Eunicea fusca and Pseudopterogorgia elisabethae as a resource for bioactive diterpenes: A journey through drug discovery, glycosylation chemistry, and chemical proteomics.

A Thesis

Submitted to the Graduate Faculty

In Partial Fulfillment of the Requirements

for the Degree of

Doctor of Philosophy

in the Department of Biomedical Sciences

Atlantic Veterinary College

University of Prince Edward Island

Douglas Hubert Marchbank

Charlottetown, P.E.I.

April, 2013

CONDITIONS FOR THE USE OF THE THESIS

PERMISSION TO USE POSTGRADUATE THESIS

Title of thesis: "Eunicea fusca and Pseudopterogorgia elisabethae as a resource for bioactive diterpenes: A journey through drug discovery, glycosylation chemistry, and chemical proteomics."

Name of Author: Douglas H. Marchbank

Department: Biomedical Sciences

Degree: Doctor of Philosophy Year: 2013

In presenting this thesis in partial fulfillment of the requirements for a postgraduate degree from the University of Prince Edward Island, I agree that the Libraries of this University may make it freely available for inspection. I further agree that permission for extensive copying of this thesis for scholarly purposes may be granted by the professor or professors who supervised my thesis work, in their absence, by the Chairman of the Department or the Dean of the Faculty in which the thesis work was done. It is understood any copying or publication or use of this thesis or parts thereof for financial gain shall not be allowed without my written permission. It is also understood that due recognition shall be given to me and to the University of Prince Edward Island in any scholarly use which may be made of any material in my thesis.

Signature: _____

Address: Department of Biomedical Sciences
Atlantic Veterinary College
University of Prince Edward Island
550 University Avenue
Charlottetown, PE C1A 4P3
CANADA

Date: _____

University of Prince Edward Island

Faculty of Veterinary Medicine

Charlottetown

CERTIFICATION OF THESIS WORK

We, the undersigned, certify that **Douglas H. Marchbank**, a candidate for the degree of **Doctor of Philosophy**, has presented his thesis with the following title: "**Eunicea fusca and Pseudopterogorgia elisabethae as a resource for bioactive diterpenes: A journey through drug discovery, glycosylation chemistry, and chemical proteomics**" and that the thesis is acceptable in form and content, and that a satisfactory knowledge of the field covered by the thesis was demonstrated by the candidate through an oral examination held on April 11, 2013.

Examiners

_____ Dr. Paul Harrison (External)

_____ Dr. Sandra McConkey (Chair)

_____ Dr. Russell Kerr

_____ Dr. Barry Linkletter

_____ Dr. Nola Etkin

Date: _____

ABSTRACT

Natural products have long been recognized for their medicinal value in traditional medicine and remain an important component of modern drug discovery. Known for their immense structural diversity, natural products are secondary metabolites that often exhibit unique pharmacological properties. In the marine habitat, alcyonacean octocorals are a rich source of diterpenes with promising therapeutic potential. For instance, Eunicea fusca contains fuscoside B, a diterpene arabinoside with potent topical anti-inflammatory activity. Notably, fuscoside B selectively inhibits 5-lipoxygenase and has a negligible effect on prostaglandin (PG) biosynthesis. Pseudopteroxazole, an amphilectane diterpene from the octocoral Pseudopterogorgia elisabethae, shows activity against Mycobacterium tuberculosis, the etiologic agent of tuberculosis.

This thesis describes a variety of approaches to discover and develop diterpenes from alcyonacean corals. An investigation of E. fusca collected from Hillsboro Ledge, Florida has led to the discovery of eunicidiol, a topical anti-inflammatory diterpene. The structure of eunicidiol was elucidated by 1D and 2D NMR spectroscopy, while the absolute configuration was unambiguously assigned by the Mosher method. The anti-inflammatory activity of eunicidiol was evaluated by measuring its ability to reduce phorbol myristate acetate (PMA)-induced edema in a mouse ear model. Topical application of a 100 μg/ear dose of eunicidiol significantly reduced edema with activity that was superior to indomethacin, an anti-inflammatory drug serving as an industry benchmark.

A library of novel fuscoside B analogues has been synthesized from fuscol and eunicol using a modified Koenigs-Knorr glycosylation approach. This semisynthesis is the first successful glycosylation of fuscol and has provided the eunicosides, a novel structural class of diterpene glycosides. In addition, glycoside mimics were prepared by introducing ethylene glycol (EG)-based substituents in place of the arabinose moiety. The library of compounds was evaluated for anti-inflammatory activity in the PMA-induced mouse ear edema assay, which demonstrated the remarkable influence of the carbohydrate substituent and its configuration on the in vivo efficacy of this glycoside class.

Pseudopteroxazole has shown activity against resistant strains of M. tuberculosis as well as in the low-oxygen-recovery assay (LORA), a mycobacterial model of non-replicating persistence (NRP). To investigate the antitubercular mechanism of action of pseudopteroxazole, a collection of semisynthetic probes was prepared to identify putative protein targets by affinity chromatography. During the course of this synthesis, structure-activity relationships (SAR) were assessed in order to maintain high binding affinity to the target protein(s). This strategy has led to the identification of several putative targets, including (3R)-hydroxyacyl-ACP dehydratase subunit C (HadC). This result suggests that pseudopteroxazole may exert its antitubercular activity, at least in part, by inhibiting mycolic acid biosynthesis.

ACKNOWLEDGEMENTS

It has been an incredible journey through my five years as a postgraduate student, an experience through which I have developed as an individual and a professional. I owe this experience to a network of support I received from the University of Prince Edward Island as well as friends and family. I want to first express my sincerest gratitude to my supervisor Russell Kerr for allowing me to pursue my academic goals in such an exceptional research group. His enthusiasm for research and discovery has served as an inspiration throughout my graduate studies. I was also fortunate to have the mentorship of the research managers in the Kerr group, Fabrice Berrue, Malcolm McCulloch, and Bradley Haltli. Their aptitude and guidance was especially important for my growth as an independent researcher. I am grateful for having such an outstanding supervisory committee, which included Tarek Saleh, Barry Linkletter, Sunny Hartwig, Bob Chapman, and Michael Shaver; their research experience and constructive feedback were invaluable. I also thank Sandra McConkey, Nola Etkin, and Paul Harrison for taking the time to participate on my examination committee.

Leigh-Anne – I am forever in your debt for the love and support you gave me, especially through the toughest moments. I will always cherish the memories that we've made, and I can't wait to see what our next step in life will be. I want to express my appreciation to the Gilroy family for all the things they've done for me, but especially for treating me like one of their own. I am also very fortunate to have a friend like Russell Campbell – his wit and humour and our conversations over a good glass of whiskey kept me sane during those stressful times. And finally, this acknowledgement would not be complete without mentioning my family. The numerous ways in which they supported and encouraged me are endless. I especially thank my parents, to whom I attribute my work ethic. If it hadn't been for their belief in me, particularly much earlier in my academic career, I wouldn't have had the ambition to pursue postgraduate studies. For these reasons, I dedicate my thesis to them.

DEDICATION

To my parents for their unconditional love and support

TABLE OF CONTENTS

LIST OF FIGURES

LIST OF TABLES

LIST OF ABBREVIATIONS

5-HPETE	5(S)-hydroperoxyeicosatetraenoic acid
5-HETE	5(S)-hydroxyeicosatetraenoic acid
5-LO	5-lipoxygenase
AAZ	acetazolamide
Ac	acetyl
Ac_2O	acetic anhydride
ACP	acyl carrier protein
AIDS	acquired immunodeficiency syndrome
APCIMS	atmospheric pressure chemical ionization-mass spectrometry
aq	aqueous
ASA	arylsulfonamide
ATP	adenosine triphosphate
BHI	brain-heart infusion
Bn	benzyl
BnOH	benzyl alcohol
BLAST	basic local alignment search tool
BP	benzophenone
BPA	benzophenone-alkyne
Bu_4NBr	tetrabutylammonium bromide
Bz	benzoyl
C_{18}	octadecylsilane
cat.	catalogue
Cip.	ciprofloxacin
CoA	coenzyme A
COSY	correlation spectroscopy
COX	cyclooxygenase
DBU	1,8-diazabicycloundec-7-ene
DCC	N,N'-dicyclohexylcarbodiimide
DI	deionized

DIC	N,N'-diisopropylcarbodiimide
DIEA	N,N-diisopropylethylamine
DMAP	4-dimethylaminopyridine
DMAPP	dimethylallyl pyrophosphate
DMF	dimethylformamide
DMSO	dimethylsulfoxide
DNA	deoxyribonucleic acid
DOS	diversity-oriented synthesis
EG_3	triethylene glycol
EG_4	tetraethylene glycol
ELSD	evaporative light scattering detection
eq	equivalents
Et_2O	diethyl ether
Et_3N	triethylamine
EtOAc	ethyl acetate
FAS	fatty acid synthase
FDA	Food and Drug Administration
FLAP	5-lipoxygenase activating protein
FT	Fourier transform
Gen.	gentamicin
GGPP	geranylgeranyl pyrophosphate
HAART	highly active anti-retroviral therapy
HIV	human immunodeficiency virus
HMBC	heteronuclear multiple bond correlation
HPLC	high-performance liquid chromatography
HRESIMS	high-resolution-electrospray ionization-mass spectrometry
HSQC	heteronuclear single quantum coherence
IC_{50}	half-maximal inhibitory concentration
IPP	isopentenyl pyrophosphate
IR	infrared spectroscopy
J	coupling constant

K_d	dissociation constant
LC	liquid chromatography
LDH	lactate dehydrogenase
LORA	low-oxygen-recovery assay
LT	leukotriene
M	monoisotopic mass
m/z	mass to charge ratio
MABA	microplate Alamar Blue assay
mCPBA	meta-chloroperbenzoic acid
MDR	multi-drug resistant
MEP	2-C-methyl-D-erythritol 4-phosphate
MIC	minimum inhibitory concentration
MPA	α-methoxyphenylacetic acid
MPLC	medium pressure liquid chromatography
MRSA	methicillin-resistant Staphylococcus aureus
MS/MS	tandem mass spectrometry
NCI	National Cancer Institute
NHS	N-hydroxysuccinimide
NMR	nuclear magnetic resonance
NOESY	nuclear Overhauser enhancement spectroscopy
NRP	non-replicating persistence
NSAID	non-steroidal anti-inflammatory drugs
NSB	non-specific binding
OTf	trifluoromethanesulfonate
P20	polysorbate 20
PBS	phosphate buffered saline
Pen.	penicillin G
PG	prostaglandin
Ph	phenyl
PhSH	thiophenol
Piv	pivaloyl

PLA_2	phospholipase A_2
PMA	phorbol 12-myristate 13-acetate
Poly.	polymyxin B
Rif.	rifampin
RP	reversed-phase
SAR	structure-activity relationship
sat.	saturated
SDS- PAGE	sodium dodecyl sulfate-polyacrylamide gel electrophoresis
SEM	standard error of the mean
t-Bu	tert-butyl
TB	tuberculosis
TBME	tert-butyl methyl ether
TBS	tert-butyldimethylsilyl
THF	tetrahydrofuran
TLC	thin layer chromatography
TMSOTf	trimethylsilyl trifluoromethanesulfonate
TOCSY	total correlation spectroscopy
t_R	retention time
TsOH	p-toluenesulfonic acid
UV	ultraviolet
Van.	vancomycin
υ_{max}	wavenumber absorption maxima
VRE	vancomycin-resistant Enterococcus
XDR	extensively-drug resistant

CHAPTER 1

GENERAL INTRODUCTION

1.1 The Role of Natural Products in Drug Discovery

Exploration of the natural environment for therapeutic agents is a concept that has its roots in traditional medicine, dating back thousands of years. Many ancient societies recognized the medicinal benefits of natural products within certain types of vegetation, and embarked on a gradual process of trial and error to identify specific varieties of plants with medicinal applications.[1] Modern drug discovery largely depends on natural products to meet current pharmaceutical needs, although the antiquated practice of administering crude plant formulations is no longer a customary practice in the developed world.[2]

A tremendous number of drugs within the current pharmacopeia have natural product origins as approximately 50 and 75% of all anticancer and antibacterial agents, respectively, are either natural products or derived therefrom.[3] Furthermore, a significant number of synthetic medicinal agents have been inspired by natural products, as demonstrated by structural similarities.[3] The ongoing role of natural products in modern drug development is underscored by the recent approval of nearly 20 natural product-based drugs between 2005 and 2010 by regulatory agencies worldwide.[4] Indeed, half of the approved small molecule drugs in 2010 were either natural products or structural mimics thereof.[3]

Natural products are secondary metabolites belonging to a unique class of biomolecules that are not required for the basic sustenance of life. The secondary metabolome includes such compounds as the alkaloids, terpenes, polyketides, and non-ribosomal peptides, and these are produced by organisms belonging to various taxonomic

lineages, including plants, animals, fungi, and bacteria. In the scientific community, natural products are renowned for their immense structural diversity and exquisite molecular complexity, as well as their unique pharmacological properties.[5] Although these compounds were once regarded as metabolic waste products with no particular function,[6] most scientists have now accepted the widely held belief that natural products provide a fitness advantage and may be required for ecological viability.[7]

1.2 Trends in Modern Drug Discovery

1.2.1 Towards combinatorial chemistry: A decline in natural products research

Despite the paramount role of natural products in modern drug discovery, towards the end of the 20th century the pharmaceutical industry scaled back or abandoned their efforts in natural product research. As technology progressed, especially in the area of automated liquid handling and detection, the throughput of biological assays was accelerated; and as a result, supplying sufficient numbers of small molecules to biological screening campaigns became a bottleneck in the drug discovery process.[8] Natural product chemistry struggled to keep up with the intense pace of high-throughput screening. Discovering a natural product is a laborious procedure requiring extensive efforts in structural determination and dereplication, a lengthy process of ensuring chemical novelty.[9] Moreover, there remains the enduring challenge of acquiring adequate material for clinical evaluation and commercial supply.

By exploiting solid-phase organic synthesis and split-and-mix techniques, combinatorial chemistry promised to deliver a staggering number of compounds for high-

throughput biological screening.[10] In fact, millions of compounds could be synthesized by a single chemist within a few weeks by applying these techniques.[11] This pace was in stark contrast to the laborious procedure of purifying and elucidating the structure of even a single natural product.[12] Unfortunately, the expectation that combinatorial chemistry would accelerate the drug discovery process was greatly exaggerated. Although this approach continues to play an important role in lead optimization,[13] the anticancer agent Sorafenib (Nexavar®) represents the only new molecular entity solely inspired by combinatorial chemistry.[3, 14]

Synthetic amenability, facile characterization, and compliance with specific rules, such as Lipinski's "rule of five", often governed the overall design of a combinatorial compound library.[15] These parameters resulted in a general restraint from incorporating chiral centers and encouraged the introduction of many aromatic rings, thus improving the overall synthetic tractability.[15-16] As a consequence, the vast majority of these compounds exhibited molecular topologies that were routinely flat and linear.[17] Furthermore, there was often little emphasis on quality control and the products of these syntheses were seldom purified.[8] Essentially, the biological relevancy of these compounds was neglected.[18]

1.2.2 Rethinking the role of natural products in drug discovery

Chemical space describes the theoretical collection of all conceivable small molecules, which is commonly estimated at approximately $10^{30} – 10^{200}$ compounds.[19] Its vastness is so great that there is insufficient matter in the known universe to supply 10 μg of every possible compound.[20] Utilizing various molecular descriptors, such as the

molecular weight, total number of stereocenters, and hydrophobicity (logP), the distribution of a compound collection across chemical space may be computationally assessed as a measure of overall structural diversity.[21] Employing such algorithms, combinatorial libraries were shown to have a confined distribution, emphasizing their low structural diversity; meanwhile the distributions of natural products and approved drugs were significantly broader, reflecting their greater overall structural diversity.[15]

Compared to the biological screening of natural product extracts, combinatorial libraries provided disappointing hit rates.[12] It has become clear that the structural diversity and molecular complexity of a library, not the number of entities, are the recipes for achieving higher hit rates.[13] Natural products are also more biologically relevant; these compounds have undergone a long process of evolutionary selection in order to attain optimal binding affinity for a particular biological target in the natural environment.[22] As a consequence, natural products occupy biologically relevant regions of chemical space and are more likely to interact with targets of pharmacological significance in humans, especially given the conservative nature of protein structure across various taxonomic lineages.[9]

Emerging from the classical ideology of combinatorial chemistry was diversity-oriented synthesis (DOS), an approach aiming to investigate biologically relevant regions of chemical space through the synthesis of molecules that mimic the structural diversity of natural products.[23] Employing a forward synthetic analysis, DOS typically involves the assembly of commercially available chiral building blocks and then pairwise combinations of various functional groups to generate products with incredible scaffold and stereochemical diversity.[24] In drug discovery, there has also been a trend towards

libraries based on natural product-like scaffolds.[25] These scaffolds should augment the drug discovery process as these scaffolds have been evolutionarily pre-validated by Nature to interact with biological targets.[26] These examples highlight an additional role of natural product chemistry; as an inspiration to synthetic chemists in their quest of novel drug discovery.

1.3 Marine Natural Products as a Source of Drugs

The diversity of life in the ocean, a habitat covering over 70% of the Earth's surface, is unparalleled by the terrestrial environment. For instance, of the 33 animal phyla, 15 are exclusively marine while five have more than 95% of their species living entirely within marine environments.[27] The tremendous biological diversity within the oceans is a reservoir of immense chemical diversity, and is therefore regarded as a rich resource for novel drug discovery.[28] Investigation of aquatic habitats was limited until the invention of scuba technology and unmanned remotely operated vehicles, and as such, marine organisms have only recently had an impact in traditional medicine.[29] Nonetheless, exploration of these untapped marine resources has revealed an exceptional number of novel natural products with pharmacological potential.[30]

Marine natural products often exhibit unique chemical scaffolds and unusual functional groups that have not been observed in terrestrial environments (**Figure 1.1**). Among these scaffolds are the macrocyclic polyketide of muironolide A (**1**)[31] and the

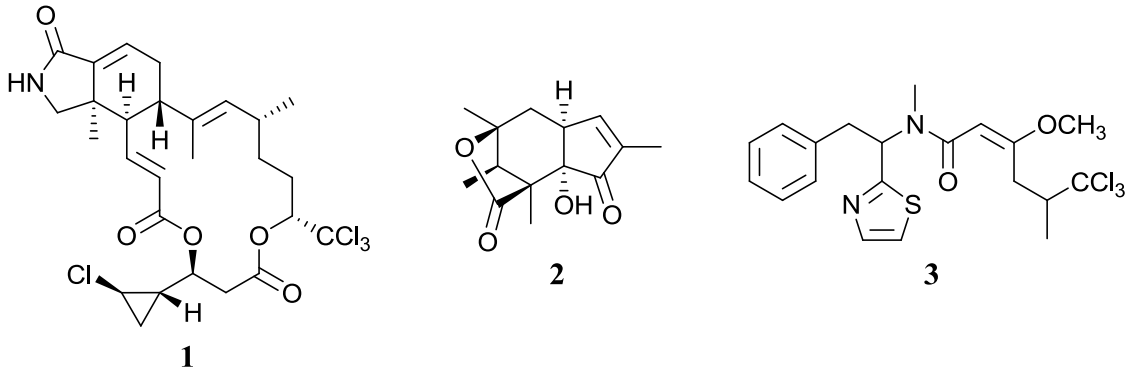

Figure 1.1. The structures of muironolide A (**1**), acremostrictin (**2**), and barbamide (**3**) as an illustration of the diversity of marine natural products.

oxygenated tricyclic lactone of acremostrictin (**2**).[32] The unusual abundance of halogenated secondary metabolites is also unique to marine organisms.[33] For instance, rhodophytes belonging to the genus Laurencia have provided a wealth of brominated terpenes and polyketides.[34] Barbamide (**3**) is a molluscicidal natural product containing an unusual trichloromethyl functionality.[35] Meanwhile, other marine organisms contain unusually high amounts of certain metabolites, such as the prostaglandins in the alcyonacean coral Plexaura homomalla.[36] The presence of such unprecedented chemistry has incited further exploration of the marine habitat for novel natural products.

1.3.1 The impact of marine natural product research on drug discovery

Cytarabine (**4**) and vidarabine (**5**) are anticancer pyrimidine and antiviral purine nucleosides, respectively, and among the first marine-derived compounds to receive FDA approval for the treatment of human disease (**Figure 1.2**).[37] The pioneering work of Bergmann et al. during the 1950's on the isolation and structural elucidation of natural products from the Caribbean sponge Tethya crypta ultimately led to the development of these two drugs,[38] inspiring other researchers to explore the marine habitat for compounds of pharmacological relevance.

It was not until approximately 30 years later that another marine-derived natural product emerged onto the drug market. Originally isolated from a tropical cone snail, ziconotide (**6**), a ω-conotoxin that selectively blocks N-type calcium channels,[39] has been clinically evaluated as an analgesic agent.[40] This marine natural product was eventually approved by the FDA in 2004 for the treatment of severe chronic pain.[41] Ziconotide is marketed under the commercial name Prialt® and is primarily administered via

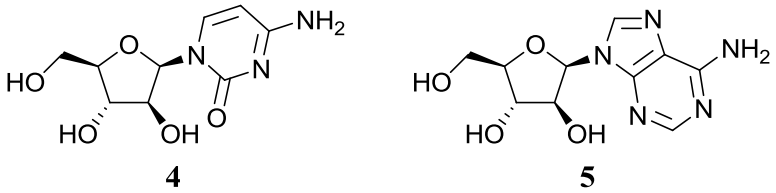

4

5

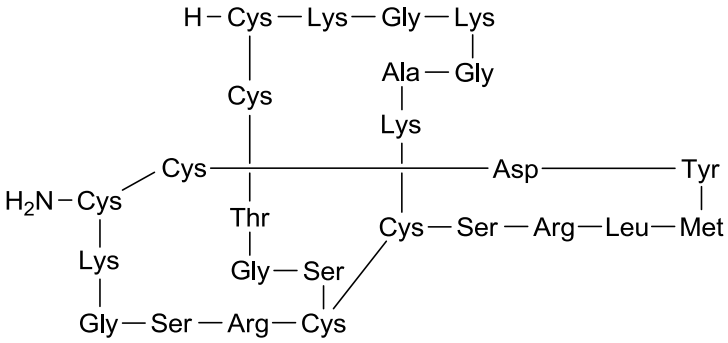

6

Figure 1.2. Marine natural products approved by the FDA, including two anticancer drugs, cytarabine (**4**) and vidarabine (**5**), and an analgesic agent, ziconotide (**6**).

.

intrathecal injection.[42] Since this accomplishment, marine natural products have steadily gained momentum in clinical drug development.

1.3.2 Ecteinascidin 743: The first anticancer drug from marine natural products

Ecteinascidin 743 (**7**, **Figure 1.3**) is a tetrahydroisoquinoline alkaloid that was discovered from the crude extract of the tunicate Ecteinascidia turbinate.[43] Known for its exceptional antitumor properties, **7** binds to the minor groove of DNA and undergoes an alkylation at the N_2 position of guanine nucleotides upon the formation of an iminium intermediate, which is generated by dehydration of the carbinolamine moiety.[44] Although the precise mechanism by which **7** exerts its antiproliferative activity is not yet fully understood, **7** has been shown to be involved in the disruption of DNA nucleotide excision repair,[45] homologous recombination DNA repair,[46] as well as transcription.[47] The first enantioselective total synthesis of **7** was completed by Corey et al. in 1996,[48] and then later by Endo et al.[49] Although these accomplishments ascertained the absolute configuration of **7**, a sustainable commercial supply had remained elusive.

The eventual development of a semisynthetic process beginning with cyanosafracin B, an antibiotic produced by fermentation of Pseudomonas fluorescens,[50] proved to be an economically feasible method of supplying **7**.[51] This achievement expedited clinical development, where **7** showed encouraging results in the treatment of various tumors, particularly soft tissue sarcoma, osteosarcoma, and ovarian cancer.[52] On the basis of its efficacy in clinical trials, **7** became the first marine-derived anticancer drug, gaining approval from the European Medicines Agency in 2007 for the treatment of advanced soft tissue sarcoma, and then in 2009 for relapsed ovarian cancer.[53] Currently

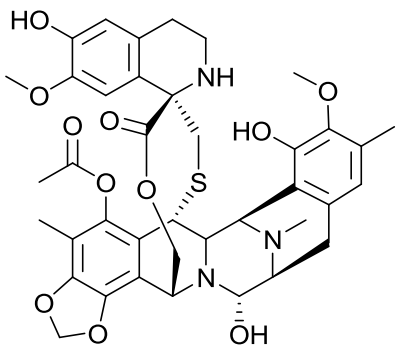

7

Figure 1.3. Chemical structure of ecteinascidin 743 (**7**), an anticancer marine natural product.

marketed by Pharmamar under the product name Yondelis®, this drug is also undergoing Phase II clinical evaluation against breast, prostate, and pediatric sarcomas.[54]

1.3.3 Eribulin mesylate: Inspiration from marine natural product chemistry

Originally isolated from the sponge Halichondria okadai by Uemura et al., the halichondrins are a family of polyether macrolides known for their remarkable anticancer properties.[55] Halichondrin B (**8**) exhibits potent cell growth inhibitory activities at nanomolar concentrations in vitro and in vivo.[56] Nearly seven years after the discovery of **8**, an elegant 90 step total synthesis was accomplished by Aicher et al., establishing the relative configuration of **8**.[57] Although the issue of supply had not been resolved, these synthetic efforts permitted the remarkable discovery of a truncated analogue with a similar biological profile as **8**.[58] Further synthetic investigation, focusing on this molecular fragment, yielded a halichondrin B mimic called eribulin mesylate (**9**, **Figure 1.4**).[59]

An investigation of the mechanism of action of **9**, utilizing an affinity chromatography approach with a biotinylated analogue, identified tubulin as a target protein of **9**.[60] Subsequent biochemical experiments later confirmed that **9** does indeed exert its anticancer activity via tubulin depolymerization. Clinical evaluation of **9** as a monotherapy for breast cancer showed that it significantly improved overall patient survival.[61] As a result, **9** received marketing authorization by the FDA for the treatment of metastatic breast cancer, and is currently marketed by Eisai Co. with the product name Halaven®.[62]

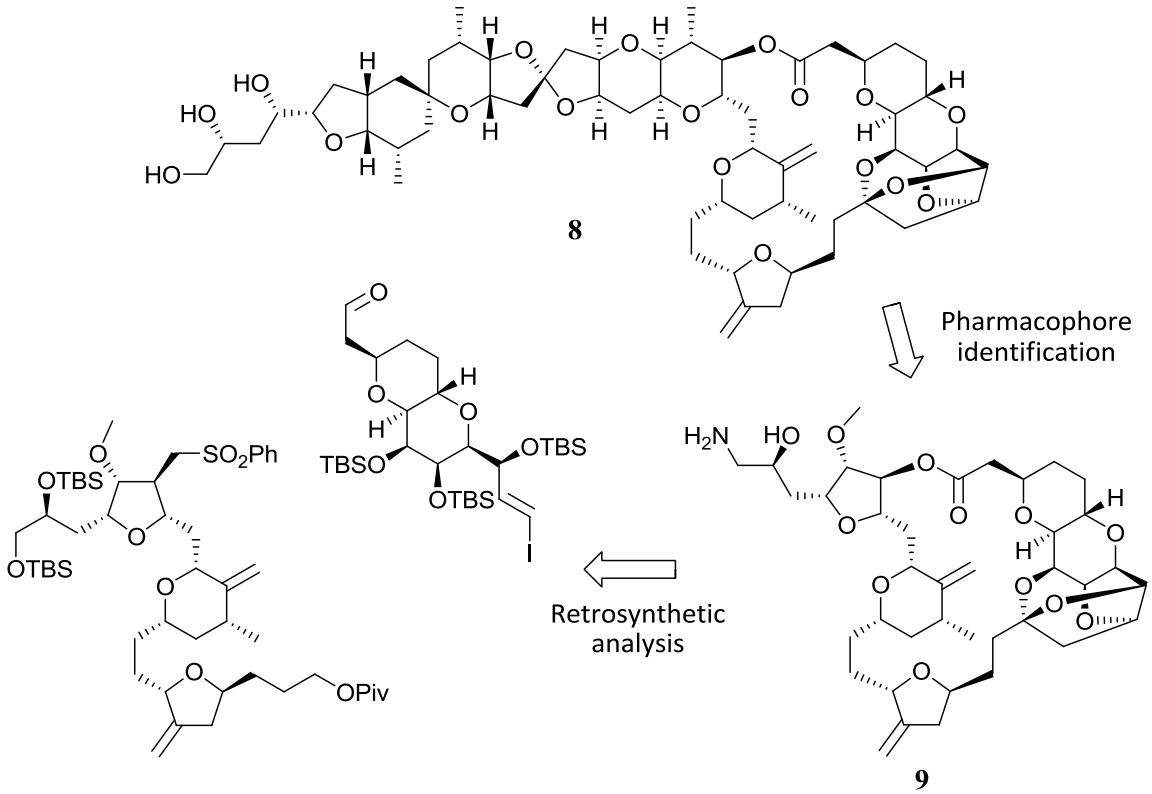

Figure 1.4. Halichondrin B (**8**) as an inspiration for the development of eribulin mesylate (**9**) by total synthesis.[63]

From the perspective of preclinical and clinical pipelines, the prospect for future drug development from marine natural products appears to be very exciting. An assessment of natural products in the clinical pipeline has indicated that 11 marine-derived compounds are in one of the three Phases of clinical development.[64] The pharmaceutical preclinical pipeline, during the period 1998 – 2008, consisted of 592 marine-derived compounds with antitumor and cytotoxic activities and an additional 666 marine-derived compounds exhibiting other pharmacological properties, such as antimicrobial and anti-inflammatory activities.[65] The exceptional wealth of candidates in these drug development phases suggests that marine natural products will be a significant contributor to the future pharmacopeia.

1.3.4 Marine diterpenes: A family of structurally diverse compounds

Terpenes are an extraordinarily diverse class of natural products with promising therapeutic and industrial potential.[66] More than 40,000 different compounds belonging to this class have been identified,[67] including the anticancer agent paclitaxel,[68] the antimalarial artemisinin,[69] and many other important pharmaceuticals. The biosynthesis of terpenes follows either the mevalonate or 2-C-methyl-D-erythritol 4-phosphate (MEP) pathway, both of which yield five-carbon isoprene subunits, isopentenyl pyrophosphate (IPP) and dimethylallyl pyrophosphate (DMAPP).[67] The origin of these precursors may be delineated through stable isotope labeling as the mevalonate pathway derives the carbon atoms from acetyl-CoA, while the latter utilizes glyceraldehyde-3-phosphate and pyruvate.[70]

Terpenes are categorized according to the number of isoprene units they carry in their structure. Diterpenes are compounds originating from geranylgeranyl pyrophosphate (GGPP), a precursor containing four isoprene units that are assembled through the iterative condensation of DMAPP with IPP.[67] In addition to varying numbers of isoprene units, the enormous skeletal diversity of terpenes is achieved by the catalytic diversity of terpene cyclases, a family of enzymes that catalyzes the cyclization of open-chain $(C_5)_n$ precursors.[66, 71] Octocorals belonging to the phylogenetic order of Alcyonacea[72] are a rich source of structurally diverse diterpenes, comprising a total of 40 skeletal classes.[73]

1.4 Fuscosides: A Family of Anti-Inflammatory Glycosides

The Caribbean alcyonacean Eunicea fusca is a source of the anti-inflammatory fuscosides (**Figure 1.5**), diterpene arabinosides that reduce phorbol 12-myristate 13 acetate (PMA)-induced mouse ear edema with activities comparable to indomethacin.[74] Topical application of a 50 μg dose of fuscosides A (**10**) and B (**11**) reduced PMA-induced edema by 85 and 52%, respectively, compared to 38 and 80% by manoalide and indomethacin.[75] Although **10** displayed greater potency, **11** was distinguished by its selective inhibition of 5-lipoxygenase (5-LO) and negligible effect on cyclooxygenase (COX) and their ability to biosynthesize the PGs.[76,77] Fuscoside E (**12**), which has recently been reported by Reina et al., is structurally related to **11** and exhibited similar anti-inflammatory activity as **11** in the mouse ear edema assay.[78] Fuscosides C (**13**) and D (**14**), despite their structural resemblance to **11**, have no reported anti-inflammatory activity.

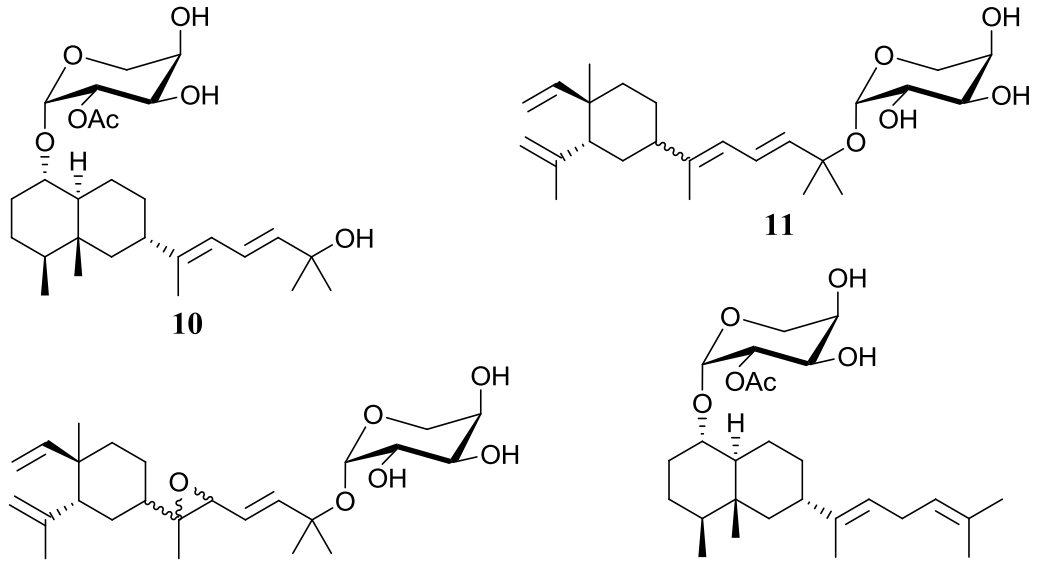

Figure 1.5. The collection of all known diterpene arabinosides isolated from Eunicea fusca.

Originally characterized by Shin et al. in 1991,[74] the fuscosides are among the few classes of marine diterpene glycosides that have been described to date.[79] While fuscoside B-D (**11**, **13**, **14**) belong to the lobane class of diterpenes, fuscosides A (**10**) and E (**12**) are diterpenoid acetylarabinosides with a unique eremophilane-type framework. Fuscosides C (**13**) and D (**14**) are a diastereomeric pair of 11,12-epoxide derivatives of **11**, adopting either the RR or SS configurations at the epoxide position. Analysis of NMR spectroscopic data revealed that the arabinoses are attached via β-glycosidic linkages.[80] Although the absolute configuration of the arabinose moiety of **10**, **11**, **13**, and **14** has not been unequivocally assigned, the D-configuration was predicted on the basis of polarimetric measurements.[74] During the recent characterization of **12**, the presence of a D-arabinose substituent was ascertained by circular dichroism spectroscopy for this particular member of the fuscoside class.[78]

Fuscol (**15**, **Figure 1.6**), the aglycone precursor of fuscoside B (**11**), was first isolated from a crude extract of E. fusca in 1978 by Gopichand et al.[81] Possessing a lobane carbon skeleton, **15** was the first non-cembranoid diterpene isolated from a Caribbean alcyonacean. This diterpene subsequently became an intriguing target for synthetic chemists such as Iwashima et al., who accomplished the total synthesis of **15** in 20 steps with an overall yield of 4.8%.[82] This enantioselective synthesis firmly established the absolute configuration of **15** as 2R, 7R, 10S, considering the identical spectroscopic properties between the synthetic and naturally occurring **15**. An alternative and more efficient synthesis was later achieved by Kosugi et al.,[83] who developed a 10-step procedure that afforded **15** with a 20% overall yield. Although **11** had served as the

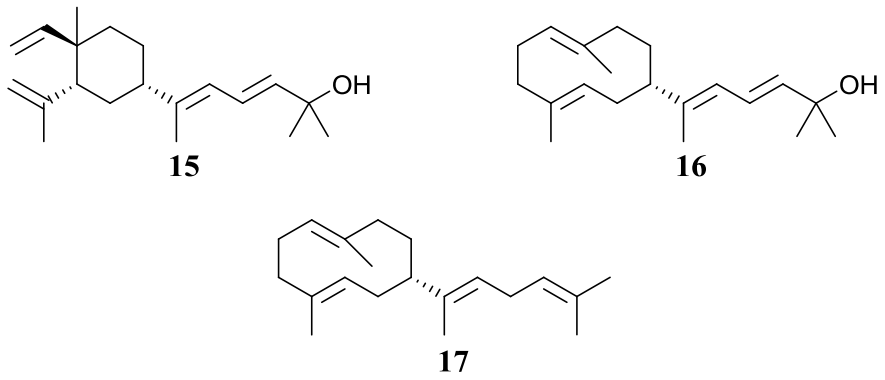

15 **16** **17**

Figure 1.6. Fuscol (**15**), the aglycone of fuscoside B (**11**), and other diterpenes isolated from Eunicea fusca.

inspiration for undertaking this research,[82,83] neither group reported any attempt to glycosylate **15**.

Originally discovered from the eggs of the alcyonacean soft coral Lobophytum microlobulatum,[84] eunicol (**16**) is a dilophol diterpene that is commonly isolated from E. fusca as a mixture with fuscol (**15**).[85] While the structural elucidation of **16** was formally described by Saleh, et al., the absolute configuration had not yet been assigned.[85] Saleh et al. also examined the metabolism of tritium labeled GGPP by E. fusca cell-free extracts, which showed that **16** and eunicene A (**17**) were biosynthetic precursors of **15** and fuscoside A (**10**). No glycosides containing the eunicol aglycone have been reported. However, the structure of such glycosides first appeared in the literature as the proposed structures of calyculaglycoside A-C;[86] a later revision revealed that these compounds instead belonged to a family of cembrane glycosides.[87] Neither the total synthesis nor any anti-inflammatory evaluation of **15**-**17** has been reported.

1.5 The Role of 5-Lipoxygenase in Inflammation

Inflammation is a complex physiological response of the immune system towards a harmful stimulus such as microbial infection or physical damage, and is essential for eliminating the distressing stimulus and promoting tissue repair.[88] Failure to revert the inflammatory response once this stimulus has been eradicated may result in a chronic state of inflammation that is detrimental towards the tissues of the host and an underlying cause of various diseases, such as rheumatoid arthritis, atherosclerosis, and cancer.[88a] The inflammatory response is regulated, to some extent, through the production of

leukotrienes (LTs) and prostaglandins (PGs), eicosanoid chemical mediators biosynthesized by 5-LO and COX, respectively.[89]

The non-steroidal anti-inflammatory drugs (NSAIDs), and particularly the selective COX-2 inhibitors known as coxibs[90], have recently received much scrutiny over their serious cardiovascular side effects.[91] Generally speaking, an NSAID is a non-selective inhibitor of COX, which are enzymes responsible for the biosynthesis of pro-inflammatory PGs.[92] The PGs produced by the housekeeping COX-1, however, also contribute to other physiological processes such as the maintenance of gastrointestinal mucosa;[93] hence the rationale for developing selective inhibitors of COX-2, an isoform whose catalytic activity is more relevant to inflammation.[91a, 94] Unfortunately, the coxibs elevated the risk of severe cardiovascular events by tipping the physiologic balance towards thrombogenic PGs.[91b, 95] Selective COX-2 inhibition also poses a significant risk of ischemic acute renal failure due to the role of PGs in maintaining renal blood supply.[96] With the exception of celecoxib (Celebrex®), all of the coxibs have been withdrawn from the market. The backlash towards selective COX-2 inhibitors has encouraged the pharmaceutical industry to develop alternative anti-inflammatory drugs, especially selective 5-LO inhibitors such as fuscoside B (**11**).

1.5.1 The 5-lipoxygenase biosynthetic pathway

5-LO belongs to a family of lipoxygenases that catalyze the addition of molecular oxygen to a 1,4-cis,cis-pentadiene.[97] Prior to the initial stages of LT biosynthesis, cytosolic phospholipase A_2 (PLA_2) releases arachidonic acid (**18**) from the nuclear envelope while 5-lipoxygenase activating protein (FLAP) aids in the transfer of **18** to

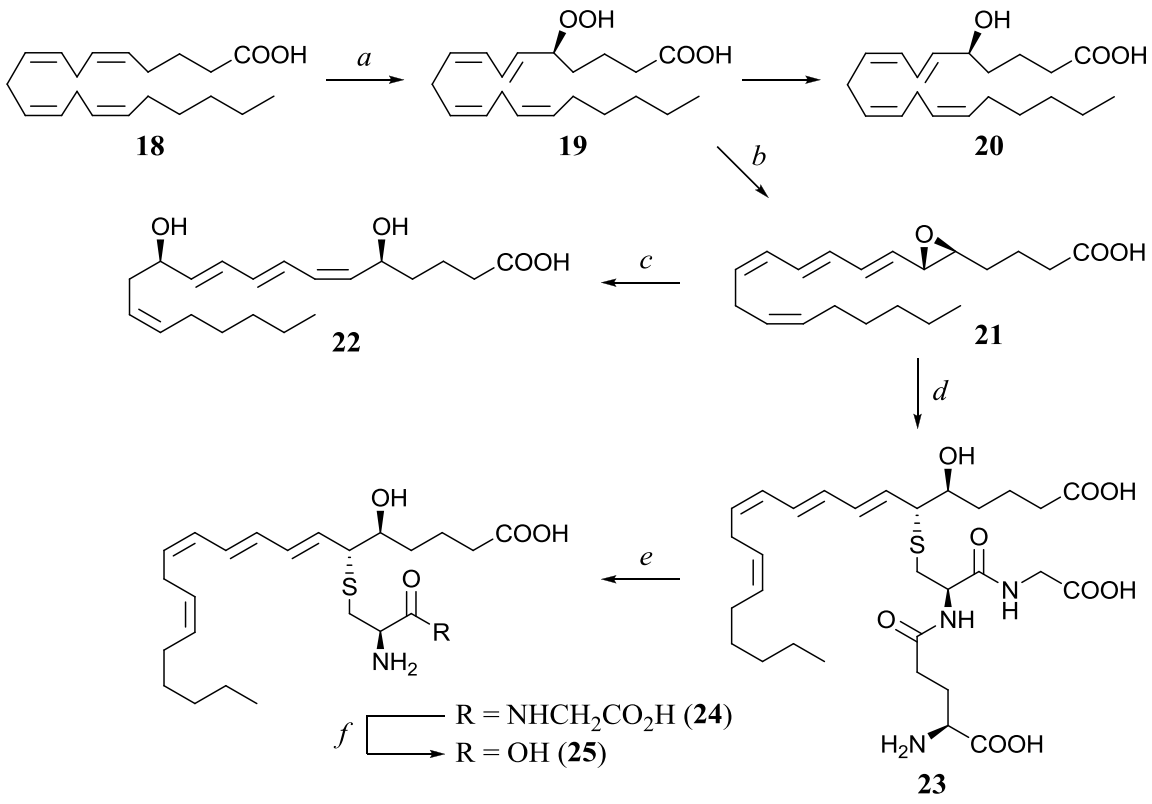

Figure 1.7. The biosynthetic pathway of LTs from arachidonic acid (**18**). The following enzymes catalyze the above transformations: (a) 5-lipoxygenase (oxygenase), (b) 5-lipoxygenase (dehydrase), (c) LTA_4 hydrolase, (d) glutathione-S-transferase, (e) γ-glutamyl transpeptidase, (f) dipeptidase.

5-LO.[98] The function of 5-LO is two-fold: it catalyzes the oxygenation of arachidonic acid to 5(S)-hydroperoxyeicosatetraenoic acid (**19**, 5-HPETE) and its subsequent dehydration to the allylic epoxide LTA_4 (**21**, **Figure 1.7**).[99] The hydroperoxide intermediate may also be reduced to 5(S)-hydroxyeicosatetraenoic acid (**20**, 5-HETE) by means of a glutathione peroxidase.[100] The unstable epoxide **21** is converted either by LTA_4 hydrolase to LTB_4 (**22**) or by glutathione-S-transferase to LTC_4 (**23**).[101] Meanwhile, the other cysteinyl-containing LTs, LTD_4 (**24**) and LTE_4 (**25**), are generated via the hydrolytic removal of the γ-glutamate and glycine appendages of **23**, which are catalyzed by γ-glutamyl transpeptidase and a dipeptidase, in that order.[99c]

LTB_4 plays a role in leukocyte recruitment by triggering the adhesion of immune cells to the luminal surface of blood vessel epithelial cells, a process that promotes their migration from the blood into the interstitial fluid.[102] Moreover, **22** is a potent chemotactic agent that directs the migration of leukocytes to the site of inflammation.[103] The cysteinyl-containing LTs (**23**-**25**) are potent broncho- and vasoconstrictors and primarily associated with the pathogenesis of asthma.[104] The pathophysiological role of LTs in atherosclerosis and other chronic illnesses has also been well-documented in the literature;[105] and thus inhibiting the biosynthesis of LTs has become recognized as an effective therapeutic strategy.

1.5.2 Classes of 5-LO inhibitors

The oxygenase activity of 5-LO is coupled to the redox cycling of its prosthetic, non-heme iron.[106] As activation of 5-LO requires oxidation of iron from the ferrous to ferric state, lipophilic reducing agents, such as nordihydroguaiaretic acid, are potent

inhibitors of 5-LO. These redox-type inhibitors, however, non-selectively perturb other physiological redox processes causing undesirable side effects.[107] As a result, redox-type 5-LO inhibitors have failed to reach the market. The iron chelating inhibitors, comprised of the hydroxamic acids, are more selective and have been successful as anti-inflammatory drugs. The FDA approved zileuton (Zyflo®) is an iron chelator and the only 5-LO inhibitor on the market to date.[108]

Non-redox 5-LO inhibitors, such as ZD-2138[109] and L-739,010,[110] have even more appeal because of their greater specificity. The non-redox inhibitors do not undergo iron chelation but instead compete for the arachidonic acid binding site. It is anticipated that fuscoside B (**11**) exerts its 5-LO inhibition through a non-redox mechanism as it lacks any functional group poised for iron chelation or redox chemistry.[77] As a result, **11** may be a valuable compound for inspiring the future development of novel 5-LO inhibitors.

1.5.3 Pharmacological properties of fuscoside B

In 1992, Jacobson and Jacobs conducted a biological and biochemical evaluation of fuscoside B (**11**) in human neutrophils and a murine model of inflammation.[76,77] According to their autoradiographic experiments, **11** specifically inhibited the LTA_4 synthase function of 5-LO with high potency, as indicated by the relative increase in 5-HETE biosynthesis.[77] Intraperitoneal administration of **11** in a mouse model was ineffective against PMA-induced swelling of the mouse ear, presumably due to the hydrophobicity of the compound.[76] Topical application of **11** at the site of PMA administration was required for the desired anti-inflammatory effect. While indomethacin

exacerbated the inflammatory response at 24 h post-PMA exposure, **11** showed long-term efficacy through its ability to prevent the early recruitment and activation of leukocytes.[76] Fuscoside B (**11**) also represents the first marine natural product to exhibit selective 5-LO inhibition.

1.6 Glycosylation Chemistry

1.6.1 The biological significance of carbohydrate substituents

Carbohydrates belong to a class of biomolecules having the characteristic empirical formula of $(CH_2O)_n$. These molecules are well known for their role in energy storage and are also indispensible as structural components for a number of biopolymers, including cellulose, peptidoglycan, and chitin. In addition, carbohydrates constitute the backbone of DNA and RNA, and are also present in over half of all human proteins.[111] Considering how ubiquitous these molecules are in nature, it is perhaps not at all surprising that an impressive number of natural products are glycosylated.[112]

The remarkable structural diversity displayed by saccharides stems from the various stereochemical and substitutional patterns displayed by the basic monosaccharide subunit.[113] Likewise, the saccharide moieties of glycoside natural products are also important contributors to the structural and stereochemical diversity of these compounds. Gaining access to new regions of chemical space can be enabled by attaching carbohydrate substituents to synthetic compounds or secondary metabolites lacking any natural glycosylation.[114] The glycan portion itself is often crucial for the biological activity of a glycoside, particularly in cases where the aglycone alone fails to elicit the

desired biological effect.[115] Moreover, the carbohydrate moiety may enhance the bioavailability of the compound by improving its water solubility.[116]

1.6.2 Mechanisms of glycoside bond formation

Probing the pharmacological significance of a carbohydrate moiety is one of the primary aims of glycosylation chemistry, a branch of organic chemistry that was developed to generate libraries of compounds with differential glycosylation. The SAR obtained from such libraries may lead to the development of analogues with greater potency[117] or reduced toxicity.[118] To establish the glycosidic linkage, glycosylation chemistry has traditionally relied on the concept of a glycosyl donor (**26**), which is a protected monosaccharide with a leaving group attached to the anomeric position (**Figure 1.8**).[119] Initiation of the S_N1 reaction begins with the removal of the anomeric leaving group. This process is facilitated by an appropriate activating reagent, frequently a Lewis acid, resulting in the transient formation of the glycosyl cation (**27**), which undergoes rapid rearrangement to an oxocarbenium ion (**28**). A hydroxyl group, belonging to the glycosyl acceptor, subsequently undergoes a nucleophilic attack at the oxocarbenium ion to generate the glycosidic linkage.

A challenge in glycosylation chemistry is controlling the stereochemical outcome of glycoside bond formation, which often results in a mixture of anomers.[119] The anomeric effect directs the anomeric substituent to the axial position of the ring, although there is a steric preference for the equatorial position.[120] The nature of this effect is widely believed to be a result of hyperconjugation between the annular oxygen lone pair and the vacant antibonding orbital of the anomeric C-O bond (n-σ* interactions),[121] but

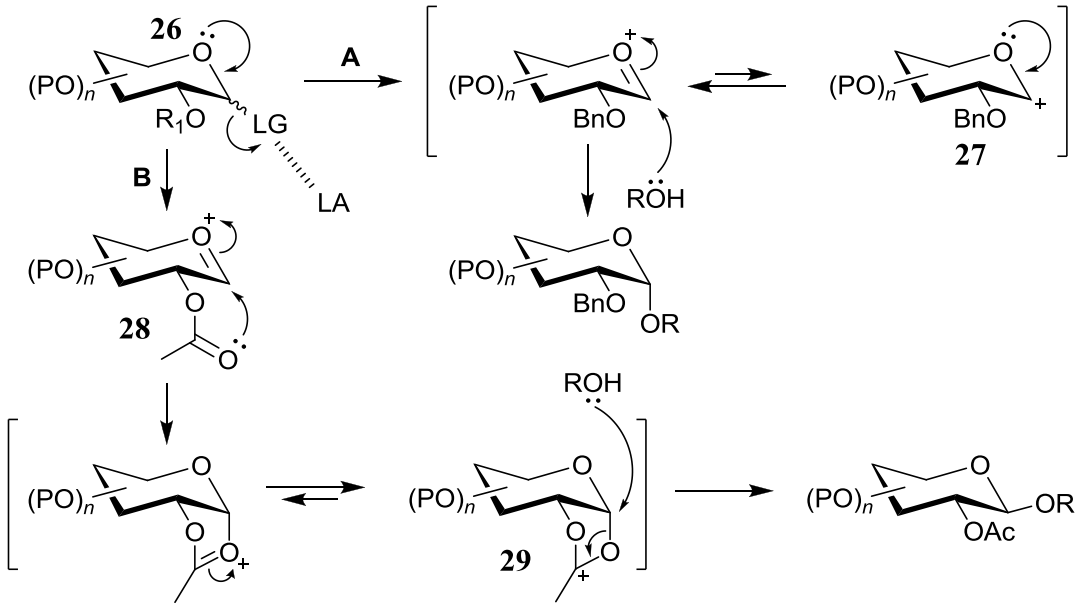

Figure 1.8. General glycosylation mechanism and the effect of neighbouring group participation on the anomeric configuration. P: protecting group; LG: leaving group; LA: Lewis acid; R: aglycone; R_1: neighbouring protecting group. Mechanism A: R_1 = Bn (anomeric effect); Mechanism B: R_1 = Ac (neighbouring group participation). Activation of the glycosyl donor (**26**) results in transient formation of the glycosyl cation (**27**), which readily rearranges to the oxocarbenium ion (**28**). Further rearrangement may occur with the participation of a neighbouring acetate protecting group, generating the acyloxonium ion (**29**).

intramolecular dipolar interactions are thought to play an important role as well.[122] As a result, axial-oriented glycosidic linkages are thermodynamically preferred. However, the anomeric configuration is also dependent on the protecting groups of the glycosyl donor.

Neighbouring group participation is defined as the interaction of a lone pair of electrons of a nearby nucleophilic substituent with a reaction center during a substitution process.[123] This phenomenon may oppose the anomeric effect and direct the formation of 1,2-trans glycosidic linkages.[124] Upon formation of the oxocarbenium ion (**28**), a rearrangement with a neighbouring participating group such as an ester functionality may occur to form a cyclic acyloxonium ion (**29**), which limits the subsequent nucleophilic attack to one side of the anomeric center. As a result, neighbouring group participation provides some degree of stereocontrol and is commonly exploited for this purpose by employing ester protecting groups, as shown in mechanism B in **Figure 1.8**.[125] However, various 1,2-cis glycosidic linkages, which are found in many natural compounds,[126] remain elusive.[127]

The protecting group also has an impact on glycosyl donor reactivity by influencing the activation energy barrier to oxocarbenium ion (**28**) formation.[128] In this regard, protecting groups have been divided into two classes: “arming” and “disarming”.[129] Electron donating protecting groups, such as benzyl ethers or acetonides, arm the glycosyl donor by lowering the energy of the oxocarbenium ion and thus increase the relative rate of glycosyl donor activation. Such glycosyl donors are less stable and have higher rates of activation. Meanwhile, electron withdrawing ester protecting groups, such as acetates and benzoates, are disarming as they invoke the destabilization of

oxocarbenium ions. These disparities in reactivity rates have recently been exploited by Zhang et al. in the development of a strategy for one-pot oligosaccharide synthesis.[130]

1.6.3 The Koenig-Knorr glycosylation method

The first chemical glycosylation was accomplished in 1901 by Koenigs and Knorr who recognized the potential of glycosyl halides as carbohydrate donors when activated by Ag_2CO_3 or Ag_2O.[131] Glycosyl bromides are typically favoured as their reactivity and hydrolytic stability is intermediate between their glycosyl chloride and iodide counterparts.[132] Since the discovery of the Koenigs-Knorr method, modifications of the procedure have improved glycosylation yields. For instance, the addition of AgOTf, a soluble silver salt with a weakly coordinating anion, increases the relative rate of glycosyl donor activation and tends to provide higher glycosylation yields.[133] In this co-promotion system, only a sub-stoichiometric amount of AgOTf is necessary as it is regenerated in situ when the glycosylation by-product TfOH reacts with Ag_2CO_3, which serves as an acid scavenger.[134] Variations of the Koenigs-Knorr method continue to be applied in the glycosylation of steroids,[135] natural products,[136] and many other glycoconjugates.[135]

The modified Koenigs-Knorr method has also found utility in the glycosylation of tertiary alcohols.[137] Owing to steric interactions, the tertiary hydroxyl group is a weaker nucleophile and notoriously difficult to glycosylate. Their relative intractability towards glycosylation is demonstrated by the fact that these functionalities are often left unprotected while glycosylating other moieties.[138] Nonetheless, Harmatha and coworkers reported a glycosylation of the tertiary alcohol 20-hydroxyecdysone in nearly 70% yield.[139] Schneider et al. also managed to introduce a carbohydrate functionality to the

tertiary hydroxyl group of the steroidal hormone gibberellin A_{20} in 40% yield.[140] More recently, the Koenigs-Knorr approach was carried out to glycosylate tertiary alcohol derivatives of an amino acid using a glycosyl bromide.[141] Multiple equivalents of glycosyl donor and long reaction times were employed in these reactions to achieve satisfactory glycosylation yields.

1.6.4 The Schmidt glycosylation method

Nearly 80 years after the discovery of the Koenigs-Knorr method, the first alternative glycosylation approach was proposed by Schmidt et al.[142] This approach utilizes glycosyl trichloroacetimidates, whose activation may be carried out with catalytic amounts of Lewis acid, usually BF_3•Et_2O or TMSOTf.[143] The Schmidt glycosylation has since gained wide popularity due to its versatility and reliability.[136, 144] Glycosylation of natural products,[145] cholesteryl glycosides,[135] and oligosaccharides[146] are among the applications of this approach. Tertiary allylic hydroxyl groups, similar to that of fuscol (**15**) and eunicol (**16**), have also been glycosylated with satisfactory yields.[144] A notable advantage of the Schmidt method is the relative hydrolytic stability of the trichloroacetimidate and the capability of activating these glycosyl donors with reagents that are less expensive and easier to handle than heavy metal salts.[143]

1.6.5 Modern strategies in glycosylation chemistry: Glycorandomization

Efforts to improve our understanding of the biological significance of carbohydrate substituents has unfortunately been curbed by the limited availability of robust glycosylation methodology.[147] Glycosylation chemistry often suffers from tedious

protecting group manipulations and variable reaction yields.[148] Polysaccharide synthesis via iterative glycoside bond formation is a formidable task requiring the tedious manipulation of protecting groups.[149] Furthermore, unlike polypeptide and polynucleotide synthesis, every glycosylation has stereochemical consequences and may result in a mixture of products.[119-120] Despite recent progress based on neighbouring group participation,[125a, 150] stereocontrol remains an issue, as exemplified by the challenge of accessing 1,2-cis glycosidic linkages of mannosides.[127]

In recent years, there has been considerable progress towards a more universal glycosylation approach. Chemoenzymatic glycorandomization is a biocatalytic approach that exploits the broad substrate specificity of various glycosyltransferases.[151] These enzymes accommodate a structurally diverse range of nucleoside diphosphate sugars in their catalysis. These activated carbohydrates are meanwhile generated in situ by an anomeric kinase and a sugar nucleotidyltransferase, a pair of enzymes also exhibiting substrate promiscuity.[151] Combining these biocatalytic syntheses greatly enhances the pace of glycoside library development. Neoglycorandomization, on the other hand, is a novel glycosylation tool that has also accelerated glycoconjugate synthesis.[152] This strategy exploits the chemoselective condensation between secondary alkoxyamines and the reducing end of unprotected and non-activated carbohydrates.[153] Although the introduction of the alkoxyamine handle to the aglycone represents a potential obstacle,[115a] this method is not restricted by the extent of enzyme flexibility.

1.7 Pseudopteroxazole: A Unique Antitubercular Diterpene

Pseudopteroxazole (**30**) is an antitubercular amphilectane diterpene first isolated by Rodríguez et al. from the alcyonacean coral Pseudopterogorgia elisabethae.[154] This compound was reported alongside seco-pseudopteroxazole (**31**), a diterpene possessing the serrulatane scaffold, while homopseudopteroxazole (**32**) was discovered at a later date.[155] The benzoxazole moiety is a characteristic feature of these compounds and exceedingly rare in marine natural product chemistry with only a few representatives in the literature.[156] After completing the enantiospecific synthesis of the proposed structure of pseudopteroxazole, Corey et al. recommended a stereochemical revision.[157] The same group later achieved the first enantiospecific synthesis of **30**, establishing its absolute configuration as shown in **Figure 1.9**.[158] A concise synthesis of **30** using a tricyclic benzothiazine was later reported by Harmata et al.[159] Diterpenes **30**-**32** were shown to inhibit the growth of Mycobacterium tuberculosis $H_{37}Rv$ by 97, 66, and 80%, respectively, at a dose of 12.5 μg/mL, and showed no signs of cytotoxicity towards the NCI-60 cell line panel.[154-155]

Although the natural abundance of pseudopteroxazole (**30**) is low, the pseudopterosins are available in multigram quantities, constituting as much as 5% of the dry weight of P. elisabethae.[160] Considering the availability of pseudopterosins G-J (**33**-**36**), as well as their structural homology to **30**, a potential semisynthetic route to **30** was realized. Hydrolysis of the carbohydrate in **33**-**36** followed by facile insertion of the oxazole ring could achieve a supply of **30**. This opportunity culminated in a semisynthesis of **30** and a library of novel analogues.[160] This work represented the first

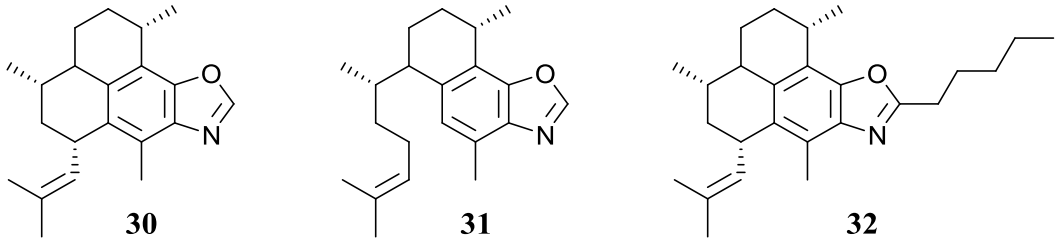

30 **31** **32**

Figure 1.9. The structures of pseudopteroxazoles **30**-**32**, antitubercular diterpenes isolated from Pseudopterogorgia elisabethae.

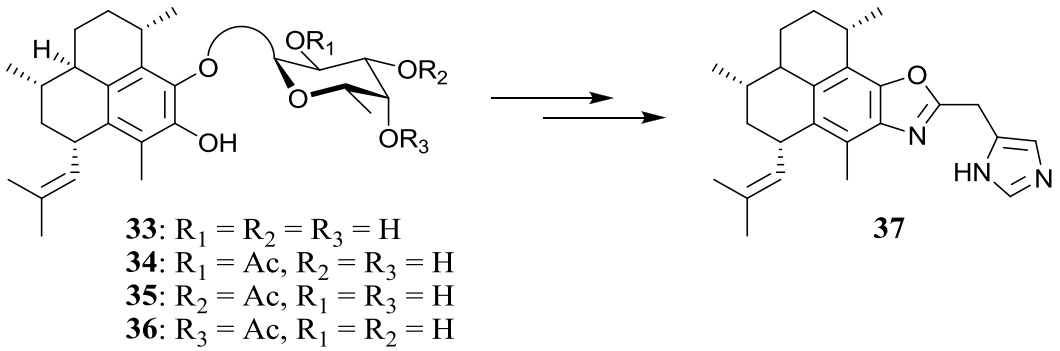

33: $R_1 = R_2 = R_3 = H$
34: $R_1 = Ac$, $R_2 = R_3 = H$
35: $R_2 = Ac$, $R_1 = R_3 = H$
36: $R_3 = Ac$, $R_1 = R_2 = H$

37

Figure 1.10. A semisynthetic route to pseudopteroxazole analogues, such as PtxHis (**37**), from a pseudopterosins G-J (**33**-**36**) mixture isolated from Pseudopterogorgia elisabethae.[161]

insight into SAR for this class of compounds (**Figure 1.10**). Within this compound collection was a histidine-derived analogue, 21-((1H-imidazol-5-yl)methyl)-pseudopteroxazole (PtxHis, **37**), which displayed greater potency than **30** against vancomycin-resistant Enterococcus (VRE), methicillin-resistant Staphylococcus aureus (MRSA), and a model of M. tuberculosis in a state of non-replicating persistence (NRP).[161]

1.8 Trends in Antimicrobial Drug Discovery

The serendipitous discovery of penicillin by Alexander Fleming in 1928 is arguably the most important medical discovery in the 20th century as it ushered in the modern era of antimicrobial drug discovery. After this breakthrough, a remarkable decrease in mortality rates from infections was achieved, convincing many that "it was time to close the book on infectious diseases".[162] Following this notion, many governmental agencies and pharmaceutical companies began diverting their resources away from antibiotic research during the early 1980s.[163] However, extensive clinical and industrial use of antibiotics imposed a selective pressure, and as a consequence, clinically relevant antibiotic resistance ensued.[164]

The mechanism of antibiotic resistance may involve altering the amino acid sequence of a protein target to vitiate drug binding interactions.[165] For instance, Staphylococcus aureus has acquired methicillin resistance by altering a penicillin binding protein, which lowered its binding affinity toward β-lactam antibiotics.[166] Obtaining resistance-associated genetic material from other organisms or the surrounding

environment may also confer antibiotic resistance.[165b] The development of vancomycin resistance in enterococci was due to the acquisition of the vanHAX gene cassette,[167] which has been thought to originate in soil-dwelling bacteria.[168] The expression of vanHAX encodes enzymes that are responsible for reinforcing the peptidoglycan layer by replacing D-Ala-D-Ala dipeptide residues with D-Ala-D-Lac.[167, 169] This alteration removes a key hydrogen bonding interaction between vancomycin and the dipeptide and thus confers resistance.

In recent years, nosocomial infections caused by drug-resistant organisms have reached epidemic proportions and are responsible for nearly 100,000 deaths per year in the United States alone.[170] Strains of MRSA possessing intermediate and high-level resistance to vancomycin, heralded as the "antibiotic of last resort", have recently been isolated from clinical cases.[171] The emergence of multidrug-resistant (MDR) Gram-negative pathogens is also alarming.[172] Regrettably, antimicrobial drug discovery has stagnated and nearly all antimicrobial drugs introduced to the clinical over the last 40 years are members of an existing class.[173] Reinvigorating antimicrobial research has now become a matter of urgency and further neglect may have grave consequences on the future of human health.

1.8.1 Tuberculosis: A global health crisis

M. tuberculosis, the etiologic agent of tuberculosis (TB) disease, causes nearly one and a half million deaths annually and has established a latent infection in one third of the human population.[174] Primarily a disease of impoverished regions, especially Africa and Asia,[175] TB is one of the leading causes of infectious disease-related mortality,

second only to HIV/AIDS.[176] The HIV/AIDS pandemic has fueled a resurgence of TB as HIV-TB co-infection accelerates the progress of both diseases.[177] As a result of compromised immunity, TB has become the leading cause of death in patients suffering from HIV.[176] The interaction between anti-HIV and antitubercular drugs may delay the initiation of highly active anti-retroviral therapy until the initial phase of antitubercular treatment has been completed.[178] Characterized as an asymptomatic and non-contagious state, a latent infection is the predominant form of TB and progresses to the active state in only 10% of all cases, though the risk increases substantially in HIV-positive patients.[179]

Pulmonary TB infections, the most common form of active TB, expedite the transmission of the disease through the expulsion of aerosolized mycobacteria as a result of chronic coughing.[180] Along with its high rate of transmission, the success of M. tuberculosis as an intracellular pathogen is attributed to its elusiveness. Upon initial infection, this obligate aerobe establishes itself within the lung and thereafter invades host immune cells, specifically alveolar macrophages.[181] After becoming internalized into a macrophage by phagocytosis, M. tuberculosis avoids destruction by inhibiting phagosome maturation.[182] By manipulating various processes within the host cell, including inhibition of phagosome-lysosome fusion,[183] the mycobacteria create a niche within the macrophage.[181] To prevent further dissemination of the mycobacteria, cell-mediated immunity is initiated with the concerted effort of macrophages, lymphocytes, and fibroblasts, which together form granulomas around the infected macrophage cells.[184]

The majority of TB infections can be cured with a six- to nine-month antibiotic treatment, involving rifampin, isoniazid, pyrazinamide, and ethambutol.[185] Eliminating TB as a major global health issue, however, has proven to be elusive. Waning patient

adherence to the lengthy antitubercular therapy has contributed to the spread of TB.[186] To improve patient compliance, the World Health Organization has recommended directly observed therapy, a program in which a health worker supervises the administration of antitubercular medication.[187] Although the program has proven to be an effective TB management strategy, its implementation is expensive compared to the low cost of the medication itself.[188] The requirement of such prolonged treatments is largely attributed to a physiological state of NRP, a quiescent form of M. tuberculosis that is unsusceptible to antitubercular treatment.[189] As a result, shortening the duration of antitubercular chemotherapy by targeting NRP mycobacteria is an important aim of current TB research.

Over the years, low patient compliance has exacerbated the emergence of drug-resistant strains, including MDR- and extensively-drug resistant (XDR)-TB.[190] Such cases, which account for approximately 5% of all TB infections, require second-line treatments, such as cycloserine, ciprofloxacin, and amikacin.[191] These drugs, however, are generally less effective, exhibit more serious side effects, or must be administered intravenously; factors that further complicate treatment or contribute to patient non-compliance.[191-192] The emergence of MDR- and XDR-TB is a serious threat to TB management, and therefore medications that are effective against resistant infections are also needed.[193]

Despite the ongoing dissemination of TB, it has been approximately 40 years since the most recent antitubercular treatment has been approved.[194] New classes of antitubercular drugs are needed to improve the outcome of TB treatments.[195] Preferably, a novel drug should shorten the course of treatment by targeting NRP mycobacteria, be

compatible with highly active anti-retroviral therapy and other antitubercular treatments, have a spectrum of activity focused on TB, and have a novel mechanism of action, such that it lacks cross-resistance with other antitubercular drugs.[196] Inhibitors of mycobacterial proteasomes,[197] ATP synthase,[198] or proteins associated with the electron transport system[196] are therefore promising candidates as they possess a unique mechanism of action and may potentially achieve the above aims.

1.9 Chemical Proteomics

Small molecules designed by Nature offer an extraordinary opportunity to explore new aspects of biological phenomena. Widely acclaimed for their pharmaceutical success, natural products also have a long history of employment as chemical tools in biological research.[199] For instance, improvements in our understanding of cellular proliferation,[200] macromolecular interactions,[201] and other fundamental aspects of biology were contingent on natural product probes.[202] Furthermore, efforts to pursue the biological function of a natural product may also lead to the realization of a novel drug target if its function is relevant to a particular disease state.[203] Owing to the supply issue, however, investigating the mechanism of action of natural products is often unfeasible.[204] Nonetheless, one of the frontiers of natural product drug discovery is the pursuit of the biological function of every natural product in order to fully understand their pharmacological and ecological significance.

The use of chemical probes has served as a complement to the more customary genetic techniques.[205] Genetic techniques, though inexpensive and fairly selective,[206] are

limited by several issues. For instance, the biological impact of genetic manipulations is permanent, which may be inappropriate for genes that are essential for viability.[207] The chronic loss of a particular gene function may also trigger a compensatory mechanism, thus confounding the study.[208] The effect of a small molecule, on the other hand, is acute and oftentimes reversible, thus enabling a temporal analysis of the biological impact.[209] The dose of a small molecule may also be fine-tuned to precisely control the extent by which a biological process is perturbed.[209] The high specificity of small molecule tools for their cellular targets also accounts for post-translational regulatory control, an aspect not captured by gene deletion techniques.[210]

1.9.1 Chemical proteomics: An approach for novel drug target discovery

Proteins are by far the most common macromolecular targets in drug discovery.[211] Within the human genome there are a predicted 16,000 protein families, of which only four are targeted by more than 50% of FDA-approved drugs.[212] Over the past decade, the discovery of new drug targets has stagnated at an average of 5.3 per year,[212] on par with the five to six "mechanistically innovative" new molecular entities approved each year.[213] Furthermore, the drugs within our current pharmacopeia exploit only approximately 500 targets.[214] As Sir James Black famously remarked, "the most fruitful basis for the discovery of a new drug is to start with an old drug".[215] But will the pursuit of new drugs for old targets provide cures for the most enduring of human illnesses?

The chemical proteomics approach exploits a small molecule as a chemical tool for the identification of its target.[216] Frequently, the small molecule is synthetically modified to enable its immobilization onto a stationary support, allowing target protein

identification by affinity chromatography.[217] The compound may otherwise be converted to a reagent that specifically labels the target protein through covalent modification. Suicide inhibitors (mechanism-based) have an intrinsic protein labeling mechanism, such as the mechanism for β-lactam ring opening of penicillin.[218] Reversible binders, on the other hand, must be modified with an electrophilic or photoreactive functionality to facilitate protein labeling.[219] In either case, the labeling reagent must also be comprised of an identifying tag to expedite the deconvolution of labeled targets.[220]

While chemical proteomics is a powerful approach for identifying biological targets, the technique is not without limitations.[221] Modifying the small molecule into a functional probe may abolish the binding activity of interest; therefore an assessment of structure-activity relationships (SAR) is a prerequisite.[222] Unfortunately, it is difficult to accurately assess the binding affinity of small molecules with unknown targets, as cell permeability and water-solubility often confound the biological data.[217] Chemical proteomics is also beset with high background as a result of non-specific binding (NSB), which often results from generic hydrophobic or ionic interactions.[223] Proteome sample preparation by cell lysis may fail to isolate the target protein or there may be issues regarding protein stability.[221, 224] These issues primarily affect affinity chromatography, whereas photoaffinity labeling and activity-based protein profiling techniques are conducive to in situ biochemical analysis.[204, 225] If these issues can be tackled successfully, chemical proteomics is a method of choice for target deconvolution.

1.9.2 Affinity chromatography as a tool for identifying protein targets

Affinity chromatography entails the biochemical isolation of a protein target through its binding interaction with a compound immobilized onto an inert stationary support.[217] The probe acts as small molecule bait for capturing and enriching the target protein on the affinity resin. This technique is most successful for probes exhibiting a high binding affinity (i.e. $K_d < 1$ μM)[225] and for protein targets of high abundance.[226] Two strategies are commonly pursued for the preparation of affinity resins: direct covalent attachment of the compound to a stationary support or immobilization of a biotinylated molecule to a streptavidin-functionalized resin.[227] The latter approach exploits the binding interaction between biotin and streptavidin, which is the strongest non-covalent association known in nature.[228]

In both cases, a spacer is frequently placed between the small molecule and the stationary support to minimize steric congestion, which can interfere with the desired binding interaction.[229] Upon binding to streptavidin, biotin is lodged within a deep binding pocket of streptavidin such that only the carboxylate protrudes from the protein surface.[230] As a result, longer spacers are usually required for the streptavidin-biotin system.[231] These spacers are typically composed of repeating ethylene glycol subunits, an alternative to long-chain hydrophobic methylene spacers that tend to increase non-specific binding.[217] A recent study by Sato et al. has also demonstrated the importance of spacer rigidity for the binding affinity of target proteins.[231] In their approach, a polyproline spacer was exploited for its ability to form a stable left-handed helix, which prevented folding of the spacer and maintained a stable distance between the small molecule and the stationary support.[231]

Deconvolution of drug targets by affinity chromatography is often complicated by the interference of NSB.[223] Nonetheless, this issue can be mitigated with the implementation of a well-designed negative control experiment.[204, 217] A competitive displacement, in which a target protein is selectively eluted from the resin via competition with unbound small molecule, is the epitome of a negative control.[232] Regrettably, the limited solubility of many small molecules in aqueous media often precludes their use as competitive ligands.[217] A probe lacking the desired activity may instead serve as a control, given the similarities in NSB. Such inactive probes are often chiral isomers,[233] structurally related analogues,[234] or may otherwise be prepared by attaching the spacer to the pharmacophore of the molecule so as to disrupt its binding activity.[235] This strategy has recently been demonstrated by Hegde et al., who elucidated the molecular basis of thiostrepton's (**38**) antiproliferative activity using the inactive probe **39** (**Figure 1.11**).[227a]

As an alternative to the negative control probe, whose design often requires extensive analysis of SAR, the principles of serial affinity chromatography may be applied.[236] In this approach, a protein preparation is incubated with multiple batches of affinity resin in an iterative fashion. During this sequential process, the relative abundance of proteins exhibiting NSB remains largely unchanged, owing to their high abundance and low binding affinity. In comparison, protein targets with higher affinity are predominantly immobilized on the affinity resins, and are therefore depleted from the lysate early in the sequence. Analysis of differential band intensities by gel

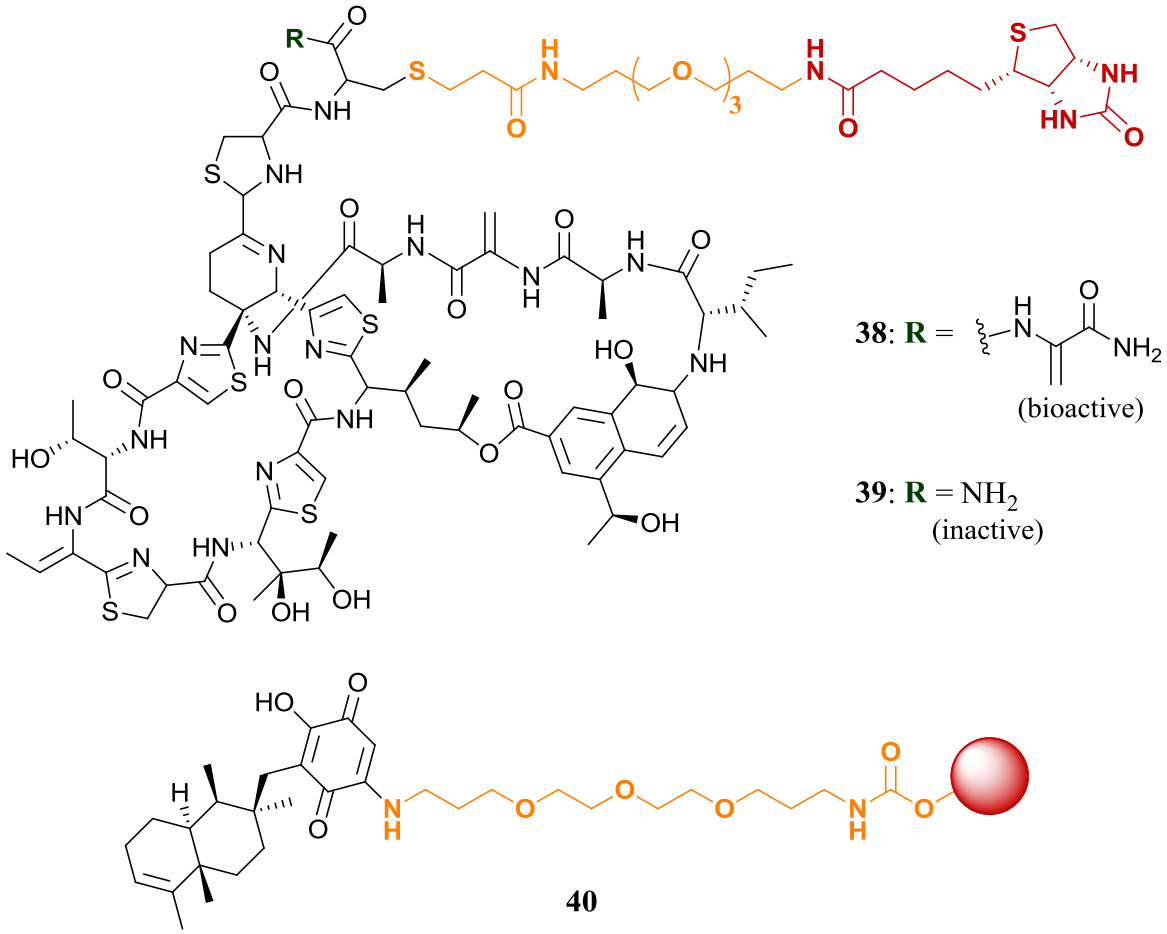

Figure 1.11. Literature examples of affinity chromatography using immobilized natural product-based probes: A biotinylated thiostrepton chemical probe (**38**) along with the inactive control probe (**39**),[227a] and bolinaquinone covalently linked to an agarose matrix (**40**).[237]

electrophoresis may allow one to differentiate between NSB and target proteins. Serial affinity chromatography was employed during the analysis of bolinaquinone (**40**, **Figure 1.11**), in which clathrin was identified as a molecular target of this anti-inflammatory marine natural product.[237]

1.9.3 Photoaffinity labeling: Target identification for reversible binders

The popularity of photoaffinity labeling in chemical proteomics has grown immensely in recent years, especially for the investigation of natural product mechanism of action.[238] This approach is commonly employed for target identification of reversible binders as these compounds, unlike suicide inhibitors, lack the intrinsic mechanism for covalently modifying their protein targets.[204] A notable advantage that this technique holds over affinity chromatography is the ability to interrogate protein binding within the context of a living cell, circumventing any potential issues regarding cell lysate preparation.[239] Furthermore, photoaffinity labeling is suitable for detecting low affinity interactions and protein targets of low abundance.[204] Labeling efficiency may be variable and depend on factors other than binding affinity.[240] For instance, conformational flexibility of the photoreactive ligand has been shown to have an impact on the overall yield of target labeling.[241]

A photoaffinity probe must be comprised of a photoreactive functional group and an identifying tag. Benzophenone has become one of the most common photoreactive groups because it exhibits excellent stability under ambient light and undergoes reversible photoexcitation instead of irreversible photolysis, resulting in higher labeling efficiency.[242] The longer wavelength of radiation required for benzophenone activation

also prevents biological macromolecules from sustaining photochemical damage.[242] To detect photolabelled targets, the probe must also present an identifying tag, commonly an alkyne group. Owing to its steric discreteness, the alkyne tag has a minimal impact on cellular uptake yet provides a synthetic handle for attaching a reporter tag, which is equipped with fluorescent and/or biotin moieties as provisions for the rapid discernment of labeled proteins.[243] For this attachment, the reporter tag must also be functionalized with an azide group to enable the azide-alkyne Huisgen cycloaddition,[244] a chemoselective ligation that is compatible with aqueous solutions.[245]

One of the preeminent applications of photoaffinity labeling was a study conducted by Koteva et al. aiming to resolve the perennial issue of inducible vancomycin resistance in enterococci.[246] The expression of vanHAX was known to be induced by vancomycin, though the exact mechanism provoking this response was the subject of much speculation.[247] A vancomycin photoaffinity probe (**41**, **Figure 1.12**) was prepared and found to be a substrate for VanS, a receptor histidine kinase that was shown to initiate transcription of vanHAX upon binding to vancomycin.[246] This discovery may lead to the development of vancomycin analogues with lower VanS binding affinity. Combining vancomycin treatment with drugs that inhibit VanS activity may also become a future strategy in the struggle against vancomycin resistant infections.[246] Using a similar protein labeling approach (**42**), Sieber et al. demonstrated the direct binding of vancomycin to other membrane targets; such binding activity may contribute to its activity against Gram-positive bacteria.[239]

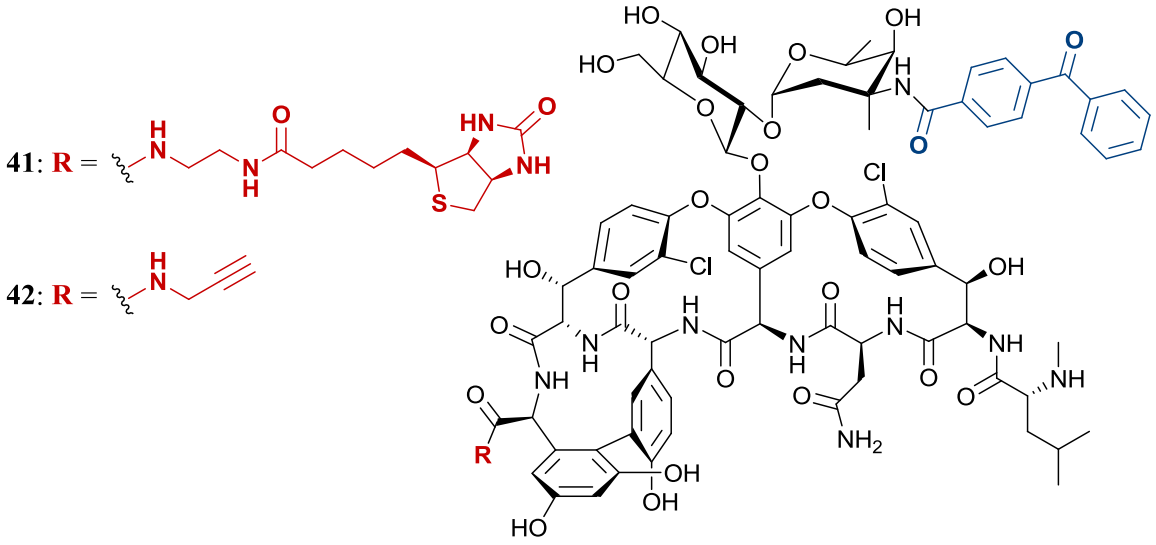

Figure 1.12. Two literature examples of vancomycin photoaffinity probes designed by Koteva et al. (**41**)[246] and Sieber et al. (**42**).[239]

1.9.4 Activity-based protein profiling: Target identification for suicide inhibitors

Activity-based protein profiling has become an effective tool for identifying the targets of natural products.[238] This approach utilizes active-site directed probes, which are compounds armed with reactive functional groups, such as α-chloroacetamides or Michael acceptors, which enable irreversible covalent binding to protein targets.[248] Similar to the photoaffinity labeling strategy, activity-based probes are commonly modified with an alkyne tag to facilitate protein target deconvolution.[249] For instance, the β-lactam antibiotics, including penicillin and ampicillin, irreversibly attach to serine residues within the active sites of penicillin binding proteins.[218] This inherent reactivity has been exploited by Staub et al. in the synthesis of β-lactam activity-based probes (**43**, **Figure 1.13**).[218] Within the context of a live cell, these β-lactam probes labeled enzymes unrelated to penicillin binding proteins, including a lipase acylhydrolase and a virulence-associated protein.[218] Activity-based probes have also been designed for the purpose of studying enzymatic function.[248b, 250] Wortmannin, a fungal natural product, has been designed into a fluorescent activity-based probe (**44**) for interrogating the biological function of phosphoinositide 3-kinase, an intracellular signaling protein with a pathophysiologic role in cancer.[251]

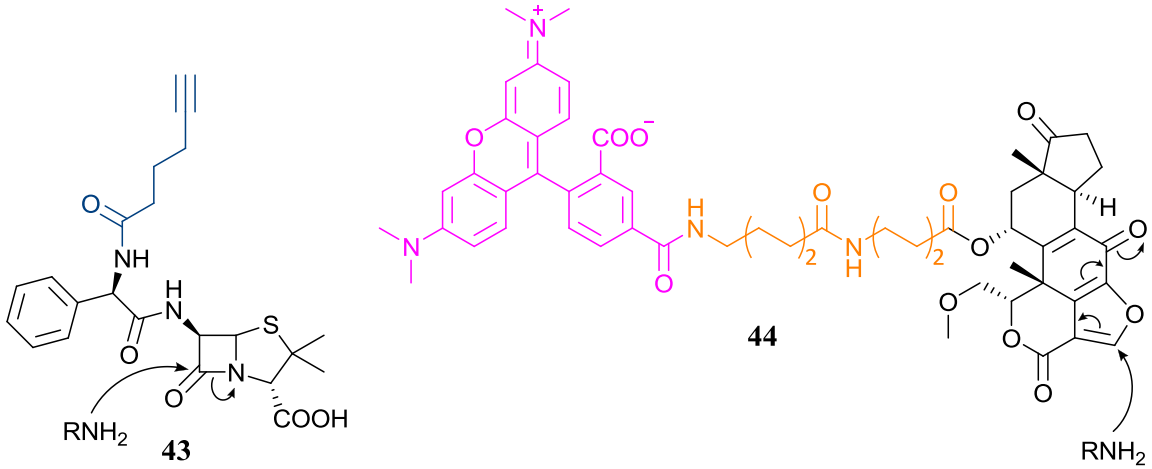

Figure 1.13. Ampicillin (**43**)[252] and wortmannin (**44**)[251] activity-based probes possessing mechanisms for protein labeling. The "R" group represents a lysine residue belonging to a target protein.

1.10 Research Goals

The general aim of this research is to investigate the biological properties of diterpenes isolated from E. fusca and P. elisabethae. While the anti-inflammatory activity of fuscoside B (**11**) has been well characterized, the biological significance of the arabinose moiety is unknown. One of the objectives of this research is to synthesize a library of fuscoside B analogues through differential glycosylation of fuscol (**15**) and eunicol (**16**). During the extraction of **15** and **16** from E. fusca, the coral shall also be investigated for diterpenes with potential therapeutic applications. The discovery of novel natural products from E. fusca, particularly those of lower abundance, is promising. The recent semisynthesis of pseudopteroxazole (**30**) from pseudopterosins G-J (**33**-**36**) in the Kerr laboratory represents a tremendous opportunity to investigate its cellular target by chemical proteomics. To identify putative targets with this strategy, a collection of pseudopteroxazole probes will be prepared for affinity chromatography or photoaffinity labeling, techniques commonly used to identify proteins exhibiting specific binding interactions. Notably, this approach may reveal a novel drug target for the treatment of TB.

Objective 1: To isolate new diterpenes from Eunicea fusca and evaluate their biological activity.

Objective 2: To synthesize a library of fuscoside B analogues and assess structure-activity relationships.

Objective 3: To investigate the antitubercular mechanism of action of pseudopteroxazole by chemical proteomics.

CHAPTER 2

EUNICIDIOL, AN ANTI-INFLAMMATORY DILOPHOL DITERPENE FROM EUNICEA FUSCA

The contents of this chapter have been published with modification as:

Marchbank, D.H.; Berrué, F.; Kerr, R.G. J. Nat. Prod. **2012**, 75, 1289.

2.1 Introduction

Marine corals belonging to the order Alcyonacea have provided a wealth of structurally diverse diterpenes with a range of potential therapeutic applications.[73, 79] The Caribbean alcyonacean Eunicea fusca is a source of the anti-inflammatory fuscosides (**Figure 2.1**), a family of diterpene arabinosides that reduce PMA-induced mouse ear edema with activities comparable to indomethacin.[74] Although fuscoside A (**10**) displays greater potency, fuscoside B (**11**) is known for its selective inhibition of 5-LO and negligible effect on prostaglandin (PG) biosynthesis.[76,77] Fuscosides C (**13**) and D (**14**) have no reported activity, while fuscoside E (**12**), a glycoside structurally related to **10**, has similar anti-inflammatory activity as **11** in the mouse ear edema assay. Although the anti-inflammatory potential of the fuscosides is well known, non-glycosidic diterpenes from E. fusca have not yet been evaluated for activity in the mouse ear edema assay.

A preliminary assessment of the anti-inflammatory properties of fuscol (**15**) was conducted by Jacobson and Jacobs in 1991.[76,77] Similar to fuscoside B (**11**), **15** had no effect on PLA_2 activity up to a concentration of 500 μM.[76] Fuscol (**15**) exhibited concentration-dependent inhibition of LTB_4 biosynthesis in adherent human polymorphonuclear leukocytes.[77] Notably, **15** [half-maximal inhibitory concentration (IC_{50}): 6 μM] was slightly more potent than **11** (IC_{50}: 10 μM) in this assay.[77] This result suggests that the carbohydrate portion is not required for in vitro 5-LO inhibition. The amount of lactate dehydrogenase (LDH) release by **11** and **15** was assessed as a measure

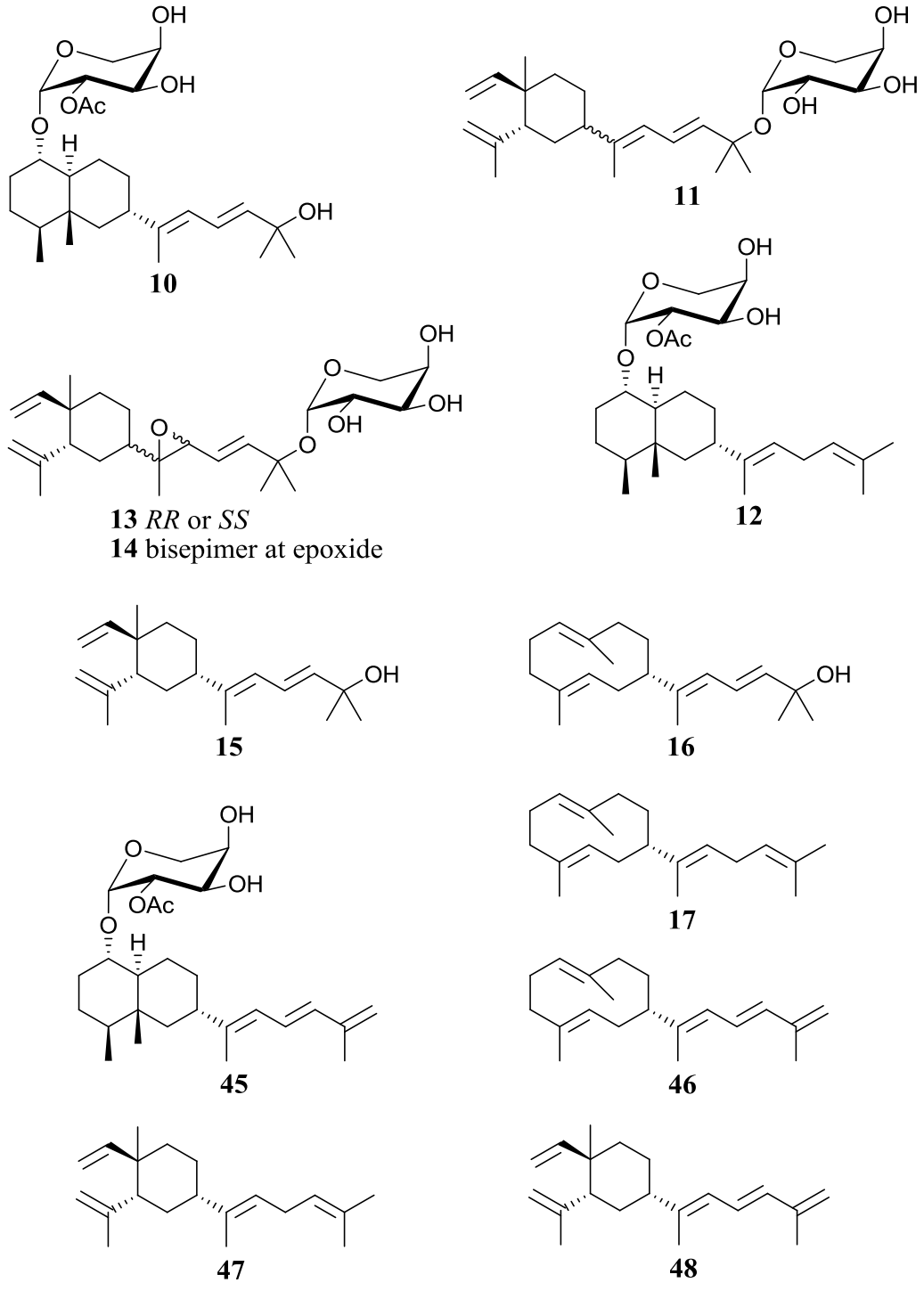

Figure 2.1. The collection of all known diterpenes and diterpene arabinosides isolated from Eunicea fusca.

of potential toxicity. Fuscoside B (**11**) showed a concentration-dependent increase in LDH release plateauing at approximately 25-30%, whereas **15** showed a maximum of 5%.[77] This result indicates lower in vitro toxicity of **15** towards adherent polymorphonuclear leukocytes, although both compounds were comparable at their respective IC_{50} concentrations. Despite a number of shared properties with fuscoside B (**11**), fuscol (**15**) was not explicitly shown to be a selective 5-LO inhibitor nor was it evaluated for in vivo anti-inflammatory activity.

Eunicol (**16**) and eunicene A (**17**), along with fuscol (**15**), are the only reported non-glycosidic diterpenes from E. fusca.[85] These diterpenes were investigated for their biosynthetic origin but were not reported to have any biological activity.[85] Newman and Hill have alleged that **15** and **16** reduce PMA-induced edema via selective inhibition of leukotriene biosynthesis,[253] however, neither compound was directly evaluated for in vivo anti-inflammatory activity and there is insufficient biochemical data to support a selective 5-LO inhibition mechanism. Other diterpenes isolated from E. fusca include fuscoside F (**45**), eunicene B (**46**), fuscene A (**47**), fuscene B (**48**),[254] (+)-germacrene D, and a variety of sterols[78] that were also isolated from extracts of sponges belonging to the order Halichondrida.[255]

The low number of literature reports on E. fusca derived secondary metabolites suggests that the coral has not yet been thoroughly investigated, thus the discovery of novel compounds remains promising. In addition, many of the reported compounds were relatively abundant in the E. fusca crude extract, indicating that much of the low-hanging fruit has been picked. An investigation of scarce natural products is therefore compelling, especially for compounds showing structural homology to fuscol (**15**) or the fuscosides.

This strategy may increase the probability of discovering novel secondary metabolites with anti-inflammatory activity. This approach may also provide an opportunity to assess the SAR of this family of natural products.

The aim of this research was to discover new compounds from E. fusca, particularly those with potential medicinal applications. The E. fusca extract was interrogated by LC-APCIMS for secondary metabolites that are structurally related to fuscol (**15**) and the fuscosides (**10**-**14**, **45**), as this approach may increase the likelihood of discovering novel natural products with anti-inflammatory properties.

2.2 Results and Discussion

2.2.1 Identification and isolation of fuscol and eunicol analogues

To discover novel secondary metabolites that are structurally related to the anti-inflammatory fuscosides, a chemistry-driven approach was pursued. A crude extract from E. fusca initially underwent chromatographic separation by medium pressure liquid chromatography (MPLC). This process of separating and enriching the metabolites into different chromatographic fractions expedited the subsequent LC-APCIMS analysis. The LC-APCIMS data was manually investigated for putative fuscoside and fuscol derivatives by searching for ions potentially arising from variations in acetylation, the degree of oxygenation, or the index of hydrogen deficiency. Compounds displaying such ions were targeted for NMR analysis and further purification. Additional structural information was also obtained by analysis of tandem APCIMS spectra.

A potentially novel diterpene was obtained as an impure sample after separating the crude extract of E. fusca by normal phase flash chromatography and RP-MPLC. Known diterpenes fuscol (**15**) and eunicol (**16**) constituted a significant proportion of the crude extract and were also collected. Preliminary analysis of the sample by low resolution LC-APCIMS revealed a quasimolecular ion of 289.2 (m/z) and a fragment ion of 269.4 (m/z), which suggested a hydroxylated analogue of **15** or **16**. Moreover, the tandem mass spectrum of this fragment ion revealed a similar fragmentation pattern as the 271.3 (m/z) fragment ion of **15** and **16** (Section 2.4), suggesting that the unknown compound was structurally related to these diterpenes. A 500 μg sample was tested in the mouse ear edema assay as a preliminary assessment of the potential anti-inflammatory

activity of this unknown diterpene. This sample strongly inhibited PMA-induced swelling by 74.5 ± 3.6% (mean ± SEM), and was significantly more potent than a 3.0 mg dose of indomethacin ($p < 0.05$, unpaired Student's t-test), a known anti-inflammatory drug employed in this study as an industry benchmark.

The diterpene was purified by semi-preparative RP-HPLC using a combination of phenylhexyl and C_{18} stationary phases (**Figure 2.2**). The molecular formula was established as $C_{20}H_{32}O_2$ by HRESIMS analysis (m/z 327.2286 $[M + Na]^+$), indicating an index of hydrogen deficiency of five. The existence of hydroxyl groups was reflected by the IR spectrum (3357 cm^{-1}) and two oxygen-bearing carbon resonances (δ_C 76.2, 70.4) in the NMR spectrum. The NMR spectroscopic data was acquired using C_6D_6 as other solvents, including CD_3OD, CD_2Cl_2, and acetone-d_6, produced poorly resolved NMR spectra with broader and weaker signals. Such signal broadening was also observed in the ^1H and ^{13}C NMR spectra of **16** (**Figure A.1**), as a consequence of conformational isomerism of the cyclodecane ring. Notably, this phenomenon has previously been observed for germacrene-type compounds.[256] Acquisition of ^1H NMR spectra at variable temperatures, ranging between -40 and 40 °C using CD_3OD or between 10 and 60 °C using C_6D_6, did not improve signal resolution.

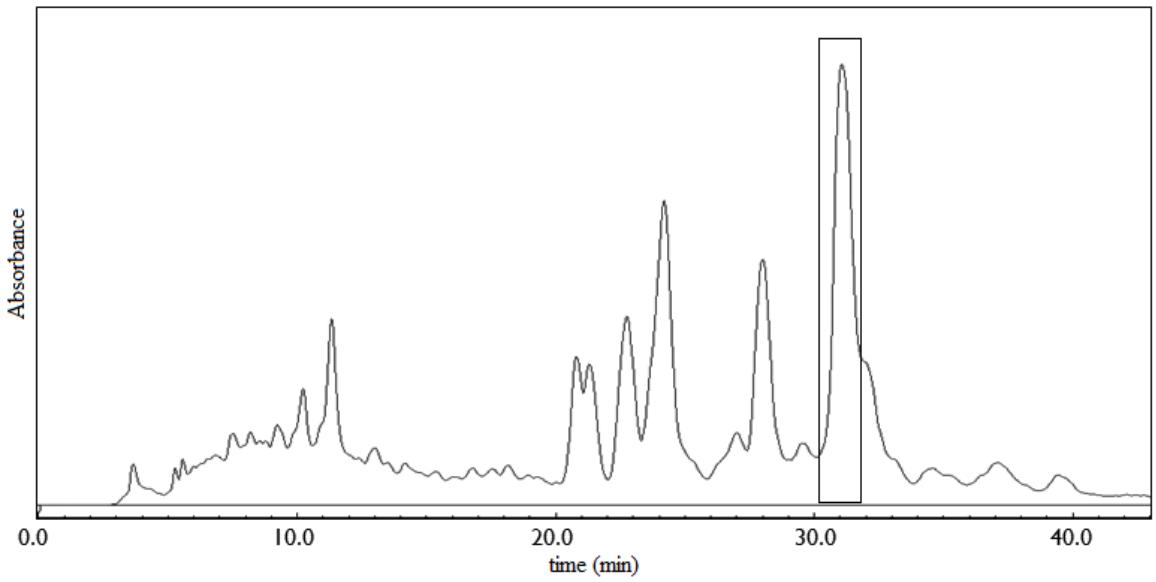

Figure 2.2. Purification of the novel diterpene by semi-preparative RP-HPLC [UV chromatogram (240 nm), phenylhexyl, 77% CH_3OH, t_R 31 min].

2.2.2 Elucidation of the planar structure of eunicidiol

The ^{1}H NMR spectrum of the novel diterpene, known as eunicidiol (**49**), indicated a conjugated diene system identical to that of fuscol (**15**) and eunicol (**16**), comprising the olefinic resonances of H-13 [δ_H 6.60 (1H, dd, J = 15.1, 10.8 Hz)], H-12 [δ_H 5.99 (1H, d, J = 10.8 Hz)], and H-14 [δ_H 5.72 (1H, d, J = 15.1 Hz)] (**Figure 2.3**, **Table 2.1**). The HMBC spectrum showed correlations between H-14 and C-19/20 (δ_C 30.2) and C-15 (δ_C 70.4), indicating the presence of geminal dimethyl groups and a tertiary hydroxyl group. The C-20 methyl protons (δ_H 1.24) displayed HMBC correlations with C-19 and C-15 to further establish this moiety. The olefinic proton H-12 exhibited HMBC coupling with C-10 (δ_C 44.8) and C-18 (δ_C 13.9), confirming that the side chain of **49** was the same as that of **15** and **16**. The C-10 methine proton showed COSY correlations with the C-1 methylene protons (δ_H 1.60), thus providing partial structure A (**Figure 2.4**). Owing to the lack of unambiguous coupling of partial structure A to other nuclei, additional partial structures were elucidated independently.

The C-3 (δ_C 150.0) and C-16 (δ_C 114.7) resonances were assigned by HMBC and HSQC coupling with terminal olefinic methylene protons H-16a/b (δ_H 5.04, 4.94). Long-range heteronuclear correlations between H-16b and C-4 (δ_C 25.7) and C-2 (δ_C 76.2) established the 1,1-disubstituted double bond. The incorporation of a secondary hydroxyl group at C-2 was established on the basis of the deshielded proton (δ_H 3.87) and carbon chemical shifts. This analysis provided a 4-carbon segment referred to as partial structure B (**Figure 2.4**). Partial structure C was composed of a trisubstituted double bond according to long range HMBC correlations between the remaining olefinic C-17 methyl group (δ_H 1.53) and multiple carbon resonances [C-5 (δ_C 25.8), C-9 (δ_C 31.2),

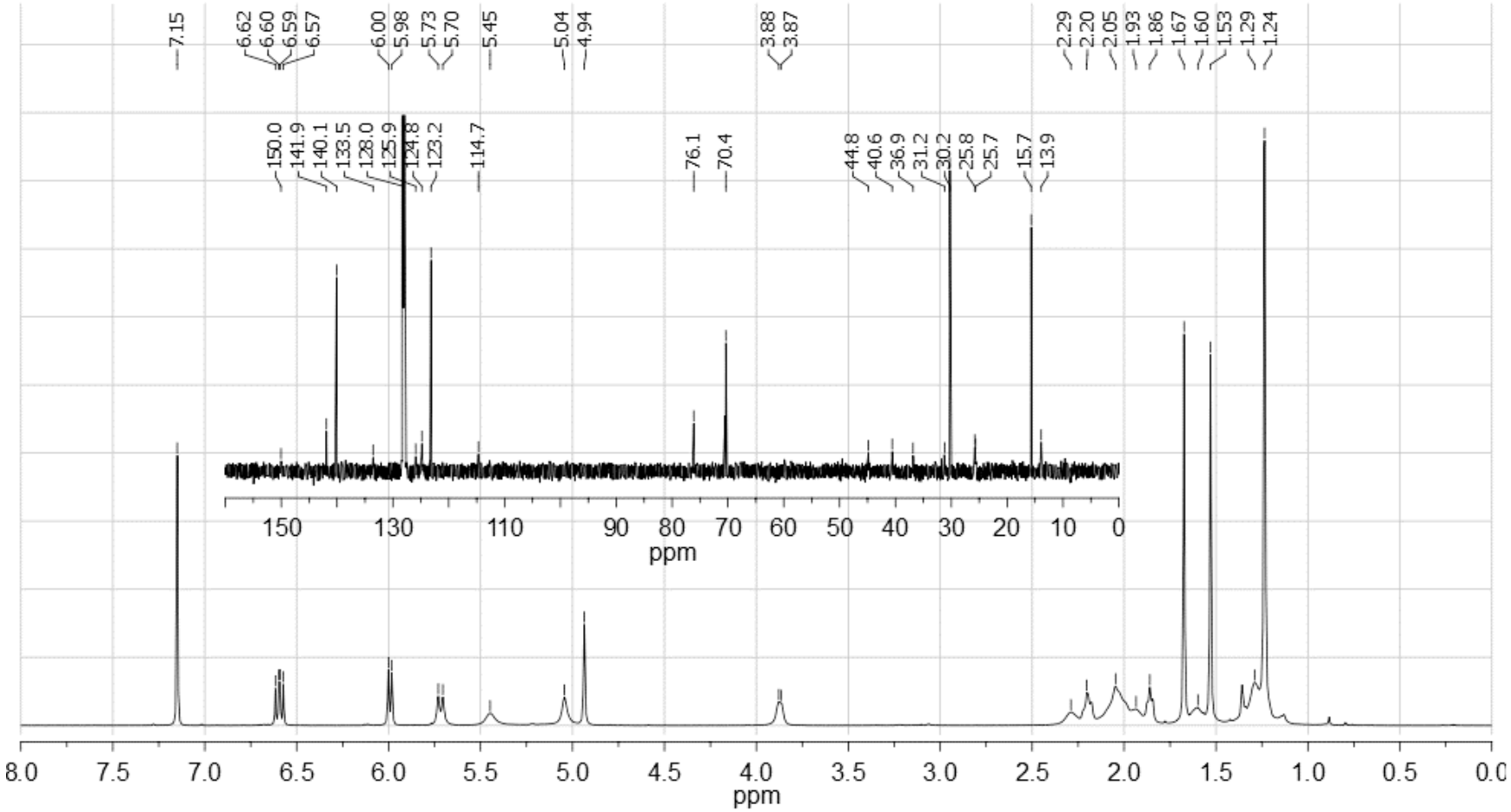

Figure 2.3. ^{1}H and ^{13}C NMR spectra (600 and 150 MHz, respectively, C_6D_6) of eunicidiol (**49**) [δ in ppm relative to residual solvent signal].

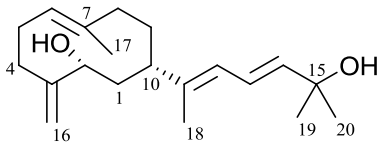

49

Table 2.1. NMR spectroscopic data (600 MHz, C_6D_6) for eunicidiol (**49**) [δ in ppm relative to residual solvent signal].[a]

Position	δ_C, type	δ_H, multiplicity (J in Hz)	COSY[b]	HMBC[c]	NOESY[b]
1	36.9, CH_2	1.60, br m	10		2
2	76.2, CH	3.87, br d (7.7)			1, 10, 12, 16a
3	150.0, C				
4a	25.7, CH_2	2.20, app. td (12.3, 3.9)	4b, 16b	2, 3, 5, 16	16b, 17
4b		2.05, m	4a, 5a, 16b		16b
5a	25.8, CH_2	2.29, m	4b, 5b, 6		
5b		2.08, m	5a		
6	125.9, CH	5.45, m	5a		8a, 10
7	133.5, C				
8a	40.6, CH_2	1.93, m	9		6
8b		2.01, m			9
9	31.2, CH_2	1.29, m	8a, 10		8b
10	44.8, CH	1.86, app. t (8.5)	1, 9	2, 8, 9, 11, 12, 18	2, 6, 12
11	141.9, C				
12	124.8, CH	5.99, d (10.8)	13, 18	10, 14, 18	1, 10, 14
13	123.2, CH	6.60, dd (15.1, 10.8)	12, 14	11, 15, 19, 20	18, 19, 20
14	140.1, CH	5.72, d (15.1)	13	12, 15, 19, 20	12, 19, 20
15	70.4, C				
16a	114.7, CH_2	5.04, br s	4a, 16b		2
16b		4.94, s	4b, 16a	2, 3, 4	4a, 4b
17	15.7, CH_3	1.53, s		5, 6, 7, 8, 9	4a
18	13.9, CH_3	1.67, s	12	10, 11, 12	13
19/20	30.2, CH_3	1.24, s		13, 14, 15, 19, 20	13, 14

[a] See **Figures A.2-A.7** for COSY, HSQC, HMBC, TOCSY and NOESY spectra. [b] COSY and NOESY correlations are from proton(s) stated to the indicated proton. [c] HMBC correlations are from proton(s) stated to the indicated carbon.

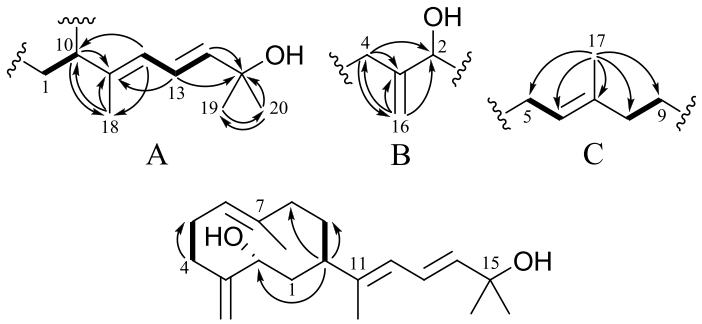

Figure 2.4. Selected HMBC ($^{1}H \rightarrow {}^{13}C$) and COSY correlations (bold bonds) of partial structures A-C as well as the assembled structure of eunicidiol (**49**).

C-6 (δ_C 125.9), C-7 (δ_C 133.5), and C-8 (δ_C 40.6)]. The COSY spectrum indicated a vicinal correlation between the C-6 olefinic methine (δ_H 5.45) and C-5 methylene (δ_H 1.93) as well as between H-8a (δ_H 1.93) and H-9 (δ_H 1.29).

The three partial structures must assemble to provide a 10-membered ring to satisfy the required index of hydrogen deficiency of five. The HMBC coupling between H-10 and C-2 provided the basis for connecting partial structures A and B at C-1 and C-2 (**Figure 2.4**). In addition, the C-10 methine proton of partial structure A displayed a COSY correlation with the C-9 methylene protons of partial structure C to signify the attachment of C-9 and C-10. Moreover, the HMBC correlations between H-10 and C-8 and C-9 confirmed this assembly. It was not possible to establish the attachment of C-4 and C-5 via COSY correlations as a result of the inability to discern between cross peaks caused by the vicinal correlation between H-4a/H-5b and the geminal correlation between H-4a/H-4b. This assignment was instead made on the basis of an HMBC correlation between H-4 and C-5. The results of a TOCSY experiment agreed with the assignment of the methylene proton resonances to the two separate spin systems of the cyclodecane ring (**Figure A.6**).

The large vicinal coupling constant (J = 15.1 Hz) across the $\Delta^{13,14}$ double bond indicated the E configuration. The $\Delta^{11,12}$ and $\Delta^{6,7}$ double bonds were also assigned E configurations given the observed NOESY correlations between H-18/H-13 and H-6/H-8a. The determination of relative configuration was also enabled by interpretation of additional NOESY correlations. The NOESY correlation between H-6 and H-10 suggested that both protons occupied the same side of the average plane of the ring. Meanwhile, the apparent lack of NOESY correlations between H-2/H-4b and H-2/H-6

implied the opposite orientation for H-2. This configuration was supported by the NOESY correlation between H-2/H-12. The observed NOESY correlations were in agreement with the MM2-minimized model of eunicidiol (**49**) (**Figure 2.5**). Considering their structural similarity, eunicidiol (**49**) and fuscol (**15**) likely have a common biosynthetic precursor, and therefore have the same configuration at C-10. On this basis, the relative configuration of **49** was determined to be 2R*,10S*.

2.2.3 Determining the absolute configuration of eunicidiol

The absolute configuration of eunicidiol (**49**) was unambiguously assigned using the Mosher method by derivatizing the asymmetric secondary hydroxyl group with (R)- and (S)-MPA (**Figure 2.6**). Although the (R)- and (S)-MPA esters of eunicidiol (**50** and **51**) were successfully synthesized using sub-milligram quantities of **49**, the tertiary allylic hydroxyl group was transformed to its methyl ether during the reaction work-up. The scarcity of **49** precluded any effort to synthesize MPA esters without methyl ethers, however such efforts were deemed unnecessary as substitution of the achiral tertiary hydroxyl group was not expected to affect the Mosher analysis. Isomerization of the conjugated diene to introduce the methyl ether at the C-11 position had not occurred during this substitution, given the geminal dimethyl signals in the ^{1}H NMR spectra. Compared to **51**, H-10, H-17, and H-18 of **50** experienced greater shielding from the phenyl ring, while H-16a and H-16b were less shielded. As a result, the $\Delta\delta^{R-S}$ values indicated the 2R configuration, establishing the absolute configuration of **49** as 2R, 10S.

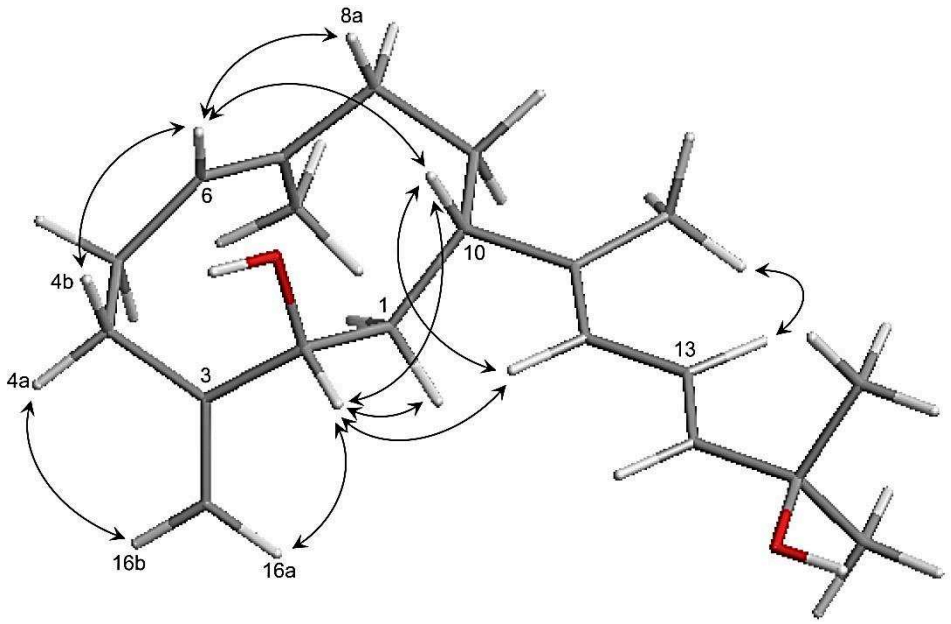

Figure 2.5. The relative configuration of eunicidiol (**49**) as indicated by key NOESY correlations ($^{1}H \leftrightarrow {}^{1}H$) [ChemBioDraw3D MM2-minimized model].

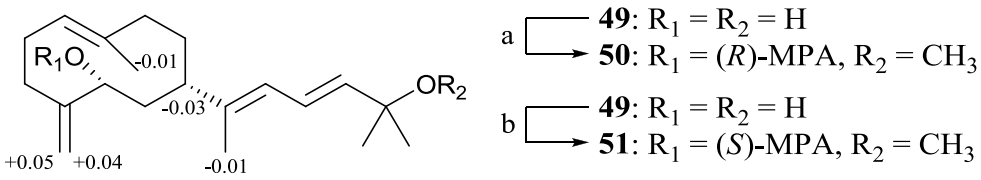

Figure 2.6. Synthesis of the (R)- and (S)-MPA esters of eunicidiol (**50** and **51**) and ^{1}H NMR chemical shift differences $\Delta\delta^{R-S}$ ($\delta^{R} - \delta^{S}$) in ppm. The ^{1}H NMR spectra for **50** and **51** are shown in **Figures A.8-A.9**. Reagents and conditions: (a) (i) (R)-MPA, DCC, DMAP, CH_2Cl_2 r.t. (ii) CH_3OH. (b) (S)-MPA, DCC, DMAP, CH_2Cl_2 r.t. (ii) CH_3OH.

2.2.4 Conformational isomerism of eunicidiol

As observed for eunicol (**16**), conformational isomerism of the cyclodecadiene ring of eunicidiol (**49**) resulted in substantial ^{1}H and ^{13}C NMR signal broadening. As a result, the NMR data was significantly more complex, and many of the correlations between atoms suffered from weak signal-to-noise ratios. This conformational phenomenon has been well characterized for germacrene A,[256] a structurally related sesquiterpene whose ^{13}C NMR spectrum displays 36 separate ^{13}C signals. Notably, the NMR data of **16** is remarkably similar to that of germacrene A.[256b] The proposed conformational isomerism of eunicidiol (**Figure 2.7**) follows that of germacrene A.[256] However, the secondary hydroxyl group may have a significant impact on the overall spatial arrangement for each conformer, an effect that may also be solvent dependent. Unfortunately, limited amount of sample precluded further NMR characterization of the conformational isomerism of **49**, which may be an important consideration during the analysis of SAR.

2.2.5 Determining the absolute configuration of eunicol

While the absolute configuration of fuscol (**15**) has been established,[8] the configuration of eunicol (**16**) was assumed to be 10S given its role as a biosynthetic precursor to **15**.[6] Recognizing that **16** may undergo an enantiospecific Cope rearrangement to **15**, its absolute configuration could be established via spectroscopic comparison of the rearranged product to a purified standard of **15**. Cope rearrangements of germacrenes and germacrenolides to elemenes and elemenolides, respectively, are known to proceed with high stereospecificity and retention of the configuration at C-10.[7]

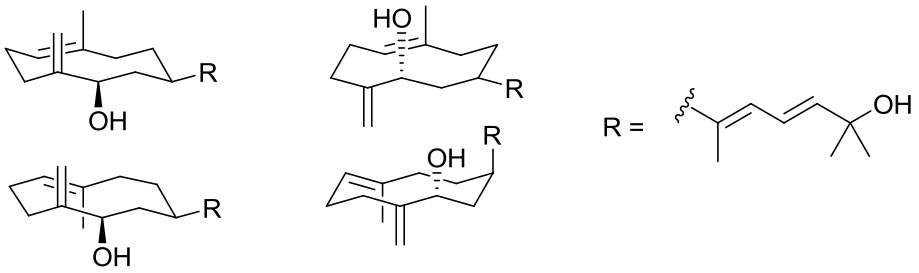

Figure 2.7. Proposed conformational isomerism of the cyclodecadiene moiety of eunicidiol (**49**).

Therefore, to unambiguously assign the absolute configuration of **16**, an enantiospecific Cope rearrangement of the cyclodecadiene moiety of **16** was carried out (**Figure 2.8**). The ^{1}H and ^{13}C NMR spectra of the rearranged product were identical to those of **15** (**Table 2.2**, **Figures A.10-A.11**), indicating the presence of a 2R,7R,10S configuration or its enantiomer. The absolute configuration of 2R,7R,10S was ascertained by comparing the specific rotation of the rearranged product ($[\alpha]^{25}_{D}$ = +28.8) with that of **15** ($[\alpha]^{25}_{D}$ = +20.4). This result is in agreement with eunicol having the 10S configuration, and for that reason the absolute configuration of eunicol was established as such.

2.2.6 Potential biosynthetic route to eunicidiol

A previous investigation of the biosynthesis of diterpenes from E. fusca has identified eunicene A (**17**) as the diterpene cyclase product and revealed that its oxidation provides eunicol (**16**).[6] Compound **16** subsequently leads to both fuscoside A (**10**) and fuscol (**15**). Eunicidiol (**49**) is conceivably derived from an oxidation of **16** as outlined in **Figure 2.9**. Considering the established biosynthetic pathway, the configurations of **10** and **17** must be consistent with their biosynthetic relatives **15**-**16**, and therefore have the absolute configurations displayed in **Figure 2.9**. A collection of diterpenes previously isolated from E. fusca,[254] which includes fuscoside F (**45**), eunicene B (**46**), fuscene A (**47**), and fuscene B (**48**), presumably share a common biosynthetic origin and have the 10S configuration as well.

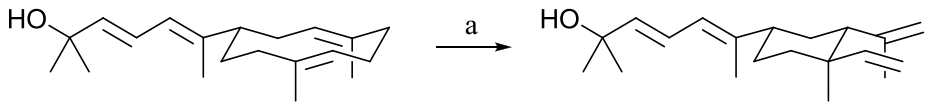

15 **16**

Figure 2.8. Semisynthesis of fuscol (**15**) by Cope rearrangement of eunicol (**16**). Reagents and conditions: (a) Δ toluene, 2.5 hr, 38%.

Table 2.2. Comparison of ^{1}H and ^{13}C NMR spectroscopic data between fuscol (**15**), semisynthetic fuscol, and eunicol (**16**) [δ in ppm relative to residual solvent signal].

	Fuscol (**15**)[a]		Semisynthetic Fuscol (**15**)[a]		Eunicol (**16**)	
Position	δ_C, type	δ_H, multiplicity (J in Hz)	δ_C, type	δ_H, multiplicity (J in Hz)	δ_C, type	δ_H, multiplicity (J in Hz)
1	33.1, CH_2	1.63, app. q (12.6) 1.60-1.56, m	33.1, CH_2	1.64, app. q (12.6) 1.61-1.56, m	35.1, CH_2	2.27-2.22, m 2.18-2.13, m
2	53.0, CH	1.93, dd (12.1, 3.9)	53.0, CH	1.93, dd (12.1, 3.9)	131.9, CH	5.20-4.83, m 4.54, app. d (10.3)
3	147.7, C		147.7, C		128.9, C	
4a	112.6, CH_2	4.92, br s	112.6, CH_2	4.92, br s	39.9, CH_2	2.13-2.08, m
4b		4.69, br s		4.69, br s		1.91-1.85, m
5a	110.1, CH_2	4.95, dd (17.5, 1.1)	110.1, CH_2	4.95, dd (17.5, 1.1)	27.1, CH_2	2.21-2.17, m
5b		4.94, dd (10.8, 1.1)		4.94, dd (10.8, 1.1)		2.07-2.02, m
6	150.5, CH	5.80, dd (17.5, 10.8)	150.5, CH	5.80, dd (17.5, 10.8)	126.9, CH	5.20-4.83, m 4.77, app. d (11.2)
7	40.0, C		40.0, C		137.7, C	
8	40.1, CH_2	1.41-1.37, m	40.1, CH_2	1.41-1.37, m	42.1, CH_2	2.37-2.31, m 2.09-2.03, m
9	26.9, CH_2	1.52-1.47, m 1.44, app. ddd (12.0, 4.0)	26.9, CH_2	1.52-1.47, m 1.44, app. ddd (12.0, 4.1)	33.9, CH_2	1.69-1.62, m 1.55-1.48, m
10	48.0, CH	1.90-1.83, m	48.0, CH	1.90-1.83, m	53.7, CH	1.98-1.93, m
11	142.2, C		142.2, C		145.7, C	
12	123.4, CH	5.99, d (10.8)	123.4, CH	6.00, d (10.8)	122.6, CH	6.07-5.92, m
13	123.2, CH	6.62, dd (10.8. 15.2)	123.2, CH	6.62, dd (10.8. 15.2)	123.2, CH	6.62-6.54, m
14	140.2, CH	5.72, d (15.2)	140.2, CH	5.71, d (15.2)	140.1, CH	5.74-5.67
15	70.5, C		70.4, C		70.5, C	
16	25.1, CH_3	1.71, s	25.1, CH_3	1.71, s	16.3, CH_3	1.45, s 1.35-1.31, br s
17	16.8, CH_3	0.99, s	16.8, CH_3	1.00, s	16.8, CH_3	1.47-1.41, br s
18	15.3, CH_3	1.68, s	15.3, CH_3	1.68, s	14.6, CH_3	1.68[b], s
19/20	30.3, CH_3	1.22, s	30.3, CH_3	1.22, s	30.3, CH_3	1.23[b], s

[a] See **Figures A.10-A.11** for NMR spectra. [b] Separate signals observed for each conformational isomer.

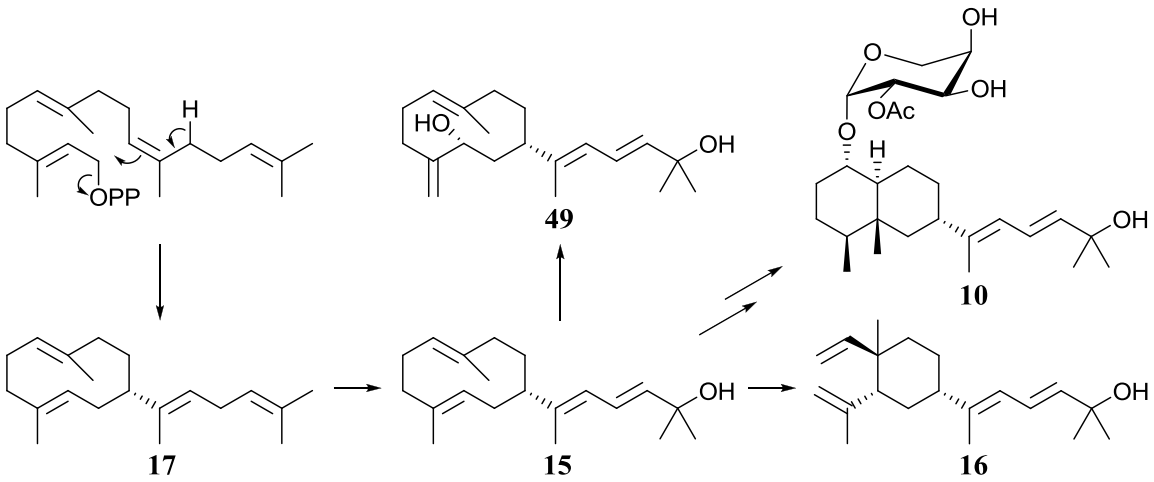

Figure 2.9. Biosynthesis of Eunicea fusca diterpenes and the proposed origin of eunicidiol (**49**).

2.2.7 Investigating the Eunicea fusca crude extract for fuscoside B

As fuscoside B (**11**) is known to exhibit potent anti-inflammatory activity, there was an interest to compare fuscol (**15**), eunicol (**16**), and eunicidiol (**49**) to this glycoside. Although **11** has been reported as an abundant metabolite in the coral extract,[74,] **11** was not available in sufficient quantities in the E. fusca extract or chromatographic fractions therefrom. Several other metabolites were isolated, however, including a significant quantity of the acetoxy methyl ester of PGA_2 (**52**, **Figure 2.10**), a metabolite also found in high concentrations in Plexaura homomalla and other alcyonacean species.[257] The methyl ethers of fuscol and eunicol (**53** and **54**) were also relatively abundant in a CH_3OH:CH_2Cl_2 (1:1) crude extract of E. fusca.[258] As substitution of the tertiary hydroxyl group with CH_3OH is known to proceed rapidly under acidic conditions,[259] these methyl ethers were likely solvent-derived artifacts. Excluding CH_3OH from the solvent during future extractions of the coral may be advised to ensure a higher isolation yield of **15** and **16**. To isolate fuscoside B (**11**) for future studies, it may also be necessary to collect E. fusca from a different collection site as there may be geographical variations in the amount of **11** present in the crude extract.

2.2.8 Assessment of anti-inflammatory activity and structure-activity relationships

Diterpenes **15**-**16** and **49** were evaluated for in vivo anti-inflammatory activity in the mouse ear edema assay at a single dose (100 μg/ear) (**Table 2.3**). Indomethacin, an NSAID that non-selectively inhibits COX-1 and -2,[260] was also included as a benchmark anti-inflammatory agent and administered as a 3 mg/ear dose.[261] Topical administration of these diterpenes significantly reduced mouse ear edema at 24 hr post-treatment. The

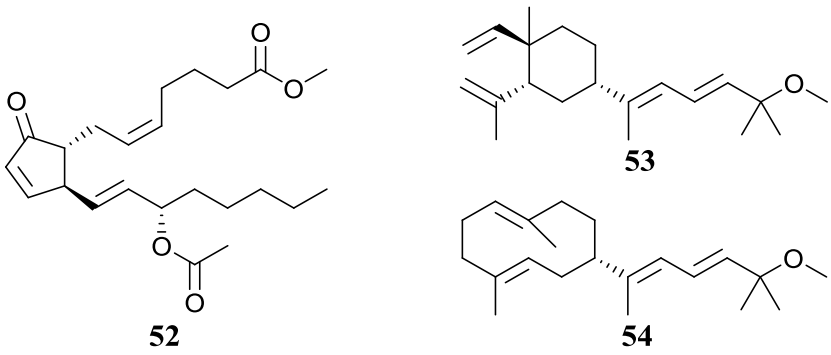

52 **53** **54**

Figure 2.10. Compounds isolated from Eunicea fusca during the search for fuscoside B (**11**).

Table 2.3. Reduction of PMA-induced mouse ear edema by diterpenes **15**-**16** and **49**.

compound	dosage (mg/ear)	reduction of ear edema (%)[a,b]
Indomethacin	3.0	51.4 ± 2.7[c]
Eunicidiol (**49**)	0.1	44.4 ± 3.2[c]
Fuscol (**15**)	0.1	46.3 ± 3.7[c]
Eunicol (**16**)	0.1	53.7 ± 4.9[c]

[a] Data is presented as the mean ± SEM. [b] Percent reduction of ear edema is relative to the vehicle control group (0.18 mm). [c] Compared to the vehicle control group, there was a statistically significant difference [unpaired Student's t-test ($p < 0.05$)]. Data for the vehicle and indomethacin control groups were obtained from six ($n = 6$) and four ($n = 4$) replicates, respectively. The diterpenes were tested in triplicate ($n = 3$).

reduction of PMA-induced edema by **15**-**16** and **49**, although comparable to indomethacin, was notably achieved with much smaller doses. Eunicol (**16**) displayed a modest increase in potency over fuscol (**15**) and eunicidiol (**49**), however, the difference between the diterpenes was not statistically significant. In addition, these diterpenes displayed no signs of toxicity (i.e. no redness of the ear or mortality) and otherwise appeared to be safe at the administered dose. The specified dose of indomethacin, on the other hand, may be less tolerable as a single mortality in this test group was observed.

An evaluation of SAR suggests that the tertiary hydroxyl group and conjugated diene moieties could be important for the observed anti-inflammatory activity, as this structural feature is present in all three anti-inflammatory diterpenes. The anti-inflammatory activity appears to tolerate structural variations on the cyclic portion of the diterpene scaffold as both lobane (e.g. **15**) and dilophol (e.g. **16**) diterpenes showed activity. Although it appears that the carbohydrate portion of fuscoside B (**11**) may not be necessary for its anti-inflammatory activity, a comparison to **11** could not be carried out due to a lack of material. While publishing this study, Reina et al. reported the characterization of fuscoside E (**12**) and a comparison of its in vivo anti-inflammatory activity to that of **11** and fuscol (**15**).[78] In their study, the reduction of PMA-induced edema by **11** and **12** was 81.5 and 80.5%, respectively, which was significantly greater than the 27.3% reduction by **15**.[78]

A comparison of the anti-inflammatory activity of fuscol (**15**) between the studies may be prohibited due to differences in the experimental protocols.[262] For instance, Reina et al. applied the phlogistic agent as a 2.5 μg dose, slightly greater than the 2.0 μg used in this study. The test samples and PMA were also administered simultaneously by Reina et

al., meanwhile in this study, topical application of the test samples preceded the PMA challenge by one hour. Furthermore, Reina et al. measured the edema only four hours after PMA administration, compared to 24 hours in this study. Regardless, fuscoside B (**11**) and fuscol (**15**) are nearly equivalent with regards to in vitro LTB_4 biosynthesis inhibition.[77] This result suggests the arabinose moiety may not be required for 5-LO inhibition but may instead have an impact on skin penetration and be responsible for improving the anti-inflammatory efficacy in vivo.

2.2.9 Assessment of the antimicrobial activity of fuscol and eunicol

Fuscol (**15**) and eunicol (**16**) were also evaluated for antimicrobial activity; eunicidiol (**49**) was not available in sufficient quantities for testing. While **15** and **16** were inactive against Candida albicans, Pseudomonas aeruginosa, methicillin-resistant Staphylococcus aureus (MRSA), and Staphylococcus warneri, **15** showed moderate activity against Mycobacterium smegmatis and M. diernhoferi. (**Table 2.4**). Fuscol (**15**) also exhibited activity against vancomycin-resistant Enterococcus (VRE), while **16** was active against the two mycobacterial species only. In addition, a crude mixture of **15** and **16** was shown to inhibit the growth of M. tuberculosis $H_{37}Rv$ with an IC_{50} of 31 μg/mL. Similar activity was observed in the low-oxygen-recovery assay [LORA, minimum inhibitory concentration (MIC) of 30 μg/mL], a model of M. tuberculosis in a state of NRP. The diterpene mixture displayed no cytotoxicity towards Vero cells (IC_{50}: >128 μg/mL). Notably, the antimicrobial properties of **15** and **16** have not previously been reported. Other members of this diterpene family, including fuscosides A (**10**) and B (**11**), may also have activity against Gram-positive organisms and, if so, these properties could

represent an additional pharmaceutical application of these anti-inflammatory natural products.

Table 2.4. Antimicrobial susceptibility testing of fuscol (**15**) and eunicol (**16**) using the microbroth dilution method (n = 3).

	IC_{50} (μg/mL)					MIC (μg/mL)	
Compound	MRSA[a]	VRE[a]	S. warneri[a]	P. aeruginosa[a]	C. albicans[a]	M. smegmatis	M. diernhoferi
Fuscol (**15**)	128 (77%)[b]	13	>128	>128	>128	8	8
Eunicol (**16**)	>128	>128	>128	>128	>128	8	8
Vancomycin	0.8	-	0.8	-	-	-	-
Rifampin	-	0.4	-	-	-	4	4
Isoniazid	-	-	-	-	-	1	0.25
Gentamicin	-	-	-	4.7	-	-	-
Nystatin	-	-	-	-	4.9	-	-

[a] Assay was completed by Martin Lanteigne. [b] Percent growth inhibition at the indicated concentration

2.3 Conclusion

In summary, a new analogue of eunicol, hereby known as eunicidiol (**49**), was isolated from Eunicea fusca using a combination of chromatographic techniques. Belonging to the dilophol skeletal class, this diterpene is comprised of an uncommon cyclodecane ring and an eight-carbon side chain, analogous to the skeleton of eunicol (**16**). The planar structure of this dilophol diterpene was elucidated by 1D and 2D NMR spectroscopic analysis, while the absolute configuration was assigned by Mosher analysis through the examination of differential shielding effects imposed by (R)- and (S)-MPA ester derivatization. Topical administration of a 100 μg/ear dose of fuscol (**15**), **16**, and **49** significantly reduced PMA-induced edema by 44, 46, and 54%, respectively, in the mouse ear assay. With regards to the administered dose, these anti-inflammatory activities were superior to indomethacin, a benchmark anti-inflammatory drug that was administered at 3 mg/ear. It remains to be determined whether diterpenes **15**-**16** and **49**, similar to fuscoside B (**11**), exert their anti-inflammatory activity via selective 5-LO inhibition.

The absolute configuration of eunicol (**16**) was unequivocally determined by carrying out a stereospecific Cope rearrangement. The product of this semisynthesis was spectroscopically identical to fuscol (**15**), whose absolute configuration has been established previously. As a result, the absolute configuration of **16** must be 10S. In consideration of the established biosynthetic pathway,[85] fuscosides A (**10**) and B (**11**), eunicene A (**17**), and other diterpenes belonging to this class (**45**-**48**) are proposed to have a 10S configuration as well. However, further analysis of each of these diterpenes

will be necessary to provide concrete evidence of their absolute configurations. This Cope rearrangement may also be employed as an alternative synthetic route to **15**, if the total synthesis of **16** is accomplished. Given the inherent stereospecificity of the Cope rearrangement, and that **16** has only one stereocenter, this may be a more efficient route to **15**.

This study represented the first in vivo anti-inflammatory evaluation of fuscol (**15**), eunicol (**16**), and eunicidiol (**49**). An analysis of SAR has suggested that the eight-carbon side chain, consisting of the tertiary hydroxyl group and conjugated diene moieties, may be important for the anti-inflammatory activity of these diterpenes, considering that it is the common structural feature. Fuscol (**15**) and **16** also showed good activity against M. smegmatis, M. diernhoferi, and M. tuberculosis, while **15** was also active against VRE. The antimicrobial activity of **15** and **16** was not previously reported and provides impetus for evaluating the fuscosides for such activities as well. Given the anti-inflammatory and antimicrobial activities exhibited by these diterpenes, other members of this natural product class (**45**-**48**) may also have unrealized pharmacological potential.

2.4 Experimental

General experimental methods as well as procedures for the mouse ear edema assay and the microbroth dilution assay are described in Appendix B.

Isolation of fuscol (15) and eunicol (16). E. fusca was collected from Hillsboro Ledge, Florida by scuba, air dried at the surface, and kept frozen during transportation. The identity of each coral was confirmed by comparing the thin layer chromatography (TLC) profile to that of a pure sample of **15**. After lyophilization, the gorgonians (124.6 g) were exhaustively extracted with CH_2Cl_2, and the combined extracts were concentrated to provide a viscous oil (11.47 g). The crude extract was initially partitioned between hexanes and CH_3OH:H_2O (9:1); afterwards the hexanes layer was evaporated (6.319 g) and separated by normal phase flash chromatography using a hexanes:EtOAc stepwise gradient elution. The hexanes:EtOAc 4:1 fraction (592.0 mg) contained **15**-**16** according to LC-APCIMS analysis. This fraction was separated by RP-MPLC (C_{18}, $H_2O \rightarrow CH_3OH$) to provide a mixture of **15**-**16** (289.9 mg, 2.3% of dry coral weight). The diterpenes were separated by semi-preparative RP-HPLC using a combination of phenylhexyl (87% CH_3OH, 3.0 mL/min, **15**: t_R 24.8 min, **16**: t_R 26.7 min) and C_{18} (83% CH_3OH, 3.0 mL/min, **15**: t_R 37.6 min, **16**: t_R 39.6 min) stationary phases. For **15**: $[\alpha]^{25}_D$ = +20.4 (c 0.06 in $CHCl_3$); IR υ_{max} 3379, 3081, 2971, 2930, 2862, 1637, 1577, 1440, 1412, 1375, 1149, 1004, 967, 907, 890 cm^{-1}. HRESIMS m/z 311.2346 $[M + Na]^+$ (calcd for $C_{20}H_{32}ONa$, 311.2345). APCIMS: m/z 271.3 $[M + H - H_2O]^+$; MS/MS spectrum (m/z 271.3): m/z 243.4, 229.4, 215.3, 201.3, 187.4, 175.3, 161.3, 147.4, 135.4, 119.3, 109.3.

For **16**: IR υ_{max} 3365, 3042, 2969, 2924, 2856, 1652, 1562, 1446, 1384, 1317, 1230, 1146, 967, 910, 844 cm^{-1}. HRESIMS m/z 311.2346 $[M + Na]^+$ (calcd for $C_{20}H_{32}ONa$, 311.2345). APCIMS: m/z 271.3 $[M + H - H_2O]^+$. All ^1H and ^{13}C NMR spectroscopic data were in agreement with the literature (**Figures A.1** and **A.10-A.11**).[6,9]

Isolation of eunicidiol (49). Eunicidiol (**49**) was present in the hexanes:EtOAc 4:1 fraction and collected alongside **15** and **16** during the above mentioned RP-MPLC separation. The compound was purified by a semi-preparative RP-HPLC using a combination of phenylhexyl (77% CH_3OH, 3.0 mL/min, t_R 31.1 min) and C_{18} (80% CH_3OH, 3.0 mL/min, t_R 21.5 min) stationary phases to provide eunicidiol (**49**, 1.5 mg, 4.9 μmol) as a colorless oil. Eunicidiol (**49**): clear oil; $[\alpha]^{25}_D$ = -33.4 (c 0.02 in CH_3OH); IR ν_{max} 3357, 3064, 3039, 2971, 2925, 2857, 1645, 1450, 1385, 1371, 1149, 1021, 968, 899. HRESIMS m/z 327.2286 $[M + Na]^+$ (calcd for $C_{20}H_{32}O_2Na$, 327.2295). APCIMS: m/z 289.2 $[M + H - H_2O]^+$; m/z 269.4 $[M + 2H - 2H_2O - H]^+$; MS/MS spectrum (m/z 269.4): 241.5, 227.4, 213.3, 199.3, 185.3, 173.3, 159.3, 145.2, 133.3, 121.3. All 2D NMR spectroscopic data of **49** (**Figures A.2**-**A.7**) are summarized in **Table 2.1**.

Synthesis of (R)- and (S)-MPA esters of eunicidiol (50 and 51). A solution containing eunicidiol (**49**, 100 μg, 0.33 μmol), DMAP (3.8 mg, 31.1 μmol), DCC (20.0 mg, 96.9 μmol), and 3Å molecular sieves (~50 mg) was stirred in freshly distilled CH_2Cl_2 (3 mL) under an N_2 atmosphere for 20 min. Subsequently, an excess of (R)- or (S)-MPA (13.8 mg, 83.0 μmol) was added and the reaction was left to stir overnight at room temperature. The reaction mixture was concentrated under a stream of N_2 and eluted through a plug of

C_{18} silica using CH_3OH. The filtrate was evaporated in vacuo to provide the reaction crude, which was separated by semi-preparative RP-HPLC (C_{18}, 5 min at 90% CH_3OH increasing linearly to 100% CH_3OH at 35 min, 3.0 mL/min, **50/51**: t_R 15.2 min). For **50**: HRESIMS m/z 489.2980 $[M + Na]^+$ (calcd for $C_{30}H_{42}O_4Na$, 489.2975). For **51**: HRESIMS m/z 489.2973 $[M + Na]^+$ (calcd for $C_{30}H_{42}O_4Na$, 489.2975). See **Figures A.8-A.9** for the ^1H NMR spectra of **50** and **51**. Product yields could not be determined with accuracy owing to the small scale of the reactions.

Semisynthesis of fuscol. A purified sample of eunicol (**16**, 1.01 mg, 3.49 μmol) was heated at reflux in toluene for 2.5 hr and evaporated in vacuo. Analysis of the reaction crude by NMR revealed the formation of fuscol (**15**, 370 μg, 1.28 μmol, 38%), which was later purified by semi-preparative RP-HPLC (C_{18}, 88% CH_3OH, 3.0 mL/min, t_R 25.6 min). Semisynthetic fuscol (**15**): $[\alpha]^{25}_D$ = +28.8 (c 0.02 in $CHCl_3$). Fuscol (lit.): $[\alpha]^{25}_D$ = +21.0 (c 0.9 in $CHCl_3$).[83] See **Figures A.10-A.11** for a comparison of ^1H and ^{13}C NMR spectra.

CHAPTER 3

THE SYNTHESIS OF A LIBRARY OF NOVEL FUSCOSIDE B ANALOGUES

The contents of this chapter have been published with modification as:

Marchbank, D.H.; Kerr, R.G. Tetrahedron **2011**, 67, 3053.

3.1 Introduction

Glycosylated diterpenes from the marine environment are a rare type of natural product whose members are found exclusively in alcyonacean species.[79] As explained in Chapter 2, Eunicea fusca is a source of the anti-inflammatory fuscosides A (**10**) and B (**11**),[74] which are diterpene arabinosides that reduce PMA-induced mouse ear edema with activities comparable to indomethacin (**Figure 3.1**).[75-77] Fuscol (**15**), the aglycone precursor of **11**,[81] is known to inhibit the biosynthesis of LTB_4 in vitro[77] and also displays in vivo anti-inflammatory activity in the mouse ear edema assay, as shown by work described in Chapter 2 as well as a report by Reina et al.[78] Considering the greater in vivo anti-inflammatory activity observed for **11** and fuscoside E (**12**),[78] the arabinose moiety appeared to be important for their in vivo efficacy. The availability of **15** and eunicol (**16**) in the E. fusca crude extract thus provided an opportunity to understand the contribution of the arabinose moiety to the observed in vivo anti-inflammatory activity of **11** through a medicinal chemistry approach.

Differential glycosylation of these aglycones could provide a collection of fuscoside B analogues, whose anti-inflammatory evaluation may lead to an improved understanding of SAR. The stereochemical configuration, ring size, and other structural variations of the carbohydrate moiety may be probed for their biological significance. Considering the near equivalent activities of fuscol (**15**) and fuscoside B (**11**) in vitro, replacing the carbohydrate with an alternative chemical moiety may also be permitted. An alternative substituent lacking the stereochemical complexity of a carbohydrate may confer greater water solubility to the relatively hydrophobic diterpene. As a result, such

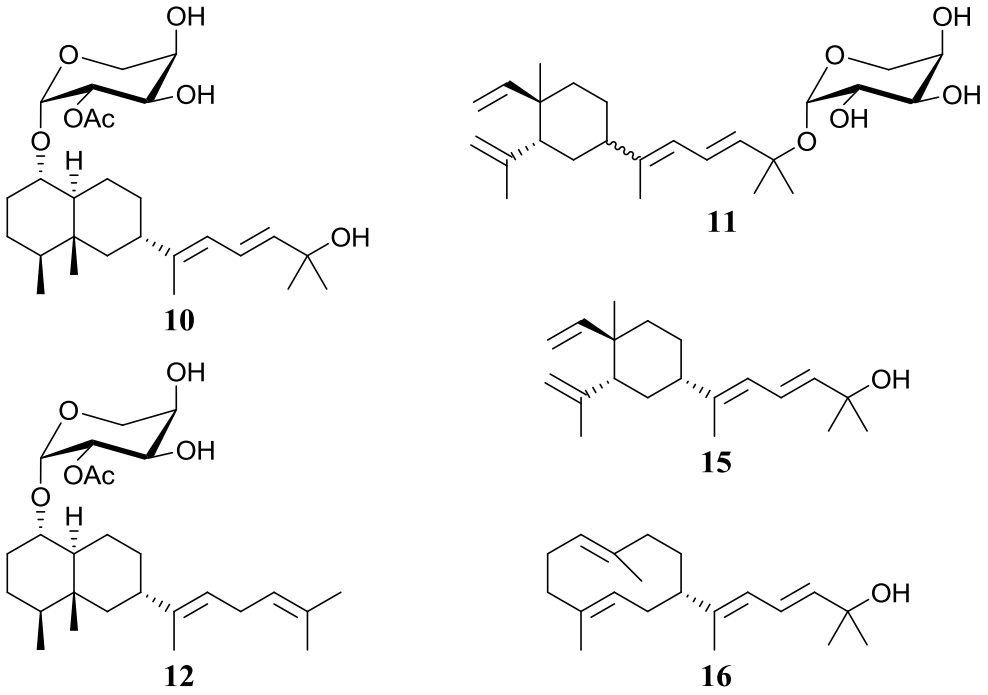

Figure 3.1. Anti-inflammatory diterpenes and diterpene arabinosides isolated from Eunicea fusca.

"glycoside mimics" may have similar anti-inflammatory properties and enable the modulation of in vivo efficacy. Synthesizing glycoside mimics may also be less difficult, and thus serve as a complement to the glycosylation approach.

Before pursuing the glycodiversification strategy, a method for glycosylating fuscol (**15**) and eunicol (**16**) must be established. While the total synthesis of **15** has been accomplished by Iwashima et al. and Kosugi et al.,[82,83] the glycosylation of **15** was not reported. This omission was curious as fuscoside B (**11**) provided the incentive for pursuing this synthetic work. Efforts to synthesize **11** may have been curbed by the challenge of glycosylating tertiary hydroxyl groups, owing to their steric hindrance. As shown by the total synthesis of erythromycin A, these functionalities often resist glycosylation, even when left unprotected.[263]

The primary aim of this research was to synthesize a collection of fuscoside B analogues via differential glycosylation of fuscol (**15**) and eunicol (**16**). To achieve this aim, methods for glycosylating these diterpenes and producing fuscoside mimics were investigated. Once the library of novel fuscosides was synthesized, the anti-inflammatory activity was evaluated using the mouse ear edema assay in an effort to assess SAR and determine the biological significance of the carbohydrate moiety.

3.2 Results and Discussion

3.2.1 The strategy for synthesizing a fuscoside library

A mixture of fuscol (**15**) and eunicol (**16**) was isolated from the E. fusca crude extract, as previously described in the preceding chapter (Section 2.4) Although the two diterpenes could be purified by RP-HPLC using a combination of phenylhexyl and C_{18} stationary phases, this approach was far too laborious to achieve a separation on a scale that would provide adequate starting material for chemical synthesis. A more realistic approach was to instead utilize **15** and **16** as a mixture. These diterpenes are essentially identical with regards to the chemical environment of the tertiary hydroxyl groups, and therefore neither one would be preferentially glycosylated. Utilizing a diterpene mixture would also increase the library by two-fold for every glycosylation reaction.

As fuscol (**15**) and eunicol (**16**) were only available in limited quantities, the glycosylation reaction was initially established using a model compound that was structurally related and had commercial availability. While 2-methyl-3-buten-2-ol (**55**) provided a suitable model for **15** and **16**, preliminary glycosylation attempts were also carried out with cholesterol. Tertiary hydroxyl groups are weak nucleophiles as a result of steric hindrance, and therefore the introduction of carbohydrate moieties remains a formidable challenge. Glycosylation of cholesterol, which contains a secondary hydroxyl group, would be facile and thus serve as a control to verify that the basic requirements for the reaction have been met; e.g. confirming that the reaction solvent was adequately dry and ensuring proper activation of the glycosyl donor by the Lewis acid.

3.2.2 Establishing a glycosylation method using a model system

A review of the glycosylation literature indicated the scope and versatility of the method reported by Schmidt,[143] which involves mild activation of glycosyl trichloroacetimidates by catalytic amounts of $BF_3 \bullet Et_2O$.[136, 144] Glycosylation reactions were initially carried out with cholesterol using 2,3,4,6-tetra-O-acetyl-α-D-galactopyranosyl trichloroacetimidate (**56**) as a glycosyl donor (**Figure 3.2**). After verifying the formation of the desired cholesteryl glycoside (**57**, **Figure 3.3**), the reaction was attempted with 2-methyl-3-buten-2-ol (**55**) but failed as this tertiary alcohol had degraded. Fuscol (**15**) and eunicol (**16**) also decomposed rapidly under these conditions. The $BF_3 \bullet Et_2O$, an oxophilic reagent, presumably cause an elimination by facilitating the formation of the tertiary π-allylic carbocation, an intermediate that is stabilized by resonance and may undergo elimination. Further attempts to glycosylate cholesterol or **55** using other glycosylation methodologies developed by Nicoloau[264] and Kahne[265] were also unsuccessful. For these reactions, the acetylated thioglycoside (**58**)[266] and phenylthiosulfoxide (**59**, **Figure 3.2**)[267] donors were too unreactive to be activated under mild conditions, owing to the disarming nature of the acetate protecting groups.

Further glycosylation efforts focused on the synthetic methodology of Koenigs and Knorr.[131b] This glycosylation may occur under neutral or basic reaction conditions, circumventing the need for acidic activating reagents.[268] Glycosyl bromides, the most common type of glycosyl donor in Koenigs-Knorr glycosylations, are frequently protected with ester functionalities, which provide more hydrolytic stability than "arming" protecting groups, such as acetonides and benzyl ethers.[128-129] Ester functionalities also undergo neighbouring group participation during the formation of an

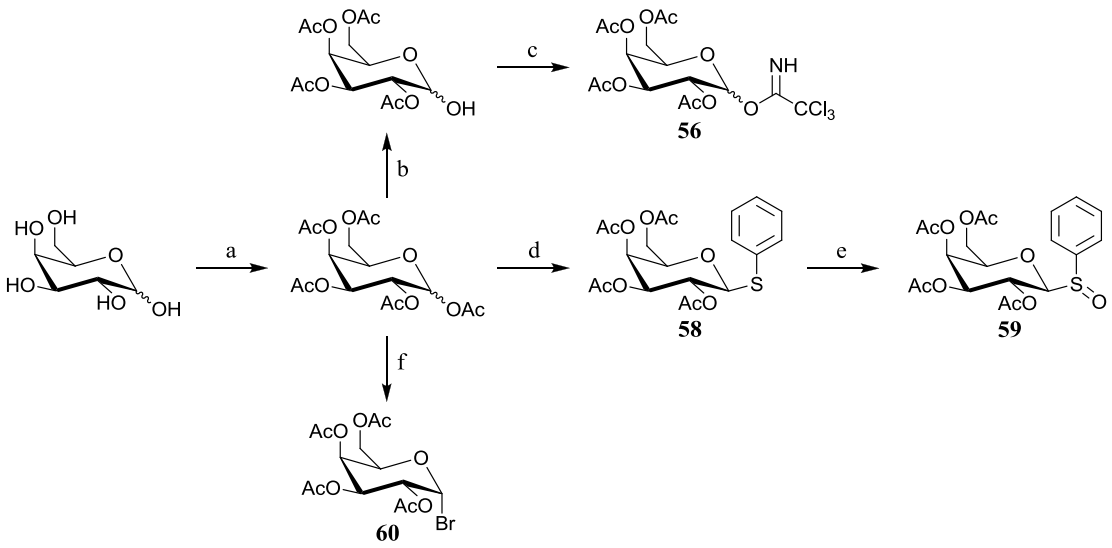

Figure 3.2. Preparation of various glycosyl donors for the preliminary glycosylation reactions. Reagents and conditions: (a) Ac_2O (18 eq), pyridine, 92%. (b) $N_2H_4 \bullet CH_3CO_2H$ (0.8 eq), DMF, -20 °C, 28%. (c) Cl_3CCN (10 eq), DBU (0.03 eq), 1,2-dichloroethane, 66%. (d) PhSH (1.6 eq), $BF_3 \bullet Et_2O$, 43% over two steps. (e) mCPBA (1.5 eq), CH_2Cl_2, 87%. (f) AcBr (3.0 eq), CH_3OH (3.3 eq), AcOH, 38% over two steps.

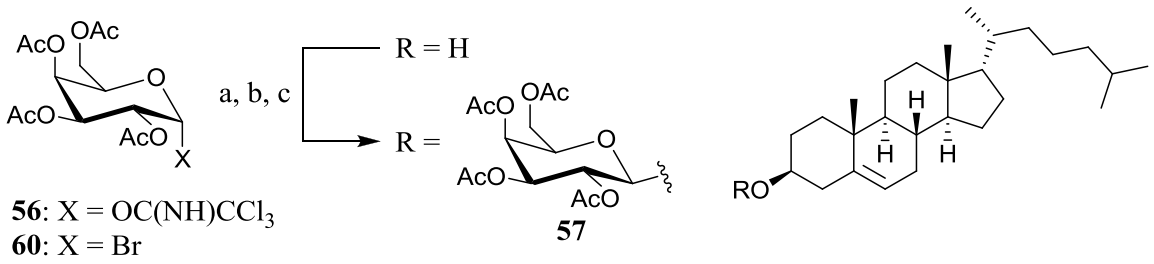

56: X = $OC(NH)CCl_3$
60: X = Br

57

Figure 3.3. Synthesis of cholesteryl glycoside (**57**) during preliminary experimentation with glycosylation methods. Reagents and conditions: (a) **56** (2.1 eq), BF_3•Et_2O, CH_2Cl_2, 40%. (b) **60** (2.1 eq), AgOTf (0.5 eq), Ag_2CO_3 (2.1 eq), CH_2Cl_2, 31%. (c) **60** (2.0 eq), Bu_4NBr (1.0 eq), DIEA (3.0 eq), DMF, 18%.

.

oxocarbenium ion, and thus provide 1',2'-trans glycosidic linkages.[125] Although this approach would fail to provide the 1',2'-cis glycoside bond of fuscoside B (**11**), only mild conditions are required for removing ester protecting groups. Acetonides and benzyl ethers were not utilized because the conditions required for their deprotection (acid hydrolysis and hydrogenolysis, respectively) would not be compatible with the desired fuscoside analogues.

2,3,4,6-Tetra-O-acetyl-α-D-galactopyranosyl bromide (**60**) was freshly prepared according to known methods (**Figure 3.2**).[269] After successfully glycosylating cholesterol (**Figure 3.3**), the method was attempted with 2-methyl-3-buten-2-ol (**55**). This glycosylation, which employed a combination of AgOTf and Ag_2CO_3 as activating agents, furnished the desired glycoside (**61**, **Figure 3.4**), which was purified by normal phase MPLC. Increasing the reaction time led to an increase in the glycosylation yield (**Table 3.1**). In an effort to further improve reaction yields, pivaloylated (**62**) and benzoylated (**63**) glycosyl donors were also prepared for these model reactions (**Figure 3.5**). A slight improvement was observed for **62**, while **63** was far superior, providing glycosylation yields that were comparable to the literature for tertiary alcohols (**Table 3.1**).[139, 141] Deprotection of **65** was later achieved by treatment with K_2CO_3/CH_3OH to afford glycoside **66**, showing that the glycosidic linkage withstood these reaction conditions.

3.2.3 Analysis of the outcome of the Koenigs-Knorr glycosylation

The protecting groups of a glycosyl donor are known to have an impact on the reactivity of the donor and overall glycosylation yields.[130, 270] With regards to the glycosylation of **55**, the steric bulkiness of the protecting groups was expected to be

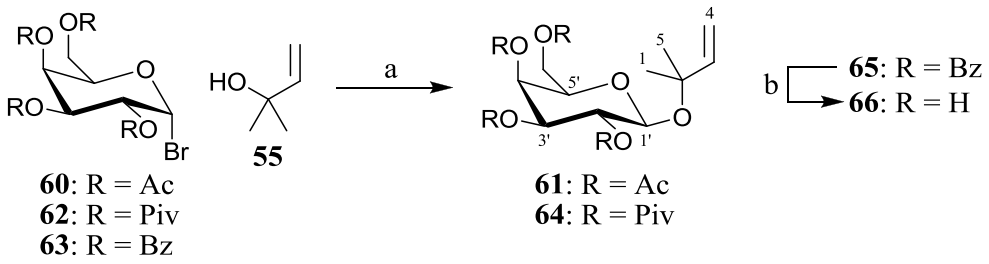

60: R = Ac
62: R = Piv
63: R = Bz

61: R = Ac
64: R = Piv

Figure 3.4. Glycosylation of 2-methyl-3-buten-2-ol (**55**) with differentially protected glycosyl bromides. Reagents and conditions: (a) **55** (1.0 eq), AgOTf (0.4 eq), Ag_2CO_3 (4.0 eq), CH_2Cl_2. (b) K_2CO_3, CH_3OH.

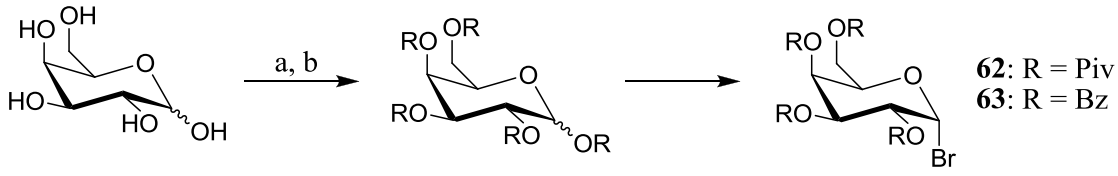

Figure 3.5. Synthesis of pivaloylated (**62**) and benzoylated (**63**) glycosyl bromides for the Koenigs-Knorr glycosylation. Reagents and conditions: (a) (i) PivCl, pyridine. (ii) AcBr (3.0 eq), CH_3OH (3.3 eq), 26% over two steps. (b) (i) BzCl, pyridine. (ii) AcBr (3.0 eq), CH_3OH (3.3 eq), 36% over two steps.

Table 3.1. Reaction conditions employed during the glycosylation of 2-methyl-3-buten-2-ol (**55**) with differentially protected glycosyl bromides.

Entry	**55** (eq)	Glycosyl bromide (eq)	Reaction time (Days)	Yield (%)
1	1.0	**60** (4.0)	0.6	(**61**) 15
2	1.0	**60** (4.1)	3.5	(**61**) 26
3	1.0	**62** (4.0)	0.6	(**64**) 36
4	1.0	**62** (4.0)	3.5	(**64**) 46
5	1.0	**63** (2.8)	1.6	(**65**) 57
6	1.0	**63** (4.2)	3.1	(**65**) 63
7	1.0	**63** (3.9)	3.5	(**65**) 67

significant. Glycosyl donors with pivaloate esters typically lower overall glycosylation yields relative to donors containing acetates.[271] Contrary to these expectations, glycosyl donor **62** provided higher glycosylation yields than **60**. Increasing the rate of glycosyl donor activation through neighbouring group participation may outweigh steric effects and have important consequences on the glycosylation yield.[272]

Greater stabilization of the acyloxonium intermediate may be achieved with the pivaloate groups via the inductive effect, thus resulting in the higher yields obtained with **62** compared to **60**. Consistent with this trend, the highest glycosylation yields were achieved with benzoylated glycosyl donor **63**, presumably due to resonance stabilization (**Figure 3.6**). The acyloxonium carbocation (**67**) may undergo delocalization across the phenyl group of the benzoate ester and further increase the rate of donor activation. Although further investigation is required to support this finding, Garegg et al. have observed a similar trend with this set of protecting groups using thioglycoside donors.[273]

3.2.4 Degradation of aglycones and deactivation of glycosyl donors: Proposed reaction mechanisms

Glycosylation yields were adversely affected by rearrangement of the glycosyl acceptor (**55**). Isolation of prenyl 2,3,4,6-tetra-O-benzoyl-β-D-galactopyranoside (**68**) and prenyl-β-D-galactopyranoside (**69**) from the glycosylation and deprotection crude products, respectively, revealed that 2-methyl-3-buten-2-ol (**55**) underwent an acid-catalyzed rearrangement to form prenyl alcohol prior to glycosylation (**Figure 3.7**). This finding supported the proposed mechanism for fuscol (**15**) and eunicol (**16**) degradation under acidic reaction conditions. Furthermore, an acid-catalyzed anomerization of **65** to

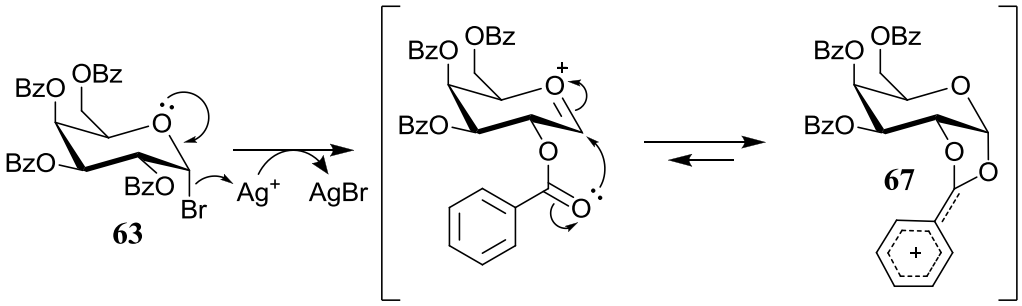

Figure 3.6. Mechanism of acyloxonium formation by neighbouring group participation and proposed resonance stabilization for benzoylated glycosyl donor **63**.

provide **70** must have occurred as an additional glycoside (**71**), featuring the thermodynamically favored α-glycosidic linkage, was isolated from the deprotection crude product (**Figure 3.7**).

Deactivation of the glycosyl donor, by way of various side reactions, also suppressed glycosylation yields. For instance, formation of a peracylated carbohydrate (**72**) had occurred. This observation indicated that hydrolysis of the anomeric bromide installed an equatorial hydroxyl group, which subsequently underwent a transesterification to furnish the anomeric pivaloate ester in the observed 1',2'-trans configuration (Mechanism A, **Figure 3.8**). The stereochemical configurations were established on the basis of coupling constants in the ^{1}H NMR spectrum and also by NOESY correlations. Transesterification, especially of the glycosyl acceptor, is common for this type of glycosylation.[274] In fact, preliminary work with cholesterol as a glycosyl acceptor showed that the aglycone underwent transesterification, which explained the presence of cholesteryl acetate in these reactions.

Isolation of the pivaloylated carbohydrate **73** suggested an alternative route to glycosyl donor inactivation. It was postulated that the origin of **73** may be the result of C-2' ester transfer to the anomeric position during neighbouring group participation,[275] a mechanism involving a molecule of water. This mechanism would furnish **73** with the observed 1',2'-cis configuration, by virtue of the axial orientation adopted by the acyloxonium ion intermediate at the anomeric position (Mechanism B, **Figure 3.8**). The 1',2'-cis configuration may also be conceived by anomerization of a 1',2'-trans intermediate, the same manner in which the α-glycoside **70** was formed. However, the

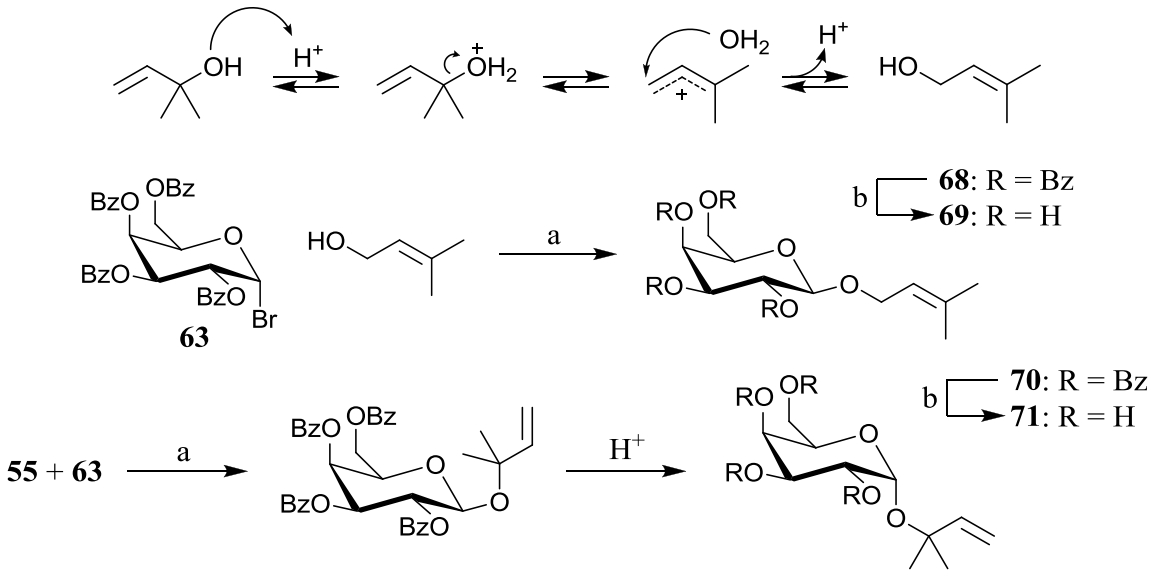

Figure 3.7. Mechanisms of prenyl 2,3,4,6-tetra-O-benzoyl-β-D-galactopyranoside (**68**) and 2-methyl-3-buten-2-yl-α-D-galactopyranoside (**71**) formation. The 2-methyl-3-buten-2-ol (**55**) underwent rearrangement to provide prenyl alcohol, which was subsequently glycosylated with the benzoylated glycosyl donor (**63**). Reagents and conditions: (a) AgOTf (0.4 eq), Ag_2CO_3 (4.0 eq), CH_2Cl_2. (b) K_2CO_3, CH_3OH.

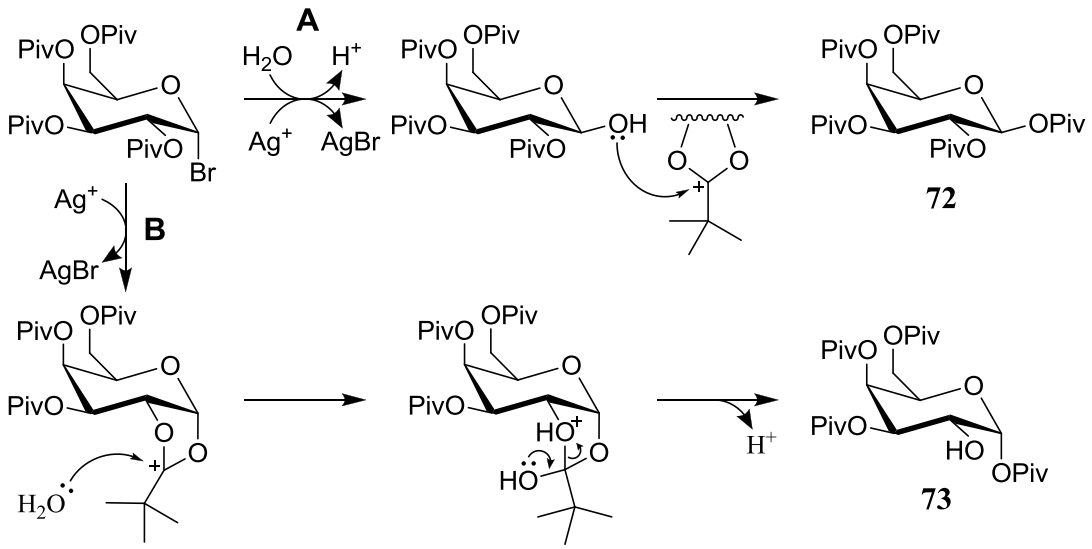

Figure 3.8. Plausible mechanisms for the formation of deactivated pivaloylated carbohydrates **72** and **73** as side products (obtained from reaction entries 3 and 4 in **Table 3.1**).[276]

1',2'-trans intermediate was not found in significant amounts in the crude product, suggesting that anomerization did not significantly contribute to the formation of **73**.

Considering that Ag_2CO_3 assumes an acid scavenging role, residual amounts of water may form spontaneously by carbonic acid decomposition. As a result, an alternative acid scavenger could be explored for future glycosylations. The decomposition of 2-methyl-3-buten-2-ol (**55**), as described earlier (**Figure 3.7**), may also produce water in situ.

3.2.5 Towards the glycosylation of fuscol and eunicol

Extending this Koenigs-Knorr method to glycosylate fuscol (**15**) and eunicol (**16**) was initially unsuccessful as it resulted in rapid degradation of the natural products. Isolation of fuscene B (**48**) and eunicene B (**46**) from the glycosylation crude product indicated that elimination had occurred, further demonstrating the inadequacy of Ag_2CO_3 as an acid scavenger. Although **15** and **16** continued to degrade in the presence of an excess of tetramethylurea, use of the stronger base DIEA proved successful as benzoylated glycosides **74** (**Figure 3.9**) and **75** (**Figure 3.10**) were synthesized. During this preliminary work, a milder glycosylation approach was also attempted, entailing the activation of glycosyl bromide with Bu_4NBr, a phase-transfer catalyst. Although cholesterol was successfully glycosylated using this approach (**Figure 3.3**), the method failed for the model tertiary alcohol (**55**).

The glycosylation crude product, containing the benzoylated glycosides **74** and **75**, was subsequently treated with K_2CO_3/CH_3OH to provide fusco-β-D-galactopyranoside (**76**) and eunico-β-D-galactopyranoside (**77**). Deprotecting the crude

product without purifying the benzoylated intermediates was advantageous as it simplified the product composition by effectively removing all carbohydrate side products. Glycoside products lacking the C-2' ester protecting group have also been documented as side products of a Koenigs-Knorr glycosylation.[277] Therefore, removing all protecting groups would simplify the HPLC purification of the desired glycosides. Therefore, the fuscoside B anomer (**78**) and eunico-β-D-arabinopyranoside (**79**) were synthesized by glycosylating fuscol (**15**) and eunicol (**16**) with the arabinopyranosyl donor (**80**, **Figure C.1**), followed by immediate deprotection of the glycosylation crude product. Unfortunately, attempts to glycosylate the diterpenes with glucosyl (**81**, **Figure C.1**) and mannosyl (**82**, **Figure C.1**) bromides were unsuccessful.

All glycosides (**74**-**79**) were purified by semi-preparative RP-HPLC and characterized by NMR spectroscopy. The glycosidic linkage was indicated by the presence of a $^{3}J_{CH}$ correlation between H-1' and C-15 on the HMBC spectrum, while the anticipated 1',2'-trans configuration was verified by analyzing vicinal ^{1}H-^{1}H coupling constants. In addition, the NOESY spectrum exhibited correlations between H-1' and the axially oriented H-3'/H-5' for all glycosides. All ^{1}H and ^{13}C assignments of the aglycones were consistent with fuscol (**15**) and eunicol (**16**).

3.2.6 Is a carbohydrate necessary? A rationale for synthesizing fuscoside mimics

Considering that fuscoside B (**11**) and its aglycone (**15**) are known to inhibit 5-LO activity in vitro,[77] it was proposed that glycoside mimics of **11** may also exhibit similar anti-inflammatory activities. Glycoside mimics with hydrophilic substituents at the carbohydrate position were prepared, bearing in mind that the overall polarity and water

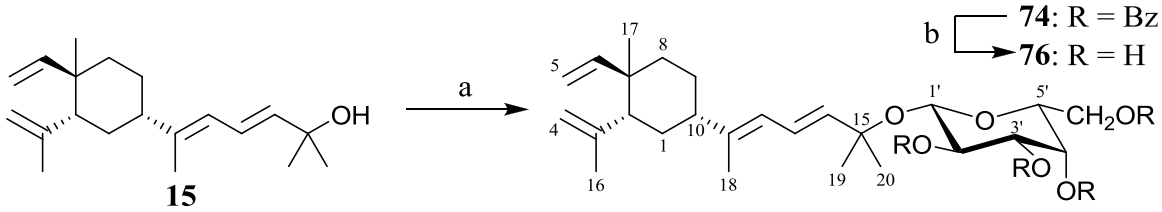

Figure 3.9. Synthesis of fusco-β-D-galactopyranoside (**76**) by glycosylation of fuscol and deprotection of benzoate esters. Reagents and conditions: (a) **15/16** (1.0 eq), AgOTf (0.4 eq), Ag_2CO_3 (4.0 eq), **63** (4.0 eq), DIEA (4.0 eq), CH_2Cl_2, 15%. (b) K_2CO_3, CH_3OH, 9% over two steps.

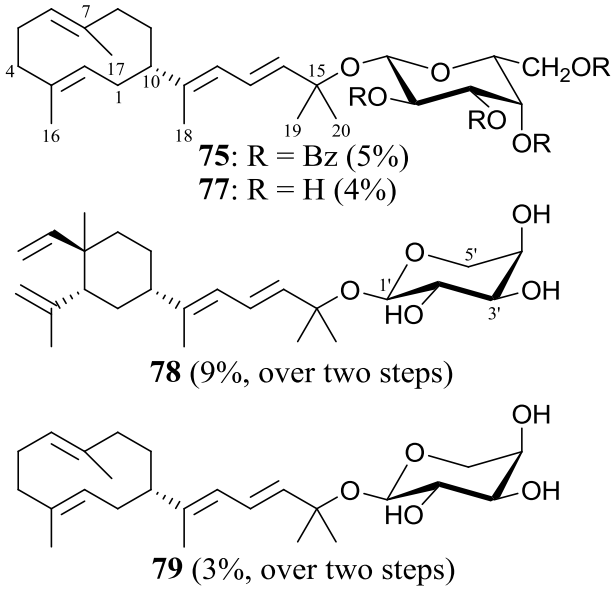

Figure 3.10. Collection of novel galactoside and arabinoside analogues of fuscoside B, including the eunicosides (reaction yields shown in parenthesis).

solubility of these mimics may be comparable to the glycosides. Moreover, the synthesis of these analogs was anticipated to be relatively straightforward, unlike the glycosylation chemistry.

Tri- and tetra-ethylene glycol (EG_3 and EG_4, respectively) were chosen as substitutes of the carbohydrate moiety as they are both hydrophilic and have molecular weights comparable to arabinose and galactose moieties. Considering the acid lability of the tertiary hydroxyl group, an S_N1 reaction was envisioned for preparing the glycoside mimics. The mimics were therefore synthesized by dissolving the diterpene mixture in either EG_3 or EG_4 and then adding $BF_3 \bullet Et_2O$ to initiate the solvolysis reaction (**Figure 3.11**). Indeed, this process was very simple and the reaction proceeded rapidly, as judged by thin layer chromatography (TLC) analysis, providing glycoside mimics **80**-**83**. While this transformation could also be effected by acetic acid or Amberlyst®, $BF_3 \bullet Et_2O$ provided the highest yields. Methyl ethers **53** and **54**, which were described previously (Section 2.2.7), were similarly prepared using CH_3OH as the reaction solvent.

After synthesizing glycoside mimics **80**-**83**, it was anticipated that the glycosylation of **15** and **16** could be achieved following a similar mechanism; the anomeric hydroxyl group could behave as an "aglycone acceptor" by undergoing a nucleophilic attack at the tertiary carbocation as the solvent did in the preceding reactions (**Figure 3.12**). This proposed glycosylation was attempted after synthesizing 2,3,4,6-tetra-O-benzoyl-β-D-galactopyranose (**84**) by Ag_2CO_3-assisted hydrolysis of the corresponding glycosyl bromide (Section 3.2.8). This initial glycosylation attempt was

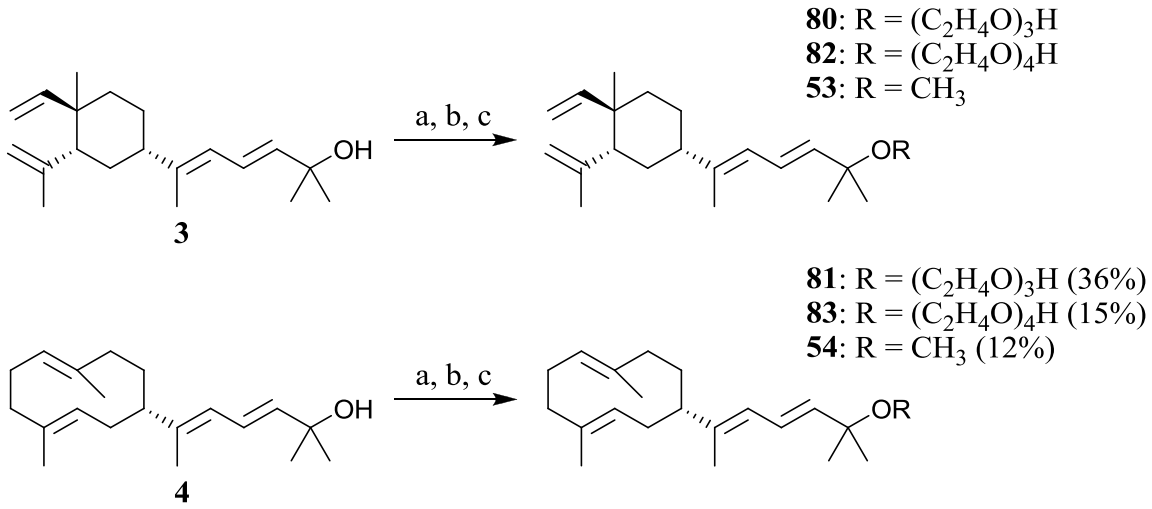

Figure 3.11. Synthesis of fuscoside mimics and methyl ether analogues of fuscol and eunicol [reaction yields for eunicoside analogues shown in parenthesis]. Reagents and conditions: (a) BF_3•Et_2O, THF:$HO(C_2H_4O)_3H$ (1:1), 60% (**80**). (b) BF_3•Et_2O, THF:$HO(C_2H_4O)_4H$ (1:1), 36% (**82**). (c) BF_3•Et_2O, CH_3OH, 54% (**53**).

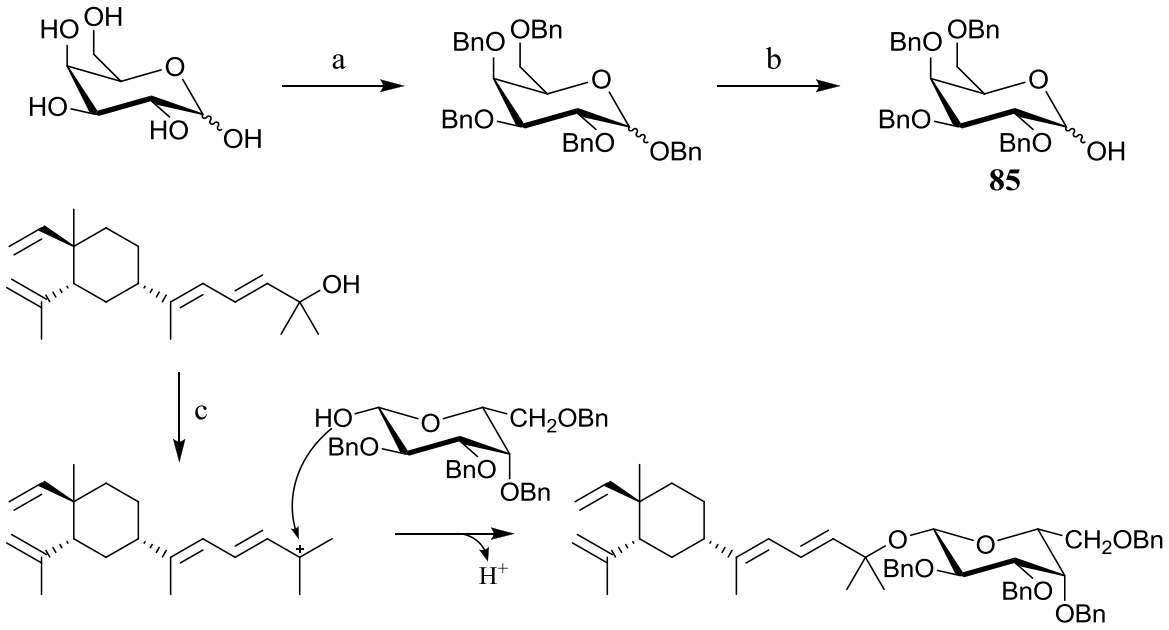

Figure 3.12. Synthesis of benzylated galactopyranose **85** and proposed mechanism for glycosylation using the aglycone acceptor method. Reagents and conditions: (a) (a) BnBr (7.3 eq), NaH (7.3 eq), DMF. (b) HOAc:1M H_2SO_4 (7:1), Δ, 25%. (c) **85**, BF_3•Et_2O, CH_2Cl_2.

unsuccessful, presumably as a result of the disarming effect of the benzoate esters on the anomeric hydroxyl group. As a result, 2,3,4,6-tetra-O-benzyl-β-D-galactopyranose (**85**, **Figure 3.12**) was synthesized and the reaction was repeated. Once again, no glycoside formation was observed. It is possible that the diterpenes must have an appropriate activating group, such as a bromide or trichloroacetimidate, to facilitate this reaction. It may be worthwhile pursuing this glycosylation ideology, coined as the aglycone acceptor method, as it could represent a powerful new approach for introducing carbohydrate functionalities to **15**, **16**, and other aglycones.

3.2.7 Assessment of anti-inflammatory activity of novel fuscoside B analogues

The new fuscosides (**76** and **78**), glycoside mimics (**80**-**83**) and methyl ethers (**53**-**54**) were assayed for in vivo anti-inflammatory activity using the PMA-induced mouse ear edema assay. Indomethacin, a known anti-inflammatory agent, was administered as an industry benchmark. As fuscoside B (**11**) was not available as a positive control, fuscol (**15**) was utilized for comparing anti-inflammatory activities. The results of this assay showed that all unnatural glycosides and glycoside mimics were either inactive or pro-inflammatory (**Table 3.2**). The unnatural anomer of **11**, fusco-α-D-arabinopyranoside (**78**), had no effect on PMA-induced swelling, while fusco-β-D-galactopyranoside (**76**) was pro-inflammatory. All glycoside mimics of fuscol (**80** and **82**) and of eunicol (**81** and **83**) were either inactive or pro-inflammatory. The tertiary hydroxyl group of fuscol (**15**) appeared to be required for activity as the methyl ethers (**53**-**54**) were also pro-inflammatory.

Although this library of glycosides and glycoside mimics was limited in size, a preliminary analysis of SAR suggested that the 1',2'-cis configuration of the arabinose moiety may be important for the in vivo anti-inflammatory activity because the anomer of fuscoside B (**78**) was inactive. However, fuscoside B (**11**) itself was not available in the coral extract for direct comparison. The glycosylation methodology also could not provide **11** as it was restricted to 1',2'-trans glycoside analogues. Nonetheless, the carbohydrate moiety appeared to modulate the anti-inflammatory efficacy, especially considering the pro-inflammatory activity of the galactoside (**76**), which nearly doubled the PMS-induced swelling compared to the vehicle control group. In addition, the hydrophilic EG-based substituents were not suitable replacements of the arabinose moiety, on the basis of the pro-inflammatory activity of the glycoside mimics (**80**-**82**).

The mouse ear edema assay does not provide a direct indication of 5-LO inhibitory activity. Although an in vitro 5-LO assay was attempted using a commercially available assay kit and 5-LO enzyme,[278] the method was unsuccessful for the fuscoside library and fuscol (**15**). Unfortunately, only the oxygenase function of 5-LO could be assessed as the assay was limited to the detection of 5(S)-hydroperoxyeicosatetraenoic acid (5-HPETE). Fuscoside B (**11**), however, is known to be a more potent inhibitor of the dehydrase function of 5-LO,[77] which may lead to an accumulation of 5-HPETE, hence the negative results. In addition, the commercially available 5-LO was non-mammalian and may not be relevant for assessing the activity of **11** and other types of non-redox inhibitors. Future efforts may instead focus on other methods for determining 5-LO inhibition, such as RP-HPLC analysis of leukotriene biosynthesis in human leukocytes.

Table 3.2. The effect of fuscoside B analogues on PMA-induced mouse ear edema.

compound	dosage (mg/ear)	relative ear edema (%)[a,b]
Indomethacin	3.0	60.0 ± 8.8[c]
Fuscol (**15**)	0.1	54.5 ± 6.3[c]
Fuscol methyl ether (**53**)	0.1	196.4 ± 21.8[c]
Fuscol-EG_3 (**80**)	0.1	218.2 ± 6.3[c]
Fuscol-EG_4 (**82**)	0.1	225.5 ± 13.1[c]
Fusco-β-D-galactoside (**76**)	0.1	192.7 ± 25.5[c]
Fusco-α-D-arabinoside (**78**)	0.1	112.7 ± 3.6
Eunicol methyl ether (**54**)	0.1	138.2 ± 9.6[c]
Eunicol-EG_3 (**81**)	0.1	138.2 ± 13.1[c]
Eunicol-EG_4 (**83**)	0.1	116.4 ± 13.1
2-Methyl-3-buten-2-yl-β-D-galactoside (**66**)	0.1	134.5 ± 3.6[c]

[a] Data is presented as the mean ± SEM. [b] Percent ear edema is relative to the vehicle control group (0.092 mm). [c] Compared to the vehicle control group there was a statistically significant difference [unpaired Student's t-test ($p < 0.05$)]. Data for the vehicle and indomethacin control groups were obtained from six replicates (n = 6). All other samples were assessed in triplicate (n = 3).

3.2.8 Preparation of truncated pseudopterosin mimics using glycosylation chemistry

Originally isolated from Pseudopterogorgia elisabethae by Look et al., the pseudopterosins are a family of diterpene glycosides with potent anti-inflammatory and antimicrobial activities.[279] These compounds possess the amphilectane skeleton and differ from one another according to the type and location of the attached carbohydrate moiety or the stereochemical configuration of the aglycone.[280] A mimic of the pseudopterosin aglycone was recently synthesized by Dr. Malcolm McCulloch through the addition of prenyl groups to 2,6-dimethoxyphenol (**86**), a commercially available substance.[161] The 3,4-diprenyl-2,6-dimethoxyphenol (**87**) showed moderate antimicrobial activity against methicillin-resistant Staphylococcus aureus (MRSA), vancomycin-resistant Enterococcus (VRE), and other Gram-positive organisms. The observed activity for **87** suggested that this compound may be a truncated analogue of the pseudopterosin aglycone as it contains similar structural features. A glycosylation of **87** was therefore proposed to generate pseudopterosin mimics with the aim of improving the antimicrobial and cytotoxicity profiles of these synthetic analogues.

Introducing carbohydrate moieties to phenolic hydroxyl groups may be a challenging task, owing to the electron-withdrawing nature of the aromatic ring.[281] A review of the literature on phenol glycosylation showed the prevalance of the Schmidt method using glycosyl trichloroacetimidates.[282] Although the preparation of these donors is more tedious, they often generate higher glycosylation yields.[283] To synthesize the glycosyl trichloroacetimidate, 2,3,4,6-tetra-O-benzoyl-β-D-galactopyranose (**84**) was first prepared by Ag_2CO_3-assisted hydrolysis of the corresponding glycosyl bromide (**63**, **Figure 3.13**). The anomeric trichloroacetimidate was then installed by nucleophilic

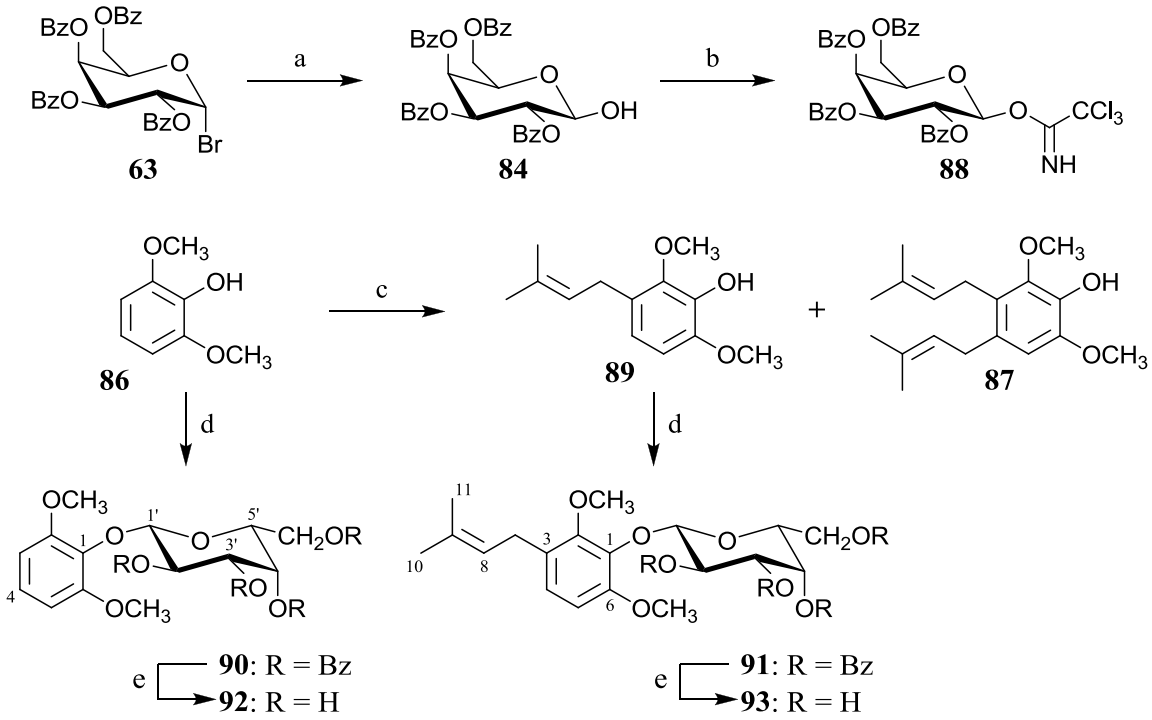

Figure 3.13. Synthesis of glycosyl trichloroacetimidate **88** for the Schmidt glycosylation of 2,6-dimethoxyphenol (**86**) and 3-prenyl-2,6-dimethoxyphenol (**89**).[284] Reagents and conditions: (a) Ag_2CO_3 (1.5 eq), acetone:H_2O (19:1), 85%. (b) Cl_3CCN (10 eq), K_2CO_3 (1.2 eq), CH_2Cl_2, 36%. (c) 2-methyl-3-buten-2-ol (1.9 eq), TsOH (cat.), Δ CH_2Cl_2/CH_3OH (3:1), 27% (**89**) and 8% (**87**). (d) **88** (1.2 eq), $BF_3{\cdot}Et_2O$, CH_2Cl_2, -78 °C, 71% (**90**) and 93% (**91**). (c) K_2CO_3, CH_3OH:TBME (5:1) , 72% (**92**) and 75% (**93**).

addition of **84** to Cl_3CCN in the presence of K_2CO_3 (**88**). The phenol glycosylation was initially carried out with 2,6-dimethoxyphenol (**86**) prior to any attempt on 3-prenyl-2,6-dimethoxyphenol (**89**) and 3,4-diprenyl-2,6-dimethoxyphenol (**87**), which were in short supply.[284] Excellent glycosylation yields were obtained during the synthesis of glycosides **90** and **91**, however, attempts to glycosylate **87** were unsuccessful (**Figure 3.13**). The benzoate esters were then removed by treatment with K_2CO_3 and CH_3OH to provide deprotected glycosides **92** and **93**.

Glycoside **93** was evaluated for antimicrobial activity against a variety of clinically relevant microorganisms using the microbroth dilution assay (**Table 3.3**). Unfortunately, the glycoside showed no improvement in the antimicrobial activity compared to 3-prenyl-2,6-dimethoxyphenol (**89**), as indicated by the loss of activity against Mycobacterium smegmatis and M. diernhoferi. Glycoside **93** also exhibited greater toxicity than 3,4-diprenyl-2,6-dimethoxyphenol (**87**) and **89** in the Vero cell cytotoxicity assay. Compared to **89** and **93**, the promising activity observed for **87** indicated that the additional prenyl group at the C-4 position may be important for antimicrobial activity. Further attempts to glycosylate **87** were not successful. The limited SAR data from this study suggested that the addition of a phenolic carbohydrate moiety may not improve the antimicrobial activity nor reduce the cytotoxicity. It is possible that the synthetic mimics may exert their antimicrobial activity through a mechanism of action that is distinct from the pseudopterosins. Nonetheless, the glycosylation methodology using the benzoylated glycosyl donor (**63**) was effective and may find applications in the synthesis of novel pseudopterosin analogues or other phenolic glycosides of biological significance.

Table 3.3. Antimicrobial susceptibility testing of the truncated pseudopterosin mimic using the microbroth dilution method (n = 3).[284]

	IC_{50} (μg/mL)		MIC (μg/mL)			IC_{50} (μg/mL)
Compound	MRSA[a]	VRE[a]	M. smegmatis	M. diernhoferi	M. tuberculosis $H_{37}Rv$	Vero cell
30	2.6	2.9	2	4	**-**	**-**
87[b]	>128	>128	128	64	>128	45
89[b]	20	3.5	8	8	59	64
93	>128	>128	>128	>128	>128	82
Vancomycin	1.2	-	-	-	-	-
Rifampin	-	0.9	4	4	0.04	-
Isoniazid	-	-	1	0.25	0.03	-

[a] Assay was completed by Martine Lanteigne. [b] Compound was synthesized and tested for antimicrobial activity by Dr. Malcolm McCulloch.

3.3 Conclusion

A modification of the Koenigs-Knorr method has enabled the glycosylation of fuscol (**15**) and eunicol (**16**), providing a collection of novel fuscoside B analogues. This glycosylation method was initially established with 2-methyl-3-buten-2-ol (**55**), a model glycosyl acceptor, using differentially protected glycosyl bromides. The glycosylation yields provided by these glycosyl donors correlated with apparent acyloxonium stability. Glycosyl bromides protected with benzoate esters provided higher yields compared to acetylated and pivaloylated variants. The glycosylation method was later adapted for the purpose of glycosylating **15** and **16** by employing DIEA as the primary acid scavenger. The acid lability of the diterpenes, although a significant hurdle in the glycosylation, was later exploited for synthesizing glycoside mimics by introducing EG_3 and EG_4 as substitutes of the arabinose moiety. Attempts to exploit this S_N1 mechanism for introducing a carbohydrate moiety, a potential glycosylation approach that was coined as the aglycone acceptor method, were unsuccessful.

The fuscoside library was evaluated for anti-inflammatory activity using the mouse ear edema assay, which showed the remarkable influence of the carbohydrate substituent on the in vivo efficacy of this glycoside class. For instance, the anomer of fuscoside B had no anti-inflammatory activity as it was unable to mount a significant reduction in PMA-induced swelling. This result suggested that the configuration of the glycosidic linkage may be important for the anti-inflammatory activity. Replacing the arabinose moiety with galactose or EG-based moieties also failed to emulate the anti-inflammatory activity of fuscoside B (**11**). The unsatisfactory performance of this

compound collection in the mouse ear edema assay was unforeseen, bearing in mind the near equivalent in vitro activities of **11** and fuscol (**15**). The activity of **15**, compared to its methyl ether (**53**), reiterated the significance of the tertiary hydroxyl group, as alluded to earlier in Chapter 2 (Section 2.2.8). Regardless, the natural products exhibited anti-inflammatory activity while all synthetic analogues were inactive.

The most significant achievement of this research was the glycosylation of fuscol (**15**), a striking omission of previous synthetic efforts. The glycosylation of eunicol (**16**) has also provided the eunicosides, a novel structural class of diterpene glycosides. The inability to install 1',2'-cis glycosidic linkages was a limitation of this glycosylation methodology, in addition to the low reaction yields that were obtained. A more precise examination of the anomeric configuration and its importance was therefore prohibited. Future glycosylation efforts should focus on applying this methodology to glycosyl donors functionalized with non-participating protecting groups. Although these donors will provide 1',2'-cis glycoside analogues, base-sensitive protecting groups should be employed as the fuscoside may not tolerate acidic conditions. Semisynthesis of fuscoside B (**11**) by introducing a 1',2'-cis D-arabinose moiety may provide a rapid route to this natural product. Unequivocal determination of the absolute configuration of **11** may also be possible by establishing this synthetic method.

3.4 Experimental

General experimental methods as well as procedures for the mouse ear edema assay and the microbroth dilution assay are described in Appendix B. Also see Appendix B for a description of the "standard work up procedure".

3.4.1 Preparation of glycosyl donors for glycosylation chemistry

2,3,4,6-tetra-O-acetyl-α/β-D-galactopyranosyl trichloroacetimidate (56). To a mixture of D-galactose (210 mg, 1.17 mmol) in pyridine (4 mL) was added Ac_2O (2.0 mL, 21 mmol). After stirring overnight at room temperature, partially acetylated carbohydrate was observed by TLC analysis (EtOAc), and thus additional Ac_2O (2.0 mL, 21 mmol) was transferred to the mixture. The reaction was stirred for 4 h and then diluted with EtOAc. After partitioning the mixture between sat. $NaHCO_{3(aq)}$ and DI H_2O, the EtOAc phase was recovered and subjected to the standard work up procedure, yielding 1,2,3,4,6-penta-O-acetyl-α/β-D-galactopyranose (418 mg, 1.07 mmol, 92%) as a colorless oil. APCIMS: m/z 331.1 $[M + H - CH_3CO_2H]^+$. The glycosyl trichloroacetimidate (**56**) was then synthesized according to an established method.[285] Without further purification, the peracetylated carbohydrate was dissolved in DMF (10 mL) and cooled to -20 °C prior to the addition of $N_2H_4 \bullet CH_3CO_2H$ (61.6 mg, 0.669 mmol). The reaction was held at -20 °C with stirring and additional $N_2H_4 \bullet CH_3CO_2H$ (total of 77.7 mg, 0.844 mmol) was added as long as peracetylated carbohydrate had remained, as judged by TLC analysis (EtOAc). The reaction mixture was then diluted with EtOAc and partitioned with DI H_2O. The

organic layer was recovered, subjected to the standard work up procedure, and separated by benchtop flash chromatography (silica, hexanes → EtOAc stepwise gradient) to provide 2,3,4,6-tetra-O-acetyl-α/β-D-galactopyranose (103.9, 0.298 mmol, 28%) as a yellow oil. APCIMS: m/z 331.1 $[M + H - H_2O]^+$. The anomerically deprotected carbohydrate (66.7 mg, 0.192 mmol) was dissolved in anhydrous 1,2-dichloroethane (1 mL) and stirred with 3Å molecular sieves (~0.1 g) under an N_2 atmosphere and cooled to 0 °C. An aliquot of Cl_3CCN (195 μL, 1.95 mmol) was added, followed by DBU (1.0 μL, 6.7 μmol) approximately 20 min later. The reaction was stirred overnight at room temperature, and was later diluted with CH_2Cl_2 and filtered through Celite®. The filtrate was evaporated in vacuo to yield **56** (62.0 mg, 0.126 mmol, 66%) as a yellow amorphous solid. All ^1H and ^{13}C NMR spectroscopic data for the product were consistent with the structure of **56**. APCIMS: m/z 331.1 $[M + H - Cl_3CCONH_2]^+$.

Phenyl 2,3,4,6-tetra-O-acetyl-1-thio-β-D-thiogalactopyranoside (58). Glycosyl donor **58** was prepared according to an established literature protocol.[266] A mixture of D-galactose (1.09 g, 6.03 mmol) was stirred in Ac_2O (3 mL) before adding BF_3•Et_2O (1.5 mL). After confirming the formation of the peracetylated intermediate by TLC analysis (EtOAc), PhSH (1 mL, 9.77 mmol) and additional BF_3•Et_2O (1 mL) was added and the reaction was stirred for 4 h. At this point, TLC analysis (TBME) indicated partial thioglycoside formation. Additional BF_3•Et_2O (1 mL) was then added and the reaction was left to stir overnight at room temperature. Afterwards, the reaction mixture was diluted with EtOAc and washed successively with $NaHCO_{3(aq)}$ and DI H_2O. The EtOAc phase was subjected to the standard work up procedure and separated by RP-MPLC (C_{18},

$H_2O \rightarrow CH_3OH$) to provide **58** (1.13 g, 2.56 mmol, 43%) as a colorless oil. All ^1H and ^{13}C NMR spectroscopic data for the product were consistent with the structure of **58**. APCIMS: m/z 463.3 $[M + Na]^+$; m/z 331.2 $[M + H - PhSH]^+$.

Phenylsulfenyl 2,3,4,6-tetra-O-acetyl-β-D-galactopyranoside (59). Glycosyl donor **59** was prepared from thioglycoside **58** following a literature protocol.[267] The thioglycoside (**58**, 89.0 mg, 0.202 mmol) was dissolved in CH_2Cl_2 (5mL) and cooled to 0 °C prior to adding mCPBA (41.1 mg, 0.238 mmol). After the reaction was stirred for 4 h, unreacted **58** had remained, according to TLC analysis (hexanes:EtOAc 1:1), and therefore an additional portion of mCPBA (11.7 mg, 0.068 mmol) was added. The reaction was left to stir for 2 h and was then diluted with EtOAc and washed successively with DI H_2O. The EtOAc phase was recovered and subjected to the standard work up procedure to provide a diastereomeric mixture of sulfoxide **59** as a colorless oil (80.0 mg, 0.175 mmol, 87%). All ^1H and ^{13}C NMR spectroscopic data for the product were consistent with the structure of **59**. APCIMS: m/z 479.2 $[M + Na]^+$; m/z 331.1 $[M + H - S(OH)Ph]^+$.

2,3,4,6-tetra-O-acyl-α-D-glycopyranosyl bromide (60, 62-63, and 81-82) and 2,3,4-tri-O-benzoyl-β-D-arabinopyranosyl bromide (80). The peracylated carbohydrate intermediates and their corresponding glycosyl bromides were synthesized by an established method,[269b] combining AcBr (3.0 eq) and CH_3OH (3.3 eq) to generate HBr in situ,[269a] and purified according to the following procedure: After formation of the desired glycosyl bromide, as judged by TLC analysis (hexanes:TBME 1:1) the reaction mixture was diluted with cold EtOAc and washed successively with cold sat. $NaHCO_{3(aq)}$, until

gas evolution ceased, followed by cold sat. $NaCl_{(aq)}$. The organic extract was subjected to the standard work up procedure to provide a crude oil, which was separated by MPLC (silica, hexanes → TBME) to provide the galactosyl bromide [**60** (R = Ac): 38%, **62** (R = Piv): 26%, **63** (R = Bz): 36%], arabinosyl bromide [**80** (R = Bz): 50%, **Figure C.1**], glucosyl bromide [**81** (R = Bz): 13%, **Figure C.1**], and mannosyl bromide [**82** (R = Bz): 35%, **Figure C.1**] as white powders. All ^{1}H and ^{13}C NMR spectroscopic data for the products were consistent with the structures of **60**, **62-63**, and **80-82**. The following $[M - Br]^+$ fragment ions were observed by APCIMS: m/z 331.3 (**60**); m/z 499.3 (**62**); m/z 579.2 (**63** and **81**-**82**); m/z 446.3 (**80**).

2,3,4,6-tetra-O-benzyl-α/β-D-galactopyranose (85). A stirred mixture of D-galactose (1.133 g, 6.289 mmol) in DMF (30 mL) was cooled to 0 °C in an ice bath before slowly adding NaH (1.10 g, 45.8 mmol). After the mixture was stirred for 30 min at 0 °C, BnBr (5.50 mL, 46.2 mmol) was added, and the reaction was stirred overnight at room temperature. Partial product formation was indicated by TLC analysis (hexanes:TBME 1:1) and additional NaH (377 mg, 15.7 mmol) and BnBr (2.00 mL, 16.8 mmol) was added. Upon stirring the reaction for 8 h, the mixture was concentrated under rotary evaporation, diluted with EtOAc, and washed successively with $NaHCO_{3(aq)}$ and deionized H_2O. The organic layer was then recovered and subjected to the standard work up procedure yielding 1,2,3,4,6-penta-O-benzyl-α/β-D-galactopyranose as a crude yellow oil, which was used without further purification. APCIMS: m/z 653.4 $[M + Na]^+$; m/z 524.2 $[M + H - BnOH]^+$. The anomeric benzyl group was then hydrolyzed by refluxing in HOAc:1M H_2SO_4 (7:1, 16 mL) for 16 hours, at which point TLC analysis

(hexanes:TBME 1:1) indicated product formation. The reaction mixture was then diluted with EtOAc and washed successively with $NaHCO_{3(aq)}$ and deionized H_2O. After recovery of the EtOAc, it was subjected to the standard work up procedure and separated by MPLC (silica, hexanes → TBME) yielding **85** (857.4 mg, 1.586 mmol, 25%) as a viscous yellow oil. All ^1H and ^{13}C NMR spectroscopic data for the product were consistent with the structure of **85**. APCIMS: m/z 524.2 $[M + H - H_2O]^+$.

2,3,4,6-tetra-O-benzoyl-β-D-galactopyranose (84). The anomeric bromide was hydrolyzed according to an established method.[286] The glycosyl bromide (**63**, 3.330 g, 5.049 mmol) was dissolved in acetone:H_2O (19:1, 20 mL) and stirred with Ag_2CO_3 (2.1389 g, 7.757 mmol) under the exclusion of light. The reaction was left to stir at room temperature for 18 h, at which point TLC analysis (hexanes:TBME 1:1) indicated product formation. The mixture was then diluted with EtOAc, filtered through Celite®, and washed successively with $NaHCO_{3(aq)}$ and DI H_2O. The EtOAc phase was recovered, subjected to the standard work up procedure, and separated by MPLC (silica, hexanes → TBME) yielding **84** (2.560 g, 4.290 mmol, 85%) as a white solid. All ^1H and ^{13}C NMR spectroscopic data for the product were consistent with the structure of **84**. APCIMS: m/z 580.3 $[M + H - H_2O]^+$.

2,3,4,6-tetra-O-benzoyl-β-D-galactopyranosyl trichloroacetimidate (88). The glycosyl donor was prepared following a literature protocol.[286] The benzoylated carbohydrate (**84**, 1.893 g, 3.173 mmol) was dissolved in anhydrous CH_2Cl_2 (30 mL) and stirred with K_2CO_3 (533.7 mg, 3.862 mmol) under a N_2 atmosphere. Shortly after, Cl_3CCN (3.20 mL,

31.9 mmol) was added and the reaction was left to stir for 60 h at room temperature. During this time, the reaction was inspected periodically and additional CH_2Cl_2 was added to avoid complete evaporation of the solvent. The reaction was completed at 60 h, as judged by TLC analysis (hexanes:acetone 7:3), and was diluted with EtOAc and partitioned between DI H_2O. The organic layer was recovered and subjected to the standard work up procedure before undergoing separation by MPLC (silica, hexanes → acetone), which yielded **88** (855.5 mg, 1.155 mmol, 36%) as a white solid. All ^{1}H and ^{13}C NMR spectroscopic data for the product were consistent with the structure of **88**. APCIMS: m/z 580.2 $[M + H - Cl_3CCONH_2]^+$.

3.4.2 Model glycosylation reactions and characterization of products

Cholesteryl 2,3,4,6-tetra-O-acetyl-β-D-galactopyranoside (57). The synthesis of the cholesteryl galactoside (**57**) was accomplished with three different glycosylation methods. All ^{1}H and ^{13}C NMR spectroscopic data for the product were consistent with the structure of **57**. APCIMS: m/z 739.4 $[M + Na]^+$; m/z 331.2 $[M + H - H_2O]^+$.

Schmidt method: Cholesterol (20.5 mg, 53.0 μmol) and glycosyl trichloroacetimidate (**56**, 53.8 mg, 0.109 mmol) were dissolved in anhydrous CH_2Cl_2 (2 mL) and stirred with 3Å molecular sieves (~0.2 g) under an atmosphere N_2 atmosphere. Upon cooling the reaction to -78 °C and stirring for 20 min, BF_3•Et_2O (5 μL) was added and the mixture was stirred for 1 h. Afterwards, the reaction was quenched with Et_3N (20 μL), diluted with EtOAc, and washed successively with $NaHCO_{3(aq)}$ and DI H_2O. The organic layer was recovered,

subjected to the standard work up procedure, and separated by flash chromatography (silica, hexanes:EtOAc stepwise gradient) to provide **57** (15.2 mg, 21.2 μmol, 40%) as a colorless oil.

Phase-transfer catalysis method: Cholesterol (137 mg, 0.354 mmol) and glycosyl bromide (**60**, 291 mg, 0.707 mmol) were stirred in anhydrous DMF (10 mL) in the presence of 3Å molecular sieves (~1.0 g) under a N_2 atmosphere. After approximately 20 min, the DIEA (185 μL, 1.06 mmol) was added along with Bu_4NBr (125 mg, 0.368 mmol), and the mixture was stirred for an additional 20 min. The reaction was heated to approximately 50 °C and stirred for 8 h. TLC analysis (hexanes:EtOAc 1:1) indicated product formation, upon which the reaction mixture was diluted with EtOAc. After filtration through Celite®, the mixture was washed successively with $NaHCO_{3(aq)}$ and DI H_2O. The organic layer was recovered, subjected to the standard work up procedure, and separated by flash chromatography (silica, hexanes:TBME stepwise gradient) to provide **57** (44.7 mg, 62.3 μmol, 18%) as a white solid. Unreacted cholesterol (81.6 mg, 0.211 mmol, 60% recovery) was also recovered.

Modified Koenigs-Knorr method: A mixture of cholesterol (61.8 mg, 0.160 mmol), Ag_2CO_3 (94.6 mg, 0.343 mmol), and AgOTf (21.6 mg, 84.1 μmol) were stirred in anhydrous CH_2Cl_2 (5 mL) with 3Å molecular sieves (~0.2 g) under an N_2 atmosphere and exclusion of light. After cooling the reaction mixture to -78 °C and stirring for 20 min, a solution of glycosyl bromide (**60**, 139 mg, 0.338 mmol) in anhydrous CH_2Cl_2 (5 mL) was added. The reaction was stirred overnight at room temperature, after which the desired glycoside was observed, as judged by TLC analysis (hexanes:TBME 1:1). Subsequently, the mixture was diluted with CH_2Cl_2, filtered through Celite®, and evaporated in vacuo.

The crude product was then separated by flash chromatography (silica, hexanes: TBME stepwise gradient), yielding **57** (35.9 mg, 50.1 μmol, 31%) as a white solid.

General procedure A: Modified Koenigs-Knorr glycosylation of 2-methyl-3-buten-2-ol. The 2-methyl-3-buten-2-ol (**55**, 50 μL, 0.48 mmol) was added to a stirring mixture of AgOTf (49 mg, 0.19 mmol), Ag_2CO_3 (530 mg, 1.92 mmol), and 3Å molecular sieves (~0.5 g) in anhydrous CH_2Cl_2 (5 mL) under a N_2 atmosphere and the exclusion of light. After stirring for 15 minutes, the mixture was cooled to -78 °C followed by the dropwise addition of glycosyl bromide (1.92 mmol) dissolved in anhydrous CH_2Cl_2 (5 mL). The mixture was stirred for 3.5 days and afterward diluted with EtOAc and filtered through Celite®. After washing with $Na_2S_2O_{3(aq)}$ and DI H_2O, the organic extract was recovered and subjected to the standard work up procedure to provide the glycosylation crude product as a colorless oil.

General procedure B: Deprotection of benzoylated glycosides. The glycosylation crude product was dissolved in CH_3OH (5 mL) and stirred with K_2CO_3 (53 mg, 0.38 mmol). The reaction was stirred until TLC analysis indicated the disappearance of benzoylated starting materials. The reaction was neutralized by addition of NH_4OAc and concentrated to 0.5 mL by rotary evaporation in vacuo. This mixture was loaded onto a C_{18} plug and washed with H_2O:CH_3OH (19:1) to separate the salts from the products. Fractions containing the deprotected glycosides, as judged by LC-APCIMS analysis, were evaporated and lyophilized to provide a white amorphous solid that was further separated by RP-HPLC.

2-Methyl-3-buten-2-yl 2,3,4,6-tetra-O-acetyl-β-D-galactopyranoside (61). The aglycone **55** was glycosylated using **60** (790 mg, 1.92 mmol) according to general procedure A. The glycosylation crude was separated by MPLC (silica, hexanes → TBME) to yield the desired glycoside (**61**, 51.8 mg, 0.124 mmol, 26%). **61**: $[\alpha]^{25}_{D}$ = +8.98 (c 0.367, CH_2Cl_2); IR υ_{max} 3088, 2982, 1744, 1643, 1216, 1072, 1040 cm^{-1}. ^1H NMR (600 MHz, C_6D_6) δ 5.86 (1H, dd, J = 17.7, 10.5 Hz, H-3), 5.57 (1H, dd, J = 10.5, 8.3 Hz, H-2'), 5.41 (1H, dd, J = 3.4, 0.8 Hz, H-4'), 5.12 (1H, dd, J = 10.5, 3.4 Hz, H-3'), 5.07 (1H, dd, J = 17.7, 1.1 Hz, H-4), 4.99 (1H, dd, J = 10.5, 1.1 Hz, H-4), 4.39 (1H, d, J = 8.3 Hz, H-1'), 4.11 (1H, dd, J = 10.9, 6.8 Hz, H-6'), 4.05 (1H, dd, J = 10.9, 6.4 Hz, H-6'), 3.24 (1H, ddd, J = 6.4, 1.1 Hz, H-5'), 1.75 (3H, s), 1.73 (3H, s), 1.65 (3H, s), 1.53 (3H, s), 1.24 (3H, s, H-1), 1.18 (3H, s, H-5). ^{13}C NMR (150 MHz, C_6D_6) δ 170.2 (C), 169.8 (C), 169.5 (C), 168.6 (C), 143.7 (CH, C-3), 113.9 (CH_2, C-4), 96.9 (CH, C-1'), 78.0 (C, C-2), 71.6 (CH, C-3'), 70.6 (CH, C-5'), 69.6 (CH, C-2'), 67.5 (CH, C-4'), 61.6 (CH_2, C-6'), 27.4 (CH_3, C-5), 26.2 (CH_3, C-1), 20.5 (CH_3), 20.3 (CH_3), 20.2 (CH_3), 19.9 (CH_3). HRESIMS m/z 439.1564 $[M + Na]^+$ (calcd for $C_{19}H_{28}O_{10}Na$, 439.1575).

2-Methyl-3-buten-2-yl 2,3,4,6-tetra-O-pivaloyl-β-D-galactopyranoside (64). The aglycone **55** was glycosylated using **62** (1.11 g, 1.92 mmol) according to general procedure A. The glycosylation crude was separated by MPLC (silica, hexanes → TBME) to yield the desired glycoside (**64**, 127.4 mg, 0.218 mmol, 46%). **64**: $[\alpha]^{25}_{D}$ = +8.56 (c 0.137, CH_2Cl_2); IR υ_{max} 2975, 2936, 2909, 2874, 1737, 1139, 1073, 1037 cm^{-1}. ^1H NMR (600 MHz, C_6D_6) δ 5.93 (1H, dd, J = 17.7, 10.9 Hz, H-3), 5.56 (1H, dd, J =

10.2 Hz, 7.9, H-2'), 5.41 (1H, dd, J = 3.0, 1.1 Hz, H-4'), 5.12 (1H, dd, J = 10.5, 3.4 Hz, H-3'), 5.06 (1H, dd, J = 17.7, 1.1 Hz, H-4), 5.00 (1H, dd, J = 10.9, 1.1 Hz, H-4), 4.42 (1H, d, J = 8.0 Hz, H-1'), 4.12 (1H, dd, J = 10.9, 7.2 Hz, H-6'), 4.06 (1H, dd, J = 10.9, 6.0 Hz, H-6'), 3.25 (1H, ddd, J = 7.2, 6.4, 1.1 Hz, H-5'), 1.28 (3H, s, H-1), 1.22 (3H, s, H-5), 1.21 (9H, s, 9H), 1.17 (9H, s, 9H), 1.17 (9H, s, 9H), 1.10 (9H, s, 9H). ^{13}C NMR (150 MHz, C_6D_6) δ 177.1 (C), 177.1 (C), 177.0 (C), 176.0 (C), 143.9 (CH, C-3), 114.1 (CH_2, C-4), 96.9 (CH, C-1'), 78.0 (C, C-2), 71.8 (CH, C-3'), 70.8 (CH, C-5'), 69.5 (CH, C-2'), 67.4 (CH, C-4'), 62.0 (CH_2, C-6'), 39.0 (C), 38.9 (C), 38.8 (C), 38.7 (C), 28.0 (CH_3, C-5), 27.5 (CH_3), 27.3 (CH_3), 27.3 (CH_3), 27.1 (CH_3), 26.2 (CH_3, C-1). HRESIMS m/z 607.3426 $[M + Na]^+$ (calcd for $C_{31}H_{52}O_{10}Na$, 607.3453).

2-Methyl-3-buten-2-yl 2,3,4,6-tetra-O-benzoyl-β-D-galactopyranoside (65). The aglycone **55** was glycosylated using **63** (1.27 g, 1.92 mmol) according to general procedure A. The glycosylation crude was separated by MPLC (silica, hexanes → TBME) to yield the desired glycoside (**65**, 225 mg, 0.339 mmol, 67%). **65**: $[\alpha]^{25}_D$ = +162.4 (c 0.2833, CH_2Cl_2); IR υ_{max} 3065, 2980, 1728, 1265, 1108, 710 cm^{-1}. ^{1}H NMR (600 MHz, C_6D_6) δ 8.21 (2H, dd), 8.12 (2H, dd), 8.08 (2H, dd), 7.98 (2H, dd), 7.11 (1H, tt), 7.06 (2H, tt), 7.03 (1H, tt), 7.00 (1H, tt), 6.95 (2H, tt), 6.87 (2H, tt), 6.83 (1H, tt), 6.71 (2H, tt), 6.29 (1H, dd, J = 10.5, 8.3 Hz, H-2'), 6.09 (1H, dd, J = 3.8, 1.1 Hz, H-4'), 5.90 (1H, dd, J = 17.6, 10.8 Hz, H-3), 5.70 (1H, dd, J = 10.2, 3.4 Hz, H-3'), 5.01 (1H, dd, J = 17.6, 1.1 Hz, H-4), 4.89 (1H, dd, J = 10.8, 1.1 Hz, H-4), 4.70 (1H, d, J = 8.0 Hz, H-1'), 4.65 (1H, dd, J = 11.3, 7.5 Hz, H-6'), 4.29 (1H, dd, J = 11.3, 5.6 Hz, H-6'), 3.58 (1H, ddd, J = 5.6, 1.1 Hz, H-5'), 1.26 (3H, s, H-1), 1.14 (3H, s, H-5). ^{13}C NMR (150 MHz,

C_6D_6) δ 165.8 (C), 165.8 (C), 165.7 (C), 165.2 (C), 143.7 (CH, C-3), 133.2 (CH), 133.1 (CH), 133.1 (CH), 133.0 (CH), 130.5 (C), 130.4 (C), 130.3 (CH), 130.0 (CH), 130.0 (CH), 129.9 (CH), 129.6 (C), 129.6 (C), 128.8 (CH), 128.6 (CH), 128.6 (CH), 128.4 (CH), 114.1 (CH_2, C-4), 97.1 (CH, C-1'), 78.4 (C, C-2), 72.5 (CH, C-3'), 71.3 (CH, C-5'), 70.7 (CH, C-2'), 68.8 (CH, C-4'), 62.6 (CH_2, C-6'), 27.2 (CH_3, C-5), 26.4 (CH_3, C-1). HRESIMS m/z 687.2186 $[M + Na]^+$ (calcd for $C_{39}H_{36}O_{10}Na$, 687.2201).

2-Methyl-3-buten-2-yl-β-D-galactopyranoside (66). The glycosylation crude from the synthesis of **65** was deprotected according to general procedure B. The desired glycoside (**66**) was isolated by RP-HPLC (C_{18}, 30% CH_3OH). **66**: $[\alpha]^{25}_D$ = -9.29 (c 0.117, CH_3OH); IR υ_{max} 3379, 3090, 2980, 2933, 2881, 1642, 1579, 1059 cm^{-1}. ^1H NMR (600 MHz, CD_3OD) δ 6.03 (1H, dd, J = 17.7, 10.9 Hz, H-3), 5.20 (1H, dd, J = 17.7, 1.1 Hz, H-4), 5.10 (1H, dd, J = 10.9, 1.1 Hz, H-4), 4.28 (1H, d, J = 7.2 Hz, H-1'), 3.83 (1H, dd, J = 3.0, 0.8 Hz, H-4'), 3.71 (1H, dd, J = 10.9, 5.7 Hz, H-6'), 3.67 (1H, dd, J = 10.9, 6.4 Hz, H-6'), 3.47 (1H, dd, J = 9.8, 7.2 Hz, H-2'), 3.44 (1H, dd, J = 9.8, 3.4 Hz, H-3'), 3.41 (1H, ddd, J = 6.4, 0.8 Hz, H-5'), 1.37 (3H, s, H-1), 1.33 (3H, s, H-5). ^{13}C NMR (150 MHz, CD_3OD) δ 145.6 (CH, C-3), 114.2 (CH_2, C-4), 100.2 (CH, C-1'), 79.0 (C, C-2), 76.3 (CH, C-5'), 75.1 (CH, C-3'), 72.6 (CH, C-2'), 70.2 (CH, C-4'), 62.3 (CH_2, C-6'), 27.9 (CH_3, C-5), 26.7 (CH_3, C-1). HRESIMS m/z 271.1159 $[M + Na]^+$ (calcd for $C_{11}H_{20}O_6Na$, 271.1152).

Prenyl 2,3,4,6-tetra-O-benzoyl-β-D-galactopyranoside (68). Glycoside **68** was isolated as a side product from the glycosylation crude reaction mixture of **65** by semi-preparative

RP-HPLC (phenylhexyl, 86% CH_3OH). **68**: IR υ_{max} 3063, 2970, 2931, 1726, 1266, 1108, 1070, 709 cm^{-1}. ^1H NMR (600 MHz, C_6D_6) δ 8.19 (2H, dd), 8.11 (2H, dd), 8.09 (2H, dd), 7.98 (2H, dd), 7.09 (2H, tt), 7.03 (2H, m), 7.03 (1H, m), 6.97 (2H, tt), 6.91 (1H, tt), 6.89 (1H, tt), 6.83 (2H, tt), 6.71 (1H, tt), 6.35 (1H, dd, J = 10.5, 7.9 Hz, H-2'), 6.19 (1H, dd, J = 3.8, 1.1 Hz, H-4'), 5.76 (1H, dd, J = 10.5, 3.8 Hz, H-3'), 5.29 (1H, m, J = 7.9, 6.4, 1.5 Hz, H-2), 4.74 (1H, dd, J = 11.3, 7.2 Hz, H-6'), 4.70 (1H, d, J = 8.0 Hz, H-1'), 4.33 (1H, dd, J = 11.3, 6.4 Hz, H-6'), 4.29 (1H, dd, J = 12.0, 6.4 Hz, H-1), 4.22 (1H, dd, J = 11.8, 7.7 Hz, H-1), 3.75 (1H, ddd, J = 6.4, 1.1 Hz, H-5'), 1.45 (3H, s, H-5), 1.39 (3H, s, H-4). ^{13}C NMR (150 MHz, C_6D_6) δ 165.3 (C), 165.2 (C), 165.2 (C), 165.1 (C), 137.8 (C, C-3), 132.7 (CH), 132.5 (CH), 132.5 (CH), 132.4 (CH), 130.4 (C), 130.2 (C), 129.8 (C), 129.8 (C), 129.6 (CH), 129.6 (CH), 129.5 (CH), 129.4 (CH), 128.3 (CH), 128.2 (CH), 128.2 (CH), 128.0 (CH) 120.4 (CH, C-2), 99.7 (CH, C-1'), 72.2 (CH, C-3'), 71.0 (CH, C-5'), 70.2 (CH, C-2'), 68.4 (CH, C-4'), 64.9 (CH_2, C-1), 62.0 (CH_2, C-6'), 25.1 (CH_3, C-5), 17.3 (CH_3, C-4). HRESIMS m/z 687.2182 $[M + Na]^+$ (calcd for $C_{39}H_{36}O_{10}Na$, 687.2201).

Prenyl-β-D-galactopyranoside (69). Glycoside **69** was isolated as a side product from the crude product of **66** by RP-HPLC (C_{18}, 30% CH_3OH). **69**: $[\alpha]^{25}_D$ = -21.4 (c 0.133, CH_3OH); IR υ_{max} 3384, 3027, 2970, 2915, 2881, 1671, 1646, 1063 cm^{-1}. ^1H NMR (600 MHz, CD_3OD) δ 5.38 (1H, m, J = 7.9, 6.4, 1.5 Hz, H-2), 4.32 (1H, dd, J = 12.0, 6.4 Hz, H-1), 4.24 (1H, d, J = 7.9 Hz, H-1'), 4.22 (1H, dd, J = 12.0, 7.9 Hz, H-1), 3.83 (1H, dd, J = 3.2, 1.0 Hz, H-4'), 3.76 (1H, dd, J = 11.3, 6.8 Hz, H-6'), 3.73 (1H, dd, J = 11.3, 5.6 Hz, H-6'), 3.51 (1H, dd, J = 9.8, 7.5 Hz, H-2'), 3.48 (1H, ddd, J = 6.8, 1.1 Hz, H-5'), 3.45 (1H, dd, J = 9.8, 3.4 Hz, H-3'), 1.69 (3H, s, H-4), 1.75 (3H, s, H-5). ^{13}C NMR (150 MHz,

CD_3OD) δ 138.4 (C, C-3), 121.9 (CH_2, C-2), 103.5 (CH, C-1'), 76.7 (CH, C-5'), 75.1 (CH, C-3'), 72.6 (CH, C-2'), 70.4 (CH, C-4'), 66.3 (CH_2, C-1), 62.5 (CH_2, C-6'), 25.9 (CH_3, C-5), 18.1 (CH_3, C-4). HRESIMS m/z 271.1157 $[M + Na]^+$ (calcd for $C_{11}H_{20}O_6Na$, 271.1152).

2-Methyl-3-buten-2-yl-α-D-galactopyranoside (71). Glycoside **71** was isolated as a side product from the crude product of **66** by RP-HPLC (C_{18}, 30% CH_3OH). **71**: ^1H NMR (600 MHz, CD_3OD) δ 5.93 (1H, dd, J = 17.6, 10.8 Hz, H-3), 5.20 (1H, dd, J = 17.6, 1.1 Hz, H-4), 5.10 (1H, dd, J = 10.8, 1.1 Hz, H-4), 5.02 (1H, d, J = 2.8 Hz, H-1'), 3.98 (1H, dd, J = 7.0, 4.8 Hz, H-3'), 3.93 (1H, dd, J = 7.0, 2.8 Hz, H-4'), 3.89 (1H, dd, J = 4.7, 2.8 Hz, H-2'), 3.68 (1H, ddd, J = 6.8, 5.8, 2.8 Hz, H-5'), 3.60 (1H, d, 5.8 Hz, H-6'), 3.59 (1H, d, J = 6.8 Hz, H-6'), 1.37 (3H, s, H-1), 1.33 (3H, s, H-5). ^{13}C NMR (150 MHz, CD_3OD) δ 145.4 (CH, C-3), 114.2 (CH_2, C-4), 104.8 (CH, C-1'), 84.2 (CH, C-2'), 83.5 (CH, C-4'), 78.0 (C, C-2), 78.0 (CH, C-3'), 72.2 (CH, C-5'), 64.8 (CH_2, C-6'), 28.5 (CH_3, C-5), 26.5 (CH_3, C-1). HRESIMS m/z 271.1140 $[M + Na]^+$ (calcd for $C_{11}H_{20}O_6Na$, 271.1152).

1,2,3,4,6-penta-O-pivaloyl-β-D-galactopyranose (72). Pivaloylated carbohydrate **72** was isolated as a side product from the crude product of **64** by MPLC (244 mg, 0.406 mmol, 21% with respect to **62**). All ^1H and ^{13}C NMR spectroscopic data for **72** were in accord with the literature.[287]

1,3,4,6-Tetra-O-pivaloyl-α-D-galactopyranose (73). Pivaloylated carbohydrate **73** was isolated as a side product from the crude product of **64** by MPLC (246 mg, 0.476 mmol,

25% with respect to **62**). **73**: (white solid); $[\alpha]^{25}_{D}$ = +105.5 (c 0.4542, CH_2Cl_2); IR: 3481, 2973, 2936, 2910, 2874, 1737, 1137, 1091, 1023 cm^{-1}. ^1H NMR (600 MHz, C_6D_6): δ 6.45 (1H, d, J = 3.8 Hz, H-1'), 5.55 (1H, dd, J = 3.4, 1.1 Hz, H-4'), 5.42 (1H, dd, J = 10.5, 3.4 Hz, H-3'), 4.28 (1H, ddd, J = 6.4, 7.2, 1.1 Hz, H-5'), 4.16 (1H, dd, J = 11.3, 7.5 Hz, H-6'), 4.13 (1H, dd, J = 10.2, 3.0 Hz, H-2'), 4.03 (1H, dd, J = 11.3, 6.0 Hz, H-6'), 1.16 (9H, s, 2'/4'-OPiv), 1.15 (9H, s, 3'-OPiv), 1.14 (9H, s, 2'/4'-OPiv), 1.12 (9H, s, 6'-OPiv). ^{13}C NMR (150 MHz, C_6D_6): 178.2 (C, 3'-OC), 177.3 (C, 6'-OC), 176.7 (C, 4'-OC),176.5 (C, 1'-OC), 92.3 (CH, C-1'), 71.0 (CH, C-3'), 69.7 (CH, C-5'), 67.9 (CH, C-4'), 67.2 (CH, C-2'), 61.9 (CH_2, C-6'), 39.3 (C, OPiv), 39.1 (C, OPiv), 39.0 (C, OPiv), 38.8 (C, OPiv), 27.2 (CH_3, OPiv), 27.2 (CH_3, OPiv), 27.2 (CH_3, OPiv), 27.1 (CH_3, OPiv). HRESIMS m/z 539.2809 $[M + Na]^+$ (calcd for $C_{26}H_{44}O_{10}Na$, 539.2827).

3.4.3 Synthesis and characterization of fuscoside analogues

Fuscene B (48) and Eunicene B (46). Diterpenes **46** and **48** were isolated as a side product from the crude product of **76** and **77** by RP-HPLC. All ^1H and ^{13}C NMR spectroscopic data for **46** and **48** were consistent with previous data.[254]

Fusco-2,3,4,6-tetra-O-benzoyl-β-D-galactopyranoside (74) and Eunico-2,3,4,6-tetra-O-benzoyl-β-D-galactopyranoside (75). Aglycones **15** and **16** (34.5 mg, 200 μmol) were glycosylated using **63** according to general procedure C. The crude product was separated by flash chromatography (silica, hexanes → TBME) and the desired glycosides were purified by RP-HPLC (C_{18}, 94% CH_3OH). **74** (8.6 mg, 9.9 μmol, 15%): $[\alpha]^{25}_{D}$ = +135.1 (c 0.1192, CH_2Cl_2); IR υ_{max} 3070, 2975, 2929, 2859, 1729, 1265, 1107, 1069, 709. ^1H

NMR (600 MHz, CD_3OD) δ 8.11 (2H, dd), 8.02 (2H, dd), 7.98 (2H, dd), 7.72 (2H, dd), 7.67 (1H, t), 7.60 (1H, t), 7.57 (1H, t), 7.54 (2H, t), 7.46 (2H, t), 7.45 (1H, t), 7.43 (2H, t), 7.25 (2H, t), 6.46 (1H, dd, J = 15.5, 10.7 Hz, H-13), 5.95 (1H, dd, J = 3.0 Hz, H-4'), 5.84 (1H, dd, J = 17.5, 10.8 Hz, H-6), 5.74 (1H, dd, J = 10.2, 3.4 Hz, H-3'), 5.71 (1H, br d, J = 10.2 Hz, H-12), 5.69 (1H, dd, J = 9.8, 7.5 Hz, H-2'), 5.50 (1H, d, J = 15.5 Hz, H-14), 5.09 (1H, d, J = 7.2 Hz, H-1'), 4.91 (1H, dd, J = 17.3, 1.4 Hz, H-5), 4.88 (1H, dd, J = 10.5, 1.5 Hz, H-5), 4.83 (1H, br s, H-4), 4.61 (1H, br s, H-4), 4.54 (1H, dd, J = 10.5, 7.2 Hz, H-6'), 4.49 (1H, ddd, J = 7.2, 5.0 Hz, H-5'), 4.44 (1H, dd, J = 10.5, 4.9 Hz, H-6'), 2.03 (1H, app. dd, J = 12.7, 3.0 Hz, H-2), 1.95-1.89 (1H, m, H-10), 1.74 (3H, s, H-18), 1.72 (3H, s, H-16), 1.63 (1H, app. ddd, J = 12.8 Hz, H-1), 1.56-1.48 (1H, m, H-8), 1.52-1.47 (2H, m, H-9), 1.46-1.40 (1H, m, H-1), 1.46-1.41 (1H, m, H-8), 1.40 (3H, s, H-19), 1.26 (3H, s, H-20), 1.02 (3H, s, H-17). ^{13}C NMR (150 MHz, CD_3OD) δ 166.8 (C), 166.7 (C), 167.4 (C), 167.3 (C), 151.5 (CH, C-6), 149.0 (C, C-3), 145.3 (C, C-11), 136.8 (CH, C-14), 134.9 (CH), 134.7 (CH), 134.6 (CH), 134.5 (CH), 131.0 (CH), 131.0 (C), 130.8 (C), 130.8 (CH), 130.8 (CH), 130.6 (CH), 130.6 (C), 130.3 (C), 129.9 (CH), 129.7 (CH), 129.7 (CH), 129.5 (CH), 127.9 (CH), 123.8 (CH, C-12), 112.8 (CH_2, C-4), 110.5 (CH_2, C-5), 97.6 (CH, C-1'), 79.9 (C, C-15), 73.4 (CH, C-3'), 72.2 (CH, C-5'), 71.8 (CH, C-2'), 70.3 (CH, C-4'), 63.8 (CH_2, C-6'), 54.0 (CH, C-2), 49.3 (CH, C-10), 41.1 (CH_2, C-8), 40.8 (C, C-7), 33.9 (CH_2, C-1), 28.8 (CH_3, C-20), 27.8 (CH_2, C-9), 26.7 (CH_3, C-19), 25.4 (CH_3, C-16), 17.2 (CH_3, C-17), 15.3 (CH_3, C-18). HRESIMS m/z 889.3950 $[M + Na]^+$ (calcd for $C_{54}H_{58}O_{10}Na$, 889.3922). **75** (6.9 mg, 8.0 μmol, 5%): $[\alpha]^{25}_D$ = +56.3 (c 0.0167, CH_2Cl_2); IR υ_{max} 3068, 3034, 2975, 2929, 2860, 1729, 1265, 1107, 1069, 710 cm^{-1}. ^1H NMR (600 MHz, C_6D_6) δ 8.23 (2H, dd), 8.19 (2H, dd), 8.08 (2H, dd), 7.97 (2H, dd),

7.12 (1H, br tt), 7.08 (1H, br tt), 7.05 (2H, m), 7.05 (2H, m), 7.02 (1H, m), 6.87 (2H, t), 6.83 (1H, br tt), 6.71 (2H, t), 6.53 (1H, dd, J = 15.8, 10.9 Hz, H-13), 6.33-6.28 (1H, m, H-2'), 6.07 (1H, dd, J = 3.0 Hz, H-4'), 6.09-5.99 (0.5H, br m, H-12), 5.94 (0.5H, br d, J = 10.5 Hz, H-12), 5.66-5.59 (1H, m, H-3'), 5.76 (1H, d, J = 15.8 Hz, H-14), 5.20-5.03 (1H, br m, H-2, H-6), 4.82 (1H, d, J = 7.5 Hz, H-1'), 4.83-4.80 (0.5H, br m, H-6), 4.72-4.67 (1H, m, H-6'), 4.55 (0.5H, br d, 10.2 Hz, H-2'), 4.32-4.26 (1H, m, H-6'), 2.39-2.33 (1H, m, J = 12.8, 7.5 Hz, H-8), 2.28-2.23 (1H, m, H-1), 2.23-2.17 (1H, m, J = 12.8, 4.5 Hz, H-5), 2.18-2.13 (1H, m, H-1), 2.14-2.09 (1H, m, H-4), 2.10-2.04 (1H, m, H-8), 2.07-2.02 (1H, m, H-5), 1.95-1.88 (1H, m, H-10), 1.92-1.87 (1H, m, H-4), 1.69 (3H, s, H-18), 1.71-1.64 (1H, m, H-9), 1.55-1.49 (1H, m, H-9), 1.47 (1.5H, s, H-16), 1.44 (3H, s, H-17), 1.44 (3H, s, H-19), 1.36-1.32 (1.5H, br s, H-16), 1.28 (3H, br s, H-20). ^{13}C NMR (150 MHz, C_6D_6) δ 165.3 (C), 165.3 (C), 165.2 (C), 165.1 (C), 146.9 (C, C-11), 137.8 (C, C-7), 137.0 (CH, C-14), 133.3 (CH), 133.2 (CH), 133.1 (CH), 133.1 (CH), 132.9 (C), 132.8 (C), 132.7 (C), 132.7 (C), 131.7 (CH, C-2), 130.4 (CH), 130.1 (CH), 130.1 (CH), 130.0 (CH), 129.6 (C, C-3), 128.7 (CH), 128.6 (CH), 128.6 (CH), 128.4 (CH), 127.0 (CH, C-6), 126.6 (CH, C-13), 122.4 (CH, C-12), 97.3 (CH, C-1'), 78.8 (C, C-15), 72.6 (CH, C-3'), 71.0 (CH, C-5'), 71.0 (CH, C-2'), 68.7 (CH, C-4'), 62.3 (CH_2, C-6'), 53.7 (CH, C-10), 42.0 (CH_2, C-8), 39.5 (CH_2, C-4), 35.2 (CH_2, C-1), 33.9 (CH_2, C-9), 28.9 (CH_3, C-20), 27.1 (CH_2, C-5), 26.3 (CH_3, C-19), 16.8 (CH_3, C-16), 16.5 (CH_3, C-17), 14.4 (CH_3, C-18). HRESIMS m/z 889.3974 $[M + Na]^+$ (calcd for $C_{54}H_{58}O_{10}Na$, 889.3922).

Fusco-β-D-galactopyranoside (76) and Eunico-β-D-galactopyranoside (**77**).

Aglycones **15** and **16** (31.0 mg, 108 μmol) were glycosylated using **63** according to

general procedure C and the crude product was deprotected according to general procedure D. The desired glycosides were separated by RP-HPLC (phenylhexyl, 81% CH_3OH). **76** (1.4 mg, 3.1 μmol, 9%): $[\alpha]^{25}_D$ = -8.06 (c 0.0500, CH_3OH); IR υ_{max} 3381, 3081, 3046, 2973, 2928, 2860, 1635, 1056 cm^{-1}. ^1H NMR (600 MHz, CD_3OD) δ 6.48 (1H, dd, J = 15.4, 10.5 Hz, H-13), 5.90 (1H, d, J = 10.5 Hz, H-12), 5.84 (1H, dd, J = 17.3, 10.8 Hz, H-6), 5.76 (1H, d, J = 15.4 Hz, H-14), 4.90 (1H, dd, J = 17.3, 1.1 Hz, H-5), 4.87 (1H, dd, J = 10.9, 1.1 Hz, H-5), 4.81 (1H, br s, H-4), 4.60 (1H, br s, H-4), 4.29 (1H, d, J = 7.5 Hz, H-1'), 3.81 (1H, dd, J = 3.4, 1.1 Hz, H-4'), 3.70 (1H, dd, J = 11.3, 6.0 Hz, H-6'), 3.68 (1H, dd, J = 11.3, 6.0 Hz, H-6'), 3.48 (1H, dd, J = 9.8, 7.5 Hz, H-2'), 3.44 (1H, dd, J = 9.8, 3.4 Hz, H-3'), 3.40 (1H, app. dd, J = 6.0, 1.1 Hz, H-5'), 2.04 (1H, app. dd, J = 12.8, 3.0 Hz, H-2), 2.03-1.97 (1H, m, H-10), 1.78 (3H, s, H-18), 1.71 (3H, s, H-16), 1.66 (1H, app. ddd, J = 12.8 Hz, H-1), 1.57-1.52 (2H, m, H-9), 1.55-1.51 (1H, m, H-8), 1.49-1.45 (1H, m, H-1), 1.46-1.42 (1H, m, H-8), 1.41 (3H, s, H-19), 1.36 (3H, s, H-20), 1.03 (3H, s, H-17). ^{13}C NMR (150 MHz, CD_3OD) δ 151.6 (CH, C-6), 149.0 (C, C-3), 144.3 (C, C-11), 138.4 (CH, C-14), 127.1 (CH, C-13), 124.2 (CH, C-12), 112.7 (CH_2, C-4), 110.4 (CH_2, C-5), 100.3 (CH, C-1'), 79.1 (C, C-15), 76.3 (CH, C-5'), 75.1 (CH, C-3'), 72.7 (CH, C-2'), 70.2 (CH, C-4'), 62.4 (CH_2, C-6'), 54.1 (CH, C-2), 49.2 (CH, C-10), 41.1 (CH_2, C-8), 40.8 (C, C-7), 34.1 (CH_2, C-1), 28.7 (CH_3, C-20), 27.8 (CH_2, C-9), 27.4 (CH_3, C-19), 25.3 (CH_3, C-16), 17.2 (CH_3, C-17), 15.4 (CH_3, C-18). HRESIMS m/z 473.2861 $[M + Na]^+$ (calcd for $C_{26}H_{42}O_6Na$, 473.2874). **77** (1.6 mg, 3.6 μmol, 4%): IR υ_{max} 3373, 3047, 2971, 2923, 2856, 1648, 1591, 1054 cm^{-1}. ^1H NMR (600 MHz, CD_3OD) δ 6.43 (1H, dd, J = 15.1, 10.5 Hz, H-13), 5.85 (1H, d, J = 10.2 Hz, H-12), 5.74 (1H, d, J = 15.4 Hz, H-14), 5.25-4.95 (1.2H, br m, H-2, H-6), 4.79 (0.4H, br d, J = 11.3 Hz, H-6),

4.55 (0.4H, br d, J = 10.2 Hz, H-2), 4.32-4.28 (1H, m, H-1'), 3.82 (1H, br dd, J = 3.0 Hz, H-4'), 3.71 (1H, dd, J = 11.3, 6.0 Hz, H-6'), 3.68 (1H, dd, J = 11.3, 6.4 Hz, H-6'), 3.50-3.45 (1H, m, H-2'), 3.47-3.43 (1H, m, H-3'), 3.43-3.39 (1H, m, H-5'), 2.40-2.33 (1H, m, H-8), 2.33-2.25 (1H, m, J = 12.4, 4.5 Hz, H-5), 2.22-2.17 (1H, m, H-1), 2.20-2.15 (1H, m, H-4), 2.10-2.05 (1H, m, H-1), 2.08-2.04 (1H, m, H-5), 2.07-2.05 (1H, m, H-8), 2.01-1.95 (1H, m, H-10), 1.94-1.88 (1H, m, H-4), 1.77 (1.2H, s, H-18), 1.75 (1.8H, s, H-18), 1.72-1.63 (2H, m, H-9), 1.59-1.53 (1.2H, br s, H-16), 1.54 (1.8H, s, H-16), 1.53-1.47 (1.8H, br s, H-17), 1.41 (1.2H, s, H-17), 1.41 (3H, s, H-19), 1.36 (3H, s, H-20). ^{13}C NMR (150 MHz, CD_3OD) δ 147.8 (C, C-11), 138.9 (C, C-7), 138.3 (CH, C-14), 132.6 (CH, C-2), 130.2 (C, C-3), 127.6 (CH, C-6), 127.0 (CH, C-13), 123.2 (CH, C-12), 100.2 (CH, C-1'), 79.1 (C, C-15), 76.3 (CH, C-5'), 75.1 (CH, C-3'), 72.7 (CH, C-2'), 70.2 (CH, C-4'), 62.4 (CH_2, C-6') 54.8 (CH, C-10), 42.8 (CH_2, C-8), 40.6 (CH_2, C-4), 35.8 (CH_2, C-1), 34.8 (CH_2, C-9), 28.8 (CH_3, C-20), 27.6 (CH_2, C-5), 27.4 (CH_3, C-19), 17.0 (CH_3, C-16), 16.6 (CH_3, C-17), 14.8 (CH_3, C-18). HRESIMS m/z 473.2868 $[M + Na]^+$ (calcd for $C_{26}H_{42}O_6Na$, 473.2874).

Fusco-α-D-arabinopyranoside (78) and Eunico-α-D-arabinopyranoside (79). Aglycones **15** and **16** (33.8 mg, 117 μmol) were glycosylated using **63** according to general procedure C and the crude product was deprotected according to general procedure D. The desired glycosides were separated by RP-HPLC (phenylhexyl, 81% CH_3OH). **78** (1.3 mg, 3.1 μmol, 9%): $[\alpha]^{25}_D$ = -6.13 (c 0.0667, CH_3OH); IR υ_{max} 3382, 3081, 2972, 2926, 2856, 1636, 1085 cm^{-1}. ^{1}H NMR (600 MHz, CD_3OD) δ 6.48 (1H, dd, J = 15.8, 10.9 Hz, H-13), 5.89 (1H, d, J = 10.5 Hz, H-12), 5.84 (1H, dd, J = 17.3, 10.9 Hz,

H-6), 5.72 (1H, d, J = 15.4 Hz, H-14), 4.90 (1H, dd, J = 17.3, 1.5 Hz, H-5), 4.88 (1H, dd, J = 10.9, 1.5 Hz, H-5), 4.81 (1H, br s, H-4), 4.61 (1H, br s, H-4), 4.27 (1H, d, J = 6.8 Hz, H-1'), 3.79 (1H, dd, J = 12.4, 2.6 Hz, H-5'), 3.78-3.76 (1H, m, H-4'), 3.51-3.49 (1H, m, H-2'), 3.51-3.49 (1H, m, H-3'), 3.47 (1H, dd, J = 12.4, 1.1 Hz, H-5'), 2.05 (1H, app. dd, J = 12.8, 3.4 Hz, H-2), 2.04-1.98 (1H, m, H-10), 1.79 (3H, s, H-18), 1.71 (3H, s, H-16), 1.67 (1H, app. ddd, J = 12.8 Hz, H-1), 1.57-1.53 (2H, m, H-9), 1.56-1.52 (1H, m, H-8), 1.49-1.45 (1H, m, H-1), 1.44 (1H, dd, J = 9.0, 2.6 Hz, H-8), 1.39 (3H, s, H-19), 1.35 (3H, s, H-20), 1.03 (3H, s, H-17). ^{13}C NMR (150 MHz, CD_3OD) δ 151.6 (CH, C-6), 149.0 (C, C-3), 144.4 (C, C-11), 138.1 (CH, C-14), 127.1 (CH, C-13), 124.1 (CH, C-12), 112.7 (CH_2, C-4), 110.4 (CH_2, C-5), 100.2 (CH, C-1'), 79.1 (C, C-15), 74.4 (CH, C-3'), 72.7 (CH, C-2'), 69.8 (CH, C-4'), 66.8 (CH, C-5'), 54.0 (CH, C-2), 49.2 (CH, C-10), 41.1 (CH_2, C-8), 40.8 (C, C-7), 34.0 (CH_2, C-1), 28.7 (CH_3, C-20), 27.9 (CH_2, C-9), 27.3 (CH_3, C-19), 25.3 (CH_3, C-16), 17.2 (CH_3, C-17), 15.3 (CH_3, C-18). HRESIMS m/z 443.2768 $[M + Na]^+$ (calcd for $C_{25}H_{40}O_5Na$, 443.2768). **79** (1.0 mg, 2.4 μmol, 3%): $[\alpha]^{25}_D$ = -34.4 (c 0.0050, CH_3OH); IR υ_{max} 3379, 3081, 3041, 2970, 2924, 2854, 1634, 1083, 1002 cm^{-1}. ^{1}H NMR (600 MHz, CD_3OD) δ 6.47-6.40 (1H, m, H-13), 5.85 (1H, d, J = 10.5 Hz, H-12), 5.71 (1H, d, J = 15.8 Hz, H-14), 4.95-5.25 (1.2H, br m, H-2, H-6), 4.80 (0.4H, br d, J = 13.2 Hz, H-6), 4.55 (0.4H, br d, J = 9.8 Hz, H-2), 4.30-4.24 (1H, m, H-1'), 3.80 (1H, dd, J = 12.4, 2.6 Hz, H-5'), 3.78-3.76 (1H, m, H-4'), 3.52-3.49 (1H, m, H-2'), 3.51-3.49 (1H, m, H-3'), 3.47 (1H, dd, J = 11.7, 3.8 Hz, H-5'), 2.40-2.34 (1H, m, H-8), 2.33-2.25 (1H, m, J = 12.8, 4.9 Hz, H-5), 2.22-2.17 (1H, m, H-1), 2.19-2.15 (1H, m, H-4), 2.10-2.04 (1H, m, H-1), 2.10-2.04 (1H, m, H-8), 2.07-2.03 (1H, m, H-5), 2.01-1.96 (1H, m, H-10), 1.94-1.87 (1H, m, J = 12.0, 4.9 Hz, H-4), 1.77 (1.2H, s, H-18), 1.75

(1.8H, s, H-18), 1.71-1.63 (2H, m, H-9), 1.60-1.52 (1.2H, br s, H-16), 1.54 (1.8H, s, H-16), 1.53-1.47 (1.8H, br s, H-17), 1.41 (1.2H, s, H-17), 1.40 (3H, s, H-19), 1.35 (3H, s, H-20). ^{13}C NMR (150 MHz, CD_3OD) δ 147.9 (C, C-11), 138.9 (C, C-7), 138.0 (CH, C-14), 132.6 (CH, C-2), 130.2 (C, C-3), 127.7 (CH, C-6), 127.1 (CH, C-13), 123.1 (CH, C-12), 100.2 (CH, C-1'), 79.1 (C, C-15), 74.4 (CH, C-3'), 72.7 (CH, C-2'), 69.8 (CH, C-4'), 66.7 (CH_2, C-5'), 54.8 (CH, C-10), 42.8 (CH_2, C-8), 40.6 (CH_2, C-4), 35.8 (CH_2, C-1), 34.8 (CH_2, C-9), 28.9 (CH_3, C-20), 27.6 (CH_2, C-5), 27.3 (CH_3, C-19), 17.0 (CH_3, C-16), 16.6 (CH_3, C-17), 14.7 (CH_3, C-18). HRESIMS m/z 443.2747 $[M + Na]^+$ (calcd for $C_{25}H_{40}O_5Na$, 443.2768).

3.4.4 Synthesis and characterization of fuscoside mimics and methyl ether analogues

EG_3-Glycoside Mimics (80 and 81). Solvolysis of **15** and **16** (3.8 mg, 13 μmol) was performed according to general procedure E using triethylene glycol (EG_3) and the desired products were separated by RP-HPLC (phenylhexyl, 87% CH_3OH). **80** (1.1 mg, 2.6 μmol, 60%): $[\alpha]^{25}_D$ = +5.31 (c 0.0583, CH_3OH); IR υ_{max} 3435, 3080, 2972, 2927, 2864, 1637, 1122, 1082 cm^{-1}. ^{1}H NMR (600 MHz, CD_3OD) δ 6.45 (1H, dd, J = 15.4, 10.5 Hz, H-13), 5.90 (1H, d, J = 10.5 Hz, H-12), 5.84 (1H, dd, J = 17.7, 10.9 Hz, H-6), 5.58 (1H, d, J = 15.4 Hz, H-14), 4.90 (1H, dd, J = 17.7, 1.1 Hz, H-5), 4.88 (1H, dd, J = 10.9, 1.1 Hz, H-5), 4.81 (1H, br s, H-4), 4.61 (1H, br s, H-4), 3.66 (2H, dd, J = 5.3, 4.2 Hz, H-6'), 3.67-3.63 (2H, m, H-3'), 3.67-3.63 (2H, m, H-4'), 3.59 (2H, dd, J = 5.8, 4.4 Hz, H-2'), 3.56 (2H, dd, J = 5.5, 4.5 Hz, H-5'), 3.47 (2H, dd, J = 5.8, 4.4 Hz, H-1'), 2.05 (1H, app. dd, J = 12.8, 3.0 Hz, H-2), 2.03-1.98 (1H, m, H-10), 1.79 (3H, s, H-18), 1.71 (3H, s, H-16), 1.67 (1H, app. ddd, J = 12.8, H-1), 1.57-1.53 (2H, m, H-9), 1.56-1.53 (1H, m, H-

8), 1.49-1.45 (1H, m, H-1), 1.46-1.43 (1H, m, H-8), 1.30 (6H, s, H-19, H-20), 1.03 (3H, s, H-17). ^{13}C NMR (150 MHz, CD_3OD) δ 151.6 (CH, C-6), 149.0 (C, C-3), 144.3 (C, C-11), 137.8 (CH, C-14), 127.4 (CH, C-13), 124.0 (CH, C-12), 112.7 (CH_2, C-4), 110.4 (CH_2, C-5), 76.7 (C, C-15), 73.7 (CH_2, C-5'), 72.2 (CH_2, C-2'), 71.7 (CH_2, C-3'), 71.5 (CH_2, C-4'), 63.2 (CH_2, C-1'), 62.3 (CH_2, C-6'), 54.0 (CH, C-2), 49.2 (CH, C-10), 41.1 (CH_2, C-8), 40.8 (C, C-7), 34.1 (CH_2, C-1), 27.9 (CH_2, C-9), 26.9 (CH_3, C-19, C-20), 25.3 (CH_3, C-16), 17.2 (CH_3, C-17), 15.3 (CH_3, C-18). HRESIMS m/z 443.3124 $[M + Na]^+$ (calcd for $C_{26}H_{44}O_4Na$, 443.3132). **81** (1.5 mg, 3.6 μmol, 36%): $[\alpha]^{25}_D$ = -14.3 (c 0.0583, CH_3OH); IR υ_{max} 3449, 3040, 2971, 2923, 2860, 1650, 1122, 1081 cm^{-1}. ^{1}H NMR (600 MHz, CD_3OD) δ 6.40 (1H, dd, J = 15.4, 10.9 Hz, H-13), 5.85 (1H, d, J = 10.5 Hz, H-12), 5.57 (1H, d, J = 15.4 Hz, H-14), 5.25-4.94 (1.2H, br m, H-2, H-6), 4.80 (0.4H, br d, J = 13.2 Hz, H-6), 4.56 (0.4H, br d, J = 10.2 Hz, H-2), 3.66 (2H, dd, J = 5.3, 4.5 Hz, H-6'), 3.66-3.62 (2H, m, H-3'), 3.66-3.62 (2H, m, H-4'), 3.61-3.58 (2H, m, H-2'), 3.57 (2H, dd, J = 5.3, 4.5 Hz, H-5'), 3.49-3.46 (2H, m, H-1'), 2.40-2.34 (1H, m, H-8), 2.33-2.25 (1H, m, H-5), 2.21-2.16 (1H, m, H-1), 2.19-2.15 (1H, m, H-4), 2.10-2.04 (1H, m, H-1), 2.08-2.03 (1H, m, H-8), 2.07-2.02 (1H, m, H-5), 2.02-1.96 (1H, m, H-10), 1.93-1.87 (1H, m, J = 11.7, 4.9 Hz, H-4), 1.78 (1.2H, s, H-18), 1.75 (1.8H, s, H-18), 1.69-1.64 (2H, m, H-9), 1.60-1.54 (1.2H, br s, H-16), 1.54 (1.8H, s, H-16), 1.54-1.46 (1.8H, br s, H-17), 1.41 (1.2H, s, H-17), 1.31 (6H, s, H-19, H-20). ^{13}C NMR (150 MHz, CD_3OD) δ 147.8 (C, C-11), 138.9 (C, C-7), 137.6 (CH, C-14), 132.6 (CH, C-2), 130.2 (C, C-3), 127.6 (CH, C-6), 127.3 (CH, C-13), 123.0 (CH, C-12), 76.8 (C, C-15), 73.7 (CH_2, C-5'), 72.1 (CH_2, C-2'), 71.6 (CH_2, C-3'), 71.4 (CH_2, C-4'), 63.1 (CH_2, C-1'), 62.2 (CH_2, C-6'), 54.8 (CH, C-10), 42.8 (CH_2, C-8), 40.6 (CH_2, C-4), 35.8 (CH_2, C-1), 34.7 (CH_2, C-9), 27.6 (CH_2, C-

5), 26.9 (CH_3, C-19, C-20), 17.0 (CH_3, C-16), 16.6 (CH_3, C-17), 14.8 (CH_3, C-18). HRESIMS m/z 443.3111 $[M + Na]^+$ (calcd for $C_{26}H_{44}O_4Na$, 443.3132).

EG_4-Glycoside Mimics (82 and 83). Solvolysis of **15** and **16** (11.4 mg, 39.5 mmol) was performed according to general procedure E using EG_4 and the desired products were separated by RP-HPLC (phenylhexyl, 86% CH_3OH). **82** (2.2 mg, 4.7 μmol, 36%): $[\alpha]^{25}_D$ = +2.38 (c 0.175, CH_3OH); IR υ_{max} 3419, 3080, 2971, 2925, 2864, 1638, 1124, 1081 cm^{-1}. ^1H NMR (600 MHz, CD_3OD) δ 6.44 (1H, dd, J = 15.4, 10.5 Hz, H-13), 5.89 (1H, d, J = 10.2 Hz, H-12), 5.84 (1H, dd, J = 17.7, 11.3 Hz, H-6), 5.58 (1H, d, J = 15.4 Hz, H-14), 4.90 (1H, dd, J = 17.3, 1.1 Hz, H-5), 4.88 (1H, dd, J = 10.5, 1.5 Hz, H-5), 4.81 (1H, br s, H-4), 4.61 (1H, br s, H-4), 3.66 (2H, dd, J = 5.5, 4.3 Hz, H-8'), 3.67-3.62 (8H, m, H-3', H-4', H-5', H-6'), 3.58 (2H, dd, J = 5.8, 4.2, H-2'), 3.56 (2H, dd, J = 5.6, 4.2 Hz, H-7'), 3.47 (2H, dd, J = 5.7, 4.1 Hz, H-1'), 2.05 (1H, app. dd, J = 12.8, 3.4 Hz, H-2), 2.04-1.98 (1H, m, H-10), 1.79 (3H, s, H-18), 1.71 (3H, s, H-16), 1.67 (1H, app. ddd, J = 12.8 Hz, H-1), 1.58-1.54 (2H, m, H-9), 1.56-1.52 (1H, m, H-8), 1.49-1.45 (1H, m, H-1), 1.46-1.41 (1H, m, H-8), 1.31 (6H, s, H-19, H-20), 1.03 (3H, s, H-17). ^{13}C NMR (150 MHz, CD_3OD) δ 151.6 (CH, C-6), 148.9 (C, C-3), 144.3 (C, C-11), 137.8 (CH, C-14), 127.3 (CH, C-13), 124.0 (CH, C-12), 112.8 (CH_2, C-4), 110.5 (CH_2, C-5), 76.8 (C, C-15), 73.7 (CH_2, C-7'), 72.1 (CH_2, C-2'), 71.6, 71.5, 71.5, 71.3 (CH_2, C-3', C-4', C-5', C-6'), 63.2 (CH_2, C-1'), 62.3 (CH_2, C-8'), 54.0 (CH, C-2), 49.2 (CH, C-10), 41.1 (CH_2, C-8), 40.8 (C, C-7), 34.1 (CH_2, C-1), 27.9 (CH_2, C-9), 26.9 (CH_3, C-19, C-20), 25.4 (CH_3, C-16), 17.2 (CH_3, C-17), 15.4 (CH_3, C-18). HRESIMS m/z 448.3394 $[M + Na]^+$ (calcd for $C_{28}H_{48}O_5Na$, 487.3394). **83** (2.0 mg, 4.3 μmol, 15%): $[\alpha]^{25}_D$ = -12.0 (c 0.0158, CH_3OH);

IR υ_{max} 3436, 3040, 2970, 2922, 2860, 1650, 1121, 1079 cm^{-1}. ^1H NMR (600 MHz, CD_3OD) δ 6.40 (1H, dd, J = 15.5, 10.9 Hz, H-13), 5.85 (1H, d, J = 9.5 Hz, H-12), 5.57 (1H, d, J = 15.6 Hz, H-14), 5.26-4.94 (1.2H, br m, H-2, H-6), 4.80 (0.4H, br d, J = 12.1 Hz, H-6), 4.55 (0.4H, br d, J = 10.4 Hz, H-2), 3.67 (2H, dd, J = 5.3, 4.5 Hz, H-8'), 3.67-3.63 (8H, m, H-3', H-4', H-5', H-6'), 3.60-3.56 (2H, m, H-2'), 3.56 (2H, dd, J = 5.3, 4.1 Hz, H-7'), 3.49-3.46 (2H, m, H-1'), 2.40-2.34 (1H, m, H-8), 2.33-2.25 (1H, m, H-5), 2.22-2.18 (1H, m, H-1), 2.20-2.15 (1H, m, H-4), 2.10-2.07 (1H, m, H-1), 2.09-2.04 (1H, m, H-8), 2.08-2.03 (1H, m, H-5), 2.02-1.96 (1H, m, H-10), 1.94-1.87 (1H, m, J = 12.4, 5.3 Hz, H-4), 1.78 (1.2H, s, H-18), 1.75 (1.8H, s, H-18), 1.70-1.64 (2H, m, H-9), 1.60-1.54 (1.2H, br s, H-16), 1.54 (1.8H, s, H-16), 1.54-1.46 (1.8H, br s, H-17), 1.41 (1.2H, s, H-17), 1.31 (6H, s, H-19, H-20). ^{13}C NMR (150 MHz, CD_3OD) δ 147.8 (C, C-11), 138.9 (C, C-7), 137.7 (CH, C-14), 132.6 (CH, C-2), 130.2 (C, C-3), 127.7 (CH, C-6), 127.3 (CH, C-13), 123.0 (CH, C-12), 76.8 (C, C-15), 73.7 (CH_2, C-7'), 72.2 (CH_2, C-2'), 71.6, 71.5, 71.5, 71.4 (CH_2, C-3', C-4', C-5', C-6'), 63.2 (CH_2, C-1'), 62.2 (CH_2, C-8'), 54.8 (CH, C-10), 42.8 (CH_2, C-8), 40.6 (CH_2, C-4), 35.8 (CH_2, C-1), 34.8 (CH_2, C-9), 27.6 (CH_2, C-5), 26.9 (CH_3, C-19, C-20), 17.0 (CH_3, C-16), 16.6 (CH_3, C-17), 14.8 (CH_3, C-18). HRESIMS m/z 487.3389 $[M + Na]^+$ (calcd for $C_{28}H_{48}O_5Na$, 487.3394).

Methyl Ethers of Fuscol and Eunicol (53 and 54). Solvolysis of **15** and **16** (9.4 mg, 33 μmol) was performed according to general procedure E (THF not required) using CH_3OH and separation by RP-HPLC (phenylhexyl, 94% CH_3OH). **53** (1.8 mg, 6.0 μmol, 54%): $[\alpha]^{25}_D$ = +3.14 (c 0.0833, CH_3OH); IR υ_{max} 3080, 2973, 2929, 2860, 1638, 1441, 1376, 1361, 1254, 1166, 1078, 969, 908, 889, 755 cm^{-1}. ^1H NMR (600 MHz, CD_3OD) δ 6.44

(1H, dd, J = 15.5, 10.7 Hz, H-13), 5.90 (1H, d, J = 10.7 Hz, H-12), 5.84 (1H, dd, J = 17.6, 10.8 Hz, H-6), 5.54 (1H, d, J = 15.5 Hz, H-14), 4.90 (1H, dd, J = 17.6, 1.4 Hz, H-5), 4.88 (1H, dd, J = 10.8, 1.4 Hz, H-5), 4.81 (1H, br s, H-4), 4.61 (1H, br s, H-4), 3.15 (3H, s, 15-OCH_3), 2.05 (1H, app. dd, J = 12.8, 3.4 Hz, H-2), 2.04-1.98 (1H, m, H-10), 1.79 (3H, s, H-18), 1.71 (3H, s, H-16), 1.67 (1H, app. ddd, J = 12.8 Hz, H-1), 1.58-1.54 (2H, m, H-9), 1.56-1.52 (1H, m, H-8), 1.49-1.45 (1H, m, H-1), 1.46-1.41 (1H, m, H-8), 1.29 (6H, s, H-19, H-20), 1.03 (3H, s, H-17). ^{13}C NMR (150 MHz, CD_3OD) δ 151.6 (CH, C-6), 148.9 (C, C-3), 144.4 (C, C-11), 137.2 (CH, C-14), 127.6 (CH, C-13), 123.9 (CH, C-12), 112.7 (CH_2, C-4), 110.4 (CH_2, C-5), 76.8 (C, C-15), 54.0 (CH, C-2), 50.6 (CH_3, 15-OCH_3), 49.2 (CH, C-10), 41.1 (CH_2, C-8), 40.8 (C, C-7), 34.0 (CH_2, C-1), 27.8 (CH_2, C-9), 26.4 (CH_3, C-19, C-20), 25.3 (CH_3, C-16), 17.2 (CH_3, C-17), 15.3 (CH_3, C-18). HRESIMS m/z 325.2512 $[M + Na]^+$ (calcd for $C_{21}H_{34}ONa$, 325.2502). **54** (0.9 mg, 3 μmol, 12%): $[\alpha]^{25}_D$ = -9.43 (c 0.0583, CH_3OH); IR υ_{max} 3040, 2973, 2857, 1651, 1446, 1383, 1359, 1253, 1165, 1075, 970, 862, 844, 756 cm^{-1}. ^{1}H NMR (600 MHz, CD_3OD) δ 6.39 (1H, dd, J = 15.5, 10.7 Hz, H-13), 5.85 (1H, d, J = 10.7 Hz, H-12), 5.53 (1H, d, J = 15.5 Hz, H-14), 5.26-4.94 (1.2H, br m, H-2, H-6), 4.79 (0.4H, br d, J = 12.0 Hz, H-6), 4.56 (0.4H, br d, J = 10.5 Hz, H-2), 3.15 (3H, br s, 15-OCH_3), 2.40-2.34 (1H, m, H-8), 2.33-2.25 (1H, m, H-5), 2.23-2.17 (1H, m, H-1), 2.20-2.15 (1H, m, H-4), 2.10-2.06 (1H, m, H-1), 2.09-2.04 (1H, m, H-8), 2.08-2.03 (1H, m, H-5), 2.02-1.96 (1H, m, H-10), 1.94-1.87 (1H, m, J = 12.4, 5.3 Hz, H-4), 1.78 (1.2H, s, H-18), 1.75 (1.8H, s, H-18), 1.72-1.63 (2H, m, H-9), 1.59-1.55 (1.2H, br s, H-16), 1.54 (1.8H, s, H-16), 1.53-1.47 (1.8H, br s, H-17), 1.41 (1.2H, s, H-17), 1.29 (6H, s, H-19, H-20). ^{13}C NMR (150 MHz, CD_3OD) δ 147.9 (C, C-11), 138.9 (C, C-7), 137.1 (CH, C-14), 132.6 (CH, C-2), 131.2 (C, C-3),

127.6 (CH, C-13), 127.5 (CH, C-6), 122.9 (CH, C-12), 76.8 (C, C-15), 54.8 (CH, C-10), 50.6, (CH_3, 15-OCH_3), 42.8 (CH_2, C-8), 40.6 (CH_2, C-4), 35.8 (CH_2, C-1), 34.8 (CH_2, C-9), 27.6 (CH_2, C-5), 26.4 (CH_3, C-19, C-20), 17.0 (CH_3, C-16), 16.6 (CH_3, C-17), 14.7 (CH_3, C-18). HRESIMS m/z 325.2499 $[M + Na]^+$ (calcd for $C_{21}H_{34}ONa$, 325.2502).

3.4.5 Synthesis and characterization of truncated pseudopterosin mimics

2,6-Dimethoxyphenolic-2,3,4,6-tetra-O-benzoyl-β-D-galactopyranoside (90). The 2,6-dimethoxyphenol (**86**, 30.0 mg, 0.195 mmol) and benzoylated glycosyl trichloroacetimidate (**88**, 151.0 mg, 0.229 mmol) were dissolved in anhydrous CH_2Cl_2 (8 mL) and stirred with 3Å molecular sieves (~0.5 g) under an N_2 atmosphere for 20 min. Afterwards, the mixture was cooled to -78 °C and $BF_3{\cdot}Et_2O$ (0.206 mmol) was added. After stirring for 2.5 h at -78 °C, the glycosyl donor had completely reacted, as indicated by TLC analysis (hexanes:TBME 1:1). The reaction was quenched with Et_3N (100 µL, excess), diluted with EtOAc, and partitioned with DI H_2O. The EtOAc phase was recovered and subjected to the standard work up procedure to provide the crude product, which was purified by MPLC (silica, hexanes → TBME) to give the desired glycoside (**90**, 101.9 mg, 0.139 mmol, 71%). **90**: (white solid); $[\alpha]^{25}_D$ +67.4 (c 0.1917, CH_2Cl_2); IR υ_{max} 3065, 2962, 2939, 2838, 1726, 1601, 1479, 1258, 1109, 1069, 709 cm^{-1}. ^1H NMR (C_6D_6, 600 MHz) δ 8.11 (2H, d, J = 7.8 Hz), 8.10 (2H, d, J = 7.8 Hz), 8.07 (2H, d, J = 7.8 Hz), 8.00 (2H, d, J = 7.8 Hz), 7.10 (1H, t, J = 7.5 Hz), 7.06 (1H, t, J = 7.5 Hz), 7.03 (2H, t, J = 7.7 Hz), 7.01 (1H, t, J = 7.5 Hz), 6.92 (2H, t, J = 7.6 Hz), 6.91 (2H, t, J = 7.6 Hz), 6.85 (1H, t, J = 7.5 Hz), 6.78 (1H, t, J = 8.4 Hz, H-4), 6.73 (2H, t, J = 7.7 Hz), 6.60 (1H,

dd, J = 10.4, 7.9 Hz, H-2′), 6.23 (2H, d, J = 8.4 Hz, H-3), 6.14 (1H, dd, J = 3.6, 1.2 Hz, H-4′), 5.80 (1H, dd, J = 10.4, 3.6 Hz, H-3′), 5.44 (1H, d, J = 7.9 Hz, H-1′), 4.67 (1H, dd, J = 11.3, 6.6 Hz, H-6′), 4.36 (1H, dd, J = 11.3, 6.6 Hz, H-6′), 3.66 (1H, app. ddd, J = 6.6, 1.2 Hz, H-5′), 3.25 (6H, s, 2-OCH_3, 6-OCH_3). ^{13}C NMR (C_6D_6, 150 MHz) δ 165.9 (C), 165.8 (C), 165.7 (C), 165.4 (C), 153.9 (C, C-2), 136.1 (C, C-1), 133.2 (CH), 133.1 (CH), 133.0 (CH), 132.7 (CH), 130.8 (CH), 130.5 (CH), 130.3 (CH), 130.1 (CH), 130.1 (C), 130.0 (C), 129.7 (C), 129.6 (C), 128.8 (CH), 128.6 (CH), 128.4 (CH), 128.3 (CH), 124.6 (CH, C-4), 106.1 (CH, C-3), 103.1 (CH, C-1′), 72.7 (CH, C-3′), 71.9 (CH, C-5′), 71.4 (CH, C-2′), 68.8 (CH, C-4′), 62.3 (CH_2, C-6′), 55.9 (CH_3, 2-OCH_3, 6-OCH_3). HRESIMS m/z 755.2088 $[M + Na]^+$ (calcd for $C_{42}H_{36}O_{12}Na$, 755.2099).

2,6-Dimethoxyphenolic-β-D-galactopyranoside (92). The benzoylated glycoside (**90**, 40.3 mg, 55.0 μmol) was stirred with K_2CO_3 (38.8 mg, 0.281 mmol) in MeOH:TBME (5:1, 3 mL) for 20 h. After the deprotection was completed, as indicated by TLC analysis (hexanes:TBME 1:1), the reaction mixture was diluted with H_2O and desalted by solid phase extraction (C_{18}, 19:1 H_2O:CH_3OH). The product was then eluted with CH_3OH and purified by RP-MPLC (C_{18}, $H_2O \rightarrow CH_3OH$) to provide **90** (12.5 mg, 39.5 μmol, 72%). **90**: (colorless solid); $[\alpha]^{25}_D$ −15.9 (c 0.8333, CH_2Cl_2); IR υ_{max} 3388, 3008, 2940, 2841, 1599, 1480, 1256, 1108, 1072 cm^{-1}. ^{1}H NMR (DMSO-d_6, 600 MHz) δ 6.97 (1H, t, J = 8.4 Hz, H-4), 6.66 (2H, d, J = 8.4 Hz, H-3), 4.83 (1H, d, J = 7.6 Hz, H-1′), 4.79–4.74 (2H, m, 2′-OH, 3′-OH), 4.50-4.44 (2H, m, 4′-OH, 6′-OH), 3.74 (6H, s, 2-OCH_3), 3.67 (1H, app. t, J = 3.3 Hz, H-4′), 3.56–3.52 (1H, m, H-2′), 3.56–3.52 (1H, m, H-6′), 3.37–3.33 (1H, m, H-3′), 3.36–3.32 (1H, m, H-6′), 3.27 (1H, app. t, J = 6.3 Hz, H-5′). ^{13}C

NMR (DMSO-d_6, 150 MHz) δ 153.0 (C, C-2), 134.9 (C, C-1), 123.7 (CH, C-4), 106.6 (CH, C-3), 103.5 (CH, C-1′), 75.5 (CH, C-5′), 73.2 (CH, C-3′), 71.4 (CH, C-2′), 67.9 (CH, C-4′), 60.1 (CH_2, C-6′), 56.4 (CH_3, 2-OCH_3). HRESIMS m/z 339.1043 $[M + Na]^+$ (calcd for $C_{14}H_{20}O_8Na$, 339.1050).

2,6-Dimethoxy-3-(3-methylbut-2-enyl)phenolic-2,3,4,6-tetra-O-benzoyl-β-D-galactopyranoside (91). The glycosylation procedure that was described for the synthesis of **90** was repeated using 3-prenyl-2,6-dimethoxyphenol (**89**, 44.6 mg, 0.201 mmol) as the glycosyl accepting substrate and the benzoylated glycosyl trichloroacetimidate (**88**, 175.6 mg, 0.266 mmol) and. The crude product was separated by MPLC (silica, hexanes → TBME) to purify the desired glycoside (**91**, 149.1 mg, 0.186 mmol, 93%). **91**: (pale yellow solid); $[\alpha]^{25}_D$ +75.9 (c 0.225, CH_2Cl_2); IR υ_{max} 3063, 2966, 2936, 1726, 1602, 1493, 1451, 1094, 1069, 709 cm^{-1}. ^1H NMR (CD_3OD, 600 MHz) δ 8.13 (2H, d, J = 7.7 Hz), 7.90 (4H, d, J = 7.8 Hz), 7.75 (2H, d, J = 7.8 Hz), 7.67 (1H, t, J = 7.7 Hz), 7.57 (1H, t, J = 7.7 Hz), 7.54 (2H, t, J = 7.7 Hz), 7.51 (1H, t, J = 7.7 Hz), 7.45 (1H, t, J = 7.6 Hz), 7.40 (2H, t, J = 7.7 Hz), 7.36 (2H, t, J = 7.7 Hz), 7.25 (2H, t, J = 7.7 Hz), 6.80 (1H, d, J = 8.6 Hz, H-4), 6.54 (1H, d, J = 8.6 Hz, H-5), 6.03 (1H, dd, J = 10.3, 8.0 Hz, H-2′), 6.00 (1H, app. d, J = 3.4 Hz, H-4′), 5.78 (1H, dd, J = 10.3, 3.4 Hz, H-3′), 5.64 (1H, d, J = 8.0 Hz, H-1′), 5.14 (1H, app. t, J = 7.4 Hz, H-8), 4.58 (1H, dd, J = 10.8, 7.0 Hz, H-6′), 4.54 (1H, app. dd, J = 7.0, 4.9 Hz, H-5′), 4.47 (1H, dd, J = 10.8, 4.9 Hz, H-6′), 3.75 (3H, s, 2-OCH_3), 3.53 (3H, s, 6-OCH_3), 3.17-3.09 (2H, m, H-7), 1.67 (3H, s, H-11), 1.64 (3H, s, H-10). ^{13}C NMR (CD_3OD, 150 MHz) δ 167.5 (C), 167.3 (C), 167.1 (C), 166.8 (C), 152.7 (C, C-2), 152.6 (C, C-6), 139.9 (C, C-1), 134.9 (CH), 134.6

(CH), 134.5 (CH), 134.4 (CH), 134.3 (C), 132.9 (C), 131.0 (C), 131.0 (C), 130.9 (CH), 130.7 (CH), 130.6 (CH), 130.5 (CH), 130.2 (C, C-9), 129.9 (CH), 129.6 (CH), 129.1 (CH, C-3), 129.0 (CH), 128.7 (CH), 125.9 (CH, C-4), 124.4 (CH, C-8), 109.0 (CH, C-5), 103.2 (CH, C-1′), 73.6 (CH, C-3′), 73.0 (CH, C-5′), 72.3 (CH, C-2′), 70.2 (CH, C-4′), 63.7 (CH_2, C-6′), 61.7 (CH_3, 2-OCH_3), 56.6 (CH_3, 6-OCH_3), 29.0 (CH_2, C-7), 25.9 (CH_3, C-11), 17.9 (CH_3, C-10). HRESIMS m/z 823.2754 $[M + Na]^+$ (calcd for $C_{47}H_{44}O_{12}Na$, 823.2725).

2,6-Dimethoxy-3-(3-methylbut-2-enyl)phenolic-β-D-galactopyranoside (93). The deprotection procedure that was described for the synthesis of **92** was repeated for **91** (38.5 mg, 48.1 μmol) and K_2CO_3 (33.4 mg, 0.242 mmol). The product was purified using the method described for **92** to yield the desired glycoside (**93**, 13.9 mg, 36.2 μmol, 75%). **93**: (colorless solid); $[\alpha]^{25}_D$ −6.44 (c 0.6917, CH_3OH); IR υ_{max} 3392, 2967, 2914, 1602, 1494, 1463, 1442, 1090 cm^{-1}. ^1H NMR (DMSO-d_6, 600 MHz) δ 6.79 (1H, d, J = 8.5 Hz, H-4), 6.70 (1H, d, J = 8.5 Hz, H-5), 5.20 (1H, app. t, J = 7.3 Hz, H-8), 4.96 (1H, d, J = 4.5 Hz, 2′-OH), 4.92 (1H, d, J = 7.6 Hz, H-1′), 4.80 (1H, d, J = 5.3 Hz, 3′-OH), 4.49 (1H, m, 4′-OH), 4.47 (1H, m, 6′-OH), 3.76 (3H, s, 6-OCH_3), 3.72 (3H, s, 2-OCH_3), 3.68 (1H, app. dd, J = 3.5 Hz, H-4′), 3.59–3.55 (1H, m, H-2′), 3.55–3.52 (1H, m, H-6′), 3.39–3.36 (1H, m, H-3′), 3.35–3.32 (2H, m, H-6′), 3.29 (1H, app. t, J = 6.2 Hz, H-5′), 3.24–3.15 (2H, m, H-7), 1.68 (3H, s, H-11), 1.67 (3H, s, H-10). ^{13}C NMR (DMSO-d_6, 150 MHz) δ 151.6 (C, C-2), 151.1 (C, C-6), 138.8 (C, C-1), 131.3 (C, C-9), 127.4 (C, C-3), 123.6 (CH, C-4), 123.4 (CH, C-8), 108.9 (CH, C-5), 103.2 (CH, C-1′), 75.5 (CH, C-5′), 73.2 (CH, C-3′), 71.4 (CH, C-2′), 67.9 (CH, C-4′), 60.7 (CH_3, 6-OCH_3), 60.1 (CH_2,

C-6′), 56.5 (CH_3, 2-OCH_3), 27.7 (CH_2, C-7), 25.5 (CH_3, C-11), 17.6 (CH_3, C-10). HRESIMS m/z 407.1687 $[M + Na]^+$ (calcd for $C_{19}H_{28}O_8Na$, 407.1676).

CHAPTER 4

IDENTIFICATION OF PUTATIVE PROTEIN TARGETS OF PSEUDOPTEROXAZOLE: A CHEMICAL PROTEOMICS APPROACH

4.1 Introduction

Mycobacterium tuberculosis, the etiologic agent of tuberculosis (TB), causes nearly one and a half million deaths annually, and is thus one of the leading causes of infectious disease-related mortality.[174a] Primarily affecting impoverished regions around the globe, M. tuberculosis has established a latent infection in one third of the human population.[175] Although TB may be cured with a six- to nine-month antibiotic treatment, low rates of patient compliance and the emergence of multidrug-resistant strains of M. tuberculosis pose a tremendous challenge for the management of TB.[190, 193] The requirement of such prolonged treatments is largely attributed to a physiological state of non-replicating persistence (NRP), a dormant phenotype of M. tuberculosis that exhibits antibiotic tolerance.[189] Shortening the duration of antitubercular chemotherapy by targeting NRP mycobacteria and combatting drug resistance are among the major goals of current TB research.

Bedaquiline (Sirturo^{TM}) was recently approved by the FDA for the treatment of drug resistant TB infections, representing the first new antitubercular drug class in approximately 40 years.[288] This diarylquinoline inhibits adenosine triphosphate (ATP) biosynthesis by interacting with ATP synthase subunit c, as demonstrated by affinity chromatography[198] and analysis of bedaquiline-resistant strains of M. tuberculosis.[289] Owing to its unique mechanism of action, bedaquiline underwent accelerated FDA approval to provide an alternative therapeutic option for patients with multi-drug resistant (MDR)- and extensively-drug resistant (XDR)-TB, despite serious concerns over the

drug's safety.[290] Therefore, a strong demand still exists for novel antitubercular drugs, particularly those exhibiting a unique mechanism of action and low toxicity.

Pseudopteroxazole (**30**, **Figure 4.1**) is an amphilectane diterpene first isolated by Rodríguez et al. from the alcyonacean coral Pseudopterogorgia elisabethae.[154] This natural product shows strong inhibitory activity against M. tuberculosis $H_{37}Rv$ [minimum inhibitory concentration (MIC): 15 μg/mL]. Exploiting the structural resemblance between **30** and the aglycone of pseudopterosins G-J (**33**-**36**), a semisynthesis of **30** and a library of novel analogues was accomplished.[160] These synthetic efforts provided structure-activity relationships (SAR) and led to the discovery of a histidine-derived analogue, 21-((1H-imidazol-5-yl)methyl)-pseudopteroxazole (PtxHis, **37**).[161]

The activity of PtxHis (**37**) against NRP M. tuberculosis (MIC: 12 μg/mL) is significantly greater than **30** (MIC: 50 μg/mL), yet on par with its potency against M. tuberculosis $H_{37}Rv$ (MIC: 13 μg/mL).[161] The selectivity index [the ratio between the Vero cell half-maximal inhibitory concentration (IC_{50}) and M. tuberculosis MIC values] of **37**, like that of **30** and **33**-**36**, is highly appealing as no cytotoxicity was observed in the Vero cell assay (IC_{50}: >128 μg/mL). Although the activity of **37** against M. tuberculosis $H_{37}Rv$ was modest (MIC: 13 μg/mL, 34 μM) in comparison to isoniazid and rifampin, its activity compared favorably to ethambutol (4.6–9.2 μM), kanamycin (2.5–10.3 μM), capreomycin (0.94–3.7 μM) and cycloserine (122–490 μM).[291]

In collaboration with Dr. Malcolm McCulloch, the MIC of **30** against a panel of isogenic mono-resistant M. tuberculosis $H_{37}Rv$ strains was determined (**Table 4.1**).[161] These strains were resistant to one of the following antitubercular drugs: rifampin, isoniazid, streptomycin, kanamycin, cycloserine, and moxifloxacin. Any cross-resistance

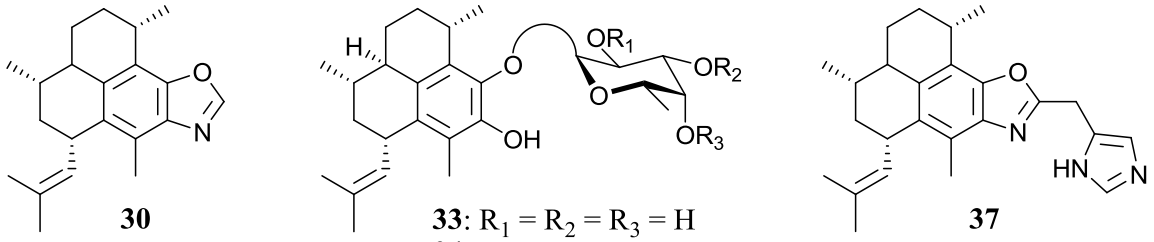

30

33: $R_1 = R_2 = R_3 = H$
34: $R_1 = Ac$, $R_2 = R_3 = H$
35: $R_2 = Ac$, $R_1 = R_3 = H$
36: $R_3 = Ac$, $R_1 = R_2 = H$

37

Figure 4.1. Chemical structures of pseudopteroxazole (**30**) and pseudopterosins G-J (**33-36**), antitubercular diterpenes isolated from Pseudopterogorgia elisabethae. Also shown is the structure of PtxHis (**37**), a semisynthetic analogue with significant activity in the low-oxygen-recovery assay (LORA).

Table 4.1. Susceptibility of isogenic mono-resistant M. tuberculosis $H_{37}Rv$ strains to pseudopteroxazole (**30**), rifampin, and isoniazid.[161]

	MIC (μg/mL)[a]						
Compound	$H_{37}Rv$	RMP^r	INH^r	SM^r	KM^r	CS^r	MOX^r
30	7	8	8	14	16	14	8
Rifampin	0.03	>3.3	0.02	0.08	0.02	0.01	0.02
Isoniazid	0.03	0.12	>1.10	0.13	0.13	0.12	0.03

[a] Microplate Alamar blue assay (MABA) against wild-type M. tuberculosis $H_{37}Rv$ ($H_{37}Rv$) and M. tuberculosis $H_{37}Rv$ isogenic strains resistant to rifampin (RMP^r), isoniazid (INH^r), streptomycin (SM^r), kanamycin (KM^r), cycloserine (CS^r) and moxifloxacin (MOX^r).

between **30** and the above clinical drugs would therefore indicate a shared mode of action. Although **30** was significantly less potent than rifampin and isoniazid, no cross-resistance was observed, suggesting that it may exert its antitubercular activity through a distinct mechanism of action.

The aim of this research is to identify putative protein targets of pseudopteroxazole (**30**) by means of chemical proteomics using one of two complementary approaches: affinity chromatography and photoaffinity labeling. Given the unique structure and antitubercular properties of **30**, this chemical proteomics approach may lead to the discovery of a novel therapeutic target for TB treatment. To achieve this aim, a collection of small molecule probes was prepared through a semisynthetic approach beginning with pseudopterosins G-J (**33**-**36**), a mixture of diterpene glycosides isolated from P. elisabethae. The molecular design of these probes was directed by SAR in order to maintain the high binding affinity of these ligands to their protein targets. The antimicrobial spectrum of **30** was also further characterized to investigate its antimicrobial properties.

4.2 Results and discussion

4.2.1 Determination of the antimicrobial spectrum of pseudopteroxazole

In addition to their activity against mycobacterial species, pseudopteroxazole (**30**) and pseudopterosins G-J (**33**-**36**) are known to inhibit the growth of methicillin-resistant Staphylococcus aureus (MRSA) and vancomycin-resistant Enterococcus (VRE) with IC_{50} values as low as 1-2 μg/mL.[160] The pseudopterosins also show activity against Streptococcus pyogenes, Staphylococcus aureus, and Enterococcus faecalis.[292] These results suggest that **30** may have clinical applications in addition to antitubercular chemotherapy. Therefore, the antimicrobial spectrum of **30** and **33** was further characterized against a taxonomically diverse panel of 22 Gram-positive and 10 Gram-negative clinical isolates using the agar disk diffusion method.[293] On account of the interesting activity of PtxHis (**37**) against NRP M. tuberculosis, this semisynthetic analogue was also evaluated in these assays.

The microbial collection included a variety of bacteria that cause human illness, including Streptococcus pneumoniaea, Pseudomonas aeruginosa, S. aureus, a number of common foodborne pathogens (Clostridium perfringens, Campylobacter jejuni, and Listeria monocytogenes), as well as Streptococcus equi subsp. equi, Rhodococcus equi, Bordetella bronchiseptica, and several other bacteria that are significant pathogens in domesticated animals and commonly encountered in veterinary medicine. Other organisms, such as Micrococcus luteus and B. bronchiseptica, are relatively innocuous or rarely infect humans. The panel of control antibiotics, which included penicillin G, vancomycin, rifampin, gentamicin, ciprofloxacin, and polymyxin, was carefully selected

so as to encompass a variety of antimicrobial mechanisms of action. Cross-resistance between pseudopteroxazole (**30**) and one of the antibiotic controls might indicate a common mechanism and aid the identification of its cellular target.

At a concentration of 50 μg/disk, diterpenes **30**, **33**, and **37** were active against Gram-positive bacteria and largely inactive against Gram-negative strains (**Tables 4.2-4.3**), presumably attributable to the low permeability of the lipopolysaccharide layer. Obstruction of peptidoglycan biosynthesis was conceivable, however, the observed activity against NRP M. tuberculosis suggested otherwise. Notably, the NRP phenotype is known to tolerate antimycobacterial drugs targeting cell wall biosynthesis, including isoniazid, cycloserine, and ethambutol.[294] Unlike penicillin G and vancomycin, the activity against MRSA and VRE was comparable to the activity against S. aureus and E. faecalis respectively, indicating their different antimicrobial mechanisms of action. Among the Gram-positive bacteria, no growth inhibition of Erysipelothrix rhusiopathiae and S. pneumoniaea was observed after administrating a 50 μg/disk concentration of each diterpene. Pseudopterosin G (**33**) typically induced larger zones of growth inhibition, presumably due to the greater aqueous solubility compared to pseudopteroxazole (**30**) and PtxHis (**37**).

The greater susceptibility of Escherichia coli imp to the antibiotic controls is due to the higher permeability of its lipopolysaccharide layer. Polymyxin B, a cationic detergent that disrupts cell membrane integrity, was an exception as the zone of growth inhibition remained unchanged. Diterpenes **30**, **33**, and **37**, however, were inactive against both E. coli strains, suggesting their low permeability across the

Table 4.2. Spectrum of antimicrobial activity of pseudopteroxazole (**30**), pseudopterosin G (**33**), and PtxHis (**37**) using the disk diffusion susceptibility method [zones of inhibition measured in mm (n = 2)].[a]

Compound	DMSO	**30**	**33**	**37**	Pen.	Van.	Rif.	Gen.	Cip.	Poly.
Concentration (μg/disk)	-	50	50	50	2	5	2	10	0.5	300[b]
Gram-negative										
Escherichia coli imp	10	9	8	9	19	17	32	31	36	22
Gram-positive										
Arcanobacterium pyogenes	10	10	11	15	50	21	48	27	9	-
Clostridium perfringens	10	12	18	9	36	21	35	13	18	14
Corynebacterium pseudotuberculosis	-	12	18	14	26	16	38	18	26	7
Erysipelothrix rhusiopathiae	-	-	-	-	35	-	-	-	28	-
Listeria monocytogenes	-	10[c]	20	11	27	15	25	26	10	11
Micrococcus luteus	8	10	21	14	38	22	43	34	10	19
Rhodococcus equi	7	11	17	9	19[c]	24	25	21	15[c]	11
Staphylococcus aureus	-	9	16	10	47	16	29	25	20	11
Staphylococcus warneri	-	9	15	9	37	16	36	33	22	21
Streptococcus agalactiae	8	12	22	10	37	17	32	10	14	16
Streptococcus canis	8	11	30	11	45	20	36	12	12	16
Streptococcus equi subsp. equi	8	11	26	13	54	20	45	34	13	21
Streptococcus equi subsp. zooepidemicus	-	12	19	12	50	21	38	28	14	23
Streptococcus pneumoniae	-	-	-	-	38	20	29	12	-	-
Streptococcus suis	-	10	19	10	32	17	24	13[c]	14	7
MRSA	-	11	16	8	-	15	38	20	15	7
Mycobacterium smegmatis	9	14	29	14	8	25	21	38	17	25
Mycobacterium diernhoferi	10	12	31	16	11	22	21	32	42	28

[a] The disk diffusions assays were completed with the assistance of Dr. Malcolm McCulloch and Nick McCarville. [b] Units/disk. [c] Zone of partial growth inhibition.

Table 4.3. Spectrum of antimicrobial activity of pseudopteroxazole (**30**), pseudopterosin G (**33**), and PtxHis (**37**) using the disk diffusion susceptibility method [zone of growth inhibition measured in mm (n = 2)].[a]

Compound	DMSO	**30**	**33**	**37**	Pen.	Van.	Rif.	Gen.	Cip.	Poly.
Concentration (μg/disk)	-	50	50	50	20	20	20	10	0.5	300[b]
Gram-negative[d]										
Actinobacillus equuli	7	9	9	-	15	-	23	17	34	21
Campylobacter jejuni	-	-	-	-	-	-	-	26	18	16
Escherichia coli	-	-	7	-	10	-	15	23	18	18
Mannheimia haemolytica	-	-	-	-	42	-	31	15	32	23
Proteus mirabilis	-	10[c]	28[c]	20[c]	16	-	18[c]	22	35	23[c]
Pseudomonas aeruginosa	-	-	-	-	-	-	10	19	22	20
Gram-positive										
Bacillus cereus	-	8	15	8	14[c]	20	21	28	20	12
Enterococcus faecalis	-	10	17	9	28	20	14	9	12	-
VRE	-	10	16	8	14	-	18	15	-	-

[a] The disk diffusions assays were completed with the assistance of Dr. Malcolm McCulloch and Nick McCarville. [b] Units/disk. [c] Zone of partial growth inhibition. [d] The diterpenes showed no activity against the following Gram-negative bacteria: Bordetella bronchiseptica, Klebsiella pneumoniae, and Salmonella enterica serovar Typhimurium.

Overall, no growth inhibition was observed for the remaining vehicle controls, with the following exceptions: H_2O and 20% CH_3OH inhibited the growth of M. diernhoferi (8 mm), while 0.3% HCO_2H inhibited the growth of A. equuli (7 mm), S. canis (7 mm), S. equi subsp. equi (8 mm), S. equi subsp. zooepidemicus (7 mm), and M. diernhoferi (10 mm). An analogue of elisabatin B, 14,15-dihydro-elisabatin B, was also tested and showed no activity.

Abbreviations for control antibiotics: penicillin G (Pen.), vancomycin (Van.), rifampin (Rif.), gentamicin (Gen.), ciprofloxacin (Cip.), polymyxin B (Poly.).

lipopolysaccharide layer may not be responsible for their inactivity against this Gram-negative bacterium. Application of these diterpenes onto the surface of the blood agar, a media used to support the growth of fastidious organisms, resulted in clear zones under the surface of the agar. This observation suggests that these diterpenes may induce hemolysis. Regardless, no cross-resistance to pseudopteroxazole (**30**) was observed for any of the control antibiotics, and as a result, there were no indications of a potential mechanism of action.

4.2.2 Designing the affinity-based pseudopteroxazole probes

The basic design of a pseudopteroxazole probe is primarily determined by the requirements of the following affinity-based techniques: affinity chromatography and photoaffinity labeling. To identify putative targets by affinity chromatography, an immobilized probe must consist of the diterpene scaffold as well as an appropriate spacer (**Figure 4.2**). The pseudopteroxazole scaffold enables the biochemical isolation of the target protein(s), by virtue of specific binding interactions, while the spacer improves binding affinity by reducing steric interactions with the stationary support.[231] Considering the hydrophobic nature of pseudopteroxazole (**30**), ethylene glycol (EG)-based spacers were chosen over their polymethylene-based counterparts in order to impart greater water solubility to the chemical probe. The 4,7,10-trioxa-1,13-tridecanediamine (**94**) was chosen as a hydrophilic spacer due to its prevalence in the affinity chromatography literature and commercial availability.[237] Owing to the remarkable binding affinity between biotin and streptavidin (dissociation constant, $K_d = 10^{-15}$ M),[228] biotinylation of small molecule probes is a common strategy for enabling their immobilization to

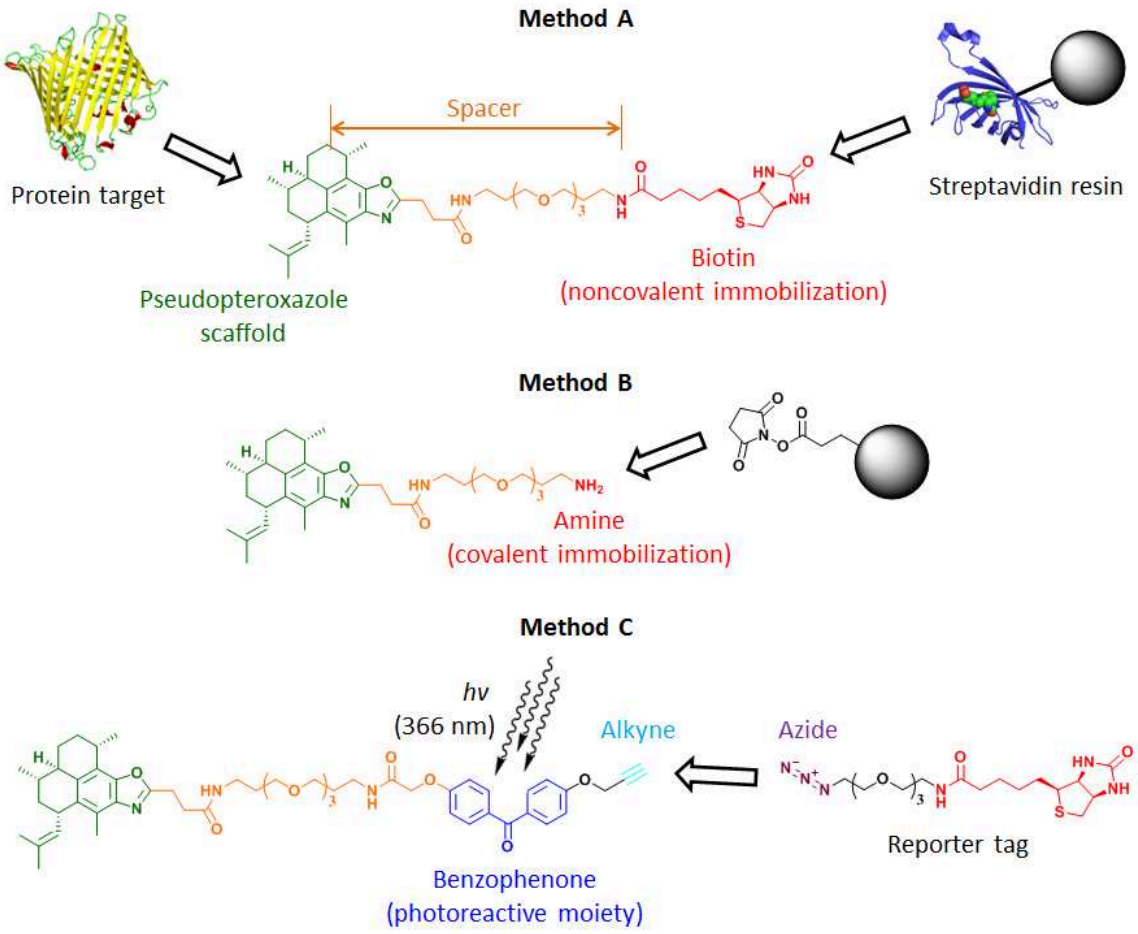

Figure 4.2. Chemical anatomy of the affinity-based pseudopteroxazole probes for the identification of protein target candidates by affinity chromatography or photoaffinity labeling approaches. Method A: Non-covalent immobilization of a biotinylated probe onto a streptavidin resin. Method B: Covalent immobilization of an amino-functionalized probe onto NHS-activated agarose. Method C: Photoaffinity labeling of a protein target by irradiation of benzophenone, followed by the attachment of a biotin reporter tag using click chemistry. Photolabeled targets may subsequently be enriched over a streptavidin resin and/or visualized by Western blotting analysis with a biotin reporter.

streptavidin resins.[227a, 229] Covalent immobilization of small molecules to an NHS-activated agarose support may otherwise be pursued.[237]

The photoaffinity probe consists of three essential features: the diterpene scaffold, a benzophenone photoreactive group, and an alkyne handle (**Figure 4.2**). The reversible binding interaction between the pseudopteroxazole scaffold and the protein target(s) maintains their close association while the benzophenone moiety, under exposure to long-wave UV light, becomes activated as a diradical and reacts with C-H bonds of amino acids to form a covalent adduct.[295] Benzophenone was selected as the photoreactive moiety for its excellent stability under ambient light, high labeling efficiency, and the lower energy required for photoexcitation.[242] After labeling the protein target(s), the alkyne moiety serves as a synthetic handle for the purpose of introducing a reporter tag via Cu(I)-catalyzed azide-alkyne [3 + 2] cycloaddition.[249]

Composed of biotin or tetramethylrhodamine moieties, the reporter tag facilitates the visualization of photolabeled proteins through Western blotting analysis or fluorescence scanning.[246, 252] The alkyne handle, unlike a reporter tag, is sterically inconspicuous and has a relatively minor impact on cellular uptake. As a result, the bioorthogonal "click chemistry" is amenable to in situ protein labeling, i.e. identifying specific binding interactions within the context of a living cell.[249] This strategy is advantageous in consideration of the limitations of cell lysate preparation, which may fail to extract the protein target(s) of interest or cause denaturation.[221, 224] The positions of the azide and alkyne moieties may be reversed, however, the directionality of the click reaction has a significant impact on the signal-to-noise ratio. Azido-functionalized reporter tags provide lower background labeling than their alkyne counterparts,[249] hence

the azide-alkyne arrangement in **Figure 4.2**. Although an EG-based spacer may not be necessary, higher photolabeling efficiency may be achieved by increasing the conformational flexibility of the benzophenone moiety.[241]

The challenge of synthesizing a pseudopteroxazole probe is the retention of the desired antimycobacterial activity, which serves as an indication of binding activity. As a result, SAR must be examined to identify positions on the diterpene scaffold that are suitable for synthetic modification. Unfortunately, only two positions on the scaffold of pseudopteroxazole (**30**) were amenable to chemical synthesis, the oxazole ring and the double bond. If the antimicrobial activity prohibits modification of these functionalities, the fucose moiety of pseudopterosin G (**33**) or the phenolic hydroxyl group of its aglycone methyl ether (**95**) could provide alternative sites for attaching the EG spacer. Although there is greater interest in **30** as an antitubercular agent, **33** and **95** are similar with regards to their structure and antimicrobial activity, suggesting they have a common mechanism of action.

4.2.3 Synthesizing the pseudopteroxazole chemical probes

The pseudopteroxazole probes were prepared using a semisynthetic approach beginning with a mixture of pseudopterosins G-J (**33**-**36**, **Figure 4.3**), which was extracted from P. elisabethae.[296] The fucose moiety of **33**-**36** was cleaved by acid hydrolysis to provide the pseudopterosin G-J aglycone ortho-quinone (**96**), an intermediate required for introducing the oxazole ring. The ortho-quinone (**96**) was condensed with 4,7,10-trioxa-1,13-tridecanediamine (**94**) to attach the EG spacer, which occurred with concomitant ring closure to install the oxazole ring, providing

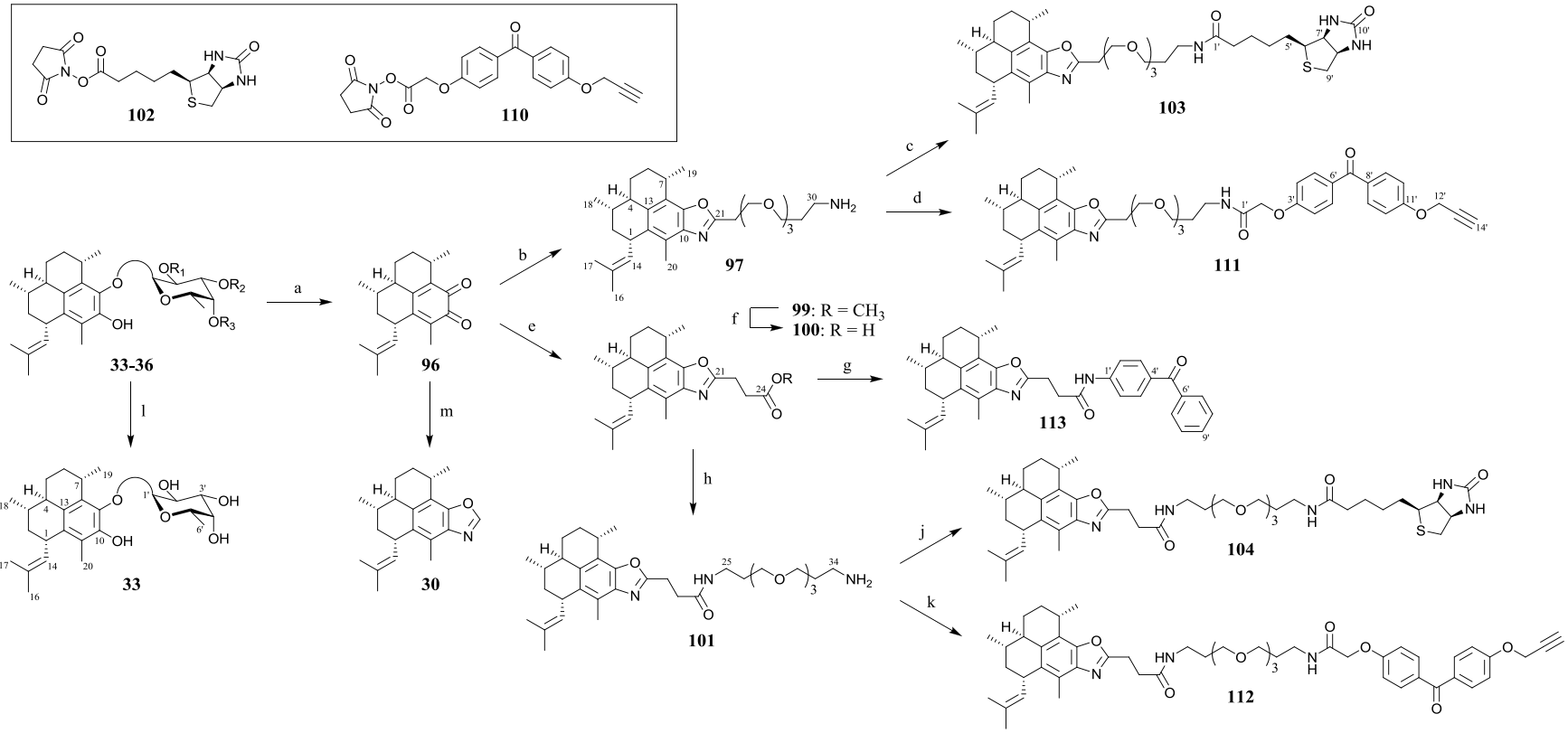

Figure 4.3. The semisynthetic route to the pseudopteroxazole probes. Reagents and conditions: (a) HCl, Δ CH_3OH:H_2O (19:1), ~59%. (b) Ag_2O (4.4 eq), 4,7,10-trioxa-1,13-tridecanediamine (**94**, 6.5 eq), Δ CH_3OH, 14% (unoptimized). (c) biotin-NHS (**102**), Et_3N, DMF, 18%. (d) BPA-NHS (**110**), Et_3N, CH_2Cl_2, 39%. (e) Ag_2O (5.5 eq), L-glutamic acid 5-methyl ester (**98**, 4.5 eq), Δ CH_3OH, 46%. (f) LiOH, acetone:H_2O (10:1), 93%. (g) (i) NHS, DCC, CH_2Cl_2. (ii) 4-aminobenzophenone, 24% over two steps. (h) (i) NHS, DCC, CH_2Cl_2. (ii) **94** (excess), 53% over two steps. (j) **102**, Et_3N, DMF, 53%. (k) **110**, Et_3N, CH_2Cl_2, 49%. (l) K_2CO_3, CH_3OH, ~62%. (m) Ag_2O (2.8 eq), glycine (13.5 eq), 16%. The synthesis of **102** and **110** is outlined in **Figure C.2**.

Ptx-EG_3-NH_2 (**97**). This one-pot synthesis, however, was low yielding and resulted in the formation of multiple side products, including a significant amount of the oxazole regioisomer (5:1 ratio), which complicated the purification and characterization of **97**.

As an alternative approach, the ortho-quinone (**96**) was condensed with L-glutamic acid 5-methyl ester (**98**) to furnish PtxGlu-CO_2CH_3 (**99**) in 46% yield (**Figure 4.3**). The methyl ester functionality of **99** was removed by base hydrolysis to provide PtxGlu-CO_2H (**100**) in high yields (93%). In a one-pot reaction, the carboxylic acid (**100**) was subsequently activated as an NHS ester and immediately reacted with 4,7,10-trioxa-1,13-tridecanediamine (**94**) to introduce the EG spacer of PtxGlu-EG_3-NH_2 (**101**). For this reaction, **94** was added in excess to prevent the formation of dimers. After activating biotin as an NHS ester (**102**, **Figure C.2**), the primary amino groups of **97** and **101** were biotinylated to provide chemical probes Ptx-EG_3-Biotin (**103**) and PtxGlu-EG_3-Biotin (**104**), respectively.

For the preparation of photoaffinity probes, a divergent strategy was envisaged. The amino-functionalized Ptx-EG_3-NH_2 (**97**) and PtxGlu-EG_3-NH_2 (**101**) could serve as synthetic precursors to the photoaffinity probes because of the synthetic accessibility of their primary amino groups. To generate an amino-specific benzophenone-alkyne (BPA) attachment, commercially available 4,4'-dihydroxybenzophenone (**105**) was O-alkylated with propargyl bromide to introduce the alkyne handle (**106**, **Figure C.2**), a reaction that also provided 4,4'-dipropargyloxy-benzophenone (**107**) as a side product. The product of this reaction underwent an additional O-alkylation using tert-butyl bromoacetate to synthesize the tert-butyl ester (**108**), which was immediately subjected to acid hydrolysis using trifluoroacetic acid to provide the carboxylic acid (**109**) in 93% overall yield.

The carboxylic acid (**109**) was then activated with NHS in the presence of DIC to provide an NHS ester intermediate (**110**, **Figure C.2**), which was cross-linked with Ptx-EG_3-NH_2 (**97**) and PtxGlu-EG_3-NH_2 (**101**) to furnish the two photoaffinity probes, Ptx-EG_3-BPA (**111**) and PtxGlu-EG_3-BPA (**112**, **Figure 4.3**). To determine if the EG spacer was necessary, a photoaffinity probe lacking the spacer was synthesized. For this synthesis, PtxGlu-CO_2H (**100**) was activated as an NHS ester, as described previously, and then reacted with 4-aminobenzophenone to attach the photoreactive moiety. This reaction provided PtxGlu-BP (**113**) with a low yield of 24%.

4.2.4 Synthesizing the pseudopterosin-derived chemical probes

The pseudopterosin G-J aglycone methyl ether (**95**), a compound that is structurally similar to pseudopteroxazole (**30**), provided an opportunity to attach the EG spacer to the phenolic hydroxyl group. The aglycone methyl ether (**95**) was prepared using a known procedure, beginning with a methylation using iodomethane followed by the removal of the fucose moiety by acid hydrolysis (**Figure 4.4**).[161, 280a] Afterwards, **95** underwent phenolic O-alkylation using tert-butyl bromoacetate to provide Ps-CO_2t-Bu (**114**), a synthetic intermediate containing a site for spacer attachment. The tert-butyl ester (**114**) was then subjected to base hydrolysis to generate Ps-CO_2H (**115**) in high yields. During the purification of **115** by RP-MPLC, the methyl ester (**116**, Ps-CO_2CH_3) was obtained as a solvent-derived artifact. Upon activation of **115** as an NHS ester, using a previously described procedure, the 4,7,10-trioxa-1,13-tridecanediamine (**94**) was added in excess to provide Ps-EG_3-NH_2 (**117**). A product of dimerization, Ps-EG_3-Ps (**118**), was also isolated from this reaction and kept for antimicrobial evaluation. After

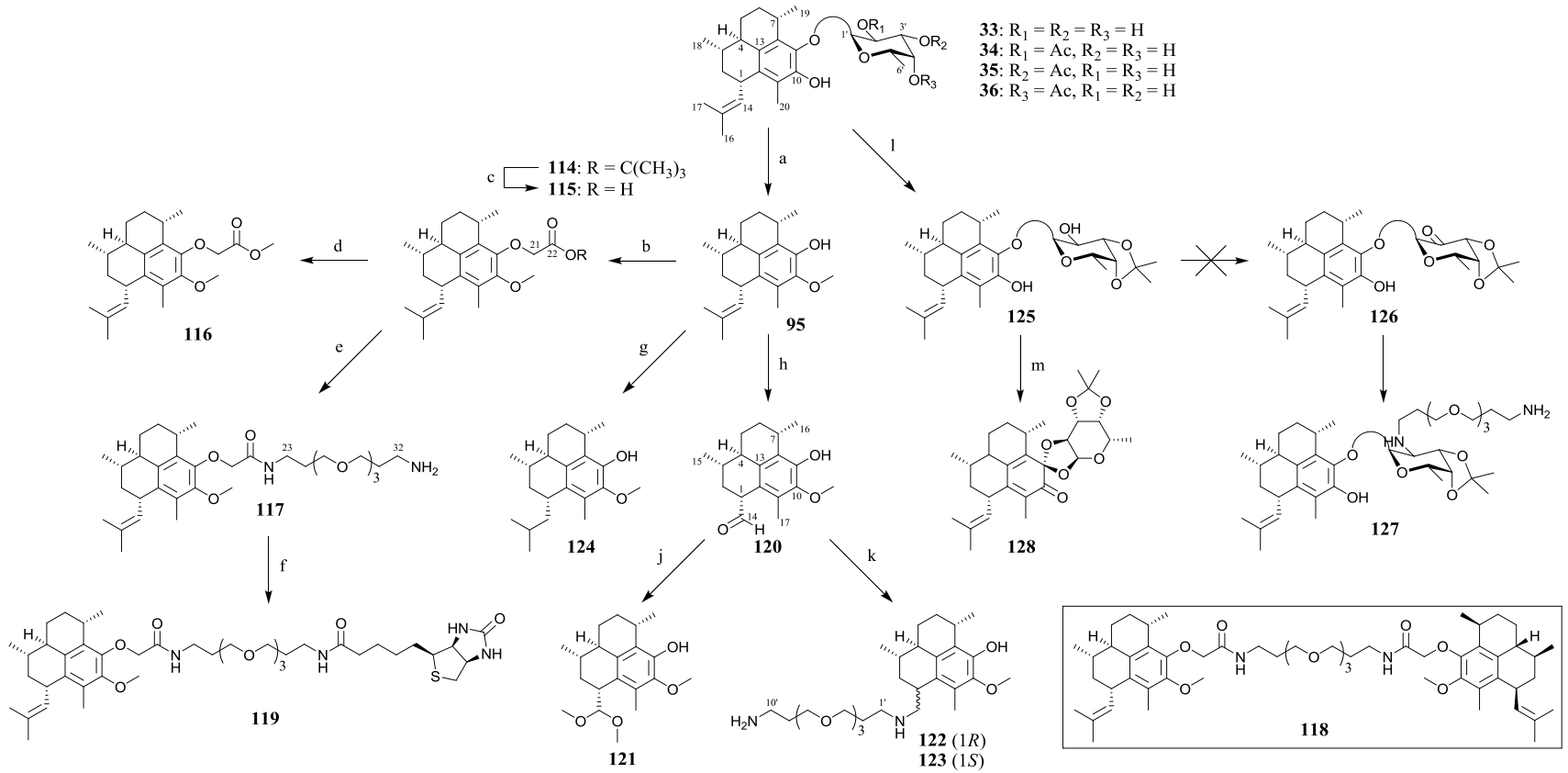

Figure 4.4. The semisynthetic route to the pseudopterosin-derived probes. Reagents and conditions: (a) (i) CH_3I, K_2CO_3, acetone. (ii) HCl, Δ CH_3OH:H_2O (19:1), ~62% over two steps. (b) tert-butyl bromoacetate (4.2 equiv.), K_2CO_3, acetone, 50%. (c) LiOH, THF, 95%. (d) **115**, CH_3OH, HCO_2H (0.1%). (e) (i) **115**, NHS, DIC, CH_2Cl_2. (ii) 4,7,10-trioxa-1,13-tridecanediamine (**94**, excess), 66% over two steps. (f) biotin-NHS (**102**), 14% over three steps. (g) H_2, Pd/C, EtOAc, 96%. (h) (i) O_3, CH_3OH:pyridine (1:1), -78°C. (ii) $(CH_3)_2S$, 69% over two steps. (j) CH_3OH:pyridine (1:1). (k) (i) **94** (excess), CH_2Cl_2. (ii) $NaBH_4$, 48% over two steps. (l) **33**, TsOH (0.03 eq), acetone, 87%. (m) Dess-Martin periodinane (1.2 eq), CH_2Cl_2, 23%. Compound **118** was obtained as a side product from reaction (e).

attaching the EG spacer, a biotin moiety was introduced to the primary amino group of **117** using biotin-NHS (**102**) to provide Ps-EG_3-Biotin (**119**) as an additional chemical probe for antimicrobial evaluation.

Previous SAR data for the oxazole position has indicated that the antimicrobial activity may tolerate structural variations at this position,[160-161] however, the biological significance of the double bond was unknown. To expedite the interrogation of SAR around this position, the pseudopterosin G-J aglycone methyl ether (**95**) was selected for derivatization instead of pseudopteroxazole (**30**). The aglycone methyl ether (**95**) was more readily available in large quantities, whereas **30** was synthesized as a mixture of regioisomers in lower yields (16%). Therefore, the double bond of **95** was oxidatively cleaved by ozonolysis and reduced with dimethyl sulfide to generate the aldehyde, CHO-PsOH (**120**), in 69% yield (**Figure 4.4**). During this synthesis, nucleophilic addition of CH_3OH to **120** also occurred, resulting in the formation of an acetal (**121**, $CH(OCH_3)_2$-PsOH). This side reaction was mitigated by shortening the duration of ozone treatment.

The carbonyl functionality of **120** provided a handle for attaching the EG spacer by way of a reductive amination. Similar to the preparation of PtxGlu-EG_3-NH_2 (**101**) and Ps-EG_3-NH_2 (**117**), this reaction was carried out with an excess of 4,7,10-trioxa-1,13-tridecanediamine (**94**) to avoid dimerization. The secondary aldimine intermediate was subsequently reduced by $NaBH_4$ to provide H_2N-EG_3-PsOH (**122**), as well as its epimerized analogue (**123**, epi-H_2N-EG_3-PsOH). These two products were separated by semi-preparative RP-HPLC and the configuration at C-1 was determined by examining NOESY correlations. To provide additional SAR data, the aglycone methyl ether (**95**)

was hydrogenated to form compound **124** by vigorously stirring a solution of **95** and Pd/C under a H_2 atmosphere.

The carbohydrate moiety of pseudopterosin G (**33**) served as an additional site for attaching the EG-based spacer. Initially, all acetate functionalities of **34**-**36** were removed through base hydrolysis, which facilitated the purification of the desired glycoside (**33**, **Figure 4.4**). To achieve regioselectivity for spacer attachment, the fucose moiety underwent acetonide protection by adding a substoichiometric amount of TsOH to an acetone solution of **33**. Preferential ketalization of the 3',4'-diol was anticipated because of their favorable cis orientation. Indeed, NMR spectroscopic analysis of the pseudopterosin G acetonide (**125**) confirmed that the acetonide moiety was located at this position.

Oxidation of the remaining secondary hydroxyl group with Dess-Martin periodinane was then attempted to provide the ketone (**126**), a synthetic intermediate poised for the attachment of an EG spacer via reductive amination (i.e. **127**, **Figure 4.4**). Unfortunately, the pseudopterosin G diketal (**128**) was obtained as an unanticipated product, whose structure was confirmed by NMR spectroscopy and comparison to the literature on pseudopterosins and their redox properties.[297] Although other synthetic strategies could have been pursued, no further efforts toward a glycosidic probe were made as other chemical probes were available for antimicrobial evaluation. Unlike the ortho-quinone (**96**), however, the diketal (**128**) possesses a single carbonyl group at C-9 and may therefore be exploited as an intermediate for synthesizing novel pseudopteroxazole analogues without simultaneous formation of regioisomer side products.

4.2.5 Antimicrobial evaluation of chemical probes and analysis of structure-activity relationships

To identify the protein target(s) of pseudopteroxazole (**30**) by chemical proteomics, an assessment of SAR must be carried out to determine the biological relevance of probe candidates. Previous work showed that the antimycobacterial activity had tolerated a variety of unnatural substituents at the oxazole position of **30**.[160] The antitubercular activities exhibited by **30**, PtxHis (**37**), pseudopterosins G-J (**33**-**36**), and the aglycone methyl ether (**95**) were also comparable,[161] further indicating that the oxazole ring is a suitable position for synthetic modification. All semisynthetic compounds were evaluated for antimicrobial activity against MRSA, VRE, S. warneri, M. smegmatis, and M. diernhoferi using the microbroth dilution method (**Table 4.4**). The SAR data from this study has again demonstrated that substituents at the oxazole position are well-tolerated. A preliminary insight into the biological significance of the double bond position has also been provided for the first time.

The PtxGlu-CO_2CH_3 (**99**) and PtxGlu-CO_2H (**100**) analogues were also synthesized and evaluated for antimicrobial activity by Dr. Malcolm McCulloch in a previous study.[160-161] The relative inactivity of the methyl ester (**99**) compared to the carboxylic acid (**100**) suggested that the attachment of an EG spacer would be detrimental for the antimicrobial activity. By contrast, PtxGlu-EG_3-NH_2 (**101**) was significantly more potent than **99** and comparable to **100**. The structurally related Ptx-EG_3-NH_2 (**97**) showed even greater activity. Although Ptx-EG_3-Biotin (**103**) and PtxGlu-EG_3-Biotin (**104**) were mostly inactive against MRSA, VRE, and S. warneri, these biotinylated probes inhibited the growth of the mycobacterial species with MICs as low

Table 4.4. Antimicrobial activity of pseudopteroxazole and pseudopterosin-derived probes as well as other synthetic intermediates, as determined by the microbroth dilution method (n = 3).

	IC_{50} (μg/mL)			MIC (μg/mL)	
Compound	MRSA[a]	VRE[a]	S. warneri[a]	M. smegmatis	M. diernhoferi
30	26	3.4	>128	2	4
33	2.6	2.9	4.0	2	4
36	2.5	4.6	5.7	4	2
95	5.4	5.9	>128	4	4
96	>128	>128	>128	128	64
97	5.2	2.7	3.1	2	2
99	>128	>128	>128	>128	>128
100	7.6	11	16	4	4
101	9.7	9.2	12	8	8
103	>128	>128	>128	8	64
104	>128	68	>128	8	16
111	>128	>128	>128	>128	>128
112	>128	>128	>128	>128	>128
113	>128	>128	>128	>128	>128
114	>128	>128	>128	>128	>128
115	21	14	48	16	16
116	>128	>128	>128	>128	>128
117	8.9	6.7	6.4	4	4
118	>128	>128	>128	>128	>128
119	>128	128 (65%)[a]	>128	8	16
120	52	59	49	64	64
121	>128	52	>128	32	32
122	>128	>128	96	128	128
123	77	52	19	64	64
124	4.2	3.6	>128	4	4
125	>128	>128	>128	>128	>128
128	>128	>128	>128	>128	>128
129	>128	>128	>128	>128	>128
130	>128	>128	>128	>128	>128
Vancomycin	0.8	-	0.8	-	-
Rifampin	-	0.4	-	2	4
Isoniazid	-	-	-	2	0.5

[a] Assay was completed by Martine Lanteigne. [b] Percent growth inhibition at the indicated concentration.

as 8 μg/mL. On the basis of their antimycobacterial activity, these biotinylated probes became promising tools for identifying putative protein targets of pseudopteroxazole (**30**) by affinity chromatography.

Attaching substituents to the phenolic hydroxyl group of the aglycone methyl ether (**95**) has previously been shown to diminish the antimicrobial activity.[161] For instance, the dimethyl ether, carbamate, and triflate analogues of **95** were largely inactive against M. tuberculosis and nonpathogenic mycobacterial species.[161] While the Ps-CO_2t-Bu (**114**) and Ps-CO_2CH_3 (**116**) analogues were consistent with this SAR data, Ps-CO_2H (**115**) showed moderate antimicrobial activity. Meanwhile, the attachment of the EG spacer to synthesize Ps-EG_3-NH_2 (**117**) further improved the activity. Similar to Ptx-EG_3-Biotin (**103**) and PtxGlu-EG_3-Biotin (**104**), the biotinylated probe Ps-EG_3-Biotin (**119**) was unable to inhibit the growth of MRSA, VRE, and S. warneri. However, the antimycobacterial activity of **119** was nearly identical to that of **103** and **104**. As a result, this biotinylated probe was selected for affinity chromatography.

In consideration of the antimycobacterial activities of Ptx-EG_3-Biotin (**103**), PtxGlu-EG_3-Biotin (**104**), and Ps-EG_3-Biotin (**119**), the photoaffinity probes Ptx-EG_3-BPA (**111**) and PtxGlu-EG_3-BPA (**112**) were anticipated to have activity as well. Unfortunately, these chemical probes were inactive, even against the mycobacterial species. According to the observed SAR trends, the binding activity of **111** and **112** to the cell target may be attained in the context of a cell lysate. An in vitro photolabeling experiment may therefore provide valuable information. The inactivity of these compounds may instead be due to their greater hydrophobicity, which may prohibit their uptake and ability to interact with the cell target(s). For instance, the Ps-EG_3-Ps (**118**), a

product of dimerization, and PtxGlu-BP (**113**) showed no activity as well. In addition, hydrophobic oxazole substituents were previously shown to weaken the antimicrobial activity of pseudopteroxazole (**30**).[160-161]

The importance of the double bond region of pseudopteroxazole (**30**) was indicated by the weak antimicrobial activity of CHO-PsOH (**120**) and $CH(OCH_3)_2$-PsOH (**121**). The H_2N-EG_3-PsOH (**122**) and epi-H_2N-EG_3-PsOH (**123**) were associated with a decrease in the activity, although the latter showed modest activity, hinting at the importance of the configuration at C-1. Regardless, the observed SAR indicated that **122** was best suited as an inactive control probe for identifying non-specific binding (NSB). The unsaturation at the double bond position did not appear to be necessary as the antimicrobial activity of the aglycone methyl ether (**95**) was nearly identical to its hydrogenated analogue (**124**). Considering that **124** showed marginal improvements against MRSA and VRE, further investigation of the SAR around the double bond position could lead to the discovery of novel analogues with greater potency.

4.2.6 Interpreting the structure-activity relationships for pseudopteroxazole analogues

The observed antimicrobial activity of the chemical probes served as a qualitative assessment of their relative binding affinity to the cell target(s). Although antimicrobial assays were necessary for examining SAR, variations in solubility and cell permeability must be taken into consideration as these are factors that may significantly impact the antimicrobial activity and confound the interpretation of SAR.[217] In a number of cases, the SAR data emanating from this study demonstrated the importance of polarity and relative aqueous solubility, particularly for the oxazole substituents of pseudopteroxazole

analogues. These results also complement previous efforts aiming to further understand the SAR of this class of natural products.[160-161]

Among the most active compounds in these antimicrobial assays, despite their long EG-based appendages, were Ptx-EG_3-NH_2 (**97**), PtxGlu-EG_3-NH_2 (**101**), and Ps-EG_3-NH_2 (**117**). Their strong activity may be due to a significant increase in polarity and aqueous solubility with the incorporation of the EG spacers. Although the methyl esters, PtxGlu-CO_2CH_3 (**99**) and Ps-CO_2CH_3 (**116**), were inactive, their carboxylic acid counterparts exhibited greater aqueous solubility and showed moderate antimicrobial activity. Biotinylation of **97** and **101** minimally impacted the antimycobacterial activity, whereas the attachment of hydrophobic benzophenone moieties, to provide the photoaffinity probes, resulted in a loss of activity. Similar SAR trends were also observed for Ps-EG_3-NH_2 (**117**) and Ps-EG_3-Biotin (**119**) which, unlike other analogues of the aglycone methyl ether (**95**), displayed good antimycobacterial activity.[161]

4.2.7 The inactive pseudopteroxazole probe: A control for non-specific binding

Identifying cell targets by chemical proteomics is often complicated by the presence of NSB.[223] The high background generated by NSB confuses the analysis and may obscure targets of low abundance. Proteins of high abundance may exhibit low binding affinity to the resin, often as a result of generic hydrophobic or electrostatic interactions.[223] Although a competitive elution may expedite the process of target deconvolution by separating the protein target(s) from NSB, the limited aqueous solubility of pseudopteroxazole (**30**) and pseudopterosin G (**33**) may hinder their application as competitive ligands.[217] To differentiate between NSB and specific binding

interactions, an inactive control probe may be employed instead. The NSB profiles exhibited by active and inactive probes are often indistinguishable, owing to their structural similarity. As a result, preferential binding to the active probe is indicative of a target protein candidate.

Three basic designs exist for an inactive probe: chiral isomers,[233] structurally related analogues,[234] or analogues with differential spacer attachment.[235] An inactive chiral isomer is generally the most effective control,[233] however, the biological significance of the chiral centers of pseudopteroxazole (**30**) is unknown. Modifying the stereochemical configuration of the diterpene skeleton also poses a formidable synthetic obstacle. As described earlier, previous SAR data indicated that an inactive structurally related probe could be obtained by attaching the EG spacer to the phenolic hydroxyl group of the aglycone methyl ether (**95**). Regrettably, this SAR trend was inconsistent with Ps-EG_3-NH_2 (**117**) and Ps-EG_3-Biotin (**119**), whose antimicrobial activity prohibited their application as inactive control probes. Attaching the spacer to the double bond position of **95** abolished the activity, as shown by H_2N-EG_3-PsOH (**122**). This data suggested that **122** may serve as an inactive control considering that the specific binding interaction with the protein target(s) appears to be disrupted by differential placement of the spacer.

In addition to the H_2N-EG_3-PsOH (**122**), a set of generic control probes was also synthesized. Unlike **122**, the generic controls contained all features of the probe except for the diterpene scaffold. As a result, any potential hydrophobic-type NSB with the scaffold may be unaccounted for. Nonetheless, the supplementary generic control probes were synthesized by reacting NHS esters **102** and **110** with an excess of 4,7,10-trioxa-

1,13-tridecanediamine (**94**) to provide Biotin-EG_3-NH_2 (**129**) and BPA-EG_3-NH_2 (**130**) (**Figure C.2**). As expected, control probe **129** showed no antimicrobial activity (**Table 4.4**), verifying that the spacer and biotin moieties were not contributing to the growth inhibitory properties of biotinylated probes.

4.2.8 Investigating the protein binding interactions of pseudopteroxazole probes by affinity chromatography

A preliminary assessment of protein binding interactions was carried out using the two biotinylated pseudopteroxazole probes, Ptx-EG_3-Biotin (**103**) and PtxGlu-EG_3-Biotin (**104**). Owing to its fast growth rate and few biosafety restrictions, M. smegmatis commonly serves as a surrogate for M. tuberculosis.[298] Considering that both mycobacterial species are susceptible to pseudopteroxazole (**30**), cell lysates of M. smegmatis were suitable for these affinity chromatography experiments. Preparation of mycobacterial lysates by sonication provided satisfactory protein extraction with minimal degradation, as indicated by the large amount of high molecular weight protein observed during gel electrophoretic analysis (data not shown). The general experimental protocol for conducting the affinity chromatography was adapted from the work of Yamamoto et al.[236] Unless specified otherwise, binding proteins were eluted from the affinity resins under denaturing conditions by heating in Laemmli buffer, as described in Section 4.4.3. Protein samples were then separated by SDS-PAGE and stained with Coomassie to visualize the binding proteins (**Figure 4.5**).

Attempts to identify protein target candidates by competitive displacement were carried out by pre-incubating the lysate with pseudopteroxazole (**30**) or pseudopterosin G

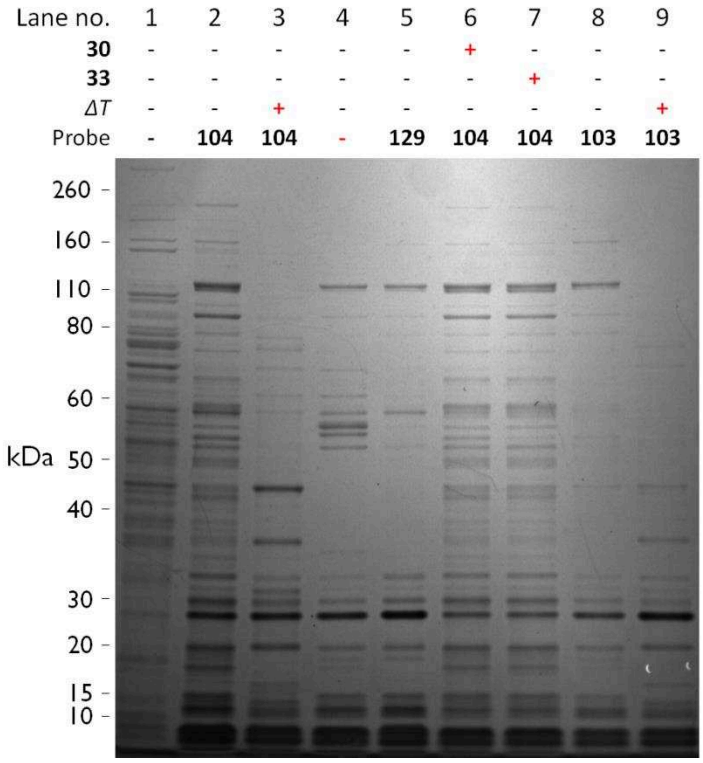

Figure 4.5. Gel electrophoretic analysis of Mycobacterium smegmatis proteins bound to the biotinylated probes, Ptx-EG_3-Biotin (**103**) and PtxGlu-EG_3-Biotin (**104**). Notes and conditions: The eluted proteins were resolved over a 4-12% polyacrylamide gel. Both competitive displacements represent a pre-incubation of the M. smegmatis lysate with either pseudopteroxazole (**30**) or pseudopterosin G (**33**). Description of gel lanes: Lane 1, M. smegmatis lysate; lane 2, affinity capture of proteins with **104**; lane 3, heat-denatured control; lane 4, affinity capture of proteins with unblocked streptavidin resin; lane 5, affinity capture of proteins with Biotin-EG_3-NH_2 (**129**); lane 6, competitive displacement control; lane 7, competitive displacement control; lane 8, affinity capture of proteins with **103**; lane 9, heat-denatured control.

(**33**). Unfortunately, these experiments were unsuccessful as no gel bands disappeared (**Figure 4.5**), a result that may be attributed to the low aqueous solubility of **30** and **33**. In addition, a considerable amount of NSB was observed, particularly for PtxGlu-EG_3-Biotin (**104**). The diterpene scaffold may have been subjected to generic hydrophobic interactions, given the distinct protein profiles exhibited by **104** and Biotin-EG_3-NH_2 (**129**). As a result, no putative targets were identified in this experiment. Efforts to lower the NSB background by varying the concentration of polysorbate 20 (P20) in the phosphate buffer were unsuccessful. The streptavidin resin, after immobilizing the biotinylated probe, was also pre-incubated with bovine serum albumin to block NSB, however, no effect on NSB was observed. Washing the affinity resin additional times with buffer also failed to lower the background.

4.2.9 Examining an arylsulfonamide model of the affinity chromatography system

Preliminary experimentation with Ptx-EG_3-Biotin (**103**) and PtxGlu-EG_3-Biotin (**104**) in the affinity chromatography experiment presented a number of potential issues. For instance, the technical aspects of the protocol, especially the pH and ionic strength of the phosphate buffer, may have a tremendous impact on protein stability and overall binding affinity. Although a comprehensive analysis of various buffer conditions may be pursued, such efforts may be futile if the probe is unable to support a specific binding interaction due to improper design. Notably, the length of the EG-based spacer may have been insufficient, resulting in steric clashing and reduced binding affinity of potential targets.[231] Therefore, the probe design was evaluated by simulating the affinity chromatography system using a model probe.

Carbonic anhydrase (CA) is a mammalian enzyme that catalyzes the interconversion of carbon dioxide and water to bicarbonate.[299] The clinical relevance of CA inhibition, particularly for the treatment of glaucoma, has long been recognized, thus a wide range of inhibitors are commercially available.[300] Arylsulfonamides (ASAs) are a family of CA inhibitors that bind to the zinc prosthetic group of the enzyme as an anion (SO_2NH^-).[301] The binding interaction between CA and ASAs is well characterized and known to tolerate a wide variety of substituents at the para position of the aromatic ring,[302] including EG-based moieties.[303] The specific binding of CA to an ASA probe of the same molecular design as PtxGlu-EG_3-Biotin (**104**) and Ps-EG_3-Biotin (**119**) could serve as a model to ensure proper functioning of the affinity chromatography system.

To synthesize the ASA model probe, an EG-based spacer was attached to 4-carboxybenzene sulfonamide (**131**), utilizing synthetic methodology described earlier for PtxGlu-EG_3-NH_2 (**101**) and Ps-EG_3-NH_2 (**117**). The product of this reaction was purified by RP-MPLC, providing ASA-EG_3-NH_2 (**132**) in 57% yield over two steps (**Figure 4.6**). The subsequent biotinylation of **132** using biotin-NHS (**102**) provided the ASA-EG_3-Biotin (**133**) probe in 78% yield. Biochemical isolation of CA by affinity chromatography was then attempted by immobilizing **133** onto a streptavidin resin and repeating the experimental protocol that was previously described for Ptx-EG_3-Biotin (**103**) and PtxGlu-EG_3-Biotin (**104**).

Regrettably, attempts to isolate CA onto the ASA-EG_3-Biotin (**133**)-immobilized streptavidin resin were unsuccessful (**Figure C.3**). Indeed, no decrease in the CA band intensity was observed for the heat-denatured control, indicating a non-specific interaction. Pre-incubating CA with acetazolamide (AAZ), a known CA inhibitor,

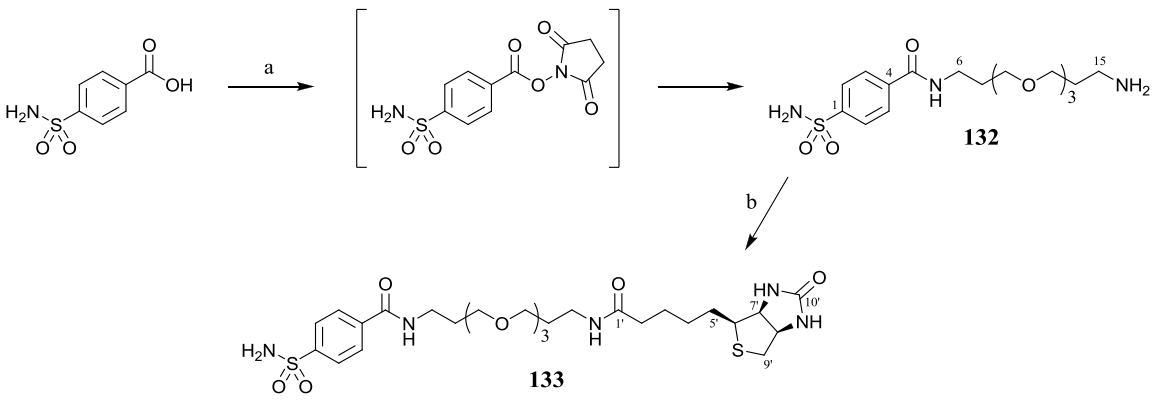

Figure 4.6. Synthesis of a biotinylated arylsulfonamide probe (**133**, ASA-EG_3-Biotin) as a simulation of the pseudopteroxazole and pseudopterosin-derived probes. Reagents and conditions: (a) (i) NHS, DIC, THF. (ii) 4,7,10-trioxa-1,13-tridecanediamine (**94**, excess), 57% over two steps. (b) biotin-NHS (**102**), DMF, 78%.

showed no decrease in band intensity either. Competitive elution of CA with AAZ was also attempted, but to no avail. The apparent lack of specific CA binding may be due to the EG spacer, whose short length may have been insufficient for minimizing the steric repulsions between CA and streptavidin. As a result, biotinylated probes ASA-EG_{23}-Biotin (**134**) and PtxGlu-EG_{23}-Biotin (**135**), whose spacers contained 20 additional EG units, were synthesized (**Figure 4.7**). The commercial availability of Biotin-EG_{23}-NH_2 (**136**) expedited the preparation of these biotinylated probes. Upon repeating the affinity chromatography experiment, no specific binding interaction between CA and the **134**-immobilized streptavidin resin was observed, despite the increased length of the EG spacer (**Figure C.4**).

4.2.10 Covalent immobilization of small molecules onto activated agarose supports

The specific binding of CA to either ASA-EG_3-Biotin (**133**) or ASA-EG_{23}-Biotin (**134**) was unsuccessful using the biotin-streptavidin system for reasons that were not clear. As a result, an alternative set of affinity resins was prepared by covalent immobilization of small molecules onto a stationary support. Although having served as synthetic precursors to biotinylated probes, PtxGlu-EG_3-NH_2 (**101**) and Ps-EG_3-NH_2 (**117**) were also poised for immobilization onto NHS-activated agarose. Immobilization of H_2N-EG_3-PsOH (**122**), an analogue showing no antimycobacterial activity, may also provide an inactive control. Furthermore, by exploiting the availability of ASA-EG_3-NH_2 (**132**), a model of the affinity chromatography system could be developed rapidly to validate the technical aspects of the experiment. Ptx-EG_3-NH_2 (**97**) and epi-H_2N-EG_3-PsOH (**123**),

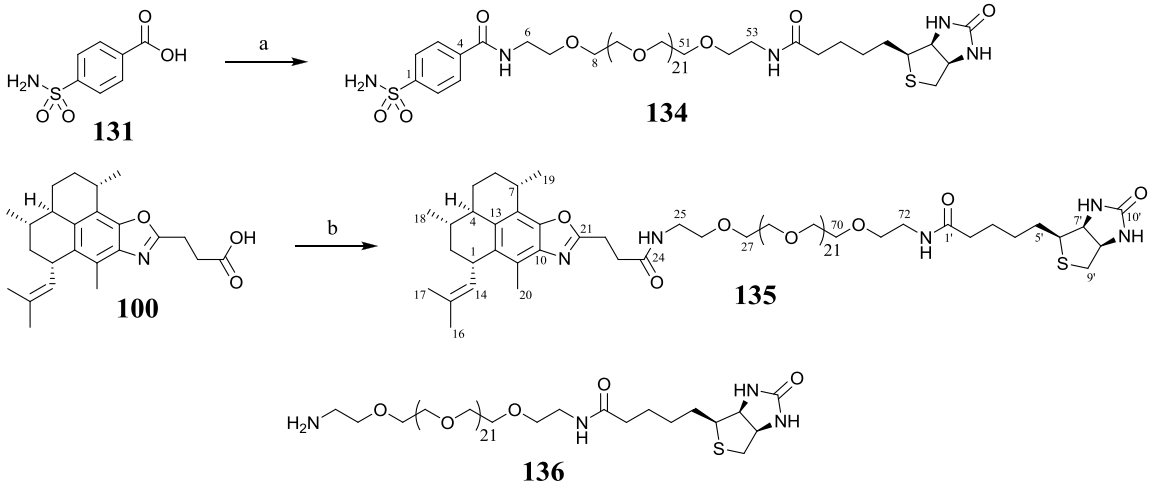

Figure 4.7. Synthesis of biotinylated arylsulfonamide (**134**, ASA-EG_{23}-Biotin) and pseudopteroxazole (**135**, PtxGlu-EG_{23}-Biotin) probes with increased EG spacer lengths. Reagents and conditions: (a) (i) PtxGlu-CO_2H (**100**, 3.2 eq), NHS (4.6 eq), DIC (13 eq), DMF. (ii) Biotin-EG_{23}-NH_2 (**136**), Et_3N (4.4 eq), 58% over two steps. (b) (i) 4-carboxybenzene sulfonamide (**131**, 2.6 eq) NHS (3.2 eq), DIC (10 eq), DMF. (ii) **136**, Et_3N (4.8 eq), 59% over two steps.

close analogues of **101** and **122**, respectively, were not available in sufficient quantities for generating additional affinity resins.

To immobilize PtxGlu-EG_3-NH_2 (**101**), Ps-EG_3-NH_2 (**117**), H_2N-EG_3-PsOH (**122**), and ASA-EG_3-NH_2 (**132**) onto a stationary support, these small molecule ligands were incubated with NHS-activated agarose in anhydrous DMSO following a literature protocol (**Figure 4.8**).[304] Although the secondary amino group of **122** remained unprotected, slower acylation at this position was anticipitated due to steric influences. Regardless, an excess of **122** was added to the activated resin to avoid potential acylation at both positions. The reaction yield and overall density of the immobilized small molecules were estimated by LC-HRESIMS quantification of unreacted primary amine (**Figures C.5-C.6**). Standard curves for each primary amine were generated and their concentrations within the reaction media were calculated. Greater than 95% of **101**, **117**, and **132** were immobilized to generate PtxGlu-EG_3-Agarose (**137**), Ps-EG_3-Agarose (**138**), and ASA-EG_3-Agarose (**139**), respectively. Meanwhile, approximately 4% of **122** had reacted to provide Agarose-EG_3-PsOH (**140**), indicating a saturation of the NHS esters. The molar density of the immobilized ligands was calculated using these reaction yields. A generic control resin (**141**) was also prepared by deactivating the NHS esters with 2-(2-aminoethoxy)ethanol (**142**), a shorter mimic of the EG spacer.

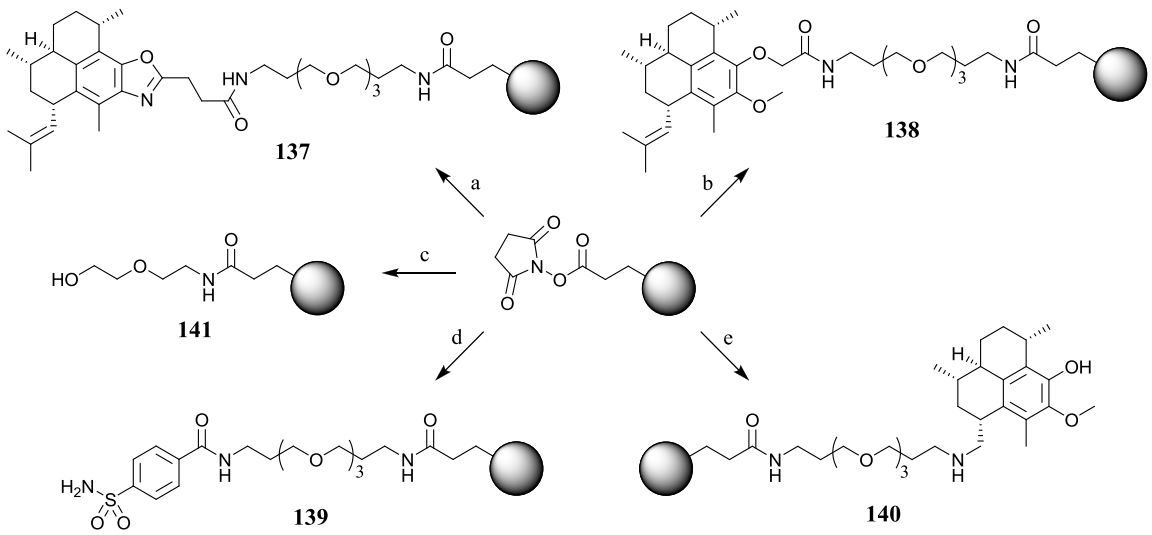

Figure 4.8. Preparation of PtxGlu-EG_3-Agarose (**137**), Ps-EG_3-Agarose (**138**), the generic control resin (**141**), ASA-EG_3-Agarose (**139**), and Agarose-EG_3-PsOH (**140**) by covalent immobilization of small molecules onto NHS-activated agarose (**143**). Reagents and conditions: (a) PtxGlu-EG_3-NH_2 (**101**), 2% Et_3N, DMSO, >95%. (b) Ps-EG_3-NH_2 (**117**), 2% Et_3N, DMSO, >95%. (c) 2-(2-aminoethoxy)ethanol (**142**), 2% Et_3N, DMSO. (d) ASA-EG_3-NH_2 (**132**), 2% Et_3N, DMSO, >95%. (e) H_2N-EG_3-PsOH (**122**) (excess), 2% pyridine, DMSO, 4.1%. Immobilization yields were estimated by LC-HRESIMS quantitation of unreacted amines, as shown in **Figures C.5-C.6**.

4.2.11 Validating the specific binding of carbonic anhydrase to the arylsulfonamide-agarose resin

The binding interaction between CA and ASA-EG_3-Agarose (**139**) was evaluated to determine the utility of the affinity resins generated by covalent immobilization of small molecule ligands. The binding experiments were performed using purified CA as well as a M. smegmatis lysate spiked with CA. By adding CA to the lysis buffer for the latter, overall enzyme stability throughout sonication could be assessed. The protocol was otherwise identical to previous experiments using biotinylated probes. The results of this model experiment demonstrated the formation of a specific CA binding interaction with the immobilized ASA ligand.

Competitive displacement and heat-denatured controls clearly demonstrated a specific binding interaction (**Figure 4.9**). For instance, the binding was disrupted by heat-denaturation or pre-incubation with AAZ, a competitive ligand that intercepted CA. Competitive elution of CA, after immobilization onto ASA-EG_3-Agarose (**139**), was also achieved using a buffer solution of AAZ. A vehicle control was also implemented to ensure solvent effects were not responsible for the elution. Owing to slow dissociation, a considerable amount of CA remained bound to the affinity resin after the competitive elution. Increasing the length of AAZ exposure may therefore maximize the elution of CA. As anticipated, the generic control resin (**141**) was incapable of binding CA, although a small band was observed due to NSB. Similar trends were observed for CA binding within the context of a M. smegmatis lysate (**Figure 4.10**).

The M. smegmatis lysate containing CA was also subjected to serial affinity chromatography (SAC), an experiment whose interpretation required the presence of

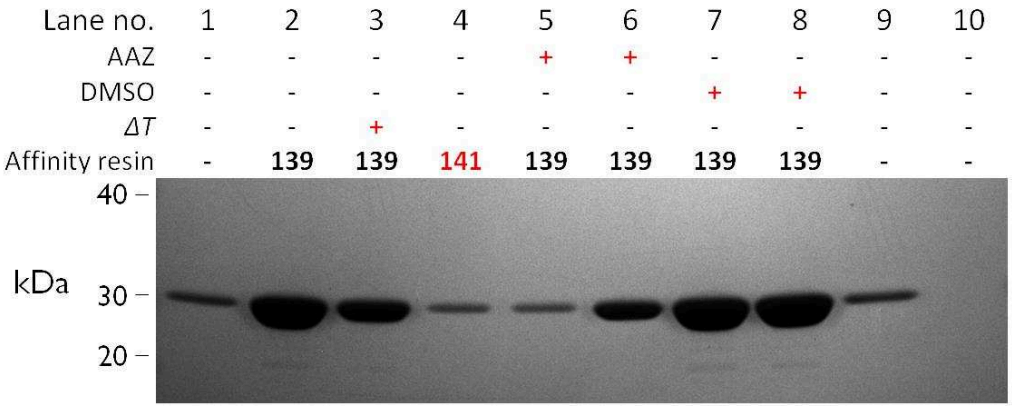

Figure 4.9. Gel electrophoretic analysis of the specific binding interaction between ASA-EG_3-Agarose (**139**) and CA. Notes and conditions: The affinity resins were incubated with a 100 μg/mL CA solution. The CA was eluted under denaturing conditions, with the exception of lanes 9-10, and resolved over a 4-12% polyacrylamide gel. Both types of competitive displacements were performed: pre-incubation of CA with AAZ and elution of CA from **139** with AAZ. Description of gel lanes: Lane 1, CA standard; lane 2, affinity capture of CA with **139**; lane 3, heat-denatured control; lane 4, affinity capture of CA with the generic control resin (**141**); lane 5, remaining CA after competitive displacement by pre-incubation of CA with AAZ; lane 6, remaining CA after competitive elution with AAZ; lane 7, remaining CA after DMSO control of competitive elution; lane 8, affinity capture of CA with **139** after DMSO control of competitive displacement; lane 9, competitively eluted CA from **139** in lane 6; lane 10, DMSO control of competitive elution from lane 7.

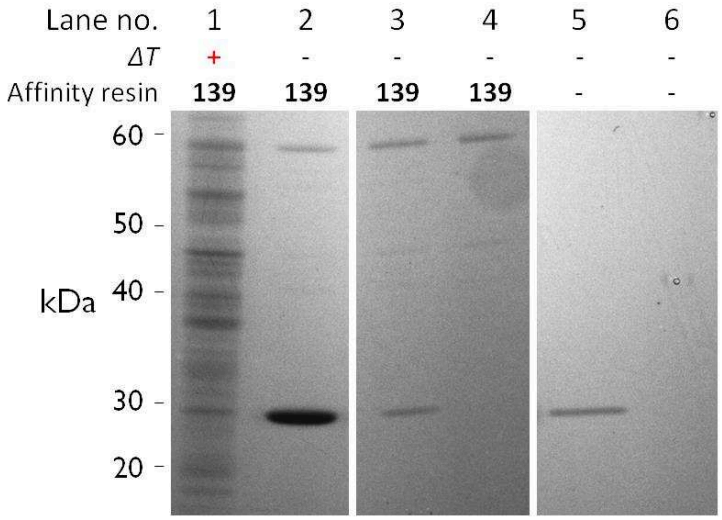

Figure 4.10. Gel electrophoretic analysis of the specific binding interaction between ASA-EG_3-Agarose (**139**) and CA within the context of a Mycobacterium smegmatis lysate. Notes and conditions: The CA was added to the lysis buffer to a total concentration of 10 μg/mL. The proteins were eluted from the resin under denaturing conditions and resolved over a 4-12%% polyacrylamide gel. To complete the SAC experiment, the lysate was incubated three times with different batches of **139** (lanes 2-4 in that order). Description of gel lanes: Lane 1, heat-denatured control; lane 2, affinity capture of CA with **139** and 1st SAC sequence; lane 3, affinity capture of CA with **139** after 2nd SAC sequence; lane 4, affinity capture of CA with **139** after 3rd SAC sequence; lane 5, competitively eluted CA from **139**; lane 6, DMSO control of competitive elution. Serial depletion trend: The intensity of the CA band (~29 kDa) decreases across lanes 2-4 relative to a NSB protein (~78 kDa).

NSB. The SAC experiment served as an alternative to a competitive displacement, which may not occur for hydrophobic ligands such as pseudopteroxazole (**30**) and pseudopterosin G (**33**).[217] As described in a preceding chapter (Section 1.9.2), SAC entails the transfer of a cell lysate from one batch of affinity resin to another, a process that may be repeated several times. During this sequence, the relative abundance of NSB remains largely unchanged because of the high abundance and low binding affinity of these proteins.[236] Protein target candidates are typically of low abundance and exhibit high binding affinity, a combination of attributes resulting in their depletion from the lysate. Indeed, the CA band intensity underwent serial depletion, meanwhile a single NSB protein (78 kDa) remained consistent throughout (**Figure 4.10**). These experiments confirmed the specific binding interaction of CA with ASA-EG_3-Agarose (**139**), and thus validated the affinity chromatography system.

4.2.12 Investigation of putative targets by affinity chromatography

After verifying the specific binding interaction between CA and ASA-EG_3-Agarose (**139**), the protein binding interactions of PtxGlu-EG_3-Agarose (**137**), Ps-EG_3-Agarose (**138**), and Agarose-EG_3-PsOH (**140**) were investigated. The latter was employed as an inactive control, while the deactivated resin **141** served as a generic control, due to the absence of the diterpene scaffold. Both **137** and **140** were utilized in the SAC experiment to identify specific binding interactions that may require the EG spacer at the double bond position of the diterpene scaffold. Both types of competitive displacements were carried out using pseudopteroxazole (**30**) or pseudopterosin G (**33**).

The ligands were either pre-incubated with the M. smegmatis lysate to intercept the target protein(s) or incubated with the affinity resin to achieve a competitive elution.

Attributable to their structural similarity, PtxGlu-EG_3-Agarose (**137**) and Ps-EG_3-Agarose (**138**) showed similar protein profiles (**Figure 4.11**), with the exception of a single protein with an apparent molecular weight of 29 kDa that interacted with **137** only. Unfortunately, the extent of NSB was significant for both affinity resins, especially within the higher molecular weight region (40-260 kDa). The interactome of Agarose-EG_3-PsOH (**140**) was quite distinct from **137** and **138**, presumably due to the cationic nature of **140** conferred by the secondary amino group (**Figure 4.12**). As a result, **140** was not a suitable inactive control for identifying NSB. Deconvolution of protein targets by competitive displacement was also unsuccessful (data not shown), likely owing to the limited aqueous solubility of the competitive ligands.

To identify protein target candidates, the SAC technique was employed to assess the relative depletion of protein band intensities, trends that are indicative of a specific binding interaction. Indeed, several protein bands of lower molecular weight underwent relative serial depletion in experiments using PtxGlu-EG_3-Agarose (**137**) and Agarose-EG_3-PsOH (**140**, **Figure 4.12**). The serial depletion profiles for **137** and **140** were quite distinct, with the exception of a single protein with an apparent molecular weight of 17.5 kDa. Although **140** has been designated as an inactive control, the formation of specific binding interactions with the immobilized ligand is conceivable. Notably, these interactions may not be identified by **137** if the attachment of an EG spacer to the oxazole ring disrupts the binding activity.

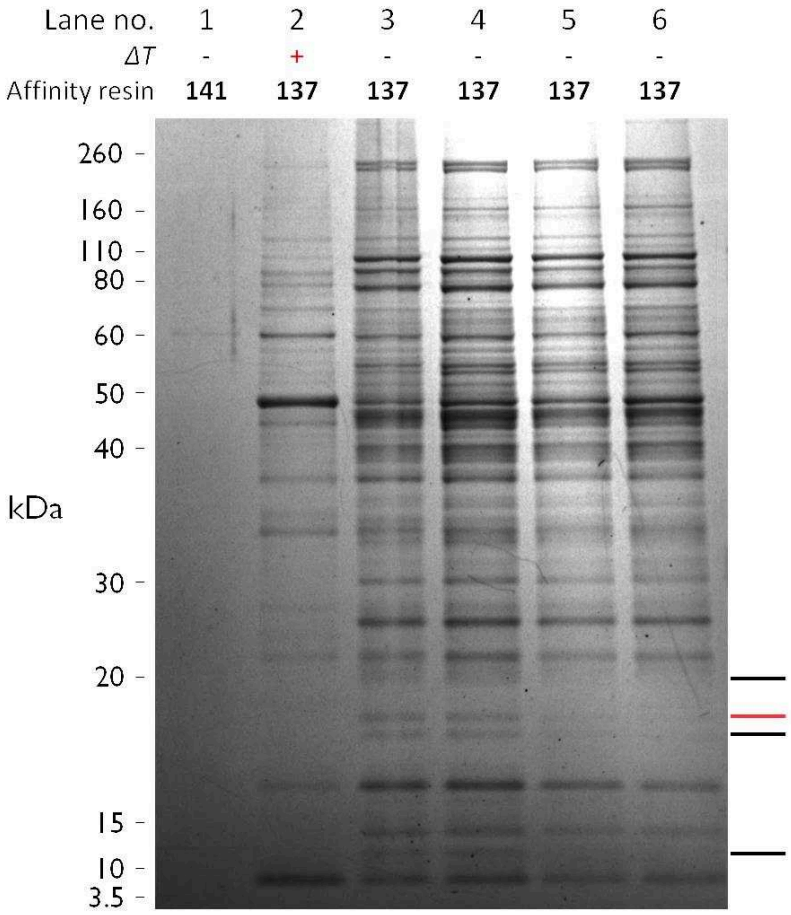

Figure 4.11. Gel electrophoretic analysis of Mycobacterium smegmatis proteins bound to PtxGlu-EG_3-Agarose (**137**). Notes and conditions: The proteins were eluted from the resin under denaturing conditions and resolved over a 12% polyacrylamide gel. To complete the SAC experiment, the M. smegmatis lysate was incubated four times with different batches of **137** (lanes 3-6 in that order). Description of gel lanes: Lane 1, affinity capture with generic control resin (**141**); lane 2, heat-denatured control; lane 3, affinity capture with **137** in 1st SAC sequence; lane 4, affinity capture with **137** in 2nd SAC sequence; lane 5, affinity capture with **137** in 3rd SAC sequence; lane 6, affinity capture with **137** in 4th SAC sequence. Serial depletion trends: The relative intensity of gel bands at 20, 18.5, 17.5, and 12 kDa decreases across lanes 3-6, as indicated by the markings on the right side of the gel image. The red marking indicates the band analyzed by tandem mass spectrometry.

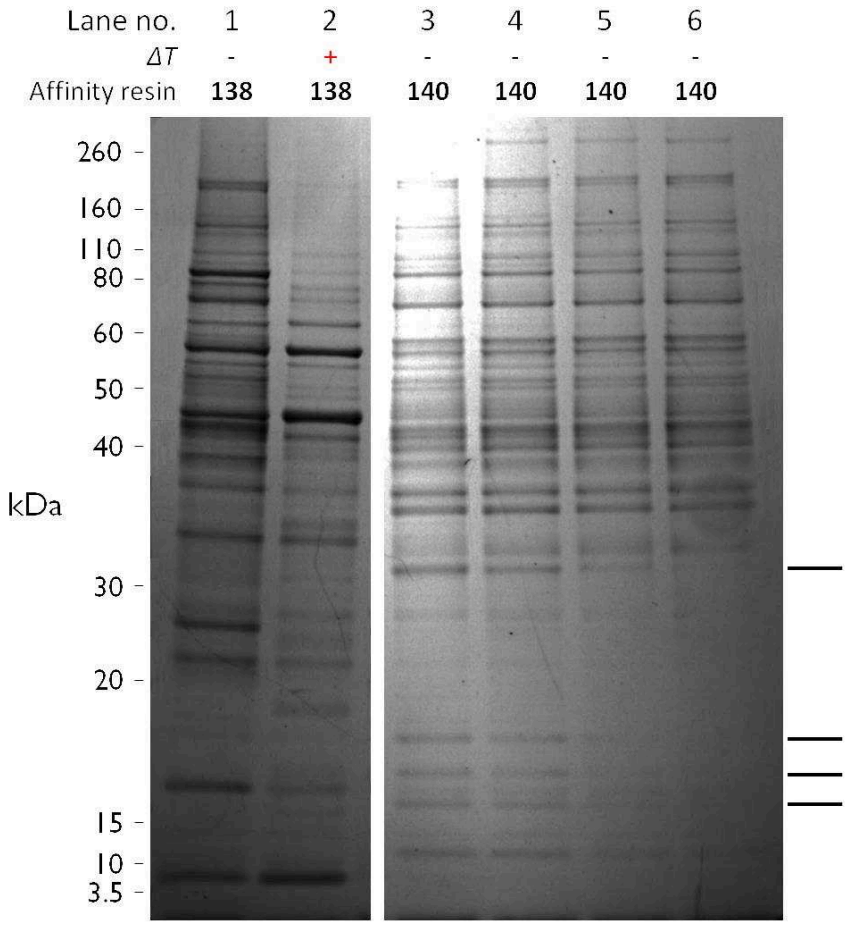

Figure 4.12. Gel electrophoretic analysis of Mycobacterium smegmatis proteins bound to Ps-EG_3-Agarose (**138**) and Agarose-EG_3-PsOH (**140**). Notes and conditions: The proteins were eluted from the resin under denaturing conditions and resolved over a 12% polyacrylamide gel. To complete the SAC experiment, the M. smegmatis lysate was incubated four times with different batches of **140** (lanes 3-6 in that order). Description of gel lanes: Lane 1, affinity capture with Ps-EG_3-Agarose (**138**); lane 2, heat-denatured control; lane 3, affinity capture with **140** in 1st SAC sequence; lane 4, affinity capture with **140** in 2nd SAC sequence; lane 5, affinity capture with **140** in 3rd SAC sequence; lane 6, affinity capture with **140** in 4th SAC sequence. Serial depletion trends: The relative intensity of gel bands at 31, 18, 17.5, and 15.5 kDa decreases across lanes 3-6, as indicated by the markings on the right side of the gel image.

The band intensities of nearly all higher molecular weight proteins (40-260 kDa) were constant, signifying the non-specificity of these binding interactions. The large number of NSB observed within this region, however, may have overlapped with and obscured the bands of putative targets. Nonetheless, protein target candidates displaying the serial depletion trend were selected for identification by tandem mass spectrometry. The gel bands were excised from the gel, as specified in **Figure 4.12**. Other bands were prioritized on the basis of differential binding to PtxGlu-EG_3-Agarose (**137**) and Agarose-EG_3-PsOH (**140**), although a serial depletion pattern was not apparent.

4.2.13 Identification of (3R)-hydroxyacyl-ACP dehydratase subunit HadC as a putative protein target

Mycolic acids are a major component of the mycobacterial cell wall, which is a lipid-rich layer known for its complexity and relative impermeability to hydrophilic antibiotics.[305] Located beyond the cell membrane and peptidoglycan layer, mycolic acids are either esterified to an underlying arabinogalactan layer or exist as free trehalose dimycolates.[306] Mycolic acids consist of long-chain, α-branched, β-hydroxylated fatty acids (**Figure 4.13**), and require both fatty acid synthase (FAS)-I and FAS-II pathways for their biosynthesis.[307] The latter is unable to carry out de novo fatty acid biosynthesis in mycobacteria, but is instead devoted to the elongation of intermediate length (C_{16}) fatty acids from the FAS-I pathway to generate long-chain (C_{48}-C_{56}) meromycolic acids.[308] The meromycolate chain may subsequently undergo cyclopropanation or oxygenation, and is then condensed with a carboxylated C_{26} fatty acid to provide the branched mycolic acid structure.[308]

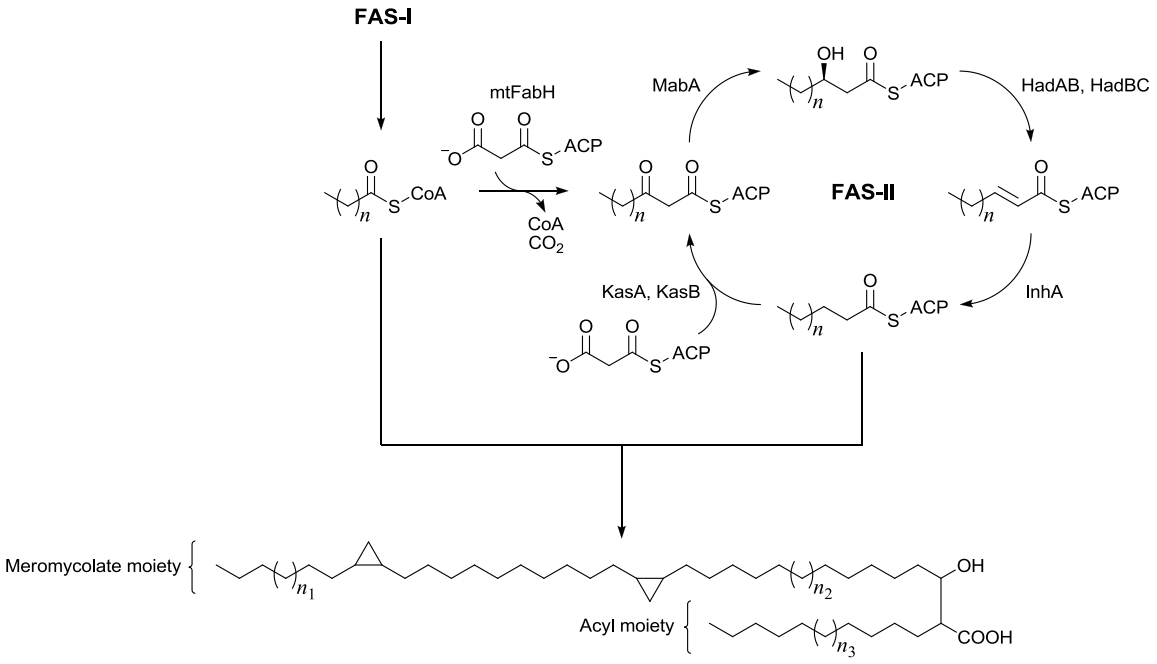

Figure 4.13. The structure of mycolic acids and their biosynthesis through the FAS-I and FAS-II pathways. The polymethylene chain length of the meromycolate and acyl moieties are as follows: $n_1 = 13$, $n_2 = 7$, $n_3 = 15$.[307, 308b]

The iterative process of elongating fatty acid chains in the FAS-II pathway is initiated by the condensation of a C_{16} acyl-coenzyme A (CoA) with malonyl-acyl carrier protein (ACP), a reaction catalyzed by β-ketoacyl-ACP synthase (mtFabH, **Figure 4.13**).[309] The β-ketoacyl-ACP intermediate subsequently undergoes reduction by β-ketoacyl-ACP reductase (MabA) and then dehydration by (3R)-hydroxyacyl-ACP dehydratases (HadAB and HadBC).[310] The trans-2-enoyl-ACP reductase (InhA) catalyzes the reduction of the unsaturated intermediate to provide an acyl chain, which may undergo another cycle of elongation via the β-ketoacyl-ACP synthase (KasA and KasB).[311] The reductive process repeats until the full length of the meromycolate chain has been completed. A functioning FAS-II pathway is known to be essential for mycobacterial viability;[312] therefore the discovery of drugs that arrest mycolic acid biosynthesis is an active area of TB research.[313] Isoniazid, one of the first-line antitubercular drugs, inhibits InhA of the FAS-II pathway.[314]

A protein with an apparent molecular weight of 18.5 kDa was selected for further analysis as it exhibited a serial depletion pattern in the SAC experiment (**Figure 4.11**), indicating a specific binding interaction. Moreover, the band was not present for the inactive control, Agarose-EG_3-PsOH (**140**), suggesting that the interaction was of antimycobacterial significance. Mass spectrometric analysis of the tryptic peptides of this protein revealed a polypeptide fragment, whose sequence (FGADIVVTR) served as a query for protein database analysis using the basic local alignment search tool (BLAST). This analysis revealed (3R)-hydroxyacyl-ACP dehydratase subunit HadC as the most probable identity of the protein. Complete sequence alignment was observed for M. tuberculosis H_{37}Rv and M. smegmatis $mc^2$155 HadC from residues 116 to 124.

Importantly, the approximated molecular weight of the gel band was also consistent with the expected 18.9 kDa reported for HadC.[307] Although no other mycobacterial proteins exhibited complete alignment with this polypeptide sequence, additional sequencing information must be acquired in the future to further substantiate the HadC identification.

The affinity chromatography data suggests that subunit HadC binds specifically to PtxGlu-EG_3-Agarose (**137**) and Ps-EG_3-Agarose (**138**) and is thus a protein target candidate of pseudopteroxazole (**30**). The HadAB and HadBC heterodimers are responsible for the dehydratase function of the FAS-II pathway in mycobacteria (**Figure 4.13**).[310b] HadAB interacts with KasA and appears to be responsible for the formation of meromycolates of intermediate length, whereas HadBC and KasB are necessary for the later stages of meromycolate biosynthesis.[315] This observation is consistent with the absence of HadC and KasB orthologs in genera containing mycolic acids of intermediate length only.[310b] Although earlier studies predicted that the hadC gene was not essential for M. tuberculosis growth in vitro,[310b, 316] overexpression of hadBC conferred high-level resistance to isoxyl and thiacetazone in vitro.[317] Notably, overexpression of either hadA, hadB, or hadC alone had a minimum impact on the MIC of these two antibiotics.

The deletion of kasB significantly diminished the virulence of M. tuberculosis H_{37}Rv in immunocompetent mice, wherein the mycobacteria persisted for more than 600 days without causing disease.[308b, 318] Undoubtedly, further studies of HadC are necessary to determine its importance in mycobacterial persistence and survival in the host. The Rv0635-Rv0637 gene cluster, which encodes HadABC, is required for M. tuberculosis growth in vitro.[310b] The functional equivalent of HadB in M. smegmatis, MSMEG1341, has also been shown to be essential.[308a] Inhibition of HadBC by pseudopteroxazole (**30**)

by binding to subunit HadC may therefore arrest the growth of M. smegmatis and M. tuberculosis, although further studies are required to determine the precise role of HadC in vitro.

The importance of HadC for mycobacterial persistence under hypoxic conditions, as is the case for the LORA, is also unknown. Given the role of HadBC in generating full-length meromycolates, a HadC binding interaction alone does not explain the antimicrobial activity against other Gram-positive bacteria, as observed in the disk diffusion assay. It remains to be determined whether affinity chromatography using Ptx-EG_3-Agarose (**137**) will identify FAS-II dehydratases in other Gram-positive organisms. Affinity resin **137** may also interact with subunit HadA, representing an additional target of pseudopteroxazole (**30**) in the mycobacterial FAS-II pathway. Notably, the SAC also demonstrated the serial depletion of a protein with a molecular weight of approximately 17.5 kDa (**Figure 4.11**), a close match to the anticipated 17.4 kDa of HadA (17.4 kDa, M. tuberculosis H_{37}Rv).

Quantification of thermodynamic parameters, particularly the dissociation constant (K_d), isothermal titration caloritmetry or surface plasmon resonance may provide formal proof of the HadC binding interaction.[221, 319] The antimycobacterial significance of the HadC interaction may also be examined through its overexpression in M. smegmatis. An increase in HadC expression may compensate for the inhibitory effects of pseudopteroxazole (**30**), resulting in partial restoration of normal dehydratase function and higher MIC values. The affinity chromatography approach pursued in this study has also revealed several other protein target candidates, whose identification may point the direction to an as yet unrecognized antitubercular treatment.

4.3 Conclusions

In addition to their antimycobacterial activity, diterpenes of the amphilectane class, pseudopteroxazole (**30**) and pseudopterosin G (**33**), showed antimicrobial activity against a variety of Gram-positive clinical isolates, but were largely inactive against Gram-negative strains. The results of this assay suggest that **30** may have clinical applications in addition to the treatment of TB, especially considering its activity against foodborne pathogens (e.g. Clostridium perfringens and Listeria monocytogenes) and other bacteria of relevance in veterinary medicine (e.g. Streptococcus equi subsp. equi). During a preliminary study, in collaboration with Dr. Malcolm McCulloch, the activity of **30** against a panel of isogenic mono-resistant M. tuberculosis H_{37}Rv strains was evaluated. Although the MIC of **30** was greater than rifampin or isoniazid, no cross-resistance with any of the clinical antitubercular drugs was observed, suggesting that **30** may exert its activity through a unique mechanism of action.

The antitubercular mechanism of action of pseudopteroxazole (**30**) was investigated by affinity chromatography using a collection of semisynthetic natural product-based probes. In an effort to retain the binding activity of the diterpene scaffold, both pseudopteroxazole and pseudopterosin-derived probes were designed by attaching the EG spacer to the oxazole ring, the phenolic hydroxyl group, and double bond positions. Antimicrobial testing of the chemical probes, and other semisynthetic intermediates, indicated that the binding activity was maintained by attaching the spacer to either the oxazole ring of **30** or the phenolic hydroxyl group of the aglycone methyl ether (**95**). According to the observed SAR trends, modifying the double bond appeared

to disrupt this binding activity, while the inactivity of Ptx-EG_3-BPA (**111**) and PtxGlu-EG_3-BPA (**112**) was attributed to their greater hydrophobicity and poor aqueous solubility. Nonetheless, these photoaffinity probes may retain their binding activity within the context of a cell lysate and have applications in future investigations of protein binding interactions.

The molecular design of these biotinylated probes was simulated by the ASA model probes, which were utilized to ensure the specific binding of CA to the affinity resin. Although the interaction was not observed for the biotin-streptavidin approach, a covalently immobilized ASA ligand proved successful. As a result, the technical aspects of the affinity chromatography experiment were validated, and therefore covalent immobilization of pseudopteroxazole and pseudopterosin-derived probes ensued. Protein target candidates were then investigated by probing the binding interactions of the M. smegmatis proteome with the affinity resins. Despite the large extent of NSB, promising protein target candidates were identified by implementing the SAC technique.

Analysis of gel bands by gel electrophoresis revealed the serial depletion of a ~18.5 kDa protein, indicative of a specific binding interaction with the PtxGlu-EG_3-Agarose (**137**) resin. Analysis of the tryptic digest by tandem mass spectrometry identified (3R)-hydroxyacyl-ACP dehydratase subunit HadC as a protein target candidate of pseudopteroxazole (**30**). As discussed earlier, the heterodimer HadBC is responsible for the dehydratase step in the FAS-II pathway, a process that is essential for mycobacterial viability.[312a] Although the biological relevance of the observed HadC binding interaction must be validated by an independent molecular- or cellular-based

assay, **30** appears to exert its antitubercular activity, at least in part, by inhibiting mycolic acid biosynthesis.

4.4 Experimental

General experimental methods as well as procedures for the mouse ear edema assay and the microbroth dilution assay are described in Appendix B. Also see Appendix B for a description of the "standard work up procedure".

4.4.1 Reagents and general experimental methods

Manufacturer procedures were followed for performing SDS-PAGE analysis, gel staining, and the Bradford protein quantification assay. The following reagents and buffers were purchased from Invitrogen Life Technologies for SDS-PAGE analysis: NuPAGE® LDS sample buffer (cat. number: NP0007), NuPAGE® sample reducing agent (cat. number: NP0004), NuPAGE® 4-12% bis-tris gradient gels (1.0 mm, cat. number: NP0322BOX), NuPAGE® 12% bis-tris gels (1.0 mm, cat. number: NP0342BOX), NuPAGE® MOPS SDS running buffer (cat. number: NP0001), NuPAGE® antioxidant (cat. number: NP0005), Novex® pre-stained protein marker (cat. number: LC5800), and SimplyBlue^{TM} SafeStain (Colloidal Coomassie® G-250 staining solution, cat. number: LC6060). The silver staining kit (Proteosilver^{TM} staining kit, cat. number: PROTSIL1-1KT), Bradford reagent (cat. number: B6916-500ML), and CA (CAS number: 9001-03-0) were purchased from Sigma-Aldrich. For the Bradford assay, a standard curve of bovine serum albumin (Thermo Scientific: HyClone BSA, cat. number: SH30574.01) was used to estimate protein quantity. The magnetic streptavidin

particles were purchased from EMD Millipore (MagPrep® P-25 streptavidin particles and PureProteome^{TM} streptavidin magnetic beads).

4.4.2 Determination of antimicrobial activity by the disk diffusion susceptibility method

The antimicrobial disk diffusion susceptibility assay was completed following the Kirby-Bauer protocol.[320] Each agar plate was prepared with 25 mL of liquid agar to establish a consistent depth of approximately 4 mm. The panel of clinical isolates was generously donated by Dr. Jeff Lewis and Beatrice Despres. All bacteria were grown on cation-adjusted Mueller-Hinton agar with the following exceptions: M. haemolytica, S. agalactiae, S. canis, S. equi subsp. equi, and S. equi subsp. zooepidemicus were grown on brain-heart infusion (BHI) agar, while A. equuli, A. pyogenes, E. rhusiopathiae, and S. pneumoniae were grown on blood agar. The indicated concentration (μg/disk) of each antimicrobial compound was delivered using 10 μL of a stock solution. Pseudopteroxazole (**30**) and pseudopterosin G (**33**) were delivered in DMSO, PtxHis (**37**) in 20% CH_3OH, ciprofloxacin in H_2O with 0.3% HCO_2H, and all other antibiotic controls in H_2O. All disks were 6 mm in diameter and made from filter paper using a hole punch. The inocula were standardized by adjusting the turbidity of the bacterial suspensions to a 0.5 McFarland standard and were spread onto agar plates use sterile cotton swabs. After incubating the plates at 37ºC for 24-72 h, the zones of growth inhibition were measured using a caliper. The assay was completed in duplicate, and as such, the reported antimicrobial activity is a consensus of two measurements. Samples of PtxHis (**37**) and 14,15-dihydro-elisabatin B were provided by Dr. Malcolm McCulloch.

4.4.3 Investigation of protein binding interactions by affinity chromatography

After streaking for purity on Middlebrook 7H10 agar, M. smegmatis was grown to stationary phase in BHI broth at 30ºC with shaking at 200 rpm. The culture was examined for purity by streaking on BHI agar. The cells were pelleted by centrifugation, washed three times with phosphate buffered saline (PBS, adjusted to pH 7.4), and stored at -80ºC until required for affinity chromatography experiments. Proteome samples were prepared by sonication of thawed M. smegmatis cells in PBS (0.01% P20), pulsing at 30% maximum power (5s pulse, 20s rest) while maintaining the temperature below 5ºC. The lysates underwent centrifugation to remove cellular debris, and the supernatants were collected for affinity chromatography.

The procedure for conducting the affinity chromatography experiment was adapted from the work of Yamamoto et al.[236] For the biotin-streptavidin system, the biotinylated probes were immobilized onto magnetic streptavidin beads (40 µL) via overnight incubation at 4ºC with gentle agitation (end-over-end rotation). The biotin binding sites were saturated by adding the biotinylated probes in excess. To remove all unbound small molecules, the streptavidin resins were subsequently washed 3-4 times with PBS (1.5 mL total volume). For experiments conducted with covalently immobilized small molecules, the agarose resins (40 µL of 50% slurry) were washed twice with PBS (1 mL total volume) to remove the 10% EtOH storage buffer.

The affinity resins were incubated with the M. smegmatis lysate for 30 min at 4ºC under gentle agitation after implementing any necessary controls. For the heat-denatured

control, the lysate was heated to 95ºC for 10 min followed by centrifugation to remove precipitated protein. Meanwhile, the competitive displacement controls were performed by pre-incubating the lysate with either 1.0 mM pseudopteroxazole (**30**) or pseudopterosin G (**33**) ligands for 30 min at 4ºC. The affinity resins were then washed three times with ice-cold PBS (1.5 mL total volume) to remove all non-binding proteins. Competitive elutions were carried out at this stage by incubating the affinity resin with 1 mM **30** or **33** for 20 min at 4ºC. Proteins were eluted from the affinity resins under denaturing conditions by heating to 95ºC in Laemmli sample buffer and then resolved by SDS-PAGE using manufacturer procedures.

4.4.4 Protein identification by tandem mass spectrometry

Gel bands were manually excised with a clean blade and transferred to 1.5 mL microcentrifuge tubes under laminar flow to avoid contamination of the samples. The preparation of the tryptic digests (in-gel procedure), as well as the LC-MS/MS analysis of tryptic peptides, was completed by Dr. Alejandro Cohen of the Life Sciences Research Institute at Dalhousie University according to an existing protocol.[321]

4.4.5 Isolation of pseudopterosins from Pseudopterogorgia elisabethae

The mixture of pseudopterosins G-J (**33**-**36**) was provided by Nautilus Biosciences Canada Inc. The pseudopterosins were extracted from samples of P. elisabethae obtained from Victory Reef, The Bahamas and purified by a combination of

liquid-liquid partitioning and chromatography. The major pseudopterosin constituents in the sample possessed the aglycone skeleton of **33**-**36**.

4.4.6 Preparation of pseudopteroxazole and pseudopterosins G and J

Pseudopterosin G-J aglycone ortho-quinone (96). Following an existing protocol, a mixture of pseudopterosins G-J (**33**-**36**) underwent acid hydrolysis to provide the ortho-quinone (**96**).[160, 279] To a solution of **33**-**36** (13.19 g) dissolved in H_2O:CH_3OH (1:19, 150 mL) were added three drops of HCl. The mixture was heated to reflux for 48 h, at which point TLC analysis (hexanes:TBME 1:1) indicated hydrolysis of the reactants. The mixture was diluted with EtOAc and partitioned between $NaHCO_{3(aq)}$ and DI H_2O. The organic layer was then subjected to the standard work up procedure and separated by MPLC (silica, hexanes → EtOAc), yielding the ortho-quinone (**96**, 7.738 g, ~59%). All ^1H and ^{13}C NMR spectroscopic data for **96** were consistent with the literature.[161, 322]

Pseudopteroxazole (30). An existing protocol was utilized to prepare pseudopteroxazole (**30**) from the pseudopterosin G-J aglycone ortho-quinone (**96**).[160] To a solution of ortho-quinone (**96**, 226.5 mg, 0.7539 mmol) dissolved in CH_3OH (30 mL) was added Ag_2O (141.5 mg, 0.6106 mmol). The reaction mixture was then heated to reflux for 2 h, and. afterwards, glycine (200.4 mg, 2.670 mmol) was transferred to the reaction along with an additional portion of Ag_2O (176.0 mg, 0.7595 mmol). The reaction was heated at reflux for an additional 2 h before adding another portion of glycine (282.1 mg, 3.758 mmol) and Ag_2O (175.5 mg, 0.7573 mmol). Additional glycine (279.9 mg, 3.729 mmol) was

added 2 h later and the reaction was heated at reflux overnight. The mixture was then filtered through Celite® and partitioned between EtOAc and DI H_2O. The EtOAc layer was subjected to the standard work up procedure and separated by MPLC (silica, hexanes → EtOAc). Fractions containing the desired product were combined and separated by semi-preparative RP-HPLC (phenylhexyl, 92% CH_3OH, 0.1% HCO_2H), yielding pseudopteroxazole (**30**, 37.7 mg, 0.122 mmol, 16%). All ^1H and ^{13}C NMR spectroscopic data for **30** were in agreement with the literature.[154, 160]

Pseudopterosins G (33) and J (36). The mixture of pseudopterosins G-J (**33-36**, 545.3 mg) was dissolved in CH_3OH (10 mL) and stirred with K_2CO_3 (102.3 mg, 740.2 mmol) at room temperature for 55 h. The reaction mixture was then diluted with EtOAc and washed successively with DI H_2O. The EtOAc layer was recovered, subjected to the standard work up procedure, and separated by flash chromatography (C_{18}, H_2O → CH_3OH, 0.1% HCO_2H) to provide pseudopterosin G (**33**, 331.1 mg, 0.7414 mmol, ~61%). The mixture of **33**-**36** was also separated by semi-preparative RP-HPLC (phenylhexyl, 86% CH_3OH, 0.1% HCO_2H), providing a sample of pseudopterosin J (**36**) in addition to **33**. All ^1H and ^{13}C NMR spectroscopic data for **33** and **36** were in agreement with the literature.[280a]

4.4.7 Synthesis and characterization pseudopteroxazole probes

The regioisomeric ratios of all pseudopteroxazole probes, and other synthetic intermediates containing oxazole rings, were determined by comparing the ^1H NMR

integrals for the region containing the benzylic methyl groups (2.40-2.25 ppm). The location of the nitrogen atom for all major regioisomers was at the C-10 position.

Ptx-EG$_3$-NH$_2$ (97). Method 1: A solution of the pseudopterosin G-J aglycone ortho-quinone (**96**, 109.5 mg, 0.3645 mmol) and Ag_2O (93.8 mg, 0.4048 mmol) in CH_3OH (25 mL) was heated to reflux for 30 min. Afterwards, 4,7,10-trioxa-1,13-tridecanediamine (**94**, 320 μL, 1.46 mmol) was added. Ag_2O (96.4 mg, 0.4160 mmol) and **94** (200 μL, 0.91 mmol) were then added after 1 h and the reaction was heated at reflux overnight. Two more portions of Ag_2O (91.4 mg, 0.394 mmol; 92.6 mg, 0.400 mmol) were added at 16 and 20 h and the reaction was kept at reflux for an additional 9 hr. The reaction mixture was then filtered through Celite® and partitioned between EtOAc and DI H_2O. The EtOAc layer was subjected to the standard work up procedure and separated by size exclusion chromatography (Sephadex® LH-20, CH_3OH 0.05% HCO_2H) to provide **97** (12.2 mg, 24.5 μmol, 7%).

Method 2: A solution of ortho-quinone (**96**, 170.6 mg, 0.5678 mmol) and Ag_2O (150.3 mg, 0.6486 mmol) in CH_3OH (20 mL) was heated to reflux and kept at that temperature for 30 min. Afterwards, the reaction was cooled to room temperature, transferred to a buret, and added dropwise to a solution of **94** (250 μL, 1.14 mmol) in CH_3OH (5 mL). The slow addition continued overnight and was completed after approximately 16 hr. The reaction mixture was then subjected to the same work up procedure as in Method 1 and separated by size exclusion chromatography (Sephadex® LH-20, CH_3OH 0.05% HCO_2H) to yield the desired primary amine (**97**, 38.0 mg, 76.2 μmol, 13%) as a regioisomeric mixture with a ratio of approximately 5:1. **97**: orange oil; $[\alpha]^{25}_D$ +74.2 (c

0.1025, $CHCl_3$); IR υ_{max} 3374, 2920, 2869, 1578, 1375, 1348, 1114 cm^{-1}. ^1H NMR ($CDCl_3$, 600 MHz) δ 4.95 (1H, d, J = 9.3 Hz, H-14), 3.94-3.88 (1H, m, H-1), 3.93 (2H, t, J = 6.7 Hz, H-23), 3.64-3.62 (2H, m, H-27), 3.62-3.58 (4H, m, H-24, H-28), 3.58-3.53 (4H, m, H-25, H-26), 3.22-3.17 (1H, m, H-7), 3.21 (2H, t, J = 6.7 Hz, H-22), 3.07 (2H, m, H-30), 2.37 (3H, s, H-20), 2.22 (1H, m, H-4), 2.20-2.14 (1H, m, H-6a), 2.17-2.12 (1H, m, H-5a), 2.11 (1H, m, H-2a), 1.91 (2H, p, J = 5.6 Hz, H-29), 1.76 (3H, s, H-17), 1.66 (3H, s, H-16), 1.42 (3H, d, J = 6.7 Hz, H-19), 1.42-1.35 (1H, m, H-6b), 1.30-1.23 (1H, m, H-2b), 1.27-1.21 (1H, m, H-3), 1.08-1.01 (1H, m, H-5b), 1.03 (3H, d, J = 5.9 Hz, H-18). ^{13}C NMR ($CDCl_3$, 150 MHz) δ 163.2 (C, C-21), 148.0 (C, C-9), 139.1 (C, C-10), 135.9 (C, C-13), 134.4 (C, C-12), 130.9 (CH, C-14), 128.9 (C, C-15), 125.7 (C, C-11), 122.0 (C, C-8), 70.4, 70.4 (CH_2, C-24, C-27), 70.2 (CH_2, C-26), 69.9, 69.9 (CH_2, C-25, C-28), 68.2 (CH_2, C-23), 44.8 (CH, C-4), 40.2 (CH_2, C-2), 39.1 (CH_2, C-30), 36.5 (CH, C-1), 34.7 (CH, C-3), 32.3 (CH_2, C-6), 30.4 (CH, C-7), 29.8 (CH_2, C-22), 28.2 (CH_2, C-5), 27.7 (CH_2, C-29), 25.6 (CH_3, C-16), 22.4 (CH_3, C-19), 19.9 (CH_3, C-18), 17.8 (CH_3, C-17), 13.7 (CH_3, C-20). HRESIMS m/z 499.3530 $[M + H]^+$ (calcd for $C_{30}H_{48}N_2O_4$, 499.3530).

Biotin N-succinimidyl ester (102). The Biotin-NHS ester (**102**) was synthesized following a known procedure.[323] Biotin (279.2 mg, 1.143 mmol) and NHS (157.7 mg, 1.370 mmol) were dissolved in DMF (12 mL) and stirred with 3Å molecular sieves (~0.8 g) under a N_2 atmosphere. After stirring for 30 min, DCC (484.4 mg, 2.348 mmol) was added and the reaction was stirred for 40 h, during which a white precipitate formed. The mixture was filtered, concentrated in vacuo, and diluted with Et_2O to precipitate the

product. The precipitate was then collected by vacuum filtration, yielding the desired biotin-NHS (**102**, 349.7 mg, 1.024 mmol, 90%). All ^{1}H and ^{13}C NMR spectroscopic data for **102** were consistent with the literature.[324]

Ptx-EG$_3$-Biotin (103): A solution of **97** (5.64 mg, 11.3 μmol) in anhydrous DMF (2 mL) was stirred with 3Å molecular sieves (~30 mg) for 20 min before adding biotin-NHS (**102**, 15.7 mg, 46.0 μmol). Et_3N (10 μL, 72 μmol) was then added and the reaction was stirred overnight at room temperature. After removing the solvent in vacuo, the crude product was separated by semi-preparative RP-HPLC (phenylhexyl, 88% CH_3OH, 0.1% HCO_2H) to provide **103** (1.45 mg, 2.00 μmol, 18%) as a regioisomeric mixture with a ratio of approximately 4:1. **103**: yellow oil; $[\alpha]^{25}_{D}$ +46.1 (c 0.1985, $CHCl_3$); IR υ_{max} 3283, 2922, 2861, 1703, 1644, 1550, 1452, 1115, 756 cm^{-1}. ^{1}H NMR ($CDCl_3$, 600 MHz) δ 6.56 (1H, t, J = 5.1 Hz, 30-NH), 6.07 (1H, br s, 7'-NH), 5.29 (1H, br s, 8'-NH), 4.95 (1H, d, J = 9.3 Hz, H-14), 4.47 (1H, dd, J = 7.5, 5.0 Hz, H-8'), 4.28 (1H, dd, J = 7.5, 4.7 Hz, H-7'), 3.95 (2H, t, J = 6.9 Hz, H-23), 3.95-3.88 (1H, m, H-1), 3.68-3.64 (2H, m, H-27), 3.64-3.61 (2H, m, H-26), 3.61-3.58 (2H, m, H-24), 3.55-3.51 (4H, m, H-25, H-28), 3.33 (2H, q, J = 6.0 Hz, H-30), 3.24-3.17 (1H, m, H-7), 3.19 (2H, t, J = 6.9 Hz, H-22), 3.12 (1H, td, J = 7.3, 4.7 Hz, H-6'), 2.88 (1H, dd, J = 12.8, 5.0 Hz, H-9'), 2.72 (1H, d, J = 12.8, H-10'), 2.38 (3H, s, H-20), 2.23 (1H, m, H-4), 2.22-2.14 (1H, m, H-6a), 2.18-2.12 (1H, m, H-5a), 2.17 (2H, t, J = 7.4 Hz, 2, H-2'), 2.11 (1H, m, H-2a), 1.77-1.72 (2H, m, H-29), 1.76 (3H, s, H-17), 1.74-1.69 (1H, m, H-5'a), 1.70-1.60 (2H, m, H-3'), 1.68-1.61 (1H, m, H-5'b), 1.66 (3H, s, H-16), 1.46-1.38 (2H, m, H-4'), 1.43-1.34 (1H, m, H-6b), 1.42 (3H, d, J = 6.8 Hz, H-19), 1.31-1.23 (1H, m, H-2b), 1.28-1.20 (1H, m, H-3), 1.09-

1.00 (1H, m, H-5b), 1.04 (3H, d, J = 6.0 Hz, H-18). ^{13}C NMR ($CDCl_3$, 150 MHz) δ 173.3 (C, C-1'), 162.8 (C, C-21), 164.1 (C, C-10'), 148.0 (C, C-9), 139.3 (C, C-10), 135.8 (C, C-13), 134.3 (C, C-12), 130.9 (CH, C-14), 128.8 (C, C-15), 125.8 (C, C-11), 121.9 (C, C-8), 70.6 (CH_2, C-24), 70.5, 70.5 (CH_2, C-26, C-27), 70.1, 70.1 (CH_2, C-25, C-28), 68.3 (CH_2, C-23), 61.9 (CH, C-7'), 60.3 (CH, C-8'), 55.8 (CH, C-6'), 44.8 (CH, C-4), 40.6 (CH_2, C-9'), 40.1 (CH_2, C-2), 37.9 (CH_2, C-30), 36.5 (CH, C-1), 36.1 (CH_2, C-2'), 34.7 (CH, C-3), 32.3 (CH_2, C-6), 30.3 (CH, C-7), 29.8 (CH_2, C-22), 29.0 (CH_2, C-29), 28.4 (CH_2, C-4'), 28.2 (CH_2, C-5), 28.2 (CH_2, C-5'), 25.8 (CH_2, C-3'), 25.5 (CH_3, C-16), 22.3 (CH_3, C-19), 19.9 (CH_3, C-18), 17.7 (CH_3, C-17), 13.6 (CH_3, C-20). HRESIMS m/z 725.4302 $[M + H]^+$ (calcd for $C_{40}H_{61}N_4O_6S$, 725.4306).

PtxGlu-CO_2CH_3 (99). A solution of pseudopterosin G-J aglycone ortho-quinone (**96**, 222.7 mg, 0.7413 mmol) and Ag_2O (189.6 mg, 0.8182 mmol) in CH_3OH (25 mL) were heated to reflux for 30 min before adding L-glutamic acid 5-methyl ester (**98**, 133.9 mg, 0.8309 mmol). The resulting mixture was kept at reflux for 4 h prior to adding additional Ag_2O (192.4 mg, 0.8303 mmol) and **98** (136.8 mg, 0.8489 mmol). After maintaining the reaction at reflux overnight, two portions of Ag_2O (380.4 mg, 1.642 mmol; 188.4 mg, 0.8130 mmol) and **98** (139.1 mg, 0.8631 mmol; 132.4 mg, 0.8216 mmol) were added 3 h apart. The reaction mixture was heated at reflux for an additional 3 h and subsequently filtered through Celite® and partitioned between EtOAc and DI H_2O. The EtOAc phase was recovered, subjected to the standard work up procedure, and separated by MPLC (silica, hexanes → EtOAc) to yield PtxGlu-CO_2CH_3 (**99**, 133.5 mg, 0.3375 mmol, 46%). All ^{1}H and ^{13}C NMR spectroscopic data for **99** were in agreement with the literature.[160]

PtxGlu-CO_2H (100). The methyl ester (**99**, 133.5 mg, 0.338 mmol) and LiOH (61.8 mg, 2.58 mmol) were dissolved in acetone:H_2O (10:1, 11 mL) and stirred for 48 hr. To quench the reaction, HCO_2H (97 μL, 2.58 mmol) was added and the solvent was removed in vacuo before separating the crude product by RP-MPLC (C_{18}, $H_2O \rightarrow CH_3OH$, 0.1% HCO_2H) to purify PtxGlu-CO_2H (**100**, 119.9 mg, 0.314 mmol, 93%). All ^1H and ^{13}C NMR spectroscopic data for **100** were in agreement with the literature.[160]

PtxGlu-EG_3-NH_2 (101). The carboxylic acid (**100**, 40.7 mg, 0.107 mmol), NHS (18.7 mg, 0.162 mmol), and 3Å MS (~100 mg) were stirred in anhydrous CH_2Cl_2 (4 mL) under a N_2 atmosphere for 20 min prior to adding DCC (35.2 mg, 0.171 mmol). The reaction was stirred overnight at room temperature and filtered through Celite®. The filtrate was evaporated in vacuo, resuspended in CH_2Cl_2 (4 mL), and 4,7,10-trioxa-1,13-tridecanediamine (**94**, 240 μL, 1.10 mmol) was added. After stirring the reaction at room temperature for 40 min, the reaction mixture was partitioned between EtOAc and DI H_2O. The EtOAc layer was subjected to the standard work up procedure and separated by RP-MPLC (C_{18}, $H_2O \rightarrow CH_3OH$, 0.1% HCO_2H) to yield **101** (33.1 mg, 56.7 μmol, 53%) as a regioisomeric mixture with a ratio of approximately 14:1. **101**: yellow oil; $[\alpha]^{25}_D$ +65.0 (c 0.1108, $CHCl_3$); IR υ_{max} 3299, 2921, 2867, 1656, 1549, 1445, 1376, 1110 cm^{-1}. ^1H NMR ($CDCl_3$, 600 MHz) δ 4.95 (1H, d, J = 9.3 Hz, H-14), 3.91 (1H, app. q, J = 8.7 Hz, H-1), 3.63-3.59 (4H, m, H-29, H-30), 3.59-3.55 (2H, m, H-31), 3.58-3.54 (2H, m, H-32), 3.55-3.52 (2H, m, H-28), 3.39 (2H, q, J = 6.2 Hz, H-34), 3.35 (2H, app. q, J = 6.1 Hz, H-25), 3.22-3.16 (1H, m, H-7), 3.21 (2H, t, J = 7.5 Hz, H-22), 2.73 (2H, t, J = 7.5 Hz, H-23), 2.36 (3H, s, H-20), 2.25-2.19 (1H, m, H-4), 2.19-2.13 (1H, m, H-6a), 2.17-

2.11 (1H, m, H-5a), 2.14-2.07 (1H, m, H-2a), 1.79-1.73 (4H, m, H-26, H-33), 1.76 (3H, s, H-17), 1.66 (3H, s, H-16), 1.41 (3H, d, J = 6.8 Hz, H-19), 1.41-1.34 (1H, m, H-6b), 1.28-1.22 (1H, m, H-2b), 1.26-1.20 (1H, m, H-3), 1.08-1.00 (1H, m, H-5b), 1.03 (3H, d, J = 5.9 Hz, H-18). ^{13}C NMR ($CDCl_3$, 150 MHz) δ 171.3 (C, C-24), 164.5 (C, C-21), 148.0 (C, C-9), 139.2 (C, C-10), 135.8 (C, C-13), 134.4 (C, C-12), 131.0 (CH, C-14), 128.8 (C, C-15), 125.7 (C, C-11), 122.0 (C, C-8), 70.6 (CH_2, C-30), 70.5 (CH_2, C-29), 70.2, 70.2 (CH_2, C-28, C-32), 69.9 (CH_2, C-31), 69.7 (CH_2, C-27), 44.8 (CH, C-4), 40.2 (CH_2, C-2), 37.8 (CH_2, C-25), 36.8 (CH_2, C-34), 36.5 (CH, C-1), 34.7 (CH, C-3), 33.3 (CH_2, C-23), 32.3 (CH_2, C-6), 30.3 (CH, C-7), 29.1 (CH_2, C-26), 28.6 (CH_2, C-33), 28.2 (CH_2, C-5), 25.6 (CH_3, C-16), 24.7 (CH_2, C-22), 22.4 (CH_3, C-19), 19.9 (CH_3, C-18), 17.7 (CH_3, C-17), 13.6 (CH_3, C-20). HRESIMS m/z 584.4059 $[M + H]^+$ (calcd for $C_{34}H_{54}N_3O_5$, 584.4058).

PtxGlu-EG$_3$-Biotin (104). To a stirred solution of **101** (5.86 mg, 10.0 μmol) and 3Å molecular sieves (~30 mg) in anhydrous DMF (2 mL) was added biotin-NHS (**102**, 16.0 mg, 46.9 μmol) and Et_3N (10 μL, 72 μmol). After stirring the reaction mixture overnight at room temperature, the solvent was removed in vacuo. The crude product was then separated by semi-preparative RP-HPLC (phenylhexyl, 88% CH_3OH, 0.1% HCO_2H) to provide **104** (3.35 mg, 4.14 μmol, 41%). No regioisomer side product was observed in the purified product. **104**: colorless oil; $[\alpha]^{25}_D$ +45.2 (c 0.3723, $CHCl_3$); IR υ_{max} 3286, 3083, 2922, 2861, 1701, 1649, 1551, 1446, 1118, 754 cm^{-1}. ^{1}H NMR ($CDCl_3$, 600 MHz) δ 6.87 (1H, t, J = 5.2 Hz, 25-NH), 6.66 (1H, t, J = 5.2 Hz, 34-NH), 6.10 (1H, br s, 7'-NH), 5.48 (1H, br s, 8'-NH), 4.94 (1H, d, J = 9.3 Hz, H-14), 4.47 (1H, dd, J = 7.5, 5.0

Hz, H-8'), 4.28 (1H, dd, J = 7.5, 4.8 Hz, H-7'), 3.91 (1H, app. q, J = 8.6 Hz, H-1), 3.65-3.60 (4H, m, H-29, H-30), 3.59-3.55 (4H, m, H-28, H-31), 3.53 (2H, app. dd, J = 5.7, 3.4 Hz, H-32), 3.52 (2H, app. dd, J = 5.9, 3.8 Hz, H-27), 3.35 (2H, app. q, J = 6.2 Hz, H-25), 3.32 (2H, app. q, J = 6.1 Hz, H-34), 3.24 (2H, t, J = 7.6 Hz, H-22), 3.23-3.15 (1H, m, H-7), 3.12 (1H, td, J = 7.3, 4.8 Hz, H-6'), 2.87 (1H, dd, J = 12.8, 5.0 Hz, H-9'a), 2.74 (2H, t, J = 7.6 Hz, H-23), 2.71 (1H, d, J = 12.8 Hz, H-9'b), 2.36 (3H, s, H-20), 2.22 (1H, app. ddd, J = 3.7 Hz, H-4), 2.19-2.13 (1H, m, H-6a), 2.17 (2H, t, J = 7.3 Hz, H-2'), 2.17-2.12 (1H, m, H-5a), 2.13-2.08 (1H, m, H-2a), 1.80-1.74 (2H, m, H-26), 1.76 (3H, s, H-17), 1.76-1.71 (2H, m, H-33), 1.74-1.69 (1H, m, H-5'a), 1.69-1.63 (2H, m, H-3'), 1.66 (3H, s, H-16), 1.66-1.60 (1H, m, H-5'b), 1.46-1.40 (2H, m, H-4'), 1.42-1.34 (1H, m, H-6b), 1.41 (3H, d, J = 6.8 Hz, H-19), 1.30-1.23 (1H, m, J = 11.8, 8.2 Hz, H-2b), 1.27-1.20 (1H, m, H-3), 1.08-1.00 (1H, m, H-5b), 1.03 (3H, d, J = 5.9 Hz, H-18). ^{13}C NMR ($CDCl_3$, 150 MHz) δ 173.3 (C, C-1'), 171.3 (C, C-24), 164.5 (C, C-21), 164.1 (C, C-10'), 147.9 (C, C-9), 139.1 (C, C-10), 135.8 (C, C-13), 134.3 (C, C-12), 130.9 (CH, C-14), 128.7 (C, C-15), 125.6 (C, C-11), 122.0 (C, C-8), 70.5, 70.5 (CH_2, C-29, C-30), 70.1, 70.1 (CH_2, C-28, C-32), 69.9 (CH_2, C-31), 69.7 (CH_2, C-27), 61.9 (CH, C-7'), 60.3 (CH, C-8'), 55.8 (CH, C-6'), 44.8 (CH, C-4), 40.6 (CH_2, C-9'), 40.1 (CH_2, C-2), 37.7, 37.7 (CH_2, C-25, C-34), 36.5 (CH, C-1), 36.1 (CH_2, C-2'), 34.6 (CH, C-3), 33.3 (CH_2, C-23), 32.3 (CH_2, C-6), 30.3 (CH, C-7), 29.1, 29.1 (CH_2, C-26, C-33), 28.3 (CH_2, C-4'), 28.2 (CH_2, C-5), 28.1 (CH_2, C-5'), 25.8 (CH_2, C-3'), 25.5 (CH_3, C-16), 24.8 (CH_2, C-22), 22.3 (CH_3, C-19), 19.9 (CH_3, C-18), 17.7 (CH_3, C-17), 13.6 (CH_3, C-20). HRESIMS m/z 810.4832 $[M + H]^+$ (calcd for $C_{40}H_{61}N_4O_6S$, 810.4834).

PtxGlu-EG$_{23}$-Biotin (135). To a stirred solution of PtxGlu-CO_2H (**100**, 19.8 mg, 51.9 μmol) and NHS (8.6 mg, 75 μmol) in anhydrous DMF (3 mL) was added DIC (35 μL, 0.22 mmol). After stirring the reaction overnight at room temperature, Biotin-EG$_{23}$-NH_2 (**136**, 21.3 mg, 16.4 μmol) and Et_3N (10 μL, 72 μmol) were added. The reaction was left to stir for 24 h, at which point analysis of the mixture by LC-HRESIMS indicated product formation. Upon removing the solvent by rotary evaporation, the crude product was resuspended in CH_3OH and eluted through a plug of C_{18}. The eluate was subsequently evaporated in vacuo, and separated by semi-preparative RP-HPLC (phenylhexyl, 94% CH_3OH, 0.1% HCO_2H) to yield PtxGlu-EG$_{23}$-Biotin (**135**, 15.8 mg, 9.50 μmol, 58%). **135**: clear oil; $[\alpha]^{25}_D$ +35.2 (c 0.5725, CH_2Cl_2) IR υ_{max} 3325, 3081, 2905, 2867, 1704, 1671, 1544, 1454, 1349, 1298, 1251, 1106, 950, 844 cm^{-1}. ^{1}H NMR ($CDCl_3$, 600 MHz) δ 4.92 (1H, d, J = 8.2 Hz, H-14), 4.48-4.44 (1H, br m, H-8'), 4.29-4.25 (1H, br m, H-7'), 3.88 (1H, app. q, J = 8.2 Hz, H-1), 3.74-3.47 (92H, H-26, H-27, …, H-70, H-71), 3.44-3.39 (2H, m, H-24), 3.41-3.36 (2H, m, H-72), 3.21 (2H, t, J = 7.2 Hz, H-21), 3.20-3.12 (1H, m, H-7), 3.12-3.07 (1H, m, H-6'), 2.85 (1H, m, H-9'a), 2.75-2.69 (2H, m, H-22), 2.70 (1H, m, H-9'b), 2.33 (3H, s, H-20), 2.22-2.14 (1H, m, H-4), 2.16-2.09 (1H, m, H-6a), 2.14-2.09 (1H, m, H-5a), 2.10-2.04 (2H, m, H-2'), 2.09-2.04 (1H, m, H-2a), 1.73 (3H, s, H-17), 1.73-1.68 (1H, m, H-5'a), 1.68-1.62 (2H, m, H-3'), 1.64-1.59 (1H, m, H-5'b), 1.62 (3H, s, H-16), 1.43-1.37 (2H, m, H-4'), 1.38 (3H, d, J = 8.2 Hz, H-19), 1.38-1.30 (1H, m, H-6b), 1.25-1.19 (1H, m, H-2b), 1.23-1.17 (1H, m, H-3), 1.04-0.97 (1H, m, H-5b), 1.00 (3H, br d, H-18). ^{13}C NMR ($CDCl_3$, 150 MHz) δ 173.4 (C, C-1'), 171.2 (C, C-24), 164.3 (C, C-21), 164.0 (C, C-10'), 147.9 (C, C-9), 139.2 (C, C-10), 135.6 (C, C-13), 134.2 (C, C-12), 130.9 (C, C-14), 128.6 (C, C-15), 125.7 (C, C-11), 121.9 (C, C-8),

70.6, 70.5, 70.4, 70.3, 70.1, 70.0, 69.9 (CH_2, C-26, C-27, …, C-70, C-71), 61.8 (CH, C-7'), 60.2 (CH, C-8'), 55.6 (CH, C-6'), 44.7 (CH, C-4), 40.5 (CH_2, C-9'), 40.1 (CH_2, C-2), 39.4 (CH_2, C-25), 39.2 (CH_2, C-72), 36.4 (CH, C-1), 35.9 (CH_2, C-2'), 34.6 (CH, C-3), 33.1 (CH_2, C-23), 32.3 (CH_2, C-6), 30.2 (CH, C-7), 28.2 (CH_2, C-4'), 28.1 (CH_2, C-5'), 28.1 (CH_2, C-5), 25.6 (CH_2, C-3'), 25.5 (CH_3, C-16), 24.6 (CH_2, C-22), 22.3 (CH_3, C-19), 19.8 (CH_3, C-18), 17.7 (CH_3, C-17), 13.5 (CH_3, C-20). HRESIMS m/z 1662.9840 $[M + H]^+$ (calcd for $C_{82}H_{144}N_5O_{27}S$, 1662.9764).

4.4.8 Synthesis and characterization of pseudopteroxazole photoaffinity probes

PtxGlu-BP (113). The carboxylic acid (**100**, 29.9 mg, 78.4 μmol), 4-aminobenzophenone (19.3 mg, 97.9 μmol), and 3Å molecular sieves (~100 mg) were stirred in anhydrous CH_2Cl_2 (6 mL) under a N_2 atmosphere for 30 min prior to adding DCC (42.8 mg, 0.207 mmol). The reaction was stirred overnight at room temperature and was then partitioned between EtOAc and DI H_2O. The EtOAc phase was recovered, subjected to the standard work up procedure, and separated by RP-MPLC (C_{18}, $H_2O \rightarrow CH_3OH$, 0.1% HCO_2H) to yield **113** (10.5 mg, 18.7 mmol, 24%). **113**: white solid; $[\alpha]^{25}_D$ +61.4 (c 0.1392, $CHCl_3$); IR υ_{max} 3326, 2922, 2855, 1703, 1656, 1596, 1528, 1446, 1408, 1374, 1312, 1280, 1175, 1603, 938, 924, 854, 743, 700 cm^{-1}. ^1H NMR ($CDCl_3$, 600 MHz) δ 9.57 (1H, s, NH), 7.80 (2H, app. d, J = 8.6 Hz, H-3'), 7.75 (2H, app. d, J = 7.5 Hz, H-7'), 7.68 (2H, app. d, J = 8.6 Hz, H-2'), 7.56 (1H, tt, J = 7.5, 1.3 Hz, H-9'), 7.46 (2H, app. t, J = 7.5 Hz, H-8'), 4.96 (1H, app. d, J = 9.3 Hz, H-14), 3.94 (1H, app. q, J = 8.8 Hz, H-1), 3.34 (2H, app. ddd, J = 7.3, 5.7, 2.6 Hz, H-22), 3.24-3.16 (1H, m, H-7), 3.06-2.95 (2H, m, H-23), 2.45

(3H, s, H-20), 2.27-2.20 (1H, m, H-4), 2.20-2.14 (1H, m, H-6a), 2.18-2.13 (1H, m, H-5a), 2.14-2.10 (1H, m, H-2a), 1.78 (3H, s, H-17), 1.68 (3H, s, H-16), 1.41 (3H, d, J = 6.8 Hz, H-19), 1.41-1.35 (1H, m, H-6b), 1.29-1.24 (1H, m, H-2b), 1.27-1.21 (1H, m, H-3), 1.07-1.01 (1H, m, H-5b), 1.04 (3H, d, J = 6.0 Hz, H-18). ^{13}C NMR ($CDCl_3$, 150 MHz) δ 195.8 (C, C-5'), 170.5 (C, C-24), 164.7 (C, C-21), 148.1 (C, C-9), 142.4 (C, C-1'), 138.6 (C, C-10), 138.1 (C, C-6'), 136.4 (C, C-13), 134.9 (C, C-12), 132.9 (C, C-4'), 132.3 (CH, C-9'), 131.7 (CH, C-3'), 130.8 (C, C-14), 130.0 (CH, C-7'), 129.1 (C, C-15), 128.4 (CH, C-8'), 125.6 (C, C-11), 122.3 (C, C-8), 118.8 (CH, C-2'), 44.9 (CH, C-4), 40.1 (CH_2, C-2), 36.6 (CH, C-1), 34.7 (CH, C-3), 34.5 (CH_2, C-23), 32.3 (CH_2, C-6), 30.3 (CH, C-7), 28.2 (CH_2, C-5), 25.6 (CH_3, C-16), 24.7 (CH_2, C-22), 22.4 (CH_3, C-19), 19.9 (CH_3, C-18), 17.8 (CH_3, C-17), 13.8 (CH_3, C-20). HRESIMS m/z 561.3087 $[M + Na]^+$ (calcd for $C_{37}H_{41}N_2O_3$, 561.3112).

4-Hydroxy-4'-propargyloxy-benzophenone (106). A stirred solution of 4,4'-dihydroxybenzophenone (**105**, 1.0358 g, 4.8352 mmol) and K_2CO_3 (333.0 mg, 2.41 mmol) in anhydrous DMF (30 mL) under an argon atmosphere was heated to 100°C prior to adding propargyl bromide (80% ($^w/_v$) in toluene, 360 µL, 2.42 mmol). After stirring overnight at 80°C, the reaction mixture was diluted with EtOAc and washed successively with DI H_2O. The EtOAc phase was then subjected to the standard work up procedure and separated by MPLC (silica, hexanes → EtOAc) to yield compounds **106** (447.1 mg, 1.772 mmol, 73%) and 4,4'-dipropargyloxy-benzophenone (**107**, 167.9 mg, 0.5783 mmol, 24%). The starting material **105** (470.0 mg, 2.194 mmol, 45% recovery) was also obtained. **106**: white solid; IR υ_{max} 3288, 1634, 1598, 1506, 1309, 1283, 1226, 1165,

1021, 929, 852, 770 cm^{-1}. ^{1}H NMR ($CDCl_3$, 600 MHz) δ 7.79 (2H, app. d, J = 8.7, H-9'), 7.73 (2H, app. d, J = 8.5, H-5'), 7.04 (2H, app. d, J = 8.7, H-10'), 6.93 (2H, app. d, J = 8.5, H-4'), 4.77 (2H, d, J = 2.3, H-12'), 2.56 (1H, t, J = 2.3 Hz, H-14'). ^{13}C NMR ($CDCl_3$, 150 MHz) δ 195.0 (C, C-7'), 160.8 (C, C-11'), 160.7 (C, C-3'), 132.8 (CH, C-5'), 132.3 (CH, C-9'), 131.7 (C, C-8'), 130.1 (C, C-6'), 115.3 (CH, C-4'), 114.5 (CH, C-10'), 78.0 (C, C-13'), 76.2 (CH, C-14'), 56.0 (CH_2, C-12'). HRESIMS m/z 253.0857 $[M + H]^+$ (calcd for $C_{16}H_{13}O_3$, 253.0859). **107**: white solid; IR υ_{max} 3289, 1644, 1597, 1504, 1418, 1305, 1284, 1220, 1166, 1018, 926, 849, 767 cm^{-1}. ^{1}H NMR ($CDCl_3$, 600 MHz) δ 7.75 (2H, app. d, J = 8.7 Hz, H-5'), 7.00 (2H, app. d, J = 8.7 Hz, H-4'), 4.72 (2H, d, J = 2.3 Hz, H-12'), 2.56 (1H, t, J = 2.3 Hz, H-14'). ^{13}C NMR ($CDCl_3$, 150 MHz) δ 194.1 (C, C-7'), 160.7 (C, C-3'), 132.1 (CH, C-5'), 131.3 (C, C-6'), 114.4 (CH, C-4'), 77.9 (C, C-13'), 76.2 (CH, C-14'), 55.8 (CH_2, C-12'). HRESIMS m/z 291.1013 $[M + H]^+$ (calcd for $C_{19}H_{15}O_3$, 291.1016).

tert-Butyl 2-(4'-propargyloxy-4-benzophenonoxy)acetate (108). To a stirred solution of **106** (323.7 mg, 1.283 mmol) and K_2CO_3 (425.7 mg, 3.080 mmol) in anhydrous acetone (10 mL) under a N_2 atmosphere was added tert-butyl bromoacetate (800 μL, 5.42 mmol). After stirring overnight at room temperature, the reaction mixture was partitioned between EtOAc and DI H_2O. The organic layer was recovered and subjected to the standard work up procedure to provide the desired tert-butyl ester (**108**, 746.0 mg). **108**: white solid; $[\alpha]^{25}_D$ +54.7 (c 0.3033, $CHCl_3$); IR υ_{max} 3288, 2979, 1749, 1647, 1601, 1508, 1369, 1307, 1222, 1168, 1152, 1076, 1023, 928, 850, 769 cm^{-1}. ^{1}H NMR ($CDCl_3$, 600 MHz) δ 7.77 (4H, app. d, J = 8.7 Hz, H-5', H-9'), 7.02 (2H, app. d, J = 8.7 Hz, H-10'),

6.94 (2H, app. d, J = 8.7 Hz, H-4'), 4.75 (2H, d, J = 2.3 Hz, H-12'), 4.58 (2H, s, H-2'), 2.56 (1H, t, J = 2.3 Hz, H-14'), 1.48 (9H, s, $C(CH_3)_3$). ^{13}C NMR ($CDCl_3$, 150 MHz) δ 194.3 (C, C-7'), 167.5 (C, C-1'), 161.2 (C, C-3'), 160.8 (C, C-11'), 132.3 (CH, C-5'), 132.2 (CH, C-9'), 131.5, 131.5 (C, C-6', C-8'), 114.5 (CH, C-10'), 114.2 (CH, C-4'), 82.8 (C, $C(CH_3)_3$), 78.0 (C, C-13'), 76.2 (CH, C-14'), 65.7 (CH_2, C-2'), 56.0 (CH_2, C-12'), 28.1 (CH_3, $C(CH_3)_3$). HRESIMS m/z 367.1523 $[M + H]^+$ (calcd for $C_{22}H_{23}O_5$, 367.1540).

2-(4'-Propargyloxy-4-benzophenonoxy)acetic acid (109). The tert-butyl ester (**108**, 746.0 mg) was dissolved in CH_2Cl_2 (10 mL) and CF_3CO_2H (2.61 mL, 34.1 mmol) was added. After stirring the reaction overnight at room temperature, the mixture was partitioned between EtOAc and $NaHCO_{3(aq)}$. The EtOAc phase was recovered and subjected to the standard work up procedure to provide the crude product, which was separated by RP-MPLC (C_{18}, $H_2O \rightarrow CH_3OH$, 0.1% HCO_2H) to yield **109** (398.1 mg, 1.283 mmol, 93% over two steps). **109**: white solid; $[\alpha]^{25}_D$ +32.3 (c 1.9169, $CHCl_3$); IR υ_{max} 3287, 1741, 1643, 1600, 1508, 1308, 1226, 1170, 1021, 929, 851, 769 cm^{-1}. ^1H NMR ($CDCl_3$, 600 MHz) δ 7.78 (4H, app. d, J = 8.8 Hz, H-5', H-9'), 7.14 (2H, app. d, J = 8.8 Hz, H-10'), 7.09 (2H, app. d, J = 8.8 Hz, H-4'), 4.86 (2H, s, H-2'), 4.92 (2H, d, J = 2.4 Hz, H-12'), 3.15 (1H, t, J = 2.4 Hz, H-14'). ^{13}C NMR ($CDCl_3$, 150 MHz) δ 193.9 (C, C-7'), 169.8 (C, C-1'), 162.3 (C, C-3'), 161.8 (C, C-11'), 132.7 (CH, C-9'), 132.7 (CH, C-5'), 132.2 (C, C-8'), 132.1 (C, C-6'), 115.3 (CH, C-10'), 115.1 (CH, C-4'), 79.2 (C, C-13'), 77.5 (CH, C-14'), 65.4 (CH_2, C-2'), 56.5 (CH_2, C-12'). HRESIMS m/z 311.0907 $[M + H]^+$ (calcd for $C_{18}H_{15}O_5$, 311.0914).

N-Succinimidyl 2-(4'-propargyloxy-4-benzophenonoxy)acetate (110). A solution of **109** (491.9 mg) and NHS (401.2 mg, 3.486 mmol) in THF (25 mL) were stirred in the presence of 3Å molecular sieves (~500 mg) under a N_2 atmosphere. After stirring for 30 min, DIC (615 μL, 3.929 mmol) was added and the reaction mixture was stirred overnight at room temperature. The mixture was then partitioned between EtOAc and DI H_2O. The EtOAc phase was recovered and subjected to the standard work up procedure to provide a crude sample of NHS ester **110** (783.5 mg), which was utilized without purification.

Ptx-EG$_3$-BPA (111). A solution of **97** (16.2 mg, 32.4 μmol) in anhydrous CH_2Cl_2 (5 mL) was stirred with 3Å molecular sieves (~100 mg) for 20 min before adding the crude sample of NHS ester **110** (33.8 mg). Afterwards, Et_3N (10 μL, 72 μmol) was added and the reaction was stirred overnight at room temperature. After removing the solvent in vacuo, the crude product was separated by RP-MPLC (C_{18}, $H_2O \rightarrow CH_3OH$, 0.1% HCO_2H) to provide **111** (9.87 mg, 12.5 μmol, 39%) as a regioisomeric mixture with a ratio of approximately 5:1. **111**: clear oil; $[\alpha]^{25}_D$ +54.7 (c 0.3033, $CHCl_3$); IR υ_{max} 3292, 2920, 2868, 1674, 1649, 1601, 1537, 1508, 1445, 1248, 1169, 1116, 928, 769 cm^{-1}. ^1H NMR ($CDCl_3$, 600 MHz) δ 7.79 (2H, app. d, J = 8.7 Hz, H-5'), 7.78 (2H, app. d, J = 8.8 Hz, H-9'), 7.11 (1H, t, J = 5.4 Hz, 30-NH), 7.03 (2H, app. d, J = 8.8 Hz, H-10'), 6.98 (2H, app. d, J = 8.7 Hz, H-4'), 4.95 (1H, d, J = 9.3 Hz, H-14), 4.76 (2H, d, J = 2.4 Hz, H-12'), 4.54 (2H, s, H-2'), 3.94-3.88 (1H, m, H-1), 3.93 (2H, t, J = 6.9 Hz, H-23), 3.65-3.62 (2H, m, H-27), 3.60-3.57 (4H, m, H-25, H-26), 3.53 (2H, t, J = 6.1 Hz, H-28), 3.54-3.51 (2H, m, H-24), 3.47 (2H, q, J = 6.1 Hz, H-30), 3.23-3.16 (1H, m, H-7), 3.17 (2H, t, J =

6.9 Hz, H-22), 2.56 (1H, t, J = 2.4 Hz, H-14'), 2.37 (3H, s, H-20), 2.22 (1H, app. ddd, J = 9.4, 3.6 Hz, H-4), 2.20-2.13 (1H, m, H-6a), 2.17-2.11 (1H, m, H-5a), 2.13-2.08 (1H, m, H-2a), 1.81 (2H, p, J = 6.1 Hz, H-29), 1.76 (3H, s, H-17), 1.65 (3H, s, H-16), 1.43-1.34 (1H, m, H-6b), 1.41 (3H, d, J = 6.8 Hz, H-19), 1.29-1.23 (1H, m, H-2b), 1.27-1.20 (1H, m, H-3), 1.09-1.00 (1H, m, H-5b), 1.03 (3H, d, J = 5.9 Hz, H-18). ^{13}C NMR ($CDCl_3$, 150 MHz) δ 194.2 (C, C-7'), 167.5 (C, C-1'), 162.7 (C, C-21), 160.9 (C, C-11'), 160.5 (C, C-3'), 148.0 (C, C-9), 139.3 (C, C-10), 135.7 (C, C-13), 134.3 (C, C-12), 132.4 (CH, C-5'), 132.3 (CH, C-9'), 132.0 (C, C-6'), 131.3 (C, C-8'), 131.0 (CH, C-14), 128.8 (C, C-15), 125.9 (C, C-11), 121.9 (C, C-8), 114.6 (CH, C-10'), 114.4 (CH, C-4'), 78.0 (C, C-13'), 76.3 (CH, C-14'), 70.6, 70.6, 70.6 (CH_2, C-25, C-26, C-27), 70.4 (CH_2, C-24), 70.0 (CH_2, C-28), 68.3 (CH_2, C-23), 67.6 (CH_2, C-2'), 56.0 (CH_2, C-12'), 44.8 (CH, C-4), 40.2 (CH_2, C-2), 37.7 (CH_2, C-30), 36.5 (CH, C-1), 34.7 (CH, C-3), 32.3 (CH_2, C-6), 30.3 (CH, C-7), 29.8 (CH_2, C-22), 29.1 (CH_2, C-29), 28.2 (CH_2, C-5), 25.5 (CH_3, C-16), 22.3 (CH_3, C-19), 19.9 (CH_3, C-18), 17.7 (CH_3, C-17), 13.6 (CH_3, C-20). HRESIMS m/z 791.4261 $[M + H]^+$ (calcd for $C_{48}H_{59}N_2O_8$, 791.4266).

PtxGlu-EG$_3$-BPA (112). Method 1: A solution of **100** (45.4 mg, 0.119 mmol) and NHS (17.8 mg, 0.155 mmol) in CH_2Cl_2 (5 mL) was stirred with 3Å molecular sieves (~500 mg) under an argon atmosphere. The 4,7,10-trioxa-1,13-tridecanediamine (**94**, 260 μL, 1.18 mmol) was then added and the reaction was stirred for 48 h at room temperature, at which point the reaction mixture was partitioned between EtOAc and DI H_2O. The EtOAc phase was then subjected to the standard work up procedure, providing a crude sample of PtxGlu-EG$_3$-NH_2 (**101**, 86.6 mg). This intermediate was dissolved in CH_2Cl_2

(5 mL) and a crude sample of NHS ester **110** (118.8 mg) was then added. After stirring the reaction for 48 h at room temperature, the reaction mixture was worked up, as described above, and separated by RP-MPLC (C_{18}, $H_2O \rightarrow CH_3OH$, 0.1% HCO_2H) to yield the desired product **112** (32.3 mg, 36.9 μmol, 31% over three steps). Method 2: To a stirred solution of PtxGlu-EG_3-NH_2 (**101**, 10.4 mg, 17.8 μmol) in CH_2Cl_2 (5 mL) was added a crude sample of NHS ester **110** (39.1 mg). After stirring the reaction was left to stir for 48 h at room temperature, the mixture was worked up, as described above, and separated by RP-MPLC (C_{18}, $H_2O \rightarrow CH_3OH$, 0.1% HCO_2H) to yield **112** (7.67 mg, 8.75 μmol, 49%). The products of both reactions were isolated as a regioisomeric mixture with a ratio of approximately 27:1. **112**: yellow oil; $[\alpha]^{25}_D$ +52.3 (c 0.9883, $CHCl_3$); IR υ_{max} 3302, 2921, 2867, 1651, 1601, 1542, 1444, 1305, 1248, 1226, 1169, 1116, 928, 851, 769 cm^{-1}. ^1H NMR ($CDCl_3$, 600 MHz) δ 7.75 (4H, app. d, J = 8.7 Hz, H-5', H-9'), 7.15 (1H, t, J = 5.5 Hz, 34-NH), 7.00 (2H, app. d, J = 8.7 Hz, H-10'), 6.95 (2H, app. d, J = 8.7 Hz, H-4'), 6.73 (1H, t, J = 5.4 Hz, 25-NH), 4.91 (1H, d, J = 9.3 Hz, H-14), 4.73 (2H, d, J = 2.4 Hz, H-12'), 4.51 (2H, s, H-2'), 3.87 (1H, app. q, J = 8.8 Hz, H-1), 3.60-3.58 (2H, m, H-29), 3.57-3.55 (2H, m, H-30), 3.55-3.52 (2H, m, H-31), 3.52-3.48 (2H, m, H-28), 3.50 (2H, t, J = 6.2 Hz, H-32), 3.48 (2H, t, J = 5.9 Hz, H-27), 3.43 (2H, q, J = 6.2 Hz, H-34), 3.32 (2H, app. q, J = 6.2 Hz, H-25), 3.21 (2H, t, J = 7.6 Hz, H-22), 3.18-3.12 (1H, m, H-7), 2.71 (2H, t, J = 7.6 Hz, H-23), 2.33 (3H, s, H-20), 2.56 (1H, t, J = 2.4 Hz, H-14'), 2.19 (1H, app. ddd, J = 10.4, 3.5 Hz, H-4), 2.16-2.10 (1H, m, H-6a), 2.14-2.08 (1H, m, H-5a), 2.10-2.04 (1H, m, H-2a), 1.77 (2H, p, J = 6.2 Hz, H-33), 1.75-1.70 (2H, m, H-26), 1.73 (3H, s, H-17), 1.63 (3H, s, H-16), 1.39-1.31 (1H, m, H-6b), 1.38 (3H, d, J = 6.8 Hz, H-19), 1.27-1.20 (1H, m, H-2b), 1.23-1.17 (1H, m, H-3), 1.05-0.96 (1H, m, H-5b), 1.00

(3H, d, J = 6.0 Hz, H-18). ^{13}C NMR ($CDCl_3$, 150 MHz) δ 194.1 (C, C-7'), 171.1 (C, C-24), 167.4 (C, C-1'), 160.8 (C, C-11'), 160.4 (C, C-3'), 164.3 (C, C-21), 147.9 (C, C-9), 139.1 (C, C-10), 135.6 (C, C-13), 134.2 (C, C-12), 132.3 (CH, C-5'), 132.1 (CH, C-9'), 131.8 (C, C-6'), 131.1 (C, C-8'), 130.9 (CH, C-14), 128.6 (C, C-15), 125.6 (C, C-11), 121.8 (C, C-8), 114.4 (CH, C-10'), 114.3 (CH, C-4'), 77.9 (C, C-13'), 76.3 (CH, C-14'), 70.5, 70.5 (CH_2, C-29, C-30), 70.3 (CH_2, C-31), 70.1 (CH_2, C-28), 69.8, 69.8 (CH_2, C-27, C-32), 67.4 (CH_2, C-2'), 55.9 (CH_2, C-12'), 44.7 (CH, C-4), 40.0 (CH_2, C-2), 37.8 (CH_2, C-25), 37.5 (CH_2, C-34), 36.4 (CH, C-1), 34.5 (CH, C-3), 33.2 (CH_2, C-23), 32.2 (CH_2, C-6), 30.2 (CH, C-7), 29.0, 29.0 (CH_2, C-26, C-33), 28.1 (CH_2, C-5), 25.4 (CH_3, C-16), 24.7 (CH_2, C-22), 22.2 (CH_3, C-19), 19.8 (CH_3, C-18), 17.6 (CH_3, C-17), 13.5 (CH_3, C-20). HRESIMS m/z 876.4785 $[M + H]^+$ (calcd for $C_{52}H_{66}N_3O_9$, 876.4794).

4.4.9 Synthesis and characterization pseudopterosin-derived probes

Pseudopterosin G-J aglycone methyl ether (95). The methyl ether (**95**) was prepared following a known procedure.[280a] To a stirred solution of pseudopterosins G-J (**33**-**36**) (10.079 g) and K_2CO_3 (15.82 g, 114.5 mmol) in freshly distilled acetone (125 mL) was added CH_3I (20 mL, 320 mmol). The reaction was heated to reflux overnight and then partitioned between EtOAc and DI H_2O. The EtOAc layer was evaporated in vacuo to provide the crude product, which was immediately dissolved in CH_3OH:H_2O (95:5, 100 mL), adjusted to pH 1 with HCl, and heated under reflux overnight. After removing approximately 90 mL of the reaction solvent in vacuo, the reaction mixture was diluted with EtOAc and washed successively with $NaHCO_{3(aq)}$. The EtOAc phase was recovered,

subjected to the standard work up procedure, and then separated by MPLC (silica, hexanes → TBME) to yield **95** (4.238 g, 13.48 mmol, ~62%). All ^{1}H and ^{13}C NMR spectroscopic data for **95** were in agreement with the literature.[280a]

Ps-CO_2t-Bu (114). A solution of aglycone methyl ether (**95**, 442.5 mg, 1.407 mmol) in anhydrous DMF (15 mL) was stirred under a N_2 atmosphere at 0 ºC. Afterwards, NaH (69.8 mg, 2.91 mmol) was slowly added and the mixture was stirred for 3 h. During this time, the reaction slowly warmed to room temperature and tert-butyl bromoacetate (415 µL, 2.81 mmol) was added. The reaction was left to stir for 72 h, after which TLC analysis (hexanes:EtOAc 7:3) showed the formation of the desired product. The reaction mixture was diluted with EtOAc and washed successively with DI H_2O. The recovered EtOAc layer was then subjected to the standard work up procedure, providing a crude product that was separated by MPLC (silica, hexanes → TBME) to yield **114** (321.3 mg, 0.7496 mmol, 50%). **114**: white solid; $[\alpha]^{25}_{D}$ +32.3 (c 1.9169, $CHCl_3$); IR υ_{max} 2925, 2861, 1758, 1730, 1456, 1413, 1368, 1321, 1223, 1160, 1098, 845 cm^{-1}. ^{1}H NMR ($CDCl_3$, 600 MHz) δ 4.96 (1H, d, J = 9.2 Hz, H-14), 4.53 (1H, d, J = 15.7 Hz, H-21a), 4.46 (1H, d, J = 15.7 Hz, H-21b), 3.74 (3H, s, 10-OCH_3), 3.72-3.66 (1H, m, H-1), 3.39 (1H, app. sextet, J = 7.2 Hz, H-7), 2.14-2.07 (1H, m, H-6a), 2.10-2.04 (1H, m, H-5a), 2.08-2.03 (1H, m, H-4), 2.07 (3H, s, H-20), 1.96 (1H, app. ddd, J = 10.3, 8.0, 1.5 Hz, H-2a), 1.73 (3H, s, H-17), 1.69 (3H, s, H-16), 1.52 (9H, s, $C(CH_3)_3$), 1.39-1.31 (1H, m, H-6b), 1.27-1.21 (1H, m, H-3), 1.26 (3H, d, J = 6.9 Hz, H-19), 1.25-1.20 (1H, m, H-2b), 1.03 (3H, d, J = 5.8 Hz, H-18), 0.97-0.89 (1H, m, H-5b). ^{13}C NMR ($CDCl_3$, 150 MHz) δ 169.1 (C, C-22), 149.0 (C, C-10), 148.0 (C, C-9), 135.6 (C, C-13), 134.6 (C, C-12), 133.3

(C, C-8), 131.0 (CH, C-14), 128.8 (C, C-15), 128.5 (C, C-11), 81.4 (C, $C(CH_3)_3$), 70.6 (CH_2, C-21), 60.4 (CH_3, 10-OCH_3), 44.1 (CH, C-4), 40.2 (CH_2, C-2), 37.4 (CH, C-1), 34.2 (CH, C-3), 31.3 (CH_2, C-6), 28.3 (CH, C-7), 28.3 (CH_3, $C(CH_3)_3$), 27.7 (CH_2, C-5), 25.6 (CH_3, C-16), 24.6 (CH_3, C-19), 20.2 (CH_3, C-18), 17.7 (CH_3, C-17), 12.2 (CH_3, C-20). HRESIMS m/z 451.2809 $[M + Na]^+$ (calcd for $C_{27}H_{40}O_4Na$, 451.2819).

Ps-CO_2H (115). To a solution of the tert-butyl ester (**114**, 308.6 mg, 0.7200 mmol) in THF (10 mL) was added LiOH (338.0 mg, 14.11 mmol). The mixture was stirred at room temperature for 96 h, at which point TLC analysis (hexanes:EtOAc 7:3) showed product formation. The reaction mixture was then diluted with EtOAc and partitioned with DI H_2O. The EtOAc layer was recovered, subjected to the standard work up procedure, and separated by RP-MPLC (C_{18}, $H_2O \rightarrow CH_3OH$, 0.1% HCO_2H) to provide the desired carboxylic acid (**115**, 254.3 mg, 0.6827 mmol, 95%). **115**: yellow oil; $[\alpha]^{25}_D$ +59.3 (c 1.3600, $CHCl_3$); IR υ_{max} 2923, 2861, 1736, 1448, 1413, 1375, 1319, 1220, 1098, 1044, 1009, 756 cm^{-1}.^{1}H NMR ($CDCl_3$, 600 MHz) δ 10.90-8.10 (1H, br s, CO_2H), 4.96 (1H, d, J = 9.2 Hz, H-14), 4.73 (1H, d, J = 16.5 Hz, H-21a), 4.53 (1H, d, J = 16.5 Hz, H-21b), 3.79 (3H, s, 10-OCH_3), 3.71 (1H, app. q, J = 8.7 Hz, H-1), 3.24 (1H, app. sextet, J = 7.2 Hz, H-7), 2.16-2.08 (1H, m, H-6a), 2.12-2.05 (1H, m, H-5a), 2.10-2.05 (1H, m, H-4), 2.09 (3H, s, H-20), 2.00 (1H, app. dd, J = 10.0, 8.2 Hz, H-2a), 1.75 (3H, s, H-17), 1.70 (3H, s, H-16), 1.41-1.32 (1H, m, H-6b), 1.26 (3H, d, J = 6.9 Hz, H-19), 1.26-1.21 (1H, m, H-3), 1.26-1.20 (1H, m, H-2b), 1.04 (3H, d, J = 5.7 Hz, H-18), 0.98-0.90 (1H, m, H-5b). ^{13}C NMR ($CDCl_3$, 150 MHz) δ 173.3 (C, C-22), 148.5 (C, C-10), 147.7 (C, C-9), 136.6 (C, C-13), 135.8 (C, C-12), 130.6 (CH, C-14), 129.1 (C, C-15), 128.6 (C, C-11), 132.9

(C, C-8), 70.4 (CH_2, C-21), 61.0 (CH_3, 10-OCH_3), 44.1 (CH, C-4), 40.1 (CH_2, C-2), 37.3 (CH, C-1), 34.2 (CH, C-3), 31.3 (CH_2, C-6), 28.8 (CH, C-7), 27.5 (CH_2, C-5), 25.5 (CH_3, C-16), 23.9 (CH_3, C-19), 20.0 (CH_3, C-18), 17.7 (CH_3, C-17), 12.3 (CH_3, C-20). HRESIMS m/z 373.2356 $[M + H]^+$ (calcd for $C_{23}H_{33}O_4$, 373.2373).

Ps-CO_2CH_3 (116). The methyl ester (**116**) was obtained as a solvent-derived artifact during the RP-MPLC purification of the carboxylic acid (**115**). **116**: yellow oil; $[\alpha]^{25}_D$ +42.0 (c 0.5517, $CHCl_3$); IR υ_{max} 2923, 2857, 1767, 1743, 1448, 1413, 1320, 1205, 1100, 1072, 1044, 839 cm^{-1}. ^1H NMR ($CDCl_3$, 600 MHz) δ 4.95 (1H, d, J = 9.2 Hz, H-14), 4.63 (2H, s, H-21), 3.81 (3H, s, 22-OCH_3), 3.73 (3H, s, 10-OCH_3), 3.69 (1H, app. q, J = 8.8 Hz, H-1), 3.35 (1H, app. sextet, J = 7.2 Hz, H-7), 2.13-2.07 (1H, m, H-6a), 2.09-2.03 (1H, m, H-5a), 2.08-2.02 (1H, m, H-4), 2.06 (3H, s, H-20), 1.96 (1H, app. ddd, J = 10.3, 8.1, 1.5 Hz, H-2a), 1.73 (3H, s, H-17), 1.68 (3H, s, H-16), 1.37-1.31 (1H, m, H-6b), 1.25 (3H, d, J = 6.9 Hz, H-19), 1.25-1.20 (1H, m, H-3), 1.24-1.18 (1H, m, H-2b), 1.03 (3H, d, J = 5.9 Hz, H-18), 0.95-0.89 (1H, m, H-5b). ^{13}C NMR ($CDCl_3$, 150 MHz) δ 170.5 (C, C-22), 149.0 (C, C-10), 147.6 (C, C-9), 135.8 (C, C-13), 134.9 (C, C-12), 133.3 (C, C-8), 130.9 (CH, C-14), 128.9 (C, C-15), 128.6 (C, C-11), 69.7 (CH_2, C-21), 60.4 (CH_3, 10-OCH_3), 51.9 (CH_3, 22-OCH_3), 44.1 (CH, C-4), 40.1 (CH_2, C-2), 37.5 (CH, C-1), 34.2 (CH, C-3), 31.3 (CH_2, C-6), 28.3 (CH, C-7), 27.7 (CH_2, C-5), 25.6 (CH_3, C-16), 24.6 (CH_3, C-19), 20.2 (CH_3, C-18), 17.7 (CH_3, C-17), 12.2 (CH_3, C-20). HRESIMS m/z 387.2529 $[M + H]^+$ (calcd for $C_{24}H_{35}O_4$, 387.2530).

Ps-EG$_3$-NH$_2$ (117). The carboxylic acid (**115**, 17.9 mg, 48.1 μmol) and NHS (8.2 mg, 71 μmol) were dissolved in anhydrous CH_2Cl_2 (5 mL) and stirred under a N_2 atmosphere. DCC (28.2 mg, 0.137 mmol) was then added and the reaction was stirred overnight at room temperature. An excess of 4,7,10-trioxa-1,13-tridecanediamine (**94**, 110 μL, 0.502 mmol) was then added and the reaction was left to stir for 7 h, at which point the mixture was diluted with EtOAc and washed successively with DI H_2O. After recovery of the EtOAc layer, the standard work up procedure was completed, and the crude product was separated by RP-MPLC (C_{18}, $H_2O \rightarrow CH_3OH$, 0.1% HCO_2H) to provide the desired product (**117**, 18.3 mg, 31.8 μmol, 66% over two steps). **117**: yellow oil; $[\alpha]^{25}_D$ -32.9 (c 0.1950, $CHCl_3$); IR υ_{max} 3332, 2923, 2867, 1660, 1587, 1538, 1456, 1413, 1375, 1348, 1319, 1109, 1072, 766 cm^{-1}.^{1}H NMR ($CDCl_3$, 600 MHz) δ 7.39 (1H, t, J = 5.5 Hz, 24-NH), 4.93 (1H, d, J = 9.2 Hz, H-14), 4.43 (2H, s, H-21), 3.68 (1H, app. q, J = 8.7 Hz, H-1), 3.70 (3H, s, 10-OCH_3), 3.64-3.60 (2H, m, H-30), 3.62-3.55 (8H, m, H-26, H-27, H-28, H-29), 3.57 (2H, t, J = 6.0 Hz, H-25), 3.46 (2H, q, J = 6.9 Hz, H-23), 3.32 (2H, q, J = 6.1 Hz, H-32), 3.14 (1H, sextet, J = 7.2 Hz, H-7), 2.12-2.05 (1H, m, H-6a), 2.08-2.02 (1H, m, H-5a), 2.06-1.99 (1H, m, H-4), 2.05 (3H, s, H-20), 1.95 (1H, app. q, J = 10.2, 8.1 Hz, H-2a), 1.94-1.88 (2H, m, H-31), 1.86 (2H, p, J = 6.5 Hz, H-24), 1.72 (3H, s, H-17), 1.67 (3H, s, H-16), 1.37-1.29 (1H, m, H-6b), 1.24-1.18 (1H, m, H-3), 1.23 (3H, d, J = 6.8 Hz, H-19), 1.22-1.17 (1H, m, H-2b), 1.01 (3H, d, J = 5.8 Hz, H-18), 0.95-0.87 (1H, m, H-5b). ^{13}C NMR ($CDCl_3$, 150 MHz) δ 170.0 (C, C-22), 149.1 (C, C-10), 147.2 (C, C-9), 136.1 (C, C-13), 135.5 (C, C-12), 132.6 (C, C-8), 130.7 (CH, C-14), 129.1 (C, C-15), 128.9 (C, C-11), 72.0 (CH_2, C-21), 70.6, 70.3, 70.3, 70.1 (CH_2, C-26, C-27, C-28, C-29), 69.9 (CH_2, C-30), 69.1 (CH_2, C-25), 60.6 (CH_3, 10-OCH_3), 44.1 (CH, C-4), 40.1 (CH_2,

C-2), 39.0 (CH_2, C-32), 37.4 (CH, C-1), 36.7 (CH_2, C-23), 34.2 (CH, C-3), 31.3 (CH_2, C-6), 29.7 (CH_2, C-24), 28.7 (CH, C-7), 27.9 (CH_2, C-31), 27.5 (CH_2, C-5), 25.6 (CH_3, C-16), 24.3 (CH_3, C-19), 20.1 (CH_3, C-18), 17.7 (CH_3, C-17), 12.3 (CH_3, C-20). HRESIMS m/z 575.4056 $[M + H]^+$ (calcd for $C_{33}H_{55}N_2O_6$, 575.4055).

Ps-EG$_3$-Biotin (119). The above procedure for synthesizing Ps-EG$_3$-NH$_2$ (**117**) was carried out using the carboxylic acid (**115**, 28.7 mg, 76.9 μmol), NHS (13.7 mg, 0.119 mmol), DCC (41.6 mg, 0.202 mmol), 4,7,10-trioxa-1,13-tridecanediamine (**94**, 170 μL, 0.775 mmol), and anhydrous CH_2Cl_2 (6 mL). Without further purification, the crude product of **117** was dissolved in anhydrous CH_2Cl_2 and added to biotin-NHS (**102**, 54.9 mg, 0.1608 mmol). The reaction was stirred for 2 h, at which point LC-HRESIMS analysis indicated the formation of the desired product. The mixture was then diluted with EtOAc and partitioned between DI H_2O. The organic layer was recovered, subjected to the standard work up procedure, and separated by RP-MPLC (C_{18}, $H_2O \rightarrow CH_3OH$, 0.1% HCO_2H). The biotinylated Ps-EG$_3$-Biotin (**119**, 8.79 mg, 11.0 μmol, 14% over three steps) was then purified by semi-preparative RP-HPLC (C_{18}, 90% CH_3OH, HCO_2H). **119**: yellow oil; $[\alpha]^{25}_D$ +75.5 (c 0.1508, $CHCl_3$); IR υ_{max} 3298, 2922, 2866, 1699, 1657, 1542, 1452, 1093, 1071, 712 cm^{-1}. ^1H NMR ($CDCl_3$, 600 MHz) δ 7.39 (1H, t, J = 5.6 Hz, 24-NH), 6.64 (1H, t, J = 5.4 Hz, 33-NH), 6.27 (1H, br s, 7'-NH), 5.48 (1H, br s, 8'-NH), 4.93 (1H, d, J = 9.2 Hz, H-14), 4.48 (1H, dd, J = 7.5, 4.9 Hz, H-8'), 4.44 (2H, s, H-21), 4.28 (1H, dd, J = 7.5, 4.8 Hz, H-7'), 3.71 (3H, s, 10-OCH_3), 3.68 (1H, app. q, J = 8.7 Hz, H-1), 3.64-3.55 (8H, m, H-26, H-27, H-28, H-29), 3.60-3.56 (2H, m, H-25), 3.54 (2H, t, J = 6.0 Hz, H-30), 3.47 (2H, q, J = 6.5 Hz, H-23), 3.32 (2H, q, J = 6.0

Hz, H-32), 3.18-3.12 (1H, m, H-7), 3.12 (1H, td, J = 7.3, 4.8 Hz, H-6'), 2.88 (1H, dd, J = 12.8, 4.9 Hz, H-9'a), 2.72 (1H, d, J = 12.8 Hz, H-9'b), 2.18 (2H, t, J = 7.5 Hz, H-2'), 2.13-2.05 (1H, m, H-6a), 2.09-2.03 (1H, m, H-5a), 2.07-2.01 (1H, m, H-4), 2.05 (3H, s, H-20), 1.96 (1H, app. q, J = 10.1, 8.2 Hz, H-2a), 1.87 (2H, p, J = 6.5 Hz, H-24), 1.76 (2H, p, J = 6.0 Hz, H-31), 1.76-1.70 (1H, m, H-5'a), 1.72 (3H, s, H-17), 1.69-1.61 (2H, m, H-3'), 1.68-1.62 (1H, m, H-5'b), 1.67 (3H, s, H-16), 1.43 (2H, p, J = 7.5 Hz, H-4'), 1.38-1.30 (1H, m, H-6b), 1.24-1.19 (1H, m, H-3), 1.24-1.17 (1H, m, H-2b), 1.23 (3H, d, J = 6.9 Hz, H-19), 1.01 (3H, d, J = 5.7 Hz, H-18), 0.96-0.88 (1H, m, H-5b). ^{13}C NMR ($CDCl_3$, 150 MHz) δ 173.2 (C, C-1'), 169.8 (C, C-22), 163.9 (C, C-10'), 149.1 (C, C-10), 147.2 (C, C-9), 136.1 (C, C-13), 135.5 (C, C-12), 132.6 (C, C-8), 130.6 (CH, C-14), 129.1 (C, C-15), 128.9 (C, C-11), 72.0 (CH_2, C-21), 70.6, 70.6, 70.4, 70.1 (CH_2, C-26, C-27, C-28, C-29), 70.1 (CH_2, C-30), 69.4 (CH_2, C-25), 61.9 (CH, C-7'), 60.6 (CH_3, 10-OCH_3), 60.3 (CH, C-8'), 55.7 (CH, C-6'), 44.1 (CH, C-4), 40.7 (CH_2, C-9'), 40.1 (CH_2, C-2), 37.8 (CH_2, C-32), 37.4 (CH, C-1), 36.8 (CH_2, C-23), 36.1 (CH_2, C-2'), 34.2 (CH, C-3), 31.3 (CH_2, C-6), 29.7 (CH_2, C-24), 29.1 (CH_2, C-31), 28.7 (CH, C-7), 28.3 (CH_2, C-4'), 28.2 (CH_2, C-5'), 27.5 (CH_2, C-5), 25.8 (CH_2, C-3'), 25.6 (CH_3, C-16), 24.3 (CH_3, C-19), 20.1 (CH_3, C-18), 17.7 (CH_3, C-17), 12.3 (CH_3, C-20). HRESIMS m/z 801.4827 $[M + H]^+$ (calcd for $C_{43}H_{69}N_4O_8S$, 801.4831).

Ps-EG$_3$-Ps (118). Compound **118** was obtained from the synthesis of Ps-EG$_3$-NH_2 (**117**) and Ps-EG$_3$-Biotin (**119**) during RP-MPLC separation. **118**: orange oil; $[\alpha]^{25}_D$ +30.6 (c 1.5707, $CHCl_3$); IR υ_{max} 3326, 2919, 2851, 1667, 1534, 1456, 1413, 1318, 1222, 1071, 838, 721 cm^{-1}. ^{1}H NMR ($CDCl_3$, 600 MHz) δ 7.38 (2H, t, J = 5.4 Hz, 23-NH), 4.93 (2H,

app. d, J = 9.2 Hz, H-14), 4.44 (4H, s, H-21), 3.71 (6H, s, 10-OCH_3), 3.68 (2H, app. q, J = 8.7 Hz, H-1), 3.58-3.54 (12H, m, H-25, H-26, H-27), 3.47 (4H, q, J = 6.4 Hz, H-23), 3.15 (2H, sextet, J = 7.3 Hz, H-7), 2.13-2.06 (2H, m, H-6a), 2.09-2.04 (2H, m, H-5a), 2.07-2.02 (2H, m, H-4), 2.05 (6H, s, H-20), 1.97 (2H, app. q, J = 10.2, 8.0 Hz, H-2a), 1.87 (4H, p, J = 6.4 Hz, H-24), 1.73 (6H, s, H-17), 1.68 (6H, s, H-16), 1.38-1.31 (2H, m, H-6b), 1.24-1.19 (2H, m, H-3), 1.24-1.18 (2H, m, H-2b), 1.23 (6H, d, J = 6.9 Hz, H-19), 1.02 (6H, d, J = 5.8 Hz, H-18), 0.95-0.88 (2H, m, H-5b). ^{13}C NMR ($CDCl_3$, 150 MHz) δ 169.7 (C, C-22), 149.2 (C, C-10), 147.2 (C, C-9), 136.1 (C, C-13), 135.5 (C, C-12), 132.6 (C, C-8), 130.7 (CH, C-14), 129.1 (C, C-15), 128.9 (C, C-11), 72.0 (CH_2, C-21), 70.7 (CH_2, C-27), 70.5 (CH_2, C-26), 69.5 (CH_2, C-25), 60.6 (CH_3, 10-OCH_3), 44.1 (CH, C-4), 40.1 (CH_2, C-2), 37.4 (CH, C-1), 36.9 (CH_2, C-23), 34.2 (CH, C-3), 31.4 (CH_2, C-6), 29.6 (CH_2, C-24), 28.7 (CH, C-7), 27.5 (CH_2, C-5), 25.6 (CH_3, C-16), 24.3 (CH_3, C-19), 20.1 (CH_3, C-18), 17.7 (CH_3, C-17), 12.3 (CH_3, C-20). HRESIMS m/z 929.6248 $[M + H]^+$ (calcd for $C_{56}H_{85}N_2O_9$, 929.6250).

CHO-PsOH (120). The aldehyde (**120**) was synthesized by ozonolysis using two different methods.

Method 1: The aglycone methyl ether (**95**, 423.6 mg, 1.347 mmol) dissolved in CH_2Cl_2:CH_3OH (5:1, 15 mL) was cooled to -78°C and ozone was bubbled through the solution for 10 min. The solution was then purged with N_2 and cooled to 0°C before adding dimethyl sulfide (3 mL, 40.8 mmol). The reaction was left to stir overnight at room temperature before removing the solvent in vacuo and separating the mixture by

MPLC (silica, hexanes → EtOAc) to yield CHO-PsOH (**120**, 268.7 mg, 0.9317 mmol, 69%).

Method 2: The ozonolysis reaction above was repeated with the aglycone methyl ether (**95**, 388.1 mg, 1.234 mmol), except the ozone was bubbled through the solution for 1 hr. After separating the reaction mixture by MPLC (silica, hexanes → EtOAc), both CHO-PsOH (**120**, 113.3 mg, 392.9 μmol, 32%) and an acetal side product (**121**) were obtained. **120**: yellow oil; $[\alpha]^{25}_{D}$ +67.8 (c 1.1262, $CHCl_3$); IR υ_{max} 3450, 2942, 2865, 1718, 1599, 1458, 1418, 1300, 1230, 1202, 1059, 1019, 891, 799 cm^{-1}. ^1H NMR ($CDCl_3$, 600 MHz) δ 9.28 (1H, d, J = 3.9 Hz, H-14), 5.95 (1H, s, 9-OH), 3.79 (1H, app. td, J = 8.8, 3.9 Hz, H-1), 3.74 (3H, s, 10-OCH_3), 3.16 (1H, app. sextet, J = 7.3 Hz, H-7), 2.17-2.11 (1H, m, H-6a), 2.11 (3H, s, H-17), 2.10-2.04 (1H, m, H-5a), 2.03-1.97 (1H, m, H-4), 2.01-1.95 (1H, m, H-2a), 1.57-1.50 (1H, m, H-2b), 1.38-1.30 (1H, m, H-6b), 1.32-1.26 (1H, m, H-3), 1.29 (3H, d, J = 6.8 Hz, H-16), 1.10 (3H, d, J = 6.5 Hz, H-15), 1.05-0.96 (1H, m, H-5b). ^{13}C NMR ($CDCl_3$, 150 MHz) δ 201.1 (CH, C-14), 146.3 (C, C-9), 143.9 (C, C-10), 136.9 (C, C-13), 127.0 (C, C-11), 126.9 (C, C-8), 120.8 (C, C-12), 60.9 (CH_3, 10-OCH_3), 51.0 (CH, C-1), 43.8 (CH, C-4), 33.1 (CH, C-3), 31.7 (CH_2, C-2), 31.6 (CH_2, C-6), 28.8 (CH, C-7), 27.3 (CH_2, C-5), 22.6 (CH_3, C-16), 19.9 (CH_3, C-15), 12.9 (CH_3, C-17). HRESIMS m/z 311.1607 $[M + Na]^+$ (calcd for $C_{20}H_{24}O_3Na$, 311.1612).

$CH(OCH_3)_2$-PsOH (121). During the synthesis and purification of CHO-PsOH (**120**), using method 2, as described above, the acetal (**121**, 57.9 mg, 173 μmol, 14%) was obtained as a side product. **121**: orange oil; $[\alpha]^{25}_{D}$ +72.0 (c 0.7069, $CHCl_3$); IR υ_{max} 3424, 2942, 2868, 2829, 1457, 1417, 1205, 1180, 1108, 1075, 1054, 883, 800, 775 cm^{-1}. ^1H

NMR ($CDCl_3$, 600 MHz) δ 5.72 (1H, s, 9-OH), 4.12 (1H, d, J = 5.3 Hz, H-14), 3.74 (3H, s, 10-OCH_3), 3.42 (1H, app. p, J = 4.9 Hz, H-1), 3.21 (3H, s, 14-OCH_3), 3.16 (6H, s, 14-OCH_3), 3.09-3.02 (1H, m, H-7), 2.27 (3H, s, H-17), 2.13-2.08 (1H, m, H-4), 2.12-2.05 (1H, m, H-6a), 2.05-1.99 (1H, m, H-5a), 1.92 (1H, ddd, J = 14.0, 10.0, 6.1 Hz, H-2a), 1.63 (1H, ddd, J = 14.0, 11.0, 4.4 Hz, H-2b), 1.33-1.25 (1H, m, H-6b), 1.28 (3H, d, J = 6.7 Hz, H-16), 1.13-1.06 (1H, m, H-3), 1.06-0.99 (1H, m, H-5b), 1.02 (3H, d, J = 6.4 Hz, H-15). ^{13}C NMR ($CDCl_3$, 150 MHz) δ 145.2 (C, C-9), 143.5 (C, C-10), 138.0 (C, C-13), 126.7 (C, C-12), 126.6 (C, C-11), 125.9 (C, C-8), 110.0 (CH, C-14), 60.9 (CH_3, 10-OCH_3), 56.3 (CH_3, 14-OCH_3), 55.8 (CH_3, 14-OCH_3), 42.5 (CH, C-4), 39.2 (CH, C-1), 35.1 (CH, C-3), 31.9 (CH_2, C-6), 31.3 (CH_2, C-2), 29.6 (CH, C-7), 27.0 (CH_2, C-5), 22.3 (CH_3, C-16), 19.9 (CH_3, C-15), 12.5 (CH_3, C-17). HRESIMS m/z 357.2026 $[M + Na]^+$ (calcd for $C_{20}H_{30}O_4Na$, 357.2036).

H_2N-EG_3-PsOH (122). A solution of CHO-PsOH (**120**, 41.2 mg, 0.143 μmol) in CH_3OH (1 mL) was slowly added to 4,7,10-trioxa-1,13-tridecanediamine (**94**, 1.00 mL, 4.56 mmol) in CH_3OH (2 mL). After the addition was complete, the mixture was stirred overnight at room temperature before adding $NaBH_4$ (118.6 mg, 3.135 mmol). The reaction was stirred for an additional 3 h, diluted with $CHCl_3$, and partitioned between DI H_2O. The $CHCl_3$ layer was recovered, subjected to the standard work up procedure, and then separated by RP-MPLC (C_{18}, $H_2O \rightarrow CH_3OH$, 0.1% HCO_2H) to provide a mixture of H_2N-EG_3-PsOH (**122**) and epi-H_2N-EG_3-PsOH (**123**) (33.8 mg, 68.6 μmol, 48% overall yield). These two compounds were separated by semi-preparative RP-HPLC (phenylhexyl, 5 min at 5% CH_3OH increasing linearly to 50% CH_3OH at 30 min, 0.1%

HCO_2H). **122**: colorless oil; $[\alpha]^{25}_D$ +16.5 (c 0.0983, $CHCl_3$); IR υ_{max} 2928, 2866, 1582, 1460, 1421, 1347, 1132, 764 cm^{-1}. ^1H NMR ($CDCl_3$, 600 MHz) δ 3.76-3.68 (2H, m, H-3'), 3.74 (3H, s, 10-OCH_3), 3.67-3.55 (10H, m, H-4', H-5', H-6', H-7', H-8'), 3.46-3.40 (1H, m, H-1), 3.29 (1H, app. sextet, J = 7.0 Hz, H-7), 3.17 (2H, br t, J = 5.0 Hz, H-1'), 3.11-3.00 (2H, m, H-10'), 2.96 (1H, app. t, J = 12.2 Hz, H-14a), 2.76 (1H, app. d, J = 12.2 Hz, H-14b), 2.28 (3H, s, H-17), 2.19-2.12 (1H, m, H-5a), 2.17-2.13 (1H, m, H-2a), 2.12-2.04 (2H, m, H-9'), 2.11-2.05 (1H, m, H-6a), 2.06-1.98 (1H, m, H-4), 2.05-1.96 (2H, m, H-2'), 1.64-1.55 (1H, m, H-3), 1.53 (1H, app. td, J = 13.1, 3.7 Hz, H-2b), 1.50-1.41 (1H, m, H-6b), 1.20 (3H, d, J = 7.0 Hz, H-16), 1.15-1.06 (1H, m, H-5b), 1.10 (3H, d, J = 6.0 Hz, H-15). ^{13}C NMR ($CDCl_3$, 150 MHz) δ 145.2 (C, C-9), 144.0 (C, C-10), 135.1 (C, C-13), 127.2 (C, C-8), 125.6 (C, C-11), 125.4 (C, C-12), 70.7 (CH_2, C-3'), 70.7, 70.1, 70.0, 69.7 (CH_2, C-4', C-5', C-6', C-7'), 68.4 (CH_2, C-8'), 60.8 (CH_3, 10-OCH_3), 50.8 (CH_2, C-14), 45.9 (CH_2, C-10'), 42.8 (CH, C-4), 39.9 (CH_2, C-1'), 33.6 (CH, C-1), 32.3 (CH_2, C-2), 30.5 (CH_2, C-6), 28.9 (CH, C-3), 28.2 (CH_2, C-5), 27.3 (CH, C-7), 26.8 (CH_2, C-2'), 26.2 (CH_2, C-9'), 22.5 (CH_3, C-16), 20.6 (CH_3, C-15), 11.7 (CH_3, C-17). HRESIMS m/z 493.3636 $[M + H]^+$ (calcd for $C_{28}H_{49}N_2O_5$, 493.3647).

epi-H_2N-EG_3-PsOH (123). The epimerized analogue (**123**) was obtained as a side product during the synthesis and purification of H_2N-EG_3-PsOH (**122**) by semi-preparative RP-HPLC. **123**: colorless oil; $[\alpha]^{25}_D$ +12.4 (c 0.4808, $CHCl_3$); IR υ_{max} 2927, 2868, 1582, 1459, 1419, 1347, 1120, 764 cm^{-1}. ^1H NMR ($CDCl_3$, 600 MHz) δ 3.70 (3H, s, 10-OCH_3), 3.68-3.62 (2H, m, H-3'), 3.61-3.54 (8H, m, H-4', H-5', H-6', H-7'), 3.59-3.52 (2H, m, H-8'), 3.59-3.51 (1H, m, H-1), 3.12 (2H, br t, J = 5.8 Hz, H-1'), 3.11-3.00

(2H, m, H-10'), 3.06-2.98 (1H, m, H-7), 2.92 (1H, app. d, J = 11.3 Hz, H-14a), 2.72 (1H, app. t, J = 11.3 Hz, H-14b), 2.25-2.19 (1H, m, H-2a), 2.22 (3H, s, H-17), 2.04-1.98 (2H, m, H-9'), 2.11-2.04 (1H, m, H-6a), 2.04-1.97 (1H, m, H-4), 2.02-1.96 (1H, m, H-5a), 1.97-1.92 (2H, m, H-2'), 1.44-1.34 (1H, m, H-2b), 1.27-1.19 (1H, m, H-6b), 1.24 (3H, d, J = 6.5 Hz, H-16), 1.15-1.07 (1H, m, H-3), 0.99 (3H, d, J = 6.0 Hz, H-15), 0.95-0.87 (1H, m, H-5b). ^{13}C NMR ($CDCl_3$, 150 MHz) δ 145.9 (C, C-9), 144.0 (C, C-10), 137.0 (C, C-13), 126.7 (C, C-8), 125.8 (C, C-11), 125.6 (C, C-12), 70.4, 70.0, 70.0, 69.8 (CH_2, C-4', C-5', C-6', C-7'), 70.2 (CH_2, C-3'), 68.5 (CH_2, C-8'), 60.6 (CH_3, 10-OCH_3), 54.9 (CH_2, C-14), 46.1 (CH_2, C-10'), 43.2 (CH, C-4), 39.2 (CH_2, C-1'), 36.2 (CH_2, C-2), 35.0 (CH, C-3), 32.8 (CH, C-1), 31.9 (CH_2, C-6), 29.5 (CH, C-7), 27.2 (CH_2, C-5), 26.6 (CH_2, C-2'), 25.7 (CH_2, C-9'), 22.3 (CH_3, C-16), 19.6 (CH_3, C-15), 12.1 (CH_3, C-17). HRESIMS m/z 493.3642 $[M + H]^+$ (calcd for $C_{28}H_{49}N_2O_5$, 493.3647).

14,15-Dihydro-pseudopterosin G-J aglycone methyl ether (124). A mixture of the aglycone methyl ether (**95**, 52.3 mg, 166 μmol) and Pd/C (29.5 mg) in EtOAc (5 mL) were stirred with vigorous agitation overnight under a H_2 atmosphere. The reaction mixture was then filtered through Celite® and separated by MPLC (silica, hexanes → EtOAc), yielding the hydrogenated product (**124**, 50.4 mg, 159 μmol, 96%). **124**: yellow oil; $[\alpha]^{25}_D$ +29.8 (c 1.1262, $CHCl_3$); IR υ_{max} 3529, 2950, 2924, 2866, 1457, 1416, 1298, 1227, 1202, 1181, 1050, 1013, 961, 799, 770 cm^{-1}. ^{1}H NMR ($CDCl_3$, 600 MHz) δ 5.71 (1H, s, 9-OH), 3.77 (3H, s, 10-OCH_3), 3.13-3.08 (1H, m, H-1), 3.12-3.07 (1H, m, H-7), 2.24 (3H, s, H-20), 2.16-2.09 (1H, m, H-6a), 2.13-2.09 (1H, m, H-2a), 2.09-2.05 (1H, m, H-4), 2.07-2.03 (1H, m, H-5a), 1.88-1.78 (1H, m, H-15), 1.36-1.30 (1H, m, H-6b), 1.33

(3H, d, J = 6.7 Hz, H-19), 1.31-1.25 (2H, m, H-14), 1.23-1.18 (1H, m, H-2b), 1.20-1.14 (1H, m, H-3), 1.04 (3H, d, J = 6.1 Hz, H-18), 1.04-1.01 (1H, m, H-5b), 1.02 (3H, d, J = 6.6 Hz, H-17), 0.92 (3H, d, J = 6.6 Hz, H-16). ^{13}C NMR ($CDCl_3$, 150 MHz) δ 144.6 (C, C-9), 143.8 (C, C-10), 136.2 (C, C-13), 132.5 (C, C-12), 125.9 (C, C-8), 124.8 (C, C-11), 60.7 (CH_3, 10-OCH_3), 48.9 (CH_2, C-14), 43.4 (CH, C-4), 38.5 (CH_2, C-2), 35.4 (CH, C-3), 32.9 (CH, C-1), 32.1 (CH_2, C-6), 29.7 (CH, C-7), 27.4 (CH_2, C-5), 25.3 (CH, C-15), 24.5 (CH_3, C-16), 22.4 (CH_3, C-19), 20.9 (CH_3, C-17), 20.3 (CH_3, C-18), 12.2 (CH_3, C-20). HRESIMS m/z 317.2468 $[M + H]^+$ (calcd for $C_{20}H_{32}O_2$, 317.2475).

Pseudopterosin G acetonide (125). A solution of pseudopterosin G (**33**, 331.1 mg, 0.7414 mmol) dissolved in acetone (10 mL) was stirred with TsOH (3.7 mg, 21 μmol) at room temperature for 40 h. The reaction mixture was then diluted with EtOAc and partitioned between DI H_2O. The EtOAc layer was recovered, subjected to the standard work up procedure, and separated MPLC (silica, hexanes → TBME) to furnish the desired acetonide (**125**, 315.5 mg, 0.6483 mmol, 87%). **125**: white solid; $[\alpha]^{25}_D$ -58.7 (c 1.8585, $CHCl_3$); IR υ_{max} 3328, 2923, 2863, 1445, 1375, 1320, 1245, 1219, 1085, 1031, 980, 868, 758 cm^{-1}. ^{1}H NMR ($CDCl_3$, 600 MHz) δ 5.07 (1H, d, J = 3.8 Hz, H-1'), 4.96 (1H, d, J = 9.2 Hz, H-14), 4.62 (1H, qd, J = 6.7, 2.2 Hz, H-5'), 4.46 (1H, t, J = 6.1 Hz, H-3'), 4.21 (1H, dd, J = 6.1, 2.2 Hz, H-4'), 4.05-3.98 (1H, m, H-2'), 3.72 (1H, app. q, J = 8.8 Hz, H-1), 3.36 (1H, sextet, J = 7.6, 7.2, 6.9 Hz, H-7), 2.13 (1H, m, H-6a), 2.09-2.03 (1H, m, H-5a), 2.05 (3H, s, H-20), 2.02 (1H, app. ddd, J = 10.0, 3.7 Hz, H-4), 2.00-1.95 (1H, m, H-2a), 1.73 (3H, s, H-17), 1.67 (3H, s, H-16), 1.52 (3H, s, $C(CH_3)_2$), 1.41 (3H, d, J = 6.7 Hz, H-6'), 1.40 (3H, s, $C(CH_3)_2$), 1.33 (1H, tdd, J = 12.8, 6.8, 4.9 Hz, H-6b),

1.25-1.19 (1H, m, H-2b), 1.27-1.21 (1H, m, H-3), 1.20 (3H, d, J = 6.9 Hz, H-19), 1.03 (3H, d, J = 5.9 Hz, H-18), 0.96 (1H, app. ddd, J = 12.5, 11.4, 4.9 Hz, H-5b). ^{13}C NMR ($CDCl_3$, 150 MHz) δ 145.7 (C, C-10), 142.4 (C, C-9), 135.8 (C, C-12), 132.6 (C, C-8), 131.3 (CH, C-14), 130.5 (C, C-13), 128.6 (C, C-15), 122.3 (C, C-11), 109.9 (C, $C(CH_3)_2$), 102.5 (CH, C-1'), 75.9 (CH, C-3'), 75.6 (CH, C-4'), 70.4 (CH, C-2'), 65.4 (CH, C-5'), 43.8 (CH, C-4), 40.2 (CH_2, C-2), 37.3 (CH, C-1), 34.3 (CH, C-3), 31.1 (CH_2, C-6), 28.1 (CH_3, $C(CH_3)_2$), 27.9 (CH, C-7), 27.7 (CH_2, C-5), 26.1 (CH_3, $C(CH_3)_2$), 25.6 (CH_3, C-16), 24.9 (CH_3, C-19), 20.2 (CH_3, C-18), 17.7 (CH_3, C-17), 16.6 (CH_3, C-6'), 12.4 (CH_3, C-20). HRESIMS m/z 487.3052 $[M + H]^+$ (calcd for $C_{29}H_{43}O_6$, 487.3054).

Pseudopterosin G diketal (128). To a stirred solution of **125** (311.9 mg, 0.6409 mmol) in CH_2Cl_2 (8 mL) was added Dess-Martin periodinane (336.3 mg, 0.7929 mmol). The reaction mixture became red upon adding the oxidant. After stirring overnight at room temperature, TLC analysis (hexanes:TBME 7:3) showed the disappearance of starting material. The mixture was then partitioned between EtOAc and DI H_2O before carrying out the standard work up procedure. The crude product was then separated by MPLC (silica, hexanes → TBME) yielding the diketal (**128**, 72.7 mg, 0.150 mmol, 23%) and ortho-quinone (**96**, 70.5 mg, 0.236 mmol, 37%). **128**: yellow solid; IR υ_{max} 2930, 2870, 1733, 1664, 1455, 1378, 1247, 1213, 1044, 1010, 965, 756 cm^{-1}.^{1}H NMR ($CDCl_3$, 600 MHz) δ 6.01 (1H, d, J = 5.8 Hz, H-1'), 5.06 (1H, d, J = 9.1 Hz, H-14), 4.54 (1H, dd, J = 8.0, 1.4 Hz, H-3'), 4.49 (1H, dd, J = 5.8, 1.4 Hz, H-2'), 4.10 (1H, qd, J = 6.5, 1.9 Hz, H-5'), 4.05 (1H, dd, J = 8.0, 1.9 Hz, H-4'), 3.46 (1H, app. q, J = 8.0 Hz, H-1), 2.98-2.91 (1H, m, H-7), 2.02-1.94 (1H, m, H-5a), 1.90-1.83 (1H, m, H-4), 1.89-1.82 (1H, m, H-2a),

1.85-1.79 (1H, m, H-6a), 1.69 (3H, s, H-20), 1.69 (3H, s, H-16), 1.67 (3H, s, H-17), 1.44 (3H, s, $C(CH_3)_2$), 1.42-1.36 (1H, m, H-6b), 1.41 (3H, d, J = 6.5 Hz, H-6'), 1.32-1.26 (1H, m, H-3), 1.32 (3H, s, $C(CH_3)_2$), 1.24-1.17 (1H, m, H-2b), 1.21-1.14 (1H, m, H-5b), 1.13 (3H, d, J = 7.1 Hz, H-19), 0.99 (3H, d, J = 6.5 Hz, H-18). ^{13}C NMR ($CDCl_3$, 150 MHz) δ 197.6 (C, C-10), 152.2 (C, C-12), 139.2 (C, C-13), 139.0 (C, C-8), 131.6 (C, C-11), 126.7 (CH, C-14), 126.2 (C, C-15), 108.8 (C, $C(CH_3)_2$), 99.4 (C, C-9), 98.4 (CH, C-1'), 72.8 (CH, C-4'), 71.8 (CH, C-3'), 69.2 (CH, C-2'), 63.3 (CH, C-5'), 41.1 (CH, C-4), 37.8 (CH, C-1), 37.6 (CH_2, C-2), 32.6 (CH, C-3), 28.5 (CH_2, C-6), 26.8 (CH, C-7), 26.2 (CH_3, $C(CH_3)_2$), 25.7 (CH_3, C-16), 24.7 (CH_2, C-5), 24.5 (CH_3, $C(CH_3)_2$), 22.0 (CH_3, C-19), 21.0 (CH_3, C-18), 17.8 (CH_3, C-17), 16.0 (CH_3, C-6'), 10.5 (CH_3, C-20). HRESIMS m/z 485.2884 $[M + H]^+$ (calcd for $C_{29}H_{41}O_6$, 485.2898).

4.4.10 Synthesis and characterization of arylsulfonamide probes

ASA-EG$_3$-NH$_2$ (132). To a stirred solution of 4-carboxybenzene sulfonamide (100.0 mg, 0.4970 mmol) and NHS (115.9 mg, 1.007 mmol) in anhydrous THF (8 mL) was added DIC (315 μL, 2.012 mmol). After stirring the reaction mixture overnight at room temperature, 4,7,10-trioxa-1,13-tridecanediamine (**94**, 1.10 mL, 5.02 mmol) was added and the reaction was stirred for an additional 8 h, at which point the mixture was concentrated in vacuo and separated by RP-MPLC (C_{18}, $H_2O \rightarrow CH_3OH$, 0.1% HCO_2H) to provide ASA-EG$_3$-NH$_2$ (**132**, 115.2 mg, 0.2855 mmol, 57%). **132**: clear oil; IR υ_{max} 3270, 3079, 2934, 2873, 1641, 1569, 1345, 1167, 1098, 762 cm^{-1}. ^1H NMR (CD_3OD, 600 MHz) δ 8.75-8.40 (1H, br m, 6-NH), 8.00-7.96 (2H, m, H-2), 7.99-7.95 (2H, m, H-3),

3.67-3.58 (8H, m, H-9, H-10, H-11, H-12), 3.65-3.60 (2H, m, H-13), 3.61-3.57 (2H, m, H-8), 3.49 (2H, t, J = 7.0 Hz, H-6), 3.15-3.04 (2H, br m, H-15), 1.96-1.90 (2H, m, H-14), 1.93-1.86 (2H, m, H-7). ^{13}C NMR (CD_3OD, 150 MHz) δ 168.6 (C, C-5), 147.6 (C, C-1), 139.0 (C, C-4), 129.0 (CH, C-3), 127.3 (CH, C-2), 71.4, 71.1, 71.1, 71.0 (CH_2, C-9, C-10, C-11, C-12), 70.2 (CH_2, C-13), 70.0 (CH_2, C-8), 39.8 (CH_2, C-15), 38.7 (CH_2, C-6), 30.3 (CH_2, C-7), 28.2 (CH_2, C-14). HRESIMS m/z 404.1851 $[M + H]^+$ (calcd for $C_{17}H_{30}N_3O_6S$, 404.1850).

ASA-EG$_3$-Biotin (133). To a stirred solution of ASA-EG$_3$-NH$_2$ (**132**, 33.6 mg, 83.3 μmol) in anhydrous DMF (3 mL) under a N_2 atmosphere was added biotin-NHS (**102**, 45.7 mg, 0.187 mmol). The reaction was stirred overnight at room temperature, at which point LC-HRESIMS indicated the formation of the desired product. The mixture was evaporated in vacuo and separated by RP-MPLC (C_{18}, $H_2O \rightarrow CH_3OH$, 0.1% HCO_2H), yielding the biotinylated probe ASA-EG$_3$-Biotin (**133**, 40.8 mg, 64.8 μmol, 78%). **133**: white solid; $[\alpha]^{25}_D$ +23.1 (c 0.6383, DMF) IR υ_{max} 3284, 3085, 2929, 2869, 1691, 1638, 1548, 1459, 1332, 1166, 1097, 858, 762 cm^{-1}. ^{1}H NMR (DMF-d$_7$, 600 MHz) δ 8.62 (1H, t, J = 5.4 Hz, 6-NH), 8.06 (2H, app. d, J = 8.4 Hz, H-2), 7.96 (2H, app. d, J = 8.4 Hz, H-3), 7.73 (1H, t, J = 5.5 Hz, 15-NH), 6.43 (1H, br s, 8'-NH), 6.35 (1H, br s, 7'-NH), 4.43 (1H, dd, J = 7.5, 5.0 Hz, H-8'), 4.25 (1H, dd, J = 7.5, 4.4 Hz, H-7'), 3.58-3.47 (8H, m, H-9, H-10, H-11, H-12), 3.45-3.40 (2H, m, H-13), 3.53-3.48 (2H, m, H-8), 3.45-3.40 (2H, m, H-6), 3.19-3.14 (1H, m, H-6'), 3.20-3.14 (2H, m, H-15), 2.89 (1H, dd, J = 12.4, 5.0 Hz, H-9'a), 2.67 (1H, d, J = 12.4 Hz, H-9'b), 2.12 (2H, t, J = 7.5 Hz, H-2'), 1.66 (2H, p, J = 6.6 Hz, H-14), 1.82 (2H, p, J = 6.6 Hz, H-7), 1.74-1.68 (1H, m, H-5'a), 1.59-1.53

(2H, m, H-3'), 1.56-1.50 (1H, m, H-5'b), 1.44-1.30 (2H, m, H-4'). ^{13}C NMR (DMF-d_7, 150 MHz) δ 173.4 (C, C-1'), 166.5 (C, C-5), 164.2 (C, C-10'), 147.7 (C, C-1), 139.1 (C, C-4), 128.9 (CH, C-3), 126.9 (CH, C-2), 71.3, 71.1, 71.1, 71.0 (CH_2, C-9, C-10, C-11, C-12), 69.7 (CH_2, C-8), 69.6 (CH_2, C-13), 62.6 (CH, C-7'), 61.0 (CH, C-8'), 56.9 (CH, C-6'), 41.2 (CH_2, C-9'), 38.3 (CH_2, C-6), 37.2 (CH_2, C-15), 36.6 (CH_2, C-2'), 30.8 (CH_2, C-14), 30.6 (CH_2, C-7), 29.6 (CH_2, C-4'), 29.4 (CH_2, C-5'), 26.7 (CH_2, C-3'). HRESIMS m/z 630.2655 $[M + H]^+$ (calcd for $C_{27}H_{44}N_5O_8S_2$, 630.2626).

ASA-EG$_{23}$-Biotin (134). The above procedure for synthesizing PtxGlu-EG$_{23}$-Biotin (**135**) was carried out using 4-carboxybenzene sulfonamide (8.0 mg, 40 μmol), NHS (5.8 mg, 50 μmol), DIC (25 μL, 0.16 mmol), Biotin-EG$_{23}$-NH$_2$ (**136**, 20.0 mg, 15.4 μmol), Et_3N (10 μL, 72 μmol), and anhydrous DMF (3 mL). The crude product was separated by semi-preparative RP-HPLC (C_{18}, 72% CH_3OH, 0.1% HCO_2H) to yield ASA-EG$_{23}$-Biotin (**134**, 13.5 mg, 9.10 μmol, 59%). **134**: clear oil; $[\alpha]^{25}_D$ +21.9 (c 0.8775, DMF) IR υ_{max} 3303, 3083, 2869, 1700, 1654, 1545, 1456, 1347, 1300, 1250, 1100, 949, 857 cm^{-1}. ^{1}H NMR (DMF-d_7, 600 MHz) δ 8.79-8.70 (1H, br m, 6-NH), 8.12 (2H, br d, J = 6.6 Hz, H-3), 8.00 (2H, br d, J = 6.6 Hz, H-2), 7.88-7.77 (1H, br m, 53-NH), 6.43 (1H, br s, 8'-NH), 6.34 (1H, br s, 7'-NH), 4.51-4.43 (1H, br m, H-8'), 4.33-4.26 (1H, br m, H-7'), 3.61-3.51 (2H, br m, H-6), 3.37-3.27 (2H, br m, H-53), 3.23-3.17 (1H, br m, H-6'), 2.98-2.90 (1H, br m, H-9'a), 2.72 (1H, d, J = 12.1 Hz, H-9'b), 2.19 (2H, br t, J = 7.2 Hz, H-2'), 1.80-1.71 (1H, br m, H-5'a), 1.65-1.57 (2H, br m, H-3'), 1.63-1.53 (1H, br m, H-5'b), 1.48-1.35 (2H, br m, H-4'). ^{13}C NMR (DMF-d_7, 150 MHz) δ 173.5 (C, C-1'), 166.6 (C, C-5), 164.2 (CH_2, C-10'), 147.7 (C, C-1), 138.8 (C, C-4), 129.0 (CH, C-3), 127.0 (CH, C-2),

71.3, 71.3, 71.1, 71.1, 70.6, 70.3 (CH_2, C-7, C-8, …, C-51, C-52), 62.6 (CH_2, C-7'), 61.0 (CH_2, C-8'), 56.9 (CH_2, C-6'), 41.2 (CH_2, C-9'), 40.8 (CH_2, C-6), 39.9 (CH_2, C-53), 36.5 (CH_2, C-2'), 29.6 (CH_2, C-4'), 29.4 (CH_2, C-5'), 26.7 (CH_2, C-3'). HRESIMS m/z 1482.7609 $[M + H]^+$ (calcd for $C_{65}H_{120}N_5O_{28}S_2$, 1482.7556).

4.4.11 Synthesis and characterization of generic control probes

Biotin-EG$_3$-NH$_2$ (129). To a stirred solution of biotin-NHS (**102**, 27.3 mg, 80.0 μmol) in anhydrous DMF (3 mL) was added 4,7,10-trioxa-1,13-tridecanediamine (**94**, 350 μL, 1.60 mmol). After stirring the reaction mixture at room temperature for 8 h, the solvent was evaporated in vacuo and the crude product separated by solid phase extraction (C_{18}, H_2O:CH_3OH stepwise gradient, 0.1% HCO_2H) to yield **129** (30.1 mg, 67.4 μmol, 84%). **129**: white solid; $[\alpha]^{25}_D$ +18.2 (c 0.7742, $CHCl_3$); IR υ_{max} 3267, 3085, 2928, 2870, 1684, 1643, 1582, 1463, 1347, 1101 cm^{-1}. ^1H NMR ($CDCl_3$, 600 MHz) δ 4.50 (dd, J = 7.8, 5.0 Hz, H-8'), 4.31 (dd, J = 7.8, 4.5 Hz, H-7'), 3.68-3.57 (8H, m, H-4, H-5, H-6, H-7), 3.66 (2H, t, J = 6.1 Hz, H-3), 3.52 (2H, t, J = 6.5 Hz, H-8), 3.25 (2H, t, J = 6.5 Hz, H-10), 3.24-3.18 (m, H-6'), 3.09 (2H, t, J = 6.1 Hz, H-1), 2.93 (dd, J = 12.8, 5.0 Hz, H-9'a), 2.71 (d, J = 12.8 Hz, H-9'b), 2.21 (t, J = 7.4 Hz, H-2'), 1.93 (2H, p, J = 6.1 Hz, H-2), 1.79-1.70 (m, H-5'a), 1.76 (2H, p, J = 6.5 Hz, H-9), 1.72-1.59 (m, H-3'), 1.64-1.55 (m, H-5'b), 1.44 (p, J = 7.7 Hz, H-4'). ^{13}C NMR ($CDCl_3$, 150 MHz) δ 176.0 (C, C-1'), 166.0 (C, C-10'), 71.4, 71.1, 71.1, 71.0 (CH_2, C-4, C-5, C-6, C-7), 70.2 (CH_2, C-3), 69.7 (CH_2, C-8), 63.4 (CH, C-7'), 61.6 (CH, C-8'), 57.0 (CH, C-6'), 41.0 (CH_2, C-9'), 39.8 (CH_2, C-1), 37.7 (CH_2, C-10), 36.8 (CH_2, C-2'), 30.5 (CH_2, C-9), 29.8 (CH_2, C-4'), 29.5 (CH_2, C-5'),

28.2 (CH_2, C-2), 26.9 (CH_2, C-3'). HRESIMS m/z 447.2616 $[M + H]^+$ (calcd for $C_{20}H_{39}N_4O_5S$, 447.2636).

BPA-EG$_3$-NH$_2$ (130). To a stirred solution of NHS ester **110** (34.3 mg, 84.2 μmol) in anhydrous THF (7 mL) was added 4,7,10-trioxa-1,13-tridecanediamine (**94**, 300 μL, 1.37 mmol). After stirring the reaction at room temperature for 8 h, the mixture was then partitioned between EtOAc and DI H_2O. The EtOAc phase was recovered and subjected to the standard work up procedure providing the crude product, which was separated by RP-MPLC (C_{18}, $H_2O \rightarrow CH_3OH$, 0.1% HCO_2H) to yield BPA-EG$_3$-NH$_2$ (**130**, 32.5 mg, 63.4 μmol, 75%). **130**: clear oil; IR υ_{max} 3238, 3070, 2924, 2873, 1646, 1600, 1508, 1307, 1285, 1250, 1170, 1115, 1020, 928, 853, 770 cm^{-1}.^{1}H NMR (CD_3OD, 600 MHz) δ 7.76 (2H, app. d, J = 8.8 Hz, H-5'), 7.75 (2H, app. d, J = 8.8 Hz, H-9'), 7.11 (2H, app. d, J = 8.8 Hz, H-4'), 7.10 (2H, app. d, J = 8.8 Hz, H-10'), 4.84 (2H, d, J = 2.3 Hz, H-12'), 4.63 (2H, s, H-2'), 3.66-3.55 (8H, m, H-4, H-5, H-6, H-7), 3.63 (2H, t, J = 6.1 Hz, H-3), 3.50 (2H, t, J = 6.5 Hz, H-8), 3.38 (2H, t, J = 6.5 Hz, H-10), 3.08 (2H, t, J = 6.1 Hz, H-1), 3.04 (1H, t, J = 2.3 Hz, H-14'), 1.91 (2H, p, J = 6.1 Hz, H-2), 1.80 (2H, p, J = 6.5 Hz, H-9). ^{13}C NMR (CD_3OD, 150 MHz) δ 196.2 (C, C-7'), 170.4 (C, C-1'), 162.7 (C, C-11'), 162.5 (C, C-3'), 133.3 (CH, C-5'), 133.2 (CH, C-9'), 132.6 (C, C-6'), 132.1 (C, C-8'), 115.7 (CH, C-10'), 115.6 (CH, C-4'), 79.2 (C, C-13'), 77.5 (CH, C-14'), 71.4, 71.1, 71.1, 71.0 (CH_2, C-4, C-5, C-6, C-7), 70.2 (CH_2, C-3), 69.9 (CH_2, C-8), 68.2 (CH_2, C-2'), 56.8 (CH_2, C-12'), 39.8 (CH_2, C-1), 37.7 (CH_2, C-10), 30.4 (CH_2, C-9), 28.2 (CH_2, C-2). HRESIMS m/z 513.2575 $[M + H]^+$ (calcd for $C_{28}H_{37}N_2O_7$, 513.2595).

4.4.12 Preparation of affinity resins by covalent immobilization of amino-functionalized pseudopteroxazole and pseudopterosin-derived probes

PtxGlu-EG$_3$-Agarose (137). To a solution of PtxGlu-EG$_3$-NH$_2$ (**101**, 1.07 mg, 1.84 μmol) dissolved in DMSO (1 mL) with 2% Et$_3$N was added NHS-activated agarose (107.8 mg). After incubating with gentle agitation (end-over-end rotation) at room temperature for 72-96 h, the agarose resin was pelleted by centrifugation. The supernatant was collected for LC-HRESIMS quantitation of unreacted **101**, which indicated an immobilization yield of >95% and a ligand density of 2.16-2.70 μmol/mL. After washing the resin three times with DMSO, 1M ethanolamine in DMSO (0.5 mL) was added and the resin was incubated for 24 h. The affinity resin was subsequently washed with PBS to remove the DMSO and any unreacted ethanolamine. The resin was stored as a ~50% slurry at 4 ºC in PBS containing 10% EtOH.

Ps-EG$_3$-Agarose (138). The procedure described for the preparation of PtxGlu-EG$_3$-Agarose (**137**) was repeated using Ps-EG$_3$-NH$_2$ (**117**, 1.14 mg, 1.99 μmol) and NHS-activated agarose (104.4 mg). The immobilization yield (>95%) and ligand density (2.42-3.02 μmol/mL) were calculated according to LC-HRESIMS quantitation, as described for PtxGlu-EG$_3$-Agarose (**137**).

ASA-EG$_3$-Agarose (139). The procedure described for the preparation of PtxGlu-EG$_3$-Agarose (**137**) was repeated using ASA-EG$_3$-NH$_2$ (**132**, 1.05 mg, 2.59 μmol) and NHS-activated agarose (101.5 mg). The immobilization yield (>95%) and ligand density (3.41-

4.26 μmol/mL) were calculated according to LC-HRESIMS, as described for PtxGlu-EG_3-Agarose (**137**).

Agarose-EG_3-PsOH (140). To prepare the inactive control resin (**140**), H_2N-EG_3-PsOH (**122**, 2.63 mg, 5.33 μmol) was dissolved in a 2% pyridine solution in DMSO (0.5 mL) and added to NHS-activated agarose (29.4 mg). The immobilization yield (0.22 μmol, 4.1%) and ligand density (4.10-5.13 μmol/mL) were calculated according to LC-HRESIMS, as described for PtxGlu-EG_3-Agarose (**137**).

Generic control agarose (141). The procedure described for the preparation of PtxGlu-EG_3-Agarose (**137**) was repeated using 2-(2-aminoethoxy)ethanol (**142**, 0.5 μL) and NHS-activated agarose (51.0 mg).

CHAPTER 5

CONCLUSIONS AND FUTURE DIRECTIONS

5.1 Marine Diterpenes: An Opportunity for Novel Drug Development

Marine corals belonging to the phylogenetic order of Alcyonacea are a rich source of structurally diverse diterpenes, such as the fuscosides and pseudopteroxazole, with promising therapeutic applications. The fuscosides are a class of anti-inflammatory diterpene arabinosides isolated from the Caribbean alcyonacean Eunicea fusca.[74-75] Fuscoside B (**11**) is known for its selective inhibition of 5-LO,[76,77] an enzyme committed to LT biosynthesis.[89] On the basis of its unique structure, **11** may exert its activity as a competitive substrate and thus belong to a novel class of 5-LO inhibitors.[77] Therefore, **11** provides a tremendous opportunity for the development of novel anti-inflammatory drugs. Pseudopteroxazole (**30**) is an amphilectane diterpene isolated from Pseudopterogorgia elisabethae with activity against M. tuberculosis,[154] the etiologic agent of TB. The inhibitory activity of **30** in the LORA, an in vitro model of the NRP phenotype, is highly intriguing. Furthermore, no cross-resistance to **30** by isogenic mono-resistant M. tuberculosis H_{37}Rv strains was observed (**Table 4.1**), suggesting the antitubercular mechanism of **30** could represent a novel strategy for TB treatment.

5.2 A New Anti-inflammatory Diterpene Isolated from Eunicea fusca

The structure of eunicidiol (**49**), a novel anti-inflammatory diterpene isolated from E. fusca, was elucidated by 1D and 2D NMR spectroscopic analysis after purification by extensive RP-HPLC separation. The absolute configuration of **49** was assigned by the Mosher method, an analysis involving the derivatization of the secondary

hydroxyl group with (R)- and (S)-MPA. In addition, the absolute configuration of eunicol (**16**), a structurally related diterpene, was unambiguously determined as 10S via stereospecific Cope rearrangement of the cyclodecadiene moiety to generate fuscol (**15**), whose configuration is known.[82,83] Fuscosides A (**10**) and B (**11**) as well as other diterpenes belonging to this class (**17** and **45**-**48**) are proposed to have a 10S configuration based on the established biosynthetic pathway.[85]

This study represents the first in vivo anti-inflammatory evaluation of fuscol (**15**), eunicol (**16**), and eunicidiol (**49**). Topical administration of diterpenes **15**-**16** and **49** at a 100 μg/ear dose significantly reduced PMA-induced edema in the mouse ear assay. The observed anti-inflammatory activity was superior to indomethacin, a benchmark anti-inflammatory drug that required a 3 mg/ear dose to achieve a similar reduction of PMA-induced edema. It remains to be determined whether diterpenes **15**-**16** and **49** exert their anti-inflammatory activity via selective 5-LO inhibition. Although **15** is known to inhibit LTB_4 biosynthesis in adherent human polymorphonuclear leukocytes,[77] the effect on 5-LO inhibition was not measured directly. In the future, enzymatic 5-LO and COX assays may be pursued in an effort to determine the anti-inflammatory mechanism of action of **15**-**16** and **49**.

An assessment of SAR has suggested that the eight-carbon side chain, consisting of the tertiary hydroxyl group and conjugated diene moieties, may be important for the anti-inflammatory activity of these diterpenes as it is the most common structural feature. To confirm the significance of this side chain, further assessment of the SAR may be pursued by isolating other structurally related diterpenes. In fact, several potentially novel diterpenes were collected during the RP-HPLC purification of **49**, as observed in the

chromatogram in Section 2.2.1. A preliminary analysis of their ^{1}H NMR spectra showed the presence of the conjugated diene moieties found in **15**-**16** and **49**. Similarities in their LC-APCIMS fragmentation suggested the presence of hydroxylated analogues of eunicidiol (**49**), but unfortunately the diterpenes were not available in sufficient quantities for complete structural elucidation. Alternatively, one may pursue the synthesis of truncated diterpene mimics containing the aforementioned eight-carbon side chain. These compounds may be prepared with commercially available building blocks, such as 2-methyl-3-buten-2-ol (**55**) or sorbic acid.

5.3 A Chemical Glycosylation of Fuscol Yields Novel Fuscoside B Analogues

The glycosylation of fuscol (**15**) and eunicol (**16**) has been accomplished for the first time using a modification of the Koenigs-Knorr method. A novel structural class of diterpene glycosides, called the eunicosides, has also been synthesized. Initially, the glycosylation methodology was established using 2-methyl-3-buten-2-ol (**55**) as a glycosyl acceptor model of **15** and **16**. The use of strong Lewis acids for glycosyl donor activation was strictly prohibited due to the instability of **15** and **16**, which also degraded in the presence of milder Lewis acids such as AgOTf. However, a combination of AgOTf and Ag_2CO_3 were capable of activating glycosyl bromides without degradation of **15** and **16** when DIEA was employed as an acid scavenger. The glycosylation yields were significantly improved by protecting the glycosyl bromides as benzoate esters, presumably due to resonance stabilization of the acyloxonium intermediate. The acid

lability of **15** and **16** was also exploited to introduce EG_3 and EG_4 substituents as mimics of the arabinose moiety.

The inhibition of LTB_4 biosynthesis by fuscol (**15**)[77] and its lower in vivo anti-inflammatory activity, relative to fuscoside B (**11**),[78] suggested that the arabinose moiety was insignificant with regards to 5-LO inhibition but instead has an overall impact on the bioavailability of fuscoside B (**11**). The results of the current study, however, have indicated otherwise. In fact, the anomer of **11** showed no anti-inflammatory activity, demonstrating the importance of a glycosidic linkage with the 1',2'-cis configuration. Replacing the arabinose moiety with galactose or an EG-based substituent also failed to emulate the anti-inflammatory activity of **11**. As a result, the significance of the arabinose moiety is much greater than originally anticipitated, although its precise role in the inhibition of 5-LO remains to be determined. The mouse ear edema assay does not serve as a direct indication of 5-LO inhibition, therefore enzymatic 5-LO assays should be carried out with future analogues of **11**.

A limitation of the modified Koenigs-Knorr approach was the inability to install 1',2'-cis glycosidic linkages. Future glycosylation efforts should therefore focus on applying this methodology to glycosyl donors protected with non-participating functional groups. Although acetonide functionalities may direct the formation of 1',2'-cis glycosidic linkages, the fuscoside may not tolerate acidic conditions required for their removal; therefore base-sensitive protecting groups are preferred. Furthermore, the proposed aglycone acceptor method may only provide 1',2'-trans glycoside products, considering that the axially-oriented hydroxyl group would be the weaker nucleophile.

Regardless, the synthesis of 1',2'-cis glycoside analogues of fuscoside B (**11**) should be pursued to understand the biological significance of anomeric configuration.

5.4 Affinity Chromatography Identifies Putative Targets of Pseudopteroxazole

A collection of semisynthetic pseudopteroxazole- and pseudopterosin-type probes were prepared from a pseudopterosin G-J (**33**-**36**) mixture that was isolated from P. elisabethae. To retain the antimicrobial activity of pseudopteroxazole (**30**), the EG spacer was attached to different positions on the diterpene scaffold, thus providing a collection of natural product-based probes. On the basis of their antimicrobial activity, the target binding interaction was maintained by attaching the EG spacer to either the oxazole ring of **30** or the phenolic hydroxyl group of the aglycone methyl ether (**95**). However, modification of the double bond appeared to disrupt the desired binding activity, as indicated by inactivity of H_2N-EG_3-PsOH (**122**). The biotinylated probes showed moderate antimycobacterial activity, while the corresponding photoaffinity probes were inactive. This result advised against the in situ labeling experiment, which would have been the primary advantage of the photolabeling approach. The observed SAR, however, suggests that the photoaffinity probes may exhibit binding activity within the context of a cell lysate.

The wealth of SAR data obtained during the antimicrobial evaluation of the natural product-based probes may be exploited for the future development of novel pseudopteroxazole analogues. As mentioned previously, the oxazole region of the diterpene scaffold can be modified without major repercussions on the antimicrobial

activity. However, there is a preference for polar substituents at this position, suggesting the importance of increasing the aqueous solubility. A preliminary investigation of SAR around the double bond indicates that this position is more significant for specific binding to the cell target(s). All synthetic modifications to this position, with the exception of a hydrogenation, were detrimental for the antimycobacterial activity. Further modification of the double bond, as well as the configuration at C-1, should be investigated in the future in an effort to identify novel pseudopteroxazole analogues with improved bioactivity.

The molecular design of the natural product-based probes was simulated in an ASA model of the affinity chromatography experiment. The results of this preliminary study demonstrated the specific binding of CA to a covalently immobilized ASA ligand, thus validating the approach. Therefore, covalent immobilization of pseudopteroxazole- and pseudopterosin-type probes onto NHS-activated agarose was pursued to identify protein target candidates. Despite the large extent of NSB and ineffectiveness of competitive displacement controls, specific binding interactions were detected by the SAC technique, according to the serial depletion of several gel bands. As a result, one of the proteins was excised and analyzed by tandem mass spectrometry for identification.

Analysis of the tryptic digest identified (3R)-hydroxyacyl-ACP dehydratase subunit HadC as a protein target candidate of pseudopteroxazole (**30**). Constituting a portion of the heterodimer HadBC, subunit HadC is responsible for carrying out the dehydratase step during mycolic acid biosynthesis in the FAS-II pathway,[310] a process that is known to be essential for mycobacterial viability.[312a] The binding interaction between HadC and **30**, as well as its antimycobacterial significance, shall be validated in

future studies to unequivocally determine whether or not **30** is arresting mycolic acid biosynthesis. In addition, the affinity chromatography has indicated several other protein target candidates, whose identification may lead to the discovery of novel targets for antitubercular drug development.

References and Notes

1. Kunle, O. F.; Egharevba, H. O.; Ahmadu, P. O. Int. J. Biodivers. Conserv. **2012,** 4, 101.
2. Firn, R. D.; Jones, C. G. Nat. Prod. Rep. **2003,** 20, 382.
3. Newman, D. J.; Cragg, G. M. J. Nat. Prod. **2012,** 75, 311.
4. Mishra, B. B.; Tiwari, V. K. Eur. J. Med. Chem. **2011,** 46, 4769.
5. Hong, J. Curr. Opin. Chem. Biol. **2011,** 15, 350.
6. Bennett, J. W. Can. J. Bot. **1995,** 73, S917.
7. Gershenzon, J.; Dudareva, N. Nat. Chem. Biol. **2007,** 3, 408.
8. Koppitz, M.; Eis, K. Drug Discov. Today **2006,** 11 (561).
9. Ortholand, J.-Y.; Ganesan, A. Curr. Opin. Chem. Biol. **2004,** 8, 271.
10. (a) Kassel, D. B. Chem. Rev. **2001,** 101, 255. (b) Bunin, B. A.; Ellman, J. A. J. Am. Chem. Soc. **1992,** 114, 10997.
11. (a) Terrett, N. K. Combinatorial Chemistry, Oxford: Oxford University Press, 1998. (b) Spring, D. R. Org. Biomol. Chem. **2003,** 1, 3867.
12. Bindseil, K. U.; Jakupovic, J.; Wolf, D.; Lavayre, J.; Leboul, J.; Van der Pyl, D. Drug Discov. Today **2001,** 6, 840.
13. Breinbauer, R.; Vetter, I. R.; Waldmann, H. Angew. Chem. Int. Ed. **2002,** 41, 2878.
14. Willhelm, S.; Carter, C.; Lynch, M.; Lowinger, T.; Dumas, J.; Smith, R. A.; Shwartz, B.; Simantov, R.; Kelley, S. Nat. Rev. Drug Discov. **2006,** 5, 835.
15. Feher, M.; Schmidt, J. M. J. Chem. Inf. Comput. Sci. **2003,** 43, 218.
16. Barker, A.; Kettle, J. G.; Nowak, T.; Pease, J. E. Drug Discov. Today **2012**, http://dx.doi.org/10.1016/j.drudis.2012.10.008.
17. (a) Spandl, R. J.; Spring, D. R. Chem. Rec. **2008,** 8, 129. (b) Burke, M. D.; Berger, E. M.; Schreiber, S. L. Science **2003,** 302, 613.
18. Mulzer, J. Natural Product Synthesis: Targets, Methods, Concepts., Springer, New York, 2005.
19. (a) Tan, D. S. Nat. Chem. Biol. **2005,** 1, 74. (b) Bohacek, R. S.; McMartin, C.; Guida, W. C. Med. Res. Rev. **1996,** 16, 3.

20. Hert, J.; Irwin, J. J.; Laggner, C.; Keiser, M. J.; Shoichet, B. K. Nat. Chem. Biol. **2009,** 5 (479).

21. Wyatt, E. E.; Fergus, S.; Galloway, W.; Bender, A.; Fox, D. J.; Plowright, A. T.; Jessiman, A. S.; Welch, M.; Spring, D. R. Chem. Commun. **2006**, 3296.

22. Grabowski, K.; Baringhaus, K.-H.; Schneider, G. Nat. Prod. Rep. **2008,** 25, 892.

23. Schreiber, S. L. Science **2000,** 287, 1964.

24. (a) Kumagai, N.; Muncipinto, G.; Schreiber, S. L. Angew. Chem. Int. Ed. **2006,** 45, 3635. (b) Burke, M. D.; Schreiber, S. L. Angew. Chem. Int. Ed. **2004,** 43, 46.

25. Thomas, G. L.; Johannes, C. W. Curr. Opin. Chem. Biol. **2011,** 15, 516.

26. (a) Breinbauer, R.; Manger, M.; Scheck, M.; Waldmann, H. Curr. Med. Chem. **2002,** 9, 2129. (b) Balamurugan, R.; Dekker, F. J.; Waldmann, H. Mol. BioSyst. **2005,** 1, 36.

27. Margulis, L.; Schwartz, K. V. W. H. Five Kingdoms: An Illustrated Guide to the Phyla of Life on Earth, Freeman & Co., New York, 1988.

28. Haefner, B. Drug Discov. Today **2003,** 8, 536.

29. Carté, B. K. Bioscience **1996,** 46, 271.

30. Molinski, T. F.; Dalisay, D. S.; Lievens, S. L.; Saludes, J. P. Nat. Rev. Drug Discov. **2009,** 8, 69.

31. Dalisay, D. S.; Morinaka, B. I.; Skepper, C. K.; Molinski, T. F. J. Am. Chem. Soc. **2009,** 131, 7552.

32. Julianti, E.; Oh, H.; Jang, K. H.; Lee, J. K.; Lee, S. K.; Oh, D.-C.; Oh, K.-B.; Shin, J. J. Nat. Prod. **2011,** 74, 2592.

33. Simmons, T. L.; Andrianasolo, E.; McPhail, K.; Flatt, P.; Gerwick, W. H. Mol. Cancer Ther. **2005,** 4, 333.

34. (a) Ji, N.-Y.; Li, X.-M.; Wang, B.-G. Molecules **2008,** 13, 2894. (b) Amsler, C. D. Algal Chemical Ecology, Springer-Verlag: Heidelberg, Germany, 2008. (c) Suzuki, M.; Vairappan, C. S. Curr. Top. Phytochem. **2005,** 7, 1.

35. (a) Chang, Z.; Sitachitta, N.; Rossi, J. V.; Roberts, M. A.; Flatt, P. M.; Jia, J.; Sherman, D. H.; Gerwick, W. H. J. Nat. Prod. **2004,** 67, 1356. (b) Orjala, J.; Gerwick, W. H. J. Nat. Prod. **1996,** 59.

36. Valmsen, K.; Järving, I.; Boeglin, W. E.; Varvas, K.; Koljak, R.; Pehk, T.; Brash, A. R.; Samel, N. Proc. Natl. Acad. Sci. **2001,** 98, 7700.

37. Mayer, A. M. S.; Glaser, K. B.; Cuevas, C.; Jacobs, R. S.; Kem, W.; Little, R. D.; McIntosh, J. M.; Newman, D. J.; Potts, B. C.; Shuster, D. E. Trends Pharm. Sci. **2009,** 31, 255.

38. (a) Bergmann, W.; Burke, D. C. J. Org. Chem. **1955,** 20, 1501. (b) Bergmann, W.; Feeney, R. J. J. Org. Chem. **1951,** 16, 981. (c) Bergmann, W.; Feeney, R. J. J. Am. Chem. Soc. **1950,** 72, 2809.

39. McIntosh, M.; Cruz, L. J.; Hunkapiller, M. W.; Gray, W. R.; Olivera, B. M. Arch. Biochem. Biophys. **1982,** 218.

40. Terlau, H.; Baldomero, O. M. Physiol. Rev. **2004,** 84.

41. Williams, J. A.; Day, M.; Heavner, J. E. Expert Opin. Pharmacother. **2008,** 9, 1575.

42. Prialt (Ziconotide). http://www.prialt.com/ (accessed Nov 15, 2012).

43. (a) Sakai, R. R., K.L.; Guan, Y.; Wang, A. H.-J. Proc. Natl. Acad. Sci. USA **1992,** 89, 11456. (b) Wright, A. E.; Forleo, D. A.; Gunawardana, P. G.; Gunasekera, S. P.; Koehn, F. E.; McConnell, O. J. J. Org. Chem. **1990,** 55, 4508.

44. Zewail-Foote, M.; Hurley, L. H. J. Med. Chem. **1999,** 42.

45. Herrero, A. B.; Martin-Castellanos, C.; Marco, E.; Gago, F.; Moreno, S. Cancer Res. **2006,** 66, 8155.

46. Tavecchio, M.; Simone, M.; Erba, E.; Chiolo, I.; Liberi, G.; Foiani, M.; D'Incalci, M.; Damia, G. Eur. J. Cancer **2008,** 44, 609.

47. Scotto, K. W. Anticancer Drugs **2002,** 13, S3.

48. (a) Martinez, E. J.; Corey, E. J. Org. Lett. **2000,** 2, 993. (b) Corey, E. J.; Gin, D. Y.; Kania, R. S. J. Am. Chem. Soc. **1996,** 118, 9202.

49. Endo, A.; Yanagisawa, A.; Abe, M.; Tohma, S.; Kan, T.; Eukuyama, T. J. Am. Chem. Soc. **2002,** 124, 6552.

50. (a) Ikeda, Y.; Idemoto, H.; Hirayama, F.; Yamamoto, K.; Iwao, K.; Asao, T.; Munakata, T. J. Antibiot. **1983,** 36, 1279. (b) Ikeda, Y.; Matsuki, H.; Ogawa, T.; Munakata, T. J. Antibiot. **1983,** 36, 1284.

51. (a) Cuevas, C.; et al. PCT Int. Appl. **2001**, WO 87895. (b) Cuevas, C.; et al. Org. Lett. **2000,** 2, 2545.

52. (a) Carter, N. J.; Keam, S. J. Drugs **2010,** 70, 335. (b) Jimeno, J.; López-Martín, J. A.; Ruiz-Casado, A.; Izquierdo, M. A.; Scheuer, P. J.; Rinehart, K. Anticancer Drugs **2004,** 15, 321.

53. European Medicines Agency. Yondelis. http://www.emea.europa.eu/pdfs/human/press/pr/43140707en.pdf (accessed Oct 16, 2012).

54. Pharmamar. Yondelis. http://www.pharmamar.com/yondelis.aspx (accessed Oct 16, 2012).

55. (a) Uemura, D.; Takahashi, K.; Yamamoto, T.; Katayama, C.; Tanaka, J.; Okumura, Y.; Hirata, Y. J. Am. Chem. Soc. **1985,** 107, 4796. (b) Hirata, Y.; Uemura, D. Pure Appl. Chem. **1986,** 58, 701.

56. Pettit, G. R.; Herald, C. L.; Boyd, M. R.; Leet, J. E.; Dufresne, C.; Doubek, D. L.; Schmidt, J. M.; Cerny, R. L.; Hooper, J. N. A.; Rutzler, K. C. J. Med. Chem. **1991,** 34, 3339.

57. Aicher, T. D.; Buszek, K. R.; Fang, F. G.; Forsyth, C. J.; Jung, S. H.; Kishi, Y.; Matelich, M. C.; Scola, P. M.; Spero, D. M.; Yoon, S. K. J. Am. Chem. Soc. **1992,** 114, 3162.

58. Kishi, Y.; Fang, F. G.; Forsyth, C. J.; Scola, P. M.; Yoon, S. K. U.S. Patent 5338866, International Patent WO 93/17650.

59. (a) Wang, Y.; Habgood, G. J.; Christ, W. J.; Kishi, Y.; Littlefield, B. A.; Yu, M. J. Bioorg. Med. Chem. Lett. **2000,** 10, 1029. (b) Littlefield, B. A.; Palme, M. H.; Seletsky, B. M.; Towle, M. J.; Yu, M. J.; Zheng, W. U.S. Patent 6214865, 6365759, and S/N 09/843617, International Patent WO 99/65894.

60. Towle, M. J.; et al. Cancer Res. **2001,** 61, 1013.

61. Twelves, C.; Cortes, J.; Vahdat, L. T.; Wanders, J.; Akerele, C.; Kaufman, P. A. Clin. Breast Cancer **2010,** 28, 3922.

62. (a) U.S. Food and Drug Administration. Halaven. http://www.accessdata.fda.gov/drugsatfda_docs/label/2010/201532lbl.pdf (accessed Oct

15, 2012). (b) Eisai Inc. Halaven. http://www.halaven.com/patients.aspx (accessed Oct 15, 2012).

63. Dong, C.-G.; Henderson, J. A.; Kaburagi, Y.; Sasaki, T.; Kim, D.-S.; Kim, J. T.; Urabe, D.; Guo, H.; Kishi, Y. J. Am. Chem. Soc. **2009,** 131, 15642.

64. (a) Gerwick, W. H.; Moore, B. S. Chem. Biol. **2012,** 19, 85. (b) Marine Pharmacology. Marine Pharmaceuticals: The Clinical Pipeline. http://marinepharmacology.mid western.edu/clinPipeline.htm (accessed Oct 16, 2012).

65. Marine Pharmacology. Marine Pharmaceuticals: The Preclinical Pipeline. http://marinepharmacology.midwestern.edu/preclinPipeline.htm (accessed Oct 16, 2012).

66. Misawa, N. Curr. Opin. Biotechnol. **2011,** 22, 1.

67. Roberts, S. C. Nat. Chem. Biol. **2007,** 3, 387.

68. Cragg, G. M. Med. Res. Rev. **1998,** 18, 315.

69. White, N. J. Science **2008,** 320, 330.

70. Eisenreich, W.; Bacher, A.; Arigoni, D.; Rohdich, F. Cell. Mol. Life Sci. **2004,** 61, 1401.

71. MacMillan, J.; Beale, M. H. Comprehensive Natural Products Chemistry, 2.06 Diterpene Biosynthesis, Meth-Cohn, O.; Barton, D.; Nakanishi, K.; Eds, Elsevier Science Ltd, 1999, ISBN: 978-0-08-091283-7.

72. The taxonomic description of Gorgonacea was amended and merged with Alcyonacea, which has become the accepted name for the order. van Ofwegen, L. Gorgonacea. WoRMS, World Register of Marine Species. http://www.marinespecies.org/aphia.php?p=taxdetails&id=1366 (accessed Nov 8, 2012).

73. Berrué, F.; Kerr, R. G. Nat. Prod. Rep. **2009,** 26, 681.

74. Shin, J.; Fenical, W. J. Org. Chem. **1991,** 56, 3153.

75. Jacobson, P. B.; Jacobs, R. S. Fed. Proc. **1991,** 805, A510.

76. Jacobson, P. B.; Jacobs, R. S. J. Pharm. Exp. Ther. **1992,** 262, 866.

77. Jacobson, P. B.; Jacobs, R. S. J. Pharm. Exp. Ther. **1992,** 262, 874.

78. Reina, E. P., C.; Rojas, J.; García, J.; Ramos, F.A.; Castellanos, L.; Aragón, M.; Ospina, L.F. Bioorg. Med. Chem. Lett. **2011,** 21, 5888.

79. Berrué, F.; McCulloch, M. W. B.; Kerr, R. G. Bioorg. Med. Chem. **2011,** 19, 6702.

80. The fuscosides were previously described as α-glycosides, prior to the revised nomenclature of carbohydrates. McNaught, A.D. Pure Appl. Chem. **1996,** 68, 1919.

81. Gopichand, Y.; Schmitz, J. Tetrahedron Lett. **1978,** 39, 3641.

82. Iwashima, M.; Nagaoka, H.; Kobayashi, K.; Yamada, Y. Tetrahedron Lett. **1992,** 33, 81.

83. Kosugi, H.; Yamabe, O.; Kata, M. J. Chem. Soc., Perkin Trans. 1 **1998**, 217.

84. Coll, J. C.; Bowden, B. B.; Konig, G. M.; Braslau, R. Bull. Soc. Chim. Belg. **1986,** 95, 815.

85. Saleh, M. B.; Kerr, R. G. Aust. J. Chem. **2010,** 63, 901.

86. Cóbar, O. M.; Rodríguez, A. D.; Padilla, O. L.; Sánchez, J. A. J. Org. Chem. **1997,** 62, 7183.

87. Shi, Y.-P.; Rodríguez, A. D.; Padilla, O. L. J. Nat. Prod. **2001,** 64, 1439.

88. (a) Ahmed, A. U. Front. Biol. **2011,** 6, 274. (b) Ferrero-Miliani, L.; Nielsen, O. H.; Andersen, P. S.; Girardin, S. E. Clin. Exp. Immun. **2006,** 147, 227.

89. Serhan, C. N.; Savill, J. Nature Immunol. **2005,** 6, 1191.

90. FitzGerald, G. A.; Patrono, C. N. Engl. J. Med. **2001,** 345, 433.

91. (a) FitzGerald, G. A. N. Engl. J. Med. **2004,** 351, 1709. (b) Topol, E. J.; Falk, G. W. Lancet **2004,** 364, 639.

92. Marnett, L. J.; Rowlinson, S. W.; Goodwin, D. C.; Kalgutkar, A. S.; Lanzo, C. A. J. Biol. Chem. **1999,** 274, 22903.

93. Crofford, L. J.; Lipsky, P. E.; Brooks, P.; Abramson, S. B.; Simon, L. S.; Van de Putte, L. B. A. Arthritis Rheum. **2000,** 43, 4.

94. Silverstein, F. E.; et al. J. Am. Med. Assoc. **2000,** 284, 1247.

95. (a) Kearney, P. M.; Baigent, C.; Godwin, J.; Halls, H.; Emberson, J. R.; Patrono, C. Br. Med. J. **2006,** 332, 1302. (b) Cotter, J.; Wooltorton, E. Can. Med. Assoc. **2005,** 172, 1299.

96. Hao, C.-M.; Breyer, M. D. Annu. Rev. Physiol. **2008,** 70, 357.

97. Jawien, J.; Gajda, M.; Rudling, M.; Mateuszuk, L.; Olszanecki, R.; Guzik, T. J.; Cichocki, T.; Chlopicki, S.; Korbut, R. Eur. J. Clin. Invest. **2006,** 36, 141.

98. (a) Evans, J. F.; Ferguson, A. D.; Mosley, R. T.; Hutchinson, J. H. Trends Pharmacol. Sci. **2008,** 29, 72. (b) Peters-Golden, M. Am. J. Respir. Crit. Care Med. **1998,** 157, S227.

99. (a) Rådmark, O.; Samuelsson, B. Lipid J. Res. **2009,** 50, S40. (b) Shimizu, T.; Rådmark, O.; Samuelsson, B. Proc. Natl. Acad. Sci. USA **1984,** 81, 689. (c) Samuelsson, B. Science **1983,** 220, 568.

100. Borgeat, P.; Hamberg, M.; Samuelsson, B. J. Biol. Chem. **1976,** 251, 7816.

101. (a) Rådmark, O.; Shimizu, T.; Jornvall, H.; Samuelsson, B. J. Biol. Chem. **1984**, 12339. (b) Samuelsson, B.; Hammarström, S. Prostaglandins **1980,** 19, 645.

102. (a) Ley, K.; Laudanna, C.; Cybulsky, M. I.; Nourshargh, S. Nat. Rev. Immunol. **2007,** 7, 678. (b) Dahlen, S.-E.; Bjork, J.; Hedqvist, P.; Arfors, K.-E.; Hammarstrom, S.; Lindgren, J.-A.; Samuelsson, B. Proc. Natl. Acad. Sci. USA **1981,** 78, 3887.

103. (a) Yokomizo, T.; Izumi, T.; Chang, K.; Takuwa, Y.; Shimizu, T. Nature **1997,** 387, 620. (b) Ford-Hutchinson, A. W.; Bray, M. V.; Doig, M. E.; Shipley, M. J.; Smith, B. Nature **1980,** 286, 264.

104. (a) Peters-Golden, M.; Gleason, M. M.; Togias, A. Clin. Exp. Allergy **2006,** 36, 689. (b) Drazen, J. M.; Israel, E.; O'Byrne, P. M. N. Engl. J. Med. **1999,** 340, 197. (c) Weiss, J.; Drazen, J.; Coles, N.; McFadden, E. J.; Weller, P.; Corey, E.; Lewis, R.; Austen, K. Science **1982,** 216, 196.

105. (a) Qiu, H.; et al. Proc. Natl. Acad. Sci. USA **2006,** 103, 8161. (b) Chen, M.; Lam, B. K.; Kanaoka, Y.; Nigrovic, P. A.; Audoly, L. P. A., K.F.; Lee, D. M. J. Exp. Med. **2006,** 203, 837. (c) Claesson, H. E.; Dahlen, S. E. J. Intern. Med. **1999,** 245, 205.

106. Werz, O.; Steinhilber, D. Pharmacol. Ther. **2006,** 112, 701.

107. Ford-Hutchinson, A. W.; Gresser, M.; Young, R. N. Annu. Rev. Biochem. **1994,** 63, 383.

108. Wenzel, S. E.; Kamada, A. K. Ann. Pharmacother. **1996,** 30, 858.

109. Crawley, G. C.; Dowell, R. I.; Edwards, P. N.; Foster, S. J.; McMillan, R. M.; Walker, E. R. J. Med. Chem. **1992,** 35, 2600.

110. Hamel, P.; al, e. J. Med. Chem. **1997,** 40, 2866.

111. Brooks, S. A. Mol. Biotechnol. **2009,** 43, 76.

112. Salas, J. A.; Méndez, C. Trends Microbiol. **2007,** 15, 219.

113. Le, G. T.; Abbenante, G.; Becker, B.; Grathwohl, M.; Halliday, J.; Tometzki, G.; Zuegg, J.; Meutermans, W. Drug Discov. Today **2003,** 8, 701.

114. Nicolaou, K. C.; Pfefferkorn, J. A.; Mitchell, H. J.; Roecker, A. J.; Cao, G.-Q. B.; Affleck, R. L.; Lillig, J. E. J. Am. Chem. Soc. **2000,** 122, 9954.

115. (a) Langenhan, J. M.; Peters, N. R.; Guzei, I. A.; Hoffman, M.; Thorson, J. S. Proc. Natl. Acad. Sci. USA **2005,** 102, 12305. (b) Ge, M.; Chen, Z.; Onishi, H. R.; Kohler, J.; Silver, L. L.; Kerns, R.; Fukuzawa, S.; Thompson, C.; Kahne, D. Science **1999,** 284, 507.

116. (a) Cao, H.; Hwang, J.; Chen, X. Opportunity, Challenge and Scope of Natural Products in Medicinal Chemistry, Tiwari, V.K., Ed.; Research Signpost: Kerala, India, 2011. (b) Hecht, S. M. Bioorganic Chemistry: Carbohydrates, Oxford: New York, 1999.

117. Ahmed, A.; Peters, N. R.; Fitzgerald, M. K.; J.A., W.; Hoffmann, F. M.; Thorson, J. S. J. Am. Chem. Soc. **2006,** 128, 14224.

118. Langenhan, J. M.; Engle, J. M.; Slevin, L. K.; Fay, L. R.; Lucker, R. W.; Smith, K. R.; Endo, M. M. Bioorg. Med. Chem. Lett. **2008,** 18, 670.

119. Demchenko, A. V. Handbook of Chemical Glycosylation: Advances in Stereoselectivity and Therapeutic Relevance, Wiley-VCH: Weinheim, Germany, 2008.

120. Demchenko, A. V. Synlett **2003**, 1225.

121. Wolfe, S.; Pinto, B. M.; Varma, V.; Leung, R. Y. N. Can. J. Chem. **1990,** 68, 1051.

122. Takahashi, O.; Yamasaki, K.; Kohno, Y.; Ohtaki, R.; Ueda, K.; Suezawa, H.; Umezawa, Y.; Nishio, M. Carbohydr. Res. **2007,** 342, 1202.

123. Carey, F. A.; Sundberg, R. G. Advanced Organic Chemistry, Springer, 2007, ISBN 978-0-387-44899-2.

124. (a) Whitfield, D. M.; Douglas, S. P. Glycoconjugate J. **1996,** 13, 5. (b) Goodman, L. Adv. Carbohydr. Chem. Biochem. **1967,** 22, 109.

125. (a) Kim, J.-H.; Yang, H.; Park, J.; Boons, G.-J. J. Am. Chem. Soc. **2005,** 127, 12090. (b) Lemieux, R.; Hayami, J. Can. J. Chem. **1965,** 43, 2162.

126. (a) Rudd, P. M.; Elliott, T.; Cresswell, P.; Wilson, I. A.; Dwek, R. A. Science **2001,** 291, 2370. (b) Dwek, R. A. Chem. Rev. **1996,** 96, 683.

127. (a) Oberli, M. A.; Bindschadler, P.; Werz, D. B.; Seeberger, P. H. Org. Lett. **2008,** 10, 905. (b) Kim, K. S.; Fulse, D. B.; Baek, J. Y.; Lee, B. Y.; Jeon, H. B. J. Am. Chem. Soc. **2008,** 130, 8537.

128. Lemieux, R. U.; Hendriks, K. B.; Stick, R. V.; James, K. J. Am. Chem. Soc. **1975,** 97, 4056.

129. Fraser-Reid, B.; Wu, Z.; Udodong, U. E.; Ottosson, H. J. Org. Chem. **1990,** 55, 6068.

130. Zhang, Z.; Ollmann, I. R.; Ye, X.-S.; Wischnat, R.; Baasov, T.; Wong, C.-H. J. Am. Chem. Soc. **1999,** 121, 734.

131. (a) Pazynina, G.; Tuzikov, A.; Chinarev, A.; Obukhova, P.; Bovin, N. Tetrahedron Lett. **2002,** 43, 8011. (b) Koenigs, W.; Knorr, E. Chem. Ber. **1901,** 34, 957.

132. van Well, R. M.; Kartha, K. P. R.; Field, R. A. J. Carbohydr. Chem. **2005,** 24, 463.

133. (a) Pozsgay, V.; Dubois, E. P.; Pannell, L. J. Org. Chem. **1997,** 62, 2832. (b) Hanessian, S.; Banoub, J. Carbohydr. Res. **1977,** 53, c13.

134. Wolfram, M. L.; Pittet, A. O.; Gillam, I. C. Proc. Nat. Acad. Sci. USA **1961,** 47, 700.

135. Pellissier, H. Tetrahedron **2004,** 60, 5123.

136. Kazunobu, T.; Tatsuta, K. Chem. Rev. **1993,** 93, 1503.

137. (a) Atopkina, L. N.; Denisenko, V. A. Chem. Nat. Compd. **2006,** 42, 452. (b) Paulsen, H.; Lê-Nguyên, B.; Sinnwell, V.; Heemann, V. S., F. Liebigs Ann. Chem. **1985,** 8, 1513.

138. (a) Anufriev, V. P.; Malinovskaya, G. V.; Denisenko, V. A. U., N.I. Elyakov, G.B.; Kim, S.-I.; Baek, N.-I. Carbohydr. Res. **1997,** 304, 179. (b) Fullerton, D. S.; Kihara, M.; Deffo, T.; Kitatsuji, E.; Ahmed, K.; Simat, B.; From, A. H. L.; Rohrer, D. C. J. Med. Chem. **1984,** 27, 256.

139. Píš, J.; Buděšinský, M.; Harmatha, J. Tetrahedron **1994,** 50, 9679.

140. Schneider, G.; Sembdner, G.; Phinney, O. J. Plant Growth Regul. **1984,** 3, 207.

141. Marin, J.; Violette, A.; Briand, J.-P.; Guichard, G. Eur. J. Org. Chem. **2004**, 3027.

142. Schmidt, R. R.; Michel, J. Angew. Chem. Int. Ed. Engl. **1980,** 19, 731.

143. Schmidt, R. R. Angew. Chem. Int. Ed. Engl. **1986,** 25, 212.

144. Reicheneder, S.; Unverzagt, C. Angew. Chem. Int. Ed. **2004,** 43, 4353.

145. (a) Ritter, T. K.; Mong, K. K. T.; Liu, H. T.; Nakatani, T.; Wong, C. H. Angew. Chem. Int. Ed. **2003,** 42, 4657. (b) Nicolaou, K. C.; Schreiner, E. P.; Iwabuchi, Y.; Suzuki, T. Angew. Chem. Int. Ed. Engl. **1992,** 31, 340.

146. Castro-Palomino, J. C.; Schmidt, R. R. Tetrahedron Lett. **1995,** 36, 5343.

147. Griffith, B. R.; Langenhan, J. M.; Thorson, J. S. Curr. Opin. Biotechnol. **2005,** 16, 622.

148. Ratner, D. M.; Murphy, E. R.; Jhunjhunwala, M.; Snyder, D. A.; Jensen, K. F.; Seeberger, P. H. Chem. Commun. **2005**, 578.

149. Wang, C.-C.; Lee, J.-C.; Luo, S.-Y.; Kulkarni, S. S.; Huang, Y.-W.; Lee, C.-C.; Chang, K.-L.; Hung, S.-C. Nature **2007,** 446, 896.

150. Cox, D. J.; Fairbanks, A. J. Tetrahedron Asymmetr. **2009,** 20, 773.

151. Fu, X.; Albermann, C.; Jiang, J.; Liao, J.; Zhang, C.; Thorson, J. S. Nat. Biotech. **2003,** 21, 1467.

152. Langenhan, J. M.; Griffith, B. R.; Thorson, J. S. J. Nat. Prod. **2005,** 68, 1696.

153. Cervigni, S. E.; Dumy, P.; Mutter, M. Angew. Chem. Int. Ed. Engl. **1996,** 35, 1230.

154. Rodríguez, A. D.; Ramírez, C.; Rodríguez, I.; González, E. Org. Lett. **1999,** 1, 527.

155. Rodríguez, I.; Rodríguez, A. D. J. Nat. Prod. **2003,** 66, 855.

156. (a) Ovenden, S. P. B.; Nielson, J. L.; Liptrot, C. H.; Willis, R. H.; Tapiolas, D. M.; Wright, A. D.; Motti, C. A. J. Nat. Prod. **2011,** 74, 65. (b) Hohmann, C.; et al. J. Antibiot. **2009,** 62, 99. (c) Stewart, M.; Fell, P. M.; Blunt, J. W.; Munro, M. H. G. Aust. J. Chem. **1997,** 50, 341. (d) Kobayashi, J.; Madono, T.; Shigemori, H. Tetrahedron Lett. **1995,** 36, 5589.

157. Johnson, T. W.; Corey, E. J. J. Am. Chem. Soc. **2001,** 123, 4475.

158. Davidson, J. P.; Corey, E. J. J. Am. Chem. Soc. **2003,** 125, 13486.

159. (a) Harmata, M.; Hong, X. Org. Lett. **2005,** 7, 3581. (b) Harmata, M.; Hong, X.; Barnes, C. L. Org. Lett. **2004,** 6, 2201.

160. McCulloch, M. W. B.; Berrué, F.; Haltli, B.; Kerr, R. G. J. Nat. Prod. **2011,** 74, 2250.

161. McCulloch, M. W. B.; Haltli, B.; Marchbank, D. H.; Kerr, R. G. Mar. Drugs **2012,** 10, 1711.

162. Cohen, M. L. Nature **2000,** 406, 762.

163. Culotta, E. Science **1994,** 264, 362.

164. (a) Tenover, F. C. Am. J. Med. **2006,** 119, S3. (b) Tenover, F. C.; McGowan, J. E. Am. J. Med. Sci. **1996,** 311, 9.

165. (a) Walsh, C. Nature **2000,** 406, 775. (b) McManus, M. C. Am. J. Health Syst. Pharm. **1997,** 61, 377.

166. Hartman, B.; Tomasz, A. Antimicrob. Agents Chemother. **1981,** 19, 726.

167. Hutchings, M. I.; Hong, H. J.; Buttner, M. J. Mol. Microbiol. **2006,** 59, 923.

168. (a) Wright, G. D. Nat. Rev. Microbiol. **2007,** 5, 175. (b) Hasman, H.; Aarestrup, F. M.; Dalsgaard, A.; Guardabassi, L. J. Antimicrob. Chemother. **2006,** 57, 648.

169. Hong, H. J.; Hutchings, M. I.; Buttner, M. J. Adv. Exp. Med. Biol. **2008,** 631, 200.

170. (a) Kung, H. C.; Hoyert, D. L.; Xu, J.; Murphy, S. L. Natl. Vital Stat. Rep. **2008,** 56, 1. (b) Klevens, R. M.; Edwards, J. R.; Richards, C. L.; Horan, T. C.; Gaynes, R. P.; Pollock, D. A.; Cardo, D. M. Public Health Rep. **2007,** 122, 160.

171. Arias, C. A.; Murray, B. E. N. Engl. J. Med. **2009,** 360, 439.

172. Giamarellou, H.; Poulakou, G. Drugs **2009,** 69, 1879.

173. (a) Boucher, H. W.; Talbot, G. H.; Bradley, J. S.; Edwards, J. E.; Gilbert, D.; Rice, L. B.; Scheld, M.; Spellberg, B.; Bartlett, J. Clin. Infect. Dis. **2009,** 48, 1. (b) Cooper, M. A.; Shlaes, D. Nature **2011,** 472, 32.

174. (a) Barry, C. E.; Boshoff, H. I.; Dartois, V.; Dick, T.; Ehrt, S.; Flynn, J.; Schnappinger, D.; Wilkinson, R. J.; Young, D. Nat. Rev. Microbiol. **2009,** 7, 845. (b) World Health Organization, Tuberculosis. http://www.who.int/topics/tuberculosis/en/ (accessed Nov 14, 2012).

175. World Health Organization, Global Tuberculosis Report 2012 http://www.who.int/tb/publications/global_report/en/ (accessed Nov 15, 2012).

176. Kim, P. S.; Makhene, M.; Sizemore, C.; Hafner, R. J. Infect. Dis. **2012,** 205, S347.

177. Lalloo, U. G.; Pillay, S. Curr. HIV/AIDS Rep. **2008,** 5, 132.

178. Dean, G. L.; Edwards, S. G.; Ives, N. J.; Matthews, G.; Fox, E. F.; Navaratne, L.; Fisher, M.; Taylor, G. P.; Miller, R.; Taylor, C. B.; de Ruiter, A.; Pozniak, A. L. AIDS **2002,** 16, 75.

179. Corbett, E. L.; Watt, C. J.; Walker, N.; Maher, D.; Williams, B. G.; Raviglione, M. C.; Dye, C. Arch. Intern. Med. **2003,** 163, 1009.

180. Cole, E. C.; Cook, C. E. Am. J. Infect. Control **1998,** 26, 453.

181. Houben, E. N. G.; Nguyen, L.; Pieters, J. Curr. Opin. Microbiol. **2006,** 9, 76.

182. Vergne, I.; Chua, J.; Singh, S. B.; Deretic, V. Annu. Rev. Cell. Dev. Biol. **2004,** 20, 367.

183. Fratti, R. A.; Chua, J.; Vergne, I.; Deretic, V. Proc. Natl. Acad. Sci. **2003,** 100, 5437.

184. Grosset, J. Antimicrob. Agents Chemother. **2003,** 47, 833.

185. Blumberg, H. M.; al, e. Am. J. Respir. Crit. Care Med. **2003,** 167, 603.

186. Sacchettini, J. C.; Rubin, E. J.; Freundlich, J. S. Nat. Rev. Microbiol. **2008,** 6, 41.

187. World Health Organization, Pursue High-Quality DOTS Expansion and Enhancement http://www.who.int/tb/dots/en/ (accessed Nov 15, 2012).

188. Holland, D. P.; Sanders, G. D.; Hamilton, C. D.; Stout, J. E. Am. J. Respir. Crit. Care Med. **2009,** 179, 1055.

189. Coates, A.; Hu, Y.; Bax, R.; Page, C. Nat. Rev. Drug Discov. **2002,** 1, 895.

190. Kingwell, K. Nat. Rev. Drug Discov. **2009,** 8, 845.

191. Kaneko, T.; Cooper, C.; Mdluli, K. Future Med. Chem. **2011,** 3, 1373.

192. Agrawal, Y. K.; Bhatt, H. G.; Raval, H. G.; Oza, P. M.; Vaidya, H. B.; Manna, K.; Gogoi, P. J. Sci. Ind. Res. **2007,** 66, 191.

193. Salomon, J. A.; Lloyd-Smith, J. O.; Getz, W. M.; Resch, S.; Sánchez, M. S.; Porco, T. C.; Borgdorff, M. W. PLoS Med. **2006,** 3, e273.

194. Andries, K.; et al. Science **2005,** 307, 223.

195. (a) Koul, A.; Arnoult, E.; Lounis, N.; Guillemont, J.; Andries, K. Nature **2011,** 469, 483. (b) Dover, L. G.; Coxon, G. D. J. Med. Chem. **2011,** 54, 6157.

196. Debnath, J.; Siricilla, S.; Wan, B.; Crick, D. C.; Lenaerts, A. J.; Franzblau, S. G.; Kurosu, M. J. Med. Chem. **2012,** 55, 3739.

197. Lin, G.; et al. Nature **2009,** 461, 621.

198. Koul, A.; et al. Nat. Chem. Biol. **2007,** 3, 323.

199. Pucheault, M. Org. Biomol. Chem. **2008,** 6, 424.

200. Hung, D. T.; Jamison, T. F.; Schreiber, S. L. Chem. Biol. **1996,** 3, 623.

201. Reayi, A.; Arya, P. Curr. Opin. Chem. Biol. **2005,** 9, 240.

202. Carlson, E. E. ACS Chem. Biol. **2010,** 5, 639.

203. Kotake, Y.; Sagane, K.; Owa, T.; Mimori-Kiyosue, Y.; Shimizu, H.; Uesugi, M.; Ishihama, Y.; Iwata, M.; Mizui, Y. Nat. Chem. Biol. **2007,** 3, 570.

204. Leslie, B. J.; Hergenrother, P. J. Chem. Soc. Rev. **2008,** 37, 1347.

205. Kawasumi, M.; Nghiem, P. J. Invest. Dermatol. **2007,** 127, 1577.

206. Lipinski, C.; Hopkins, A. Nature **2004,** 432, 855.

207. Stockwell, B. R. Nat. Rev. Genet. **2000,** 1, 116.

208. Knight, Z. A.; Shokat, K. M. Cell **2007,** 5, 262.

209. Zamir, E.; Bastiaens, P. I. H. Nat. Chem. Biol. **2008,** 4, 643.

210. Cong, F.; Cheung, A. K.; Huang, S.-M. A. Annu. Rev. Pharmacol. Toxicol. **2012,** 52, 57.

211. Landry, Y.; Gies, J.-P. Fundam. Clin. Pharm. **2008,** 22, 1.

212. Overington, J. P.; Al-Lazikani, B.; Hopkins, A. L. Nat. Rev. Drug Discov. **2006,** 5, 993.

213. Paul, S. M.; Mytelka, D. S.; Dunwiddie, C. T.; Persinger, C. C.; Munos, B. H.; Lindborg, S. R.; Schacht, A. L. Nat. Rev. Drug Discov. **2010,** 9, 203.

214. Meisner, N.-C.; Hintersteiner, M.; Uhl, V.; Weidemann, T.; Schmied, M.; Gstach, H.; Auer, M. Curr. Opin. Chem. Biol. **2004,** 8, 424.

215. Raju, T. N. Lancet **2000,** 355, 1022.

216. Cho, Y. S.; Kwon, H. J. Bioorg. Med. Chem. **2012,** 20, 1922.

217. Sato, S.-I.; Murata, A.; Shirakawa, T.; Uesugi, M. Chem. Biol. **2010,** 17, 616.

218. Yocum, R. R.; Rasmussen, J. R.; Strominger, J. L. J. Biol. Chem. **1980,** 255, 3977.

219. Battenberg, O. A.; Nodwell, M. B.; Sieber, S. A. J. Org. Chem. **2011,** 76, 6075.

220. Sadaghiani, A. M.; Verhelst, S. H. L.; Bogyo, M. Curr. Opin. Chem. Biol. **2007,** 11, 20.

221. Rix, U.; Superti-Furga, G. Nat. Chem. Biol. **2009,** 5, 616.

222. (a) Lomenick, B.; Olsen, R. W.; Huang, J. ACS Chem. Biol. **2011,** 6, 34. (b) Jung, D.-W.; Williams, D.; Khersonsky, S. M.; Kang, T.-W.; Heidary, N.; Chang, Y.-T.; Orlow, S. J. Mol. BioSyst. **2005,** 1, 85.

223. (a) Lee, W.-C.; Lee, K. H. Anal. Biochem. **2004,** 324, 1. (b) Tamura, T.; Terada, T.; Tanaka, A. Bioconj. Chem. **2003,** 14, 1222.

224. Baruch, A.; Jeffrey, D. A.; Bogyo, M. Trends Cell Biol. **2004,** 14, 29.

225. Krysiak, J.; Breinbauer, R. Top. Curr. Chem. **2012,** 324, 43.

226. Szardenings, K.; Li, B.; Ma, L.; Wu, M. Drug Discov. Today **2004,** 1, 9.

227. (a) Hegde, N. S.; Sanders, D. A.; Rodriguez, R.; Balasubramanian, S. Nat. Chem. **2011,** 3, 725. (b) Knockaert, M.; et al. Chem. Biol. **2000,** 7, 411.

228. Weber, P. C.; Ohlendorf, D. H.; Wendoloski, J. J.; Salemme, F. R. Science **1989,** 243, 85.

229. Savage, M. D.; Mattson, G.; Desai, S.; Nielander, G. W.; Morgensen, S.; Conklin, E. J. Avidin-Biotin Chemistry: A Handbook. Pierce: Rockford, 1992.

230. Hendrickson, W. A.; Pähler, A.; Smith, J. L.; Satow, Y.; Merritt, E. A.; Phizackerley, R. P. Proc. Natl. Acad. Sci. USA **1989,** 86, 2190.

231. Sato, S.-I.; Kwon, Y.; Kamisuki, S.; Srivastava, N.; Mao, Q.; Kawazoe, Y.; Uesugi, M. J. Am. Chem. Soc. **2007,** 129, 873.

232. Emami, K. H.; et al. Proc. Natl. Acad. Sci. USA **2004,** 101, 12682.

233. Nakamura, Y.; Miyatake, R.; Ueda, M. Angew. Chem. Int. Ed. **2008,** 47, 7289.

234. Wang, G.; Shang, L.; Burgett, A. W.; Harran, P. G.; Wang, X. Proc. Natl. Acad. Sci. USA **2007,** 104, 2068.

235. Ding, S.; Wu, T. Y.; Brinker, A.; Peters, E. C.; Hur, W.; Gray, N. S.; Schultz, P. G. Proc. Natl. Acad. Sci. USA **2003,** 100, 7632.

236. Yamamoto, K.; Yamazaki, A.; Takeuchi, M.; Tanaka, A. Anal. Biochem. **2006,** 352, 15.

237. Margarucci, L.; Monti, M. C.; Fontanella, B.; Riccio, R.; Casapullo, A. Mol. BioSyst. **2011,** 7, 480.

238. Böttcher, T.; Pitscheider, M.; Sieber, S. A. Angew. Chem. Int. Ed. **2010,** 49, 2680.

239. Eirich, J.; Orth, R.; Sieber, S. A. J. Am. Chem. Soc. **2011,** 133, 12144.

240. Salisbury, C. M.; Cravatt, B. F. J. Am. Chem. Soc. **2008,** 130, 2184.

241. Kawamura, A.; Hindi, S.; Mihai, D. M.; James, L.; Aminova, O. Bioorg. Med. Chem. **2008,** 16, 8824.

242. Vera, M. D.; Joulié, M. M. Med. Res. Rev. **2002,** 22, 102.

243. Evans, M. J.; Cravatt, B. F. Chem. Rev. **2006,** 106, 3279.

244. Huisgen, R. 1,3-Dipolar Cycloaddition Chemistry, Padwa, A., Ed.; Wiley: New York, 1984, ISBN: 978-0-471-08364-1.

245. Rostovtsev, V. V.; Green, J. G.; Fokin, V. V.; Sharpless, K. B. Angew. Chem. Int. Ed. **2002,** 41, 2596.

246. Koteva, K.; Hong, H.-J.; Wang, X. D.; Nazi, I.; Hughes, D.; Naldrett, M. J.; Buttner, M. J.; Wright, G. D. Nat. Chem. Biol. **2010,** 6, 327.

247. Arthur, M.; Molinas, C.; Courvalin, P. J. Bacteriol. **1992,** 174, 2582.

248. (a) Weerapana, E.; Speers, A. E.; Cravatt, B. F. Nat. Protoc. **2007,** 2, 1414. (b) Cravatt, B. F.; Wright, A. T.; Kozarich, J. W. Annu. Rev. Biochem. **2008,** 77, 383.

249. Speers, A. E.; Cravatt, B. F. Chem. Biol. **2004,** 11, 535.

250. (a) Li, N.; Overkleeft, H. S.; Florea, B. I. Curr. Opin. Chem. Biol. **2012,** 16, 1. (b) Sieber, S. A.; Niessen, S.; Hoover, H. S.; Cravatt, B. F. Nat. Chem. Biol. **2006,** 2, 274.

251. Yee, M.-C.; Fas, S. C.; Stohlmeyer, M. M.; Wandless, T. J.; Cimprich, K. A. J. Biol. Chem. **2005,** 280, 29053.

252. Staub, I.; Sieber, S. A. J. Am. Chem. Soc. **2008,** 130, 13400.

253. Newman, D. J.; Hill, R. T. J. Ind. Microbiol. Biotechnol. **2006,** 33, 539.

254. Saleh, M. B. Natural Product Biosynthesis in the Gorgonian Eunicea fusca and other Marine Invertebrates, Ph.D. Dissertation, Florida Atlantic University, Boca Raton, FL, 2005.

255. Castellanos, L.; Zea, S.; Osorno, O.; Duque, C. Biochem. Syst. Ecol. **2003,** 31, 1163.

256. (a) Adio, A. M. Tetrahedron **2009,** 65, 1533. (b) Faraldos, J. A.; Wu, S.; Chappell, J.; Coates, R. M. Tetrahedron **2007,** 63, 7733. (c) Wharton, P. S.; Poon, Y.; Kluender, H. C. J. Org. Chem. **1973,** 38, 735.

257. Pawlik, J. R. Chem. Rev. **1993,** 93, 1911.

258. This E. fusca crude extract was previously obtained by other personnel from the Kerr lab.

259. See Chapter 3 for more details on the acid degradation of fuscol (**15**) and eunicol (**16**).

260. Scholz, M.; Blobaum, A. L.; Marnett, L. J.; Hey-Hawkins, E. Bioorg. Med. Chem. **2011,** 19, 3242.

261. Topical administration of a 100 μg dose of indomethacin shows no reduction of PMA-induced edema, according to previous experiments conducted by Amplia Pharmatek.

262. For a description of the mouse ear edema assay conducted by Reina et al., refer to the following: Correa, H.; Valenzuela, A.L.; Ospina, L.F.; Duque, C. J. Inflamm. **2009,** 6, doi:10.1186/1476-9255-6-5.

263. Toshima, K.; Mukaiyama, S.; Yoshida, T.; Tamai, T.; Tatsuta, K. Tetrahedron Lett. **1991,** 32, 6155.

264. Nicolaou, K. C.; Seitz, S. P.; Papahatjis, D. P. J. Am. Chem. Soc. **1983,** 105, 2430.

265. Kahne, D.; Walker, S.; Cheng, Y.; Van Engen, D. J. Am. Chem. Soc. **1989,** 111, 6881.

266. Agnihotri, G.; Tiwari, P.; Misra, A. K. Carbohydr. Res. **2005,** 340, 1393.

267. Kim, S.-H.; Augeri, D.; Yang, D.; Kahne, D. J. Am. Chem. Soc. **1994,** 116, 1766.

268. Figueroa-Pérez, S.; Vérez-Bencomo, V. Carbohydr. Res. **1999,** 317, 29.

269. (a) Hunsen, M.; Long, D. A.; D'Ardenne, C. R.; Smith, A. L. Carbohydr. Res. **2005,** 340, 2670. (b) Mateusz, M.; Schlueter, U.; Mathew, F.; Fraser-Reid, B.; Hazen, K. C. Tetrahedron **2002,** 58, 7345.

270. (a) Premathilake, H. D.; Mydock, L. K.; Demchenko, A. V. J. Org. Chem. **2010,** 75, 1095. (b) Lee, D. J.; Kowalczyk, R.; Muir, V. J.; Rendle, P. M.; Brimble, M. A. Carbohydr. Res. **2007,** 342, 2628.

271. Thompson, C.; Ge, M.; Kahne, D. J. Am. Chem. Soc. **1999,** 121, 1237.

272. Mydock, L.; Demchenko, A. V. Org. Lett. **2008,** 10, 2103.

273. Garegg, P. J.; Olsson, L.; Oscarson, S. J. Org. Chem. **1995,** 60, 2200.

274. Ziegler, T.; Kováč, P.; Glaudemans, C. P. J. Liebigs. Ann. Chem. **1990**, 613.

275. Whitfield, D. M.; Douglas, S. P.; Tang, T.-H.; Csizmadia, I. G.; Pang, H. Y. S.; Moolten, F. L.; Krepinsky, J. J. Can. J. Chem. **1994,** 72, 2225.

276. For the sake of brevity, not every reaction intermediate is shown in **Figure 3.8**.

277. Garegg, P. J.; Konradsson, P.; Kvarnström, I.; Norberg, T.; Svensson, S. C. T.; Wigilius, B. Acta Chem. Scand. B **1985,** 39, 569.

278. The 5-LO inhibitor screening assay kit (cat. number: 760700) and 5-LO enzyme (cat. number: 60400) were obtained from Cayman Chemical.

279. Look, S. A.; Fenical, W.; Jacobs, R. S.; Clardy, J. Proc. Natl. Acad. Sci. USA **1986,** 83, 6238.

280. (a) Roussis, V.; Wu, Z.; Fenical, W.; Strobel, S. A.; Van Duyne, G. D.; Clardy, J. J. Org. Chem. **1990,** 55, 4916. (b) Ata, A.; Kerr, R. G.; Moya, C. E.; Jacobs, R. S. Tetrahedron **2003,** 59, 4215.

281. Jacobsson, M.; Malmberg, J.; Ellervik, U. Carbohydr. Res. **2006,** 341, 1266.

282. (a) Thompson, M. J.; Hutchinson, E. J.; Stratford, T. H.; Bowler, W. B.; Blackburn, G. M. Tetrahedron Lett. **2004,** 45, 1207. (b) Nicolaou, K. C.; Mitchell, H. J.; Jain, N. F.; Bando, T.; Hughes, R.; Winssinger, N.; Natarjan, S.; Koumbis, A. E. Chem. Eur. J. **1999,** 5, 2648.

283. Kröger, L.; Thiem, J. J. Carbohydr. Chem. **2003,** 22, 9.

284. The 3,4-diprenyl-2,6-dimethoxyphenol (**87**) and 3-prenyl-2,6-dimethoxyphenol (**89**) were provided by Dr. Malcolm McCulloch.

285. Kerékgyártó, J.; Kamerling, J. P.; Bouwstra, J. B.; Vliegenthart, J. F. G. Carbohydr. Res. **1989,** 186, 51.

286. Mbadugha, B. N. A.; Menger, F. M. Org. Lett. **2003,** 5, 4041.

287. Becker, D.; Galili, N. Carbohydr. Res. **1993,** 248, 129.

288. U.S. Food and Drug Administration. http://www.fda.gov/NewsEvents/Newsroom/PressAnnouncements/ucm333695.htm (accessed Jan 26, 2013).

289. Petrella, S.; Cambau, E.; Chauffour, A.; Andries, K.; Jarlier, V.; Sougakoff, W. Antimicrob. Agents. Chemother. **2006,** 50, 2853.

290. Marshall, H. New drug approved for MDR tuberculosis, despite concerns. http://download.thelancet.com/flatcontentassets/lanres/edch/140113_2_1.pdf (accessed Jan 26, 2013).

291. Collins, L.; Franzblau, S. G. Antimicrob. Agents Chemother. **1997,** 41, 1004.

292. Ata, A.; Win, H. Y.; Holt, D.; Holloway, P.; Segstro, E. P.; Jayatilake, G. S. Helv. Chim. Acta. **2004,** 87, 1090.

293. Obtained from Dr. Jeff Lewis at the Atlantic Veterinary College, University of Prince Edward Island.

294. Cho, S. H.; Warit, S.; Wan, B.; Hwang, C. H.; Pauli, G. F.; Franzblau, S. G. Antimicrob. Agents Chemother. **2007,** 51, 1380.

295. Tanaka, Y.; Bond, M. R.; Kohler, J. J. Mol. BioSyst. **2008,** 4, 473.

296. The extraction of pseudopterosins G-J (**33**-**36**) was completed by research technicians at Nautilus Biosciences.

297. Zhong, W.; Little, R. D. Tetrahedron **2009,** 65, 10784.

298. Reyrat, J.-M.; Kahn, D. Trends Microbiol. **2001,** 9, 472.

299. Dodgson, S. J.; Tashian, R. E.; Gros, G.; Carter, N. D. The carbonic anhydrases: Cellular physiology and molecular genetics. Plenum Press: New York, 1991.

300. Supuran, C. T. Bioorg. Med. Chem. Lett. **2010,** 20, 3467.

301. Lahiri, J.; Isaacs, L.; Grzybowski, B.; Carbeck, J. D.; Whitesides, G. M. Langmuir **1999,** 15, 7186.

302. Poulson, S.-A.; Bornaghi, L. F.; Healy, P. C. Bioorg. Med. Chem. **2005,** 15, 5429.

303. Arslan, O.; Cakir, U.; Ugras, H. I. Biochemistry (Moscow) **2002,** 67, 1055.

304. Lolli, G.; Thaler, F.; Valsasina, B.; Roletto, F.; Knapp, S.; Uggeri, M.; Bachi, A.; Matafora, V.; Storici, P.; Stewart, A.; Kalisz, H. M.; Isacchi, A. Proteomics **2003,** 3, 1287.

305. Minnikin, D. E. Lipids: complex lipids, their chemistry, biosynthesis and roles. The biology of the mycobacteria: Physiology, identification and classification., Ratledge, C.; Stanford, J., Ed.; Academic Press: London, UK, 1982.

306. Dover, L. G.; Cerdeno-Tarraga, A. M.; Pallen, M. J.; Parkhill, J.; Besra, G. S. FEMS Microbiol. Rev. **2004,** 28, 225.

307. Sacco, E.; Legendre, V.; Laval, F.; Zerbib, D.; Montrozier, H.; Eynard, N.; Guilhot, C.; Daffé, M.; Quémard, A. Biochim. Biophys. Acta **2007,** 1774, 303.

308. (a) Brown, A. K.; Bhatt, A.; Singh, A.; Saparia, E.; Evans, A. F.; Besra, G. S. Microbiology **2007,** 153, 4166. (b) Bhatt, A.; Molle, V.; Besra, G. S.; Jacobs, W. R. J.; Kremer, L. Mol. Microbiol. **2007,** 64, 1442.

309. Cohen-Gonsaud, M.; Ducasse, S.; Hoh, F.; Zerbib, D.; Labesse, G.; Quémard, A. J. Mol. Biol. **2002,** 320, 249.

310. (a) Banerjee, A.; Sugantino, M.; Sacchettini, J. C.; Jacobs, W. R. J. Microbiology **1998,** 144, 2697. (b) Sacco, E.; Covarrubias, A. S.; O'Hare, H. M.; Carroll, P.; Eynard, N.; Jones, T. A.; Parish, T.; Daffé, M.; Bäckbro, K.; Quémard, A. Proc. Nat. Acad. Sci. USA **2007,** 104, 14628.

311. Banerjee, A.; Dubnau, E.; Quémard, A.; Balasubramanian, V.; Um, K. S.; Wilson, T.; Collins, D.; de Lisle, G.; Jacobs, W. R. J. Science **1994,** 263, 227.

312. (a) Kremer, B. A.; Dai, L.; Sacchettini, J. C.; Jacobs, W. R. J. J. Bacteriol. **2005,** 187, 7596. (b) Vilcheze, C.; Morbidoni, H. R.; Weisbrod, T. R.; Iwamoto, H.; Kuo, M.; Sacchettini, J. C.; Jacobs, W. R. J. J. Bacteriol. **2000,** 182, 4059.

313. Fulmer, T. SciBX **2009,** 2, doi:10.1038/scibx.2009.430.

314. Rawat, R.; Whitty, A.; Tonge, P. J. Proc. Nat. Acad. Sci. USA **2003,** 100, 13881.

315. Cantaloube, S.; Veyron-Churlet, R.; Haddache, N.; Daffé, M.; Zerbib, D. PloS ONE **2011,** 6, e29564.

316. Sassetti, C. M.; Boyd, D. H.; Rubin, E. J. Mol. Microbiol. **2003,** 48, 77.

317. (a) Grzegorzewicz, A. E.; et al. J. Biol. Chem. **2012,** 287, 38434. (b) Belardinelli, J. M.; Morbidoni, H. R. Mol. Microbiol. **2012,** 86, 568.

318. Bhatt, A.; Fujiwara, N.; Bhatt, K.; Gurcha, S. S.; Kremer, L.; Chen, B.; Chan, J.; Porcelli, S. A.; Kobayashi, K.; Besra, G. S.; Jacobs, W. R. J. Proc. Nat. Acad. Sci. USA **2007,** 104, 5157.

319. Oda, Y.; Owa, T.; Sato, T.; Boucher, B.; Daniels, S.; Yamanaka, H.; Shinohara, Y.; Yokok, A.; Kuromitsu, J.; Nagasu, T. Anal. Chem. **2003,** 75, 2159.

320. (a) Hudzicki, J. Kirby-Bauer Disk Diffusion Susceptibility Test Protocol. http://www.microbelibrary.org/component/resource/laboratory-test/3189-kirby-bauer-disk-diffusion-susceptibility-test-protocol (accessed Jan 26, 2013). (b) Singh, M. P.; Petersen, P. J.; Weiss, W. J.; Janso, J. E.; Luckman, S. W.; Lenoy, E. B.; Bradford, P. A.; Testa, R. T.; Greenstein, M. Antimicrob. Agents Chemother. **2003,** 47, 62.

321. Kinter, M.; Sherman, N. Protein sequencing and identification using tandem mass spectrometry. Desiderio, D.M.; Nibbering, N.M.M., Ed.; Wiley-Interscience: New York, US, 2000.

322. Lazerwith, S. E.; Johnson, T. W.; Corey, E. J. Org. Lett. **2000,** 2, 2389.

323. Susumu, K.; Mei, B. C.; Mattoussi, H. Nat. Protoc. **2009,** 4, 424.

324. Wei, Y.; Wesson, P. J.; Kourkine, I.; Grzybowski, B. A. Anal. Chem. **2010,** 82, 8780.

325. (a) Martinez, J.; Silván, A. M.; Abad, M. J.; Bermejo, P.; Villar, A.; Söllhuber, M. J. Nat. Prod. **1997,** 60, 142. (b) Carlsson, R. P.; O'Neill-Davis, L.; Chang, J.; Lewis, A. Agents Actions **1985,** 17, 198.

326. (a) Methods for Dilution Antimicrobial Susceptibility Tests for Bacteria that Grow Aerobically, Approved Standard, 6th Ed, M7-A6, Volume 23, Number 2. (b) Susceptibility Testing of Mycobacteria, Nocardiae, and other Aerobic Actinomycetes, Approved Standard, M24-A, Volume 23, Number 18.

327. Franzblau, S. G.; Witzig, R. S.; McLaughlin, J. C.; Torres, P.; Madico, G.; Hernandez, A.; Degnan, M. T.; Cook, M. B.; Quenzer, V. K.; Ferguson, R. M.; Gilman, R. H. J. Clin. Microbiol. **1998,** 36, 362.

APPENDIX A

CHAPTER 2 SUPPORTING INFORMATION:

NMR SPECTROSCOPIC DATA

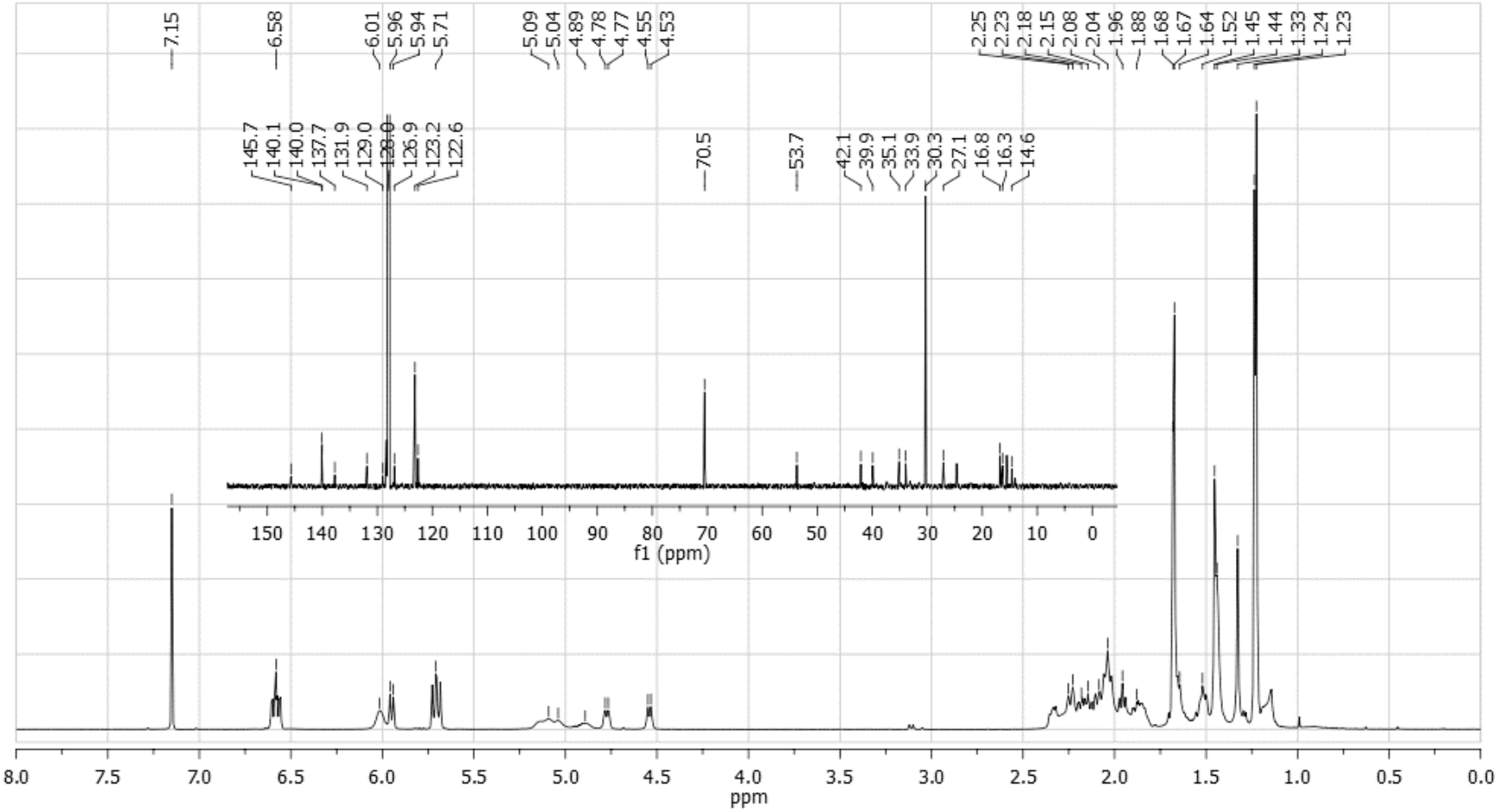

Figure A.1. The ^{1}H and ^{13}C NMR spectra (600 and 150 MHz, respectively, C_6D_6) of eunicol (**16**) [δ in ppm relative to residual solvent signal].

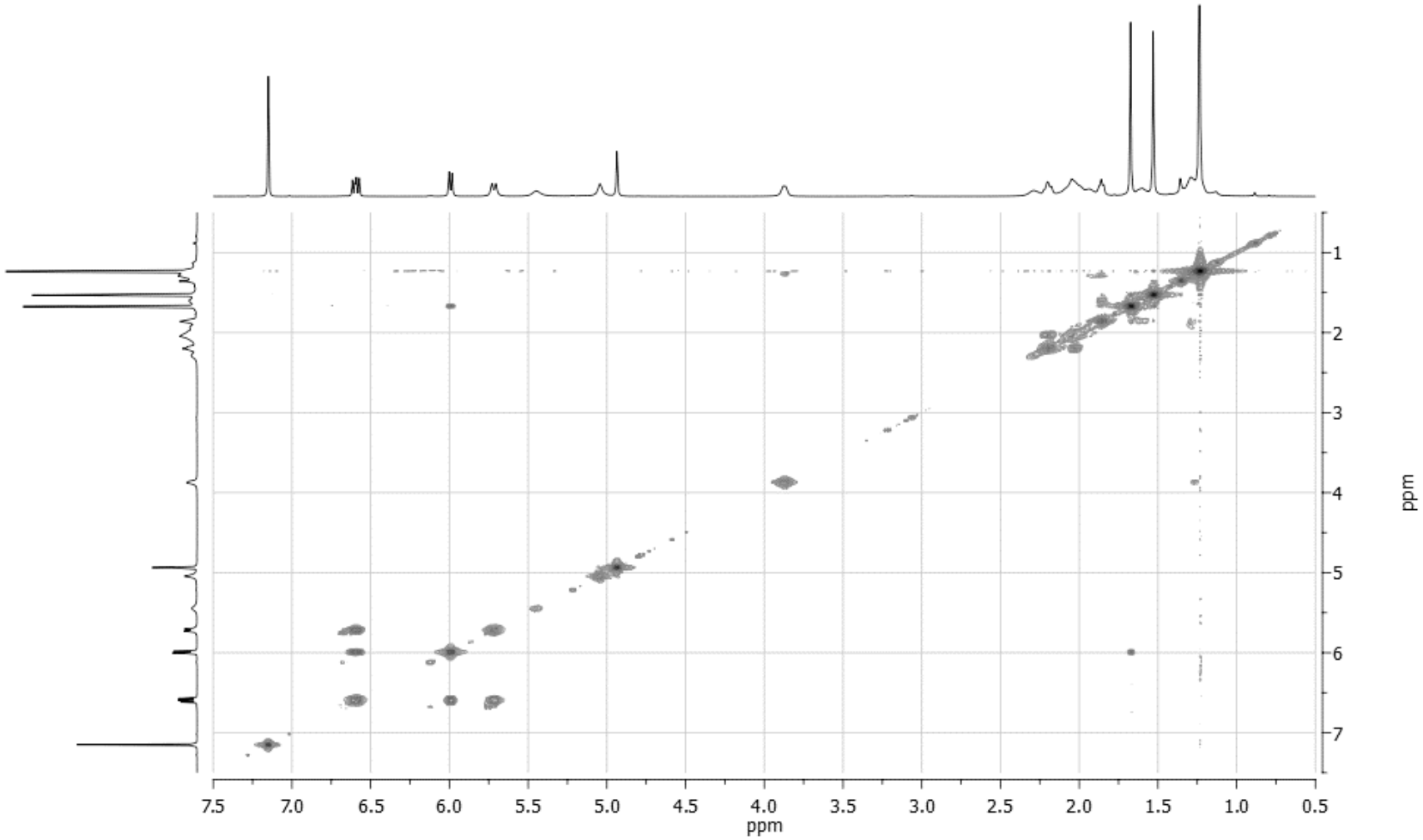

Figure A.2. The COSY spectrum of eunicidiol (**49**) [δ in ppm relative to residual solvent signal].

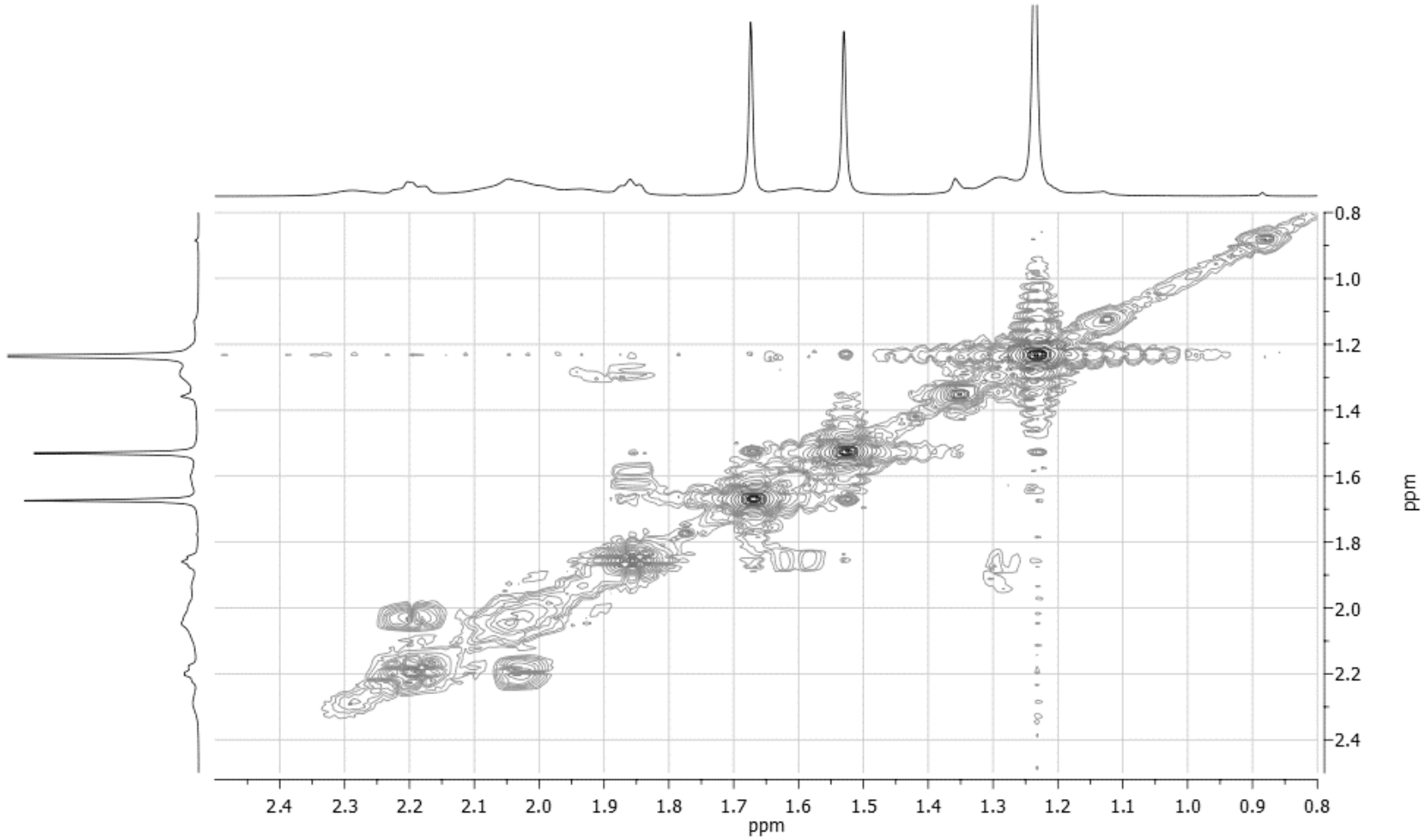

Figure A.3. The upfield region of the COSY spectrum of eunicidiol (**49**) [δ in ppm relative to residual solvent signal].

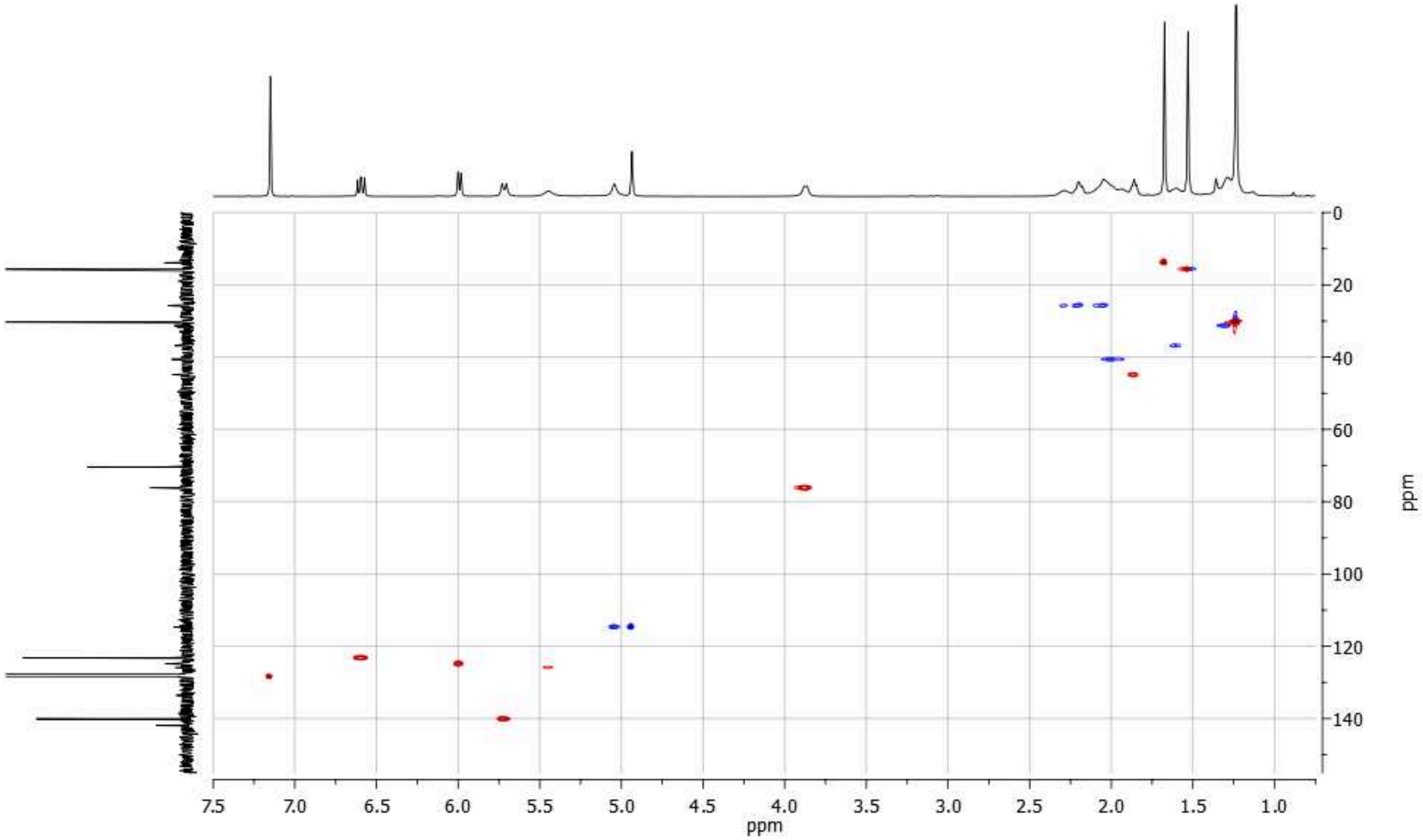

Figure A.4. The HSQC spectrum of eunicidiol (**49**) [δ in ppm relative to residual solvent signal].

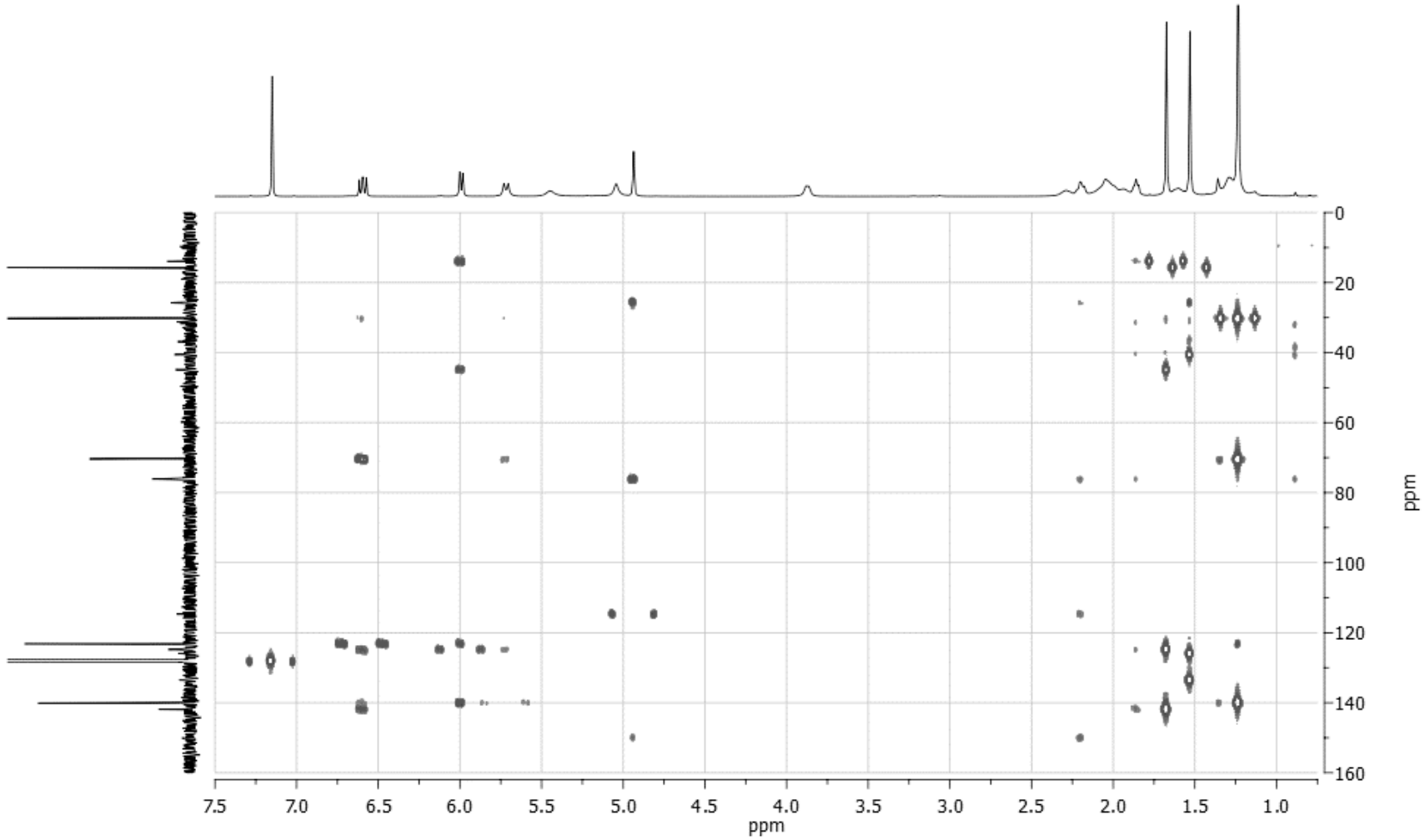

Figure A.5. The HMBC spectrum of eunicidiol (**49**) [δ in ppm relative to residual solvent signal].

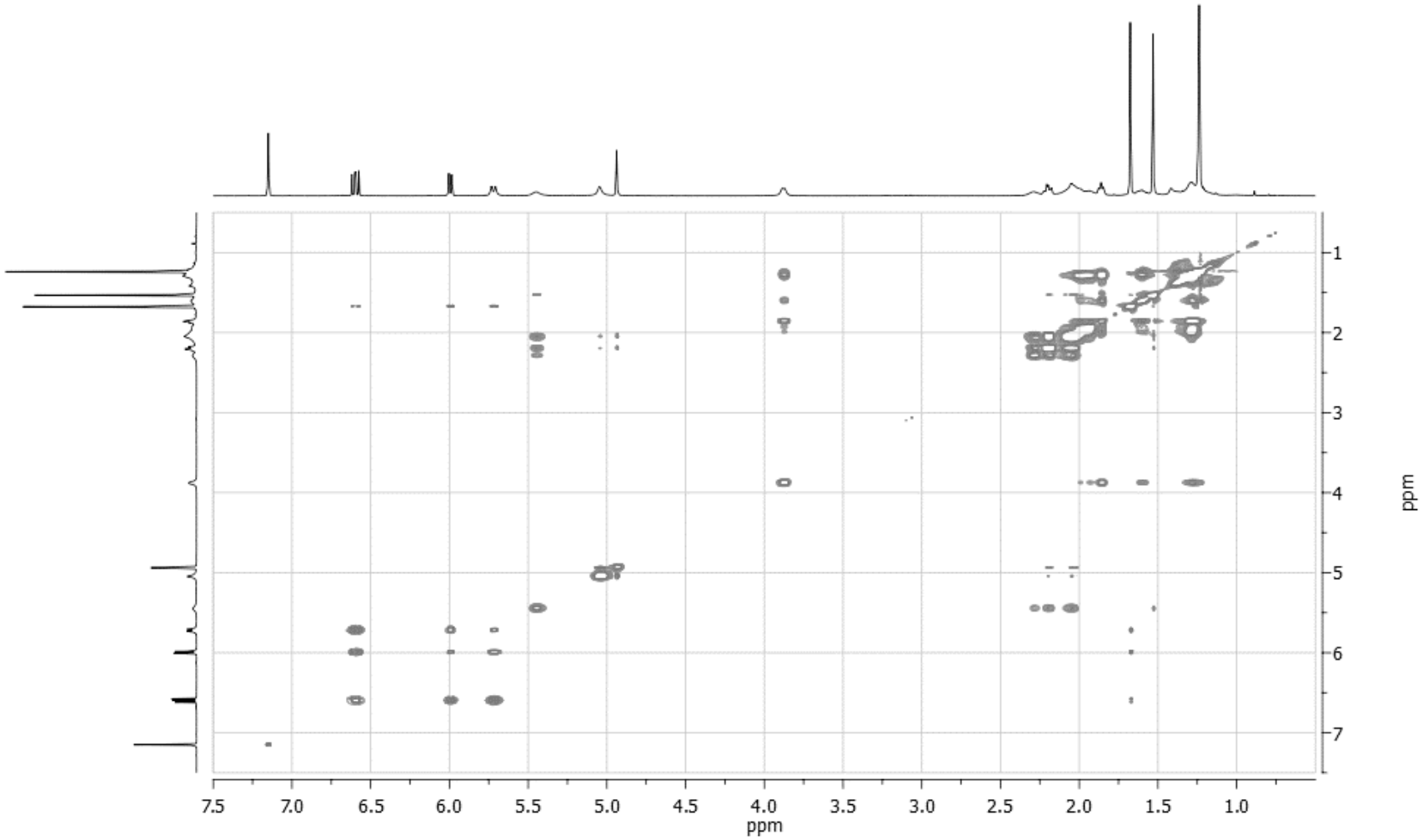

Figure A.6. The TOCSY spectrum of eunicidiol (**49**) [δ in ppm relative to residual solvent signal].

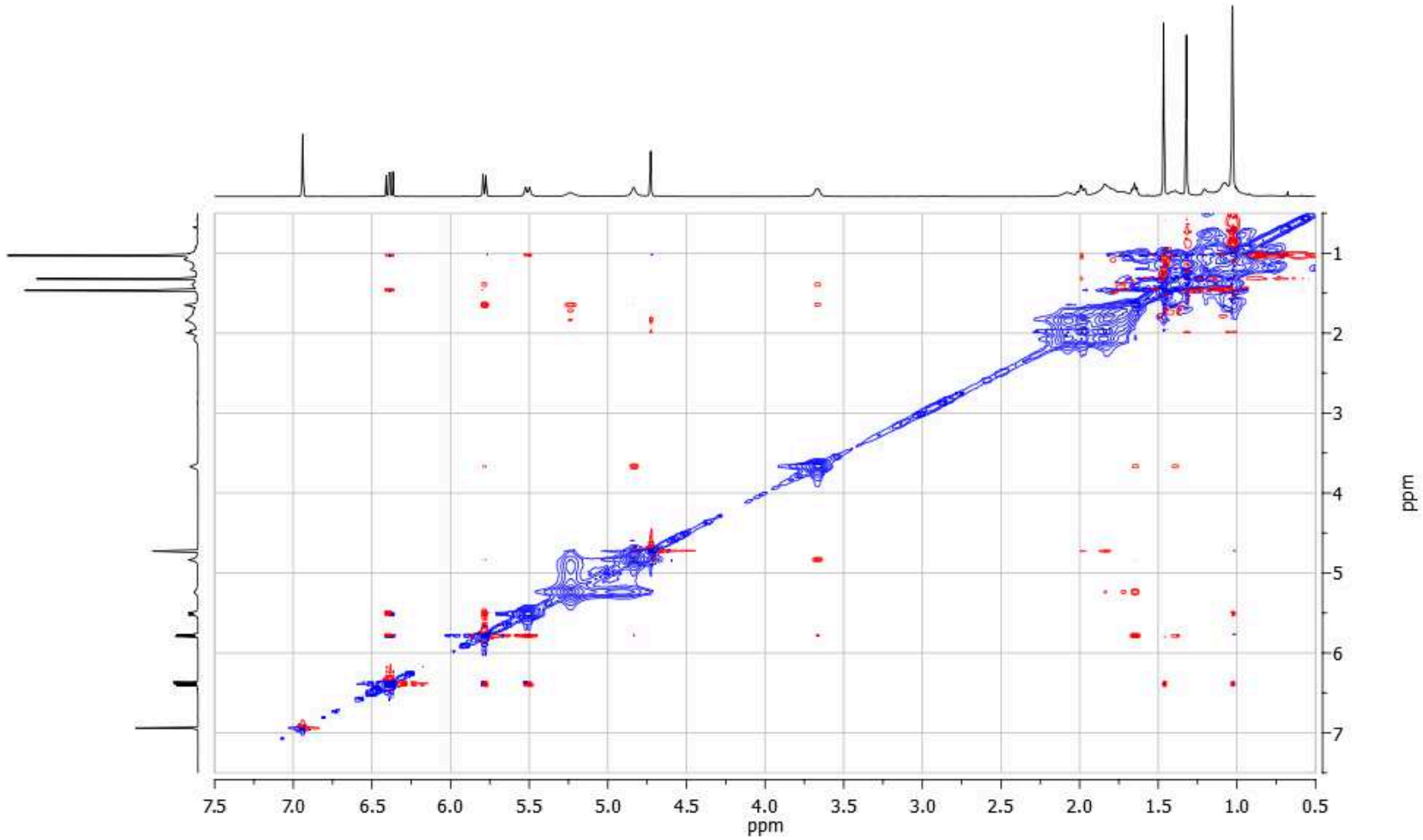

Figure A.7. The NOESY spectrum of eunicidiol (**49**) [δ in ppm relative to residual solvent signal].

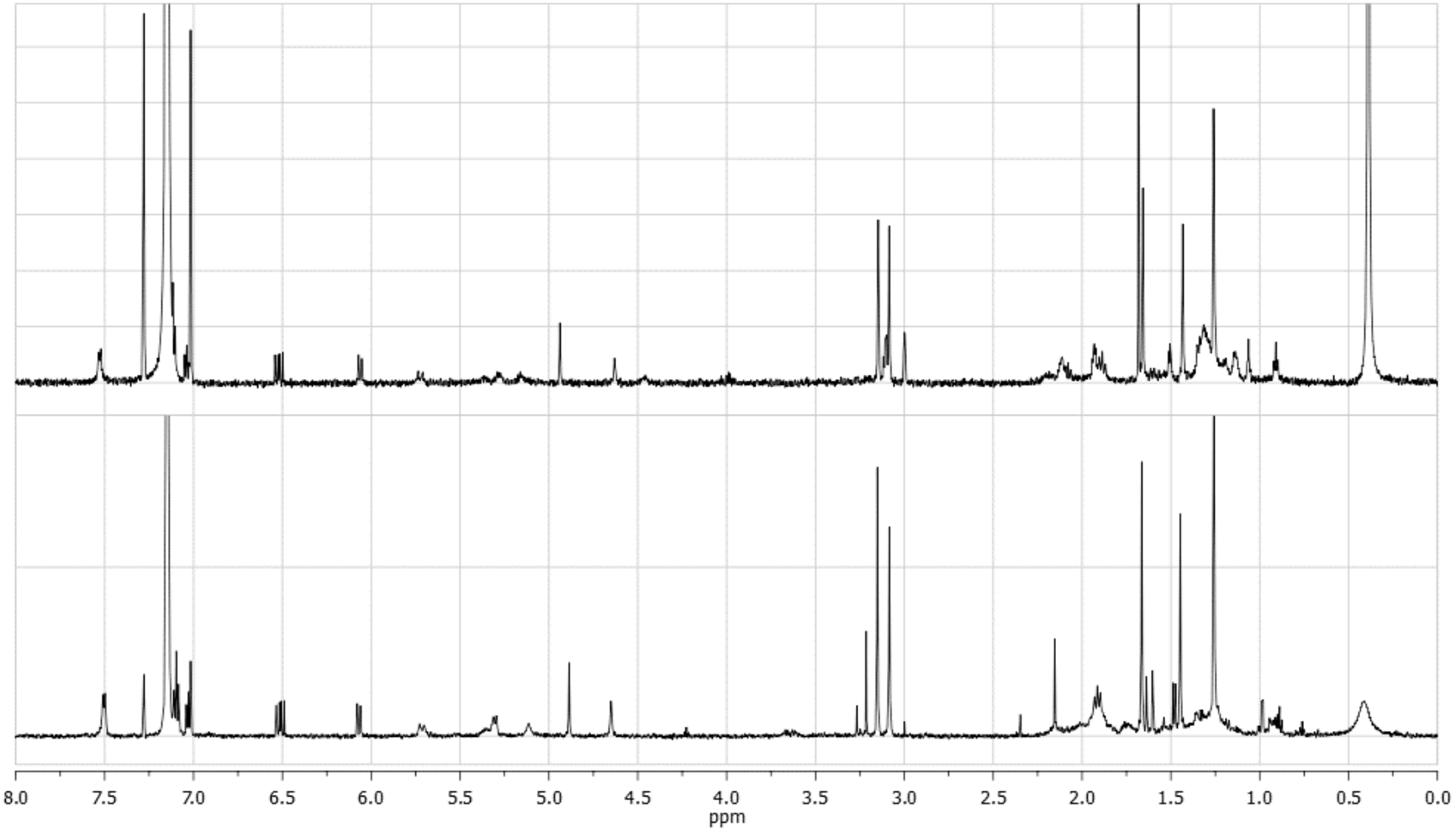

Figure A.8. The stack plot of ^{1}H NMR spectra (600 MHz, C_6D_6) of (R)- and (S)-MPA esters of eunicidiol [**50** (above) and **51** (below), respectively, δ in ppm relative to residual solvent signal].

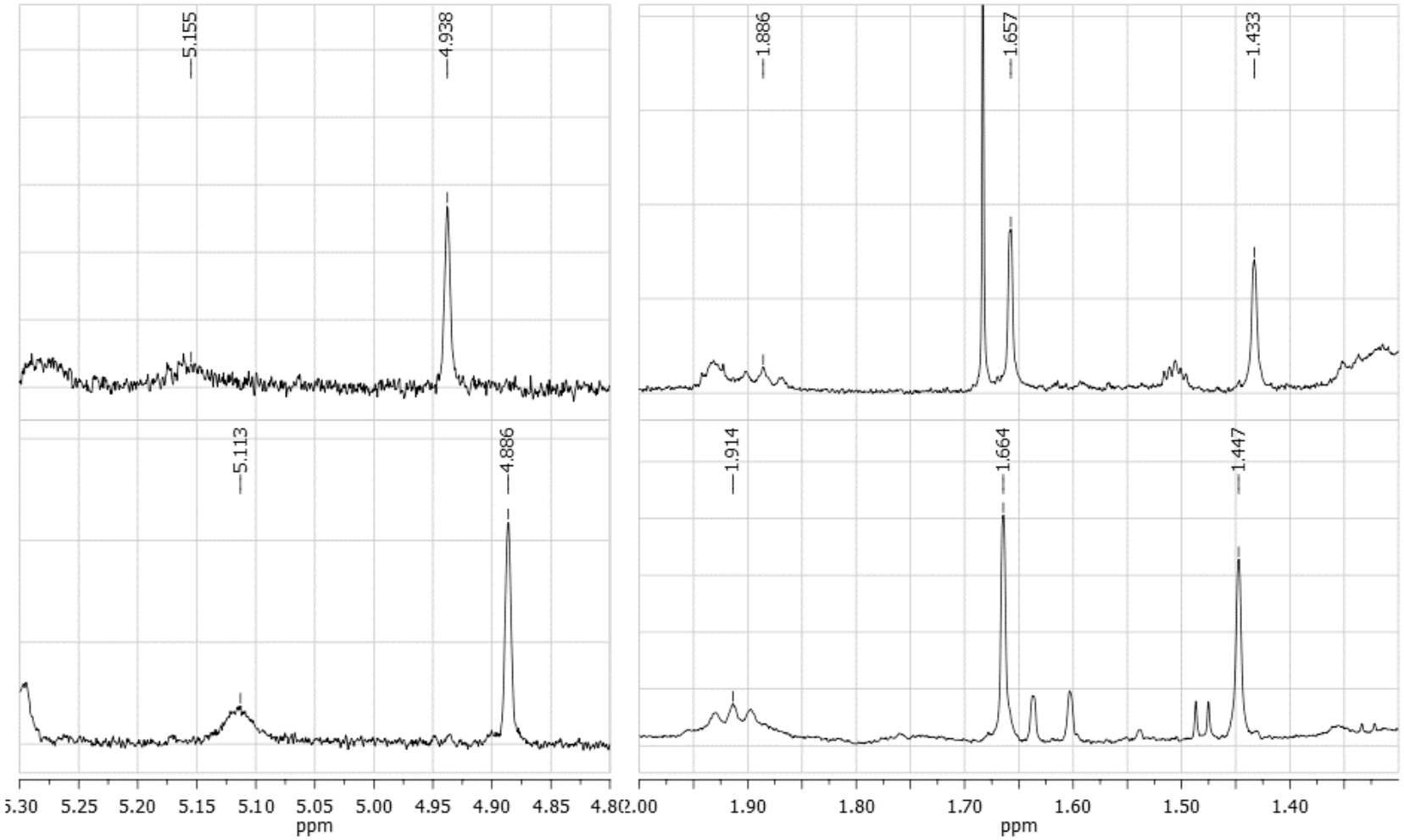

Figure A.9. Enlarged regions within the ^{1}H NMR spectra (600 MHz, C_6D_6) of (R)- and (S)-MPA esters of eunicidiol [**50** (above) and **51** (below), respectively, δ in ppm relative to residual solvent signal].

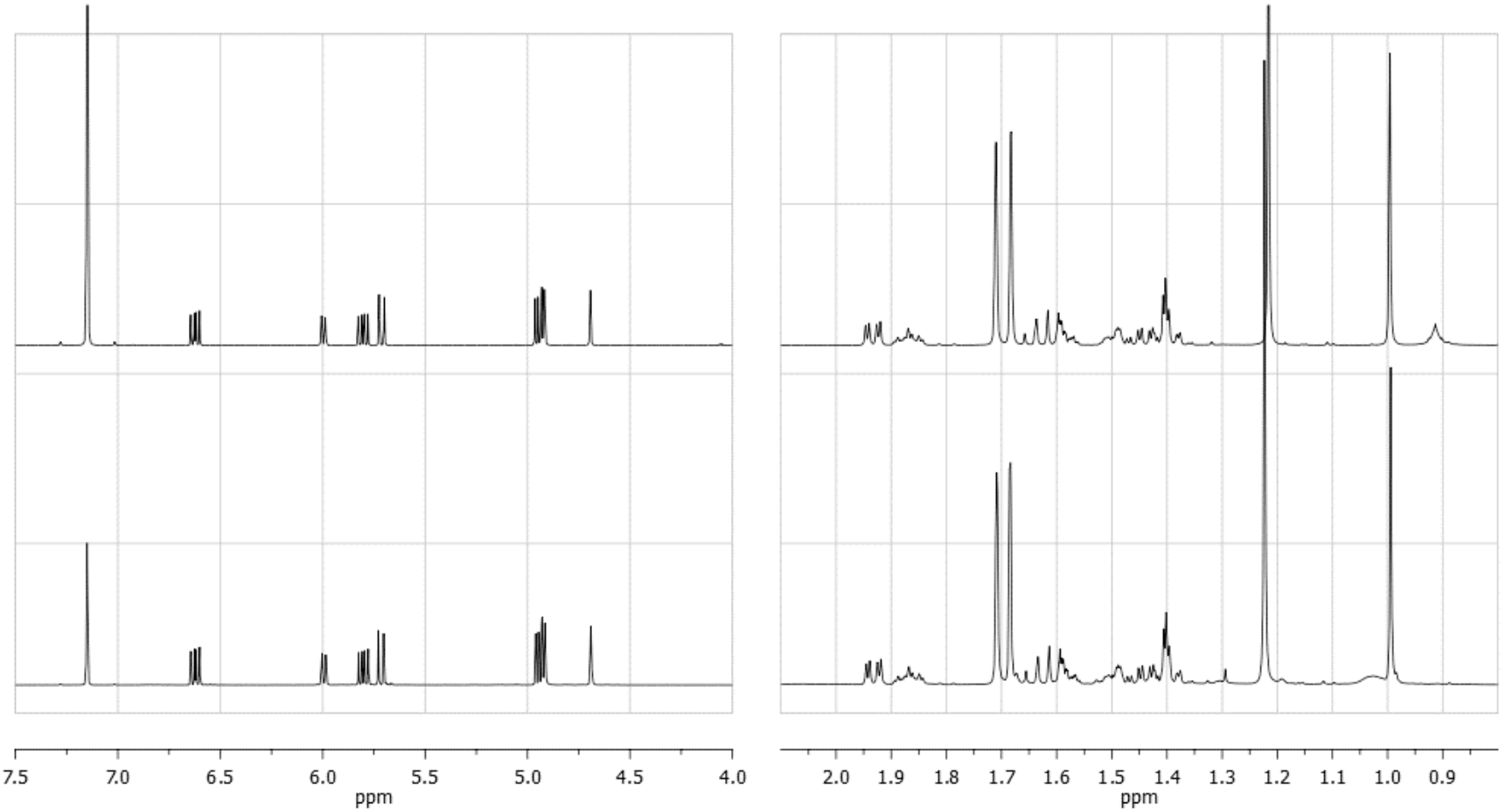

Figure A.10. The stack plot of ^{1}H NMR spectra (600 MHz, C_6D_6) of semisynthetic fuscol (above) and fuscol (**15**) isolated from Eunicea fusca (below) [δ in ppm relative to residual solvent signal].

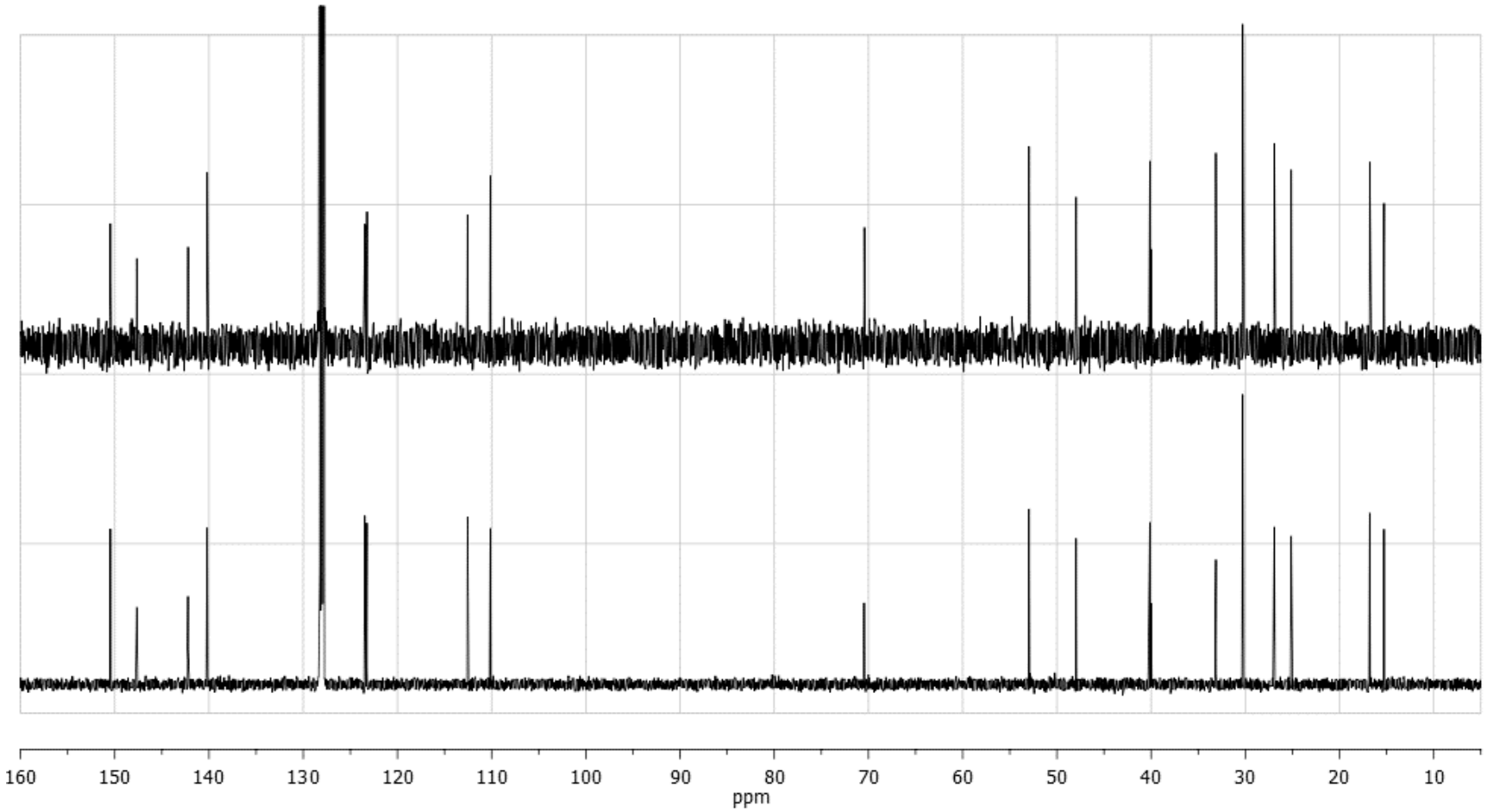

Figure A.11. The stack plot of ^{13}C NMR spectra (150 MHz, C_6D_6) of semisynthetic fuscol (**15**, above) and **15** isolated from Eunicea fusca (below) [δ in ppm relative to residual solvent signal].

APPENDIX B

GENERAL EXPERIMENTAL METHODS

B.1 General experimental information

Medium pressure liquid chromatography (MPLC) was performed using pre-packaged RediSep® Rf columns and a CombiFlash® Rf system (Teledyne Isco) with UV-triggered fraction collection. All flash chromatography was carried out on silica gel (230-400 mesh, Fisher), while TLC was performed using aluminum-backed silica plates (Whatman®, cat. number: 4420 222). Separation of products by RP-HPLC was performed using Phenomenex Luna Phenyl-Hexyl (250 × 10 mm, 5 μm) or Phenomenex Gemini C_{18} (250 × 10 mm, 5 μm) semi-preparative columns. Analysis of samples by LC-APCIMS and LC-HRESIMS with hyphenated ELSD-UV detection was performed with Finnigan™ LXQ™ linear ion trap and Thermo Scientific Exactive™ mass spectrometers, respectively, using a Kinetex C_{18} (50 × 2.1 mm, 1.7 μm) analytical column. The Thermo Scientific Exactive™ instrument was operated by Patricia Boland. Optical rotations were measured on a Rudolph Autopol III Polarimeter. Infrared spectra were acquired using attenuated total reflectance on a Thermo Scientific Nicolet 6700 FT-IR spectrometer (Smart iTR™).

All ^{1}H and ^{13}C NMR spectra were acquired by Dr. Chris Kirby or Lloyd Kerry on a Bruker Avance III 600 MHz NMR spectrometer operating at 600 and 150 MHz for ^{1}H and ^{13}C, respectively. Chemical shifts are reported in ppm and were relative to residual solvent signals: $CDCl_3$ (^{1}H: 7.26 ppm, ^{13}C: 77.16 ppm), CD_3OD (^{1}H: 3.31 ppm, ^{13}C: 49.05 ppm), C_6D_6 (^{1}H: 7.15 ppm, ^{13}C: 128.02 ppm), DMSO-d_6 (^{1}H: 2.50 ppm, ^{13}C: 39.52 ppm), DMF-d_7 (^{1}H: 2.75 ppm, ^{13}C: 163.15 ppm). All ^{1}H and ^{13}C NMR spectral assignments were made on the basis of 2D NMR techniques, primarily COSY, HSQC, and HMBC. Coupling constants are reported along with their multiplicity: singlet (s),

doublet (d), triplet (t), quartet (q), pentet (p), multiplet (m), broad (br), apparent (app.). All deuterated solvents were purchased from Sigma-Aldrich.

All commercially available anhydrous solvents and reagents were obtained from VWR, Sigma-Aldrich, or Fisher Scientific and utilized without further purification. Molecular sieves (3Å pore size) were activated by microwave heating, and all anhydrous reactions were carried out with oven-dried glassware. All reactions were performed at room temperature unless otherwise specified. Rotary evaporation of all solutions was performed in vacuo at 30 °C, except for DMF solutions which were heated to 55 °C. Glycosyl bromides were utilized within one month, during which they were stored under high vacuum over anhydrous $CaSO_4$ to prevent hydrolytic degradation. The model glycosyl acceptor, 2-methyl-3-buten-2-ol (**55**) was dried in the presence of 3Å molecular sieves to remove traces of water. On the basis of BF_3 content, the BF_3•Et_2O (Sigma-Aldrich) was between 46.5 and 53.5%.

B.2 Determination of anti-inflammatory activity by the mouse ear edema assay

The mouse ear edema assay was completed by Amplia PharmaTek Inc. according to a protocol adapted from Martinez et al.[325] The 6-7 week-old female CD-1 mice (Charles River Canada Inc.) were provided with food and water ad libitum and acclimatized for at least 5 days. Indomethacin (150 mg/mL) and the test samples (5 mg/mL) were formulated in DMSO, while PMA (100 μg/mL) was prepared as an acetone solution. Initially, the right ears were treated with 20 μL DMSO (vehicle control group, n = 6), indomethacin (20 μL, 3 mg total, n = 6), or test sample (20 μL, 100 μg total, n = 3). All left ears received 20 μL DMSO as a vehicle control. One hour later, the phlogistic

agent, PMA (20 μL, 2 μg total), was administered by topical application to the right ears of each mouse, while the left ears received 20 μL acetone as a vehicle control. Edema was measured at 6 and 24 hr post-PMA treatment using a digital caliper and calculated by subtracting the thickness of the left ear from the right ear. The data is represented as the mean ± SEM in terms of percent reduction of edema, relative to the vehicle control group. The statistical significance of the comparison between test groups and the vehicle control was assessed by Student's unpaired t-test. A p value <0.05 was considered to indicate statistical significance.

B.3 Determination of antimicrobial activity by the microbroth dilution method

The determination of antimicrobial activity against MRSA (ATCC 33591), VRE (Enterococcus faecium, VREF Ef 379), S. warneri (ATCC 17917), M. smegmatis (ATCC 12051), and M. diernhoferi (ATCC 19340) was conducted in accordance with the testing standards of the Clinical Laboratory Standards Institute.[326] The antimicrobial assays against the former three organisms were carried out by Martin Lanteigne. Eight concentrations of each compound were prepared by serial two-fold dilutions in 20% DMSO so as to achieve testing concentrations of 1-128 μg/mL in the assay wells. All bacteria were grown in cation-adjusted Mueller-Hinton broth under static conditions. The IC_{50} values were determined by measuring the optical density of the plates at 600 nm before and after incubation at 37ºC for 22 h, as described previously.[160] For the mycobacterial species only, the MIC values were determined by visually inspecting the plates after incubation at 30ºC for 96 h, as described previously.[160] All antimicrobial testing against M. tuberculosis $H_{37}Rv$ (ATCC 27294) was conducted by the Institute for

Tuberculosis Research using the microplate Alamar blue assay (MABA).[327] Activities in the low-oxygen-recovery assay (LORA)[294] and against the Vero cell line were also determined by the Institute for Tuberculosis Research.

B.4 Standard procedure for reaction workup

The following protocol is referred to as the "standard work up procedure" throughout the experimental sections of each chapter: The organic layer from the liquid/liquid partition was recovered, dried with anhydrous $MgSO_4$, filtered, and evaporated in vacuo to provide the crude product.

APPENDIX C

CHAPTER 2 AND 3 SUPPORTING INFORMATION:

SUPPLEMENTARY FIGURES

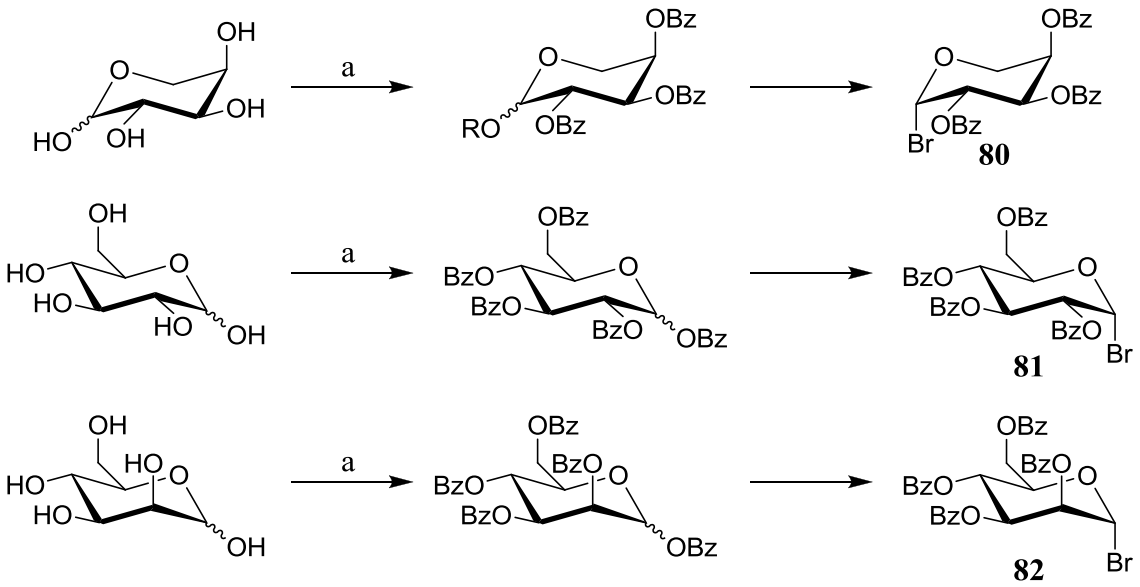

Figure C.1. Synthesis of the arabinosyl (**80**), glucosyl (**81**), and mannosyl (**82**) bromides. Reagents and conditions: (a) (i) BzCl, pyridine. (ii) AcBr (3.0 eq), CH_3OH (3.3 eq), 50% (**80**), 13% (**81**), and 35% (**82**) over two steps.

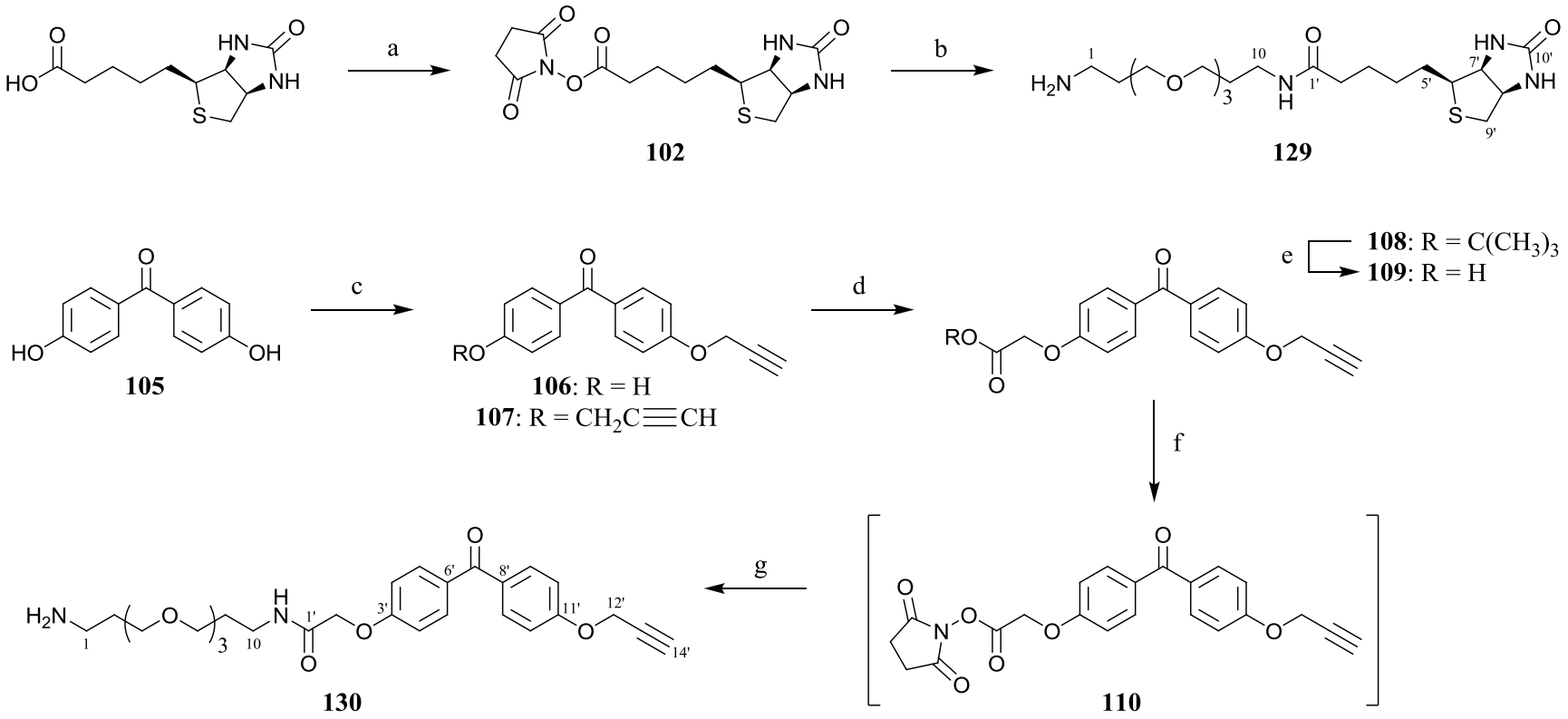

Figure C.2. Preparation of activated NHS esters (**102** and **110**) and generic control probes (**129** and **130**) of biotin and the benzophenone-alkyne (BPA) conjugate. Reagents and conditions: (a) biotin, NHS (1.2 eq), DCC (2.1 eq), DMF, 90%. (b) 4,7,10-trioxa-1,13-tridecanediamine (**94**, excess), DMF, 84%. (c) propargyl bromide (0.7 eq), K_2CO_3, DMF, 73% (**106**) and 24% (**107**). (d) **106**, tert-butyl bromoacetate (4.2 eq), K_2CO_3, DMF. (e) CF_3COOH (excess), CH_2Cl_2, 92% over two steps. (f) NHS, DCC, CH_2Cl_2. (g) **94** (excess), CH_2Cl_2, 75% over two steps.

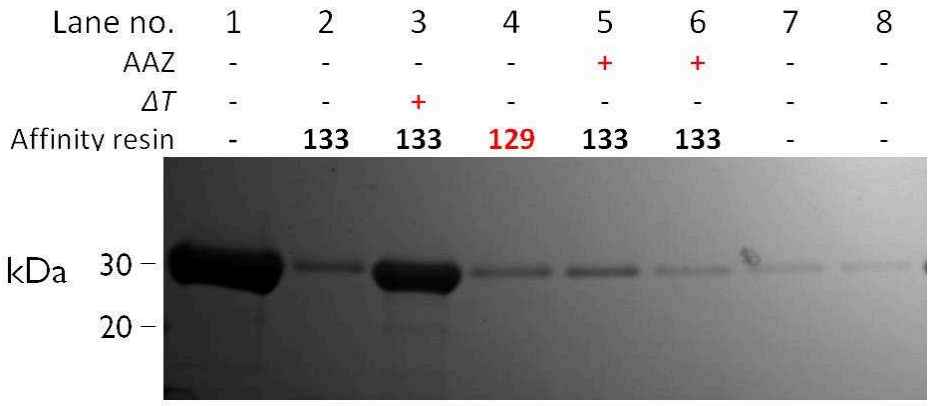

Figure C.3. Gel electrophoretic analysis of the specific binding interaction between ASA-EG_3-Biotin (**133**) and CA. Notes and conditions: The affinity resins were incubated with a 1 mg/mL CA solution. The CA was eluted under denaturing conditions, with the exception of lanes 7-8, and resolved over a 4-12% polyacrylamide gel. Both types of competitive displacements were performed: pre-incubation of CA with AAZ and elution of CA from **133** with AAZ. Description of gel lanes: Lane 1, CA standard; lane 2, affinity capture of CA with **133**; lane 3, heat-denatured control; lane 4, affinity capture of CA with the generic control Biotin-EG_3-NH_2 (**129**); lane 5, remaining CA after competitive displacement by pre-incubation of CA with AAZ; lane 6, remaining CA after competitive elution with AAZ; lane 7, 1st fraction of competitively eluted CA from **133** in lane 6; lane 8, 2nd fraction of competitively eluted CA from **133** in lane 6.

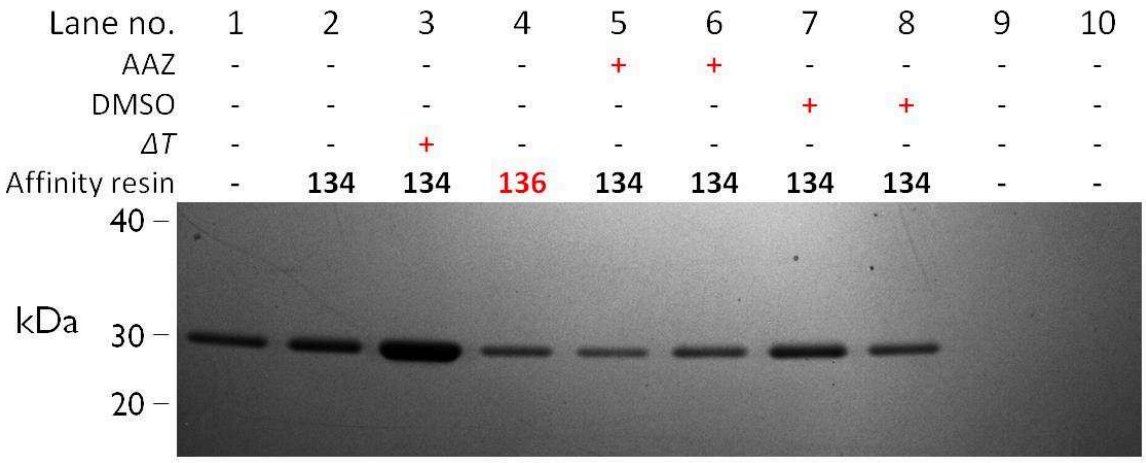

Figure C.4. Gel electrophoretic analysis of the specific binding interaction between ASA-EG_{23}-Biotin (**134**) and CA. Notes and conditions: The affinity resins were incubated with a 100 μg/mL CA solution. The CA was eluted under denaturing conditions, with the exception of lanes 9-10, and resolved over a 4-12% polyacrylamide gel. Both types of competitive displacements were performed: pre-incubation of CA with AAZ and elution of CA from **134** with AAZ. Description of gel lanes: Lane 1, CA standard; lane 2, affinity capture of CA with **134**; lane 3, heat-denatured control; lane 4, affinity capture of CA with the generic control Biotin-EG_{23}-NH_2 (**136**); lane 5, remaining CA after competitive displacement by pre-incubation of CA with AAZ; lane 6, remaining CA after competitive elution with AAZ; lane 7, remaining CA after DMSO control of competitive elution; lane 8, affinity capture of CA with **134** after DMSO control of competitive displacement; lane 9, competitively eluted CA from **134** in lane 6; lane 10, DMSO control of competitive elution from lane 7.

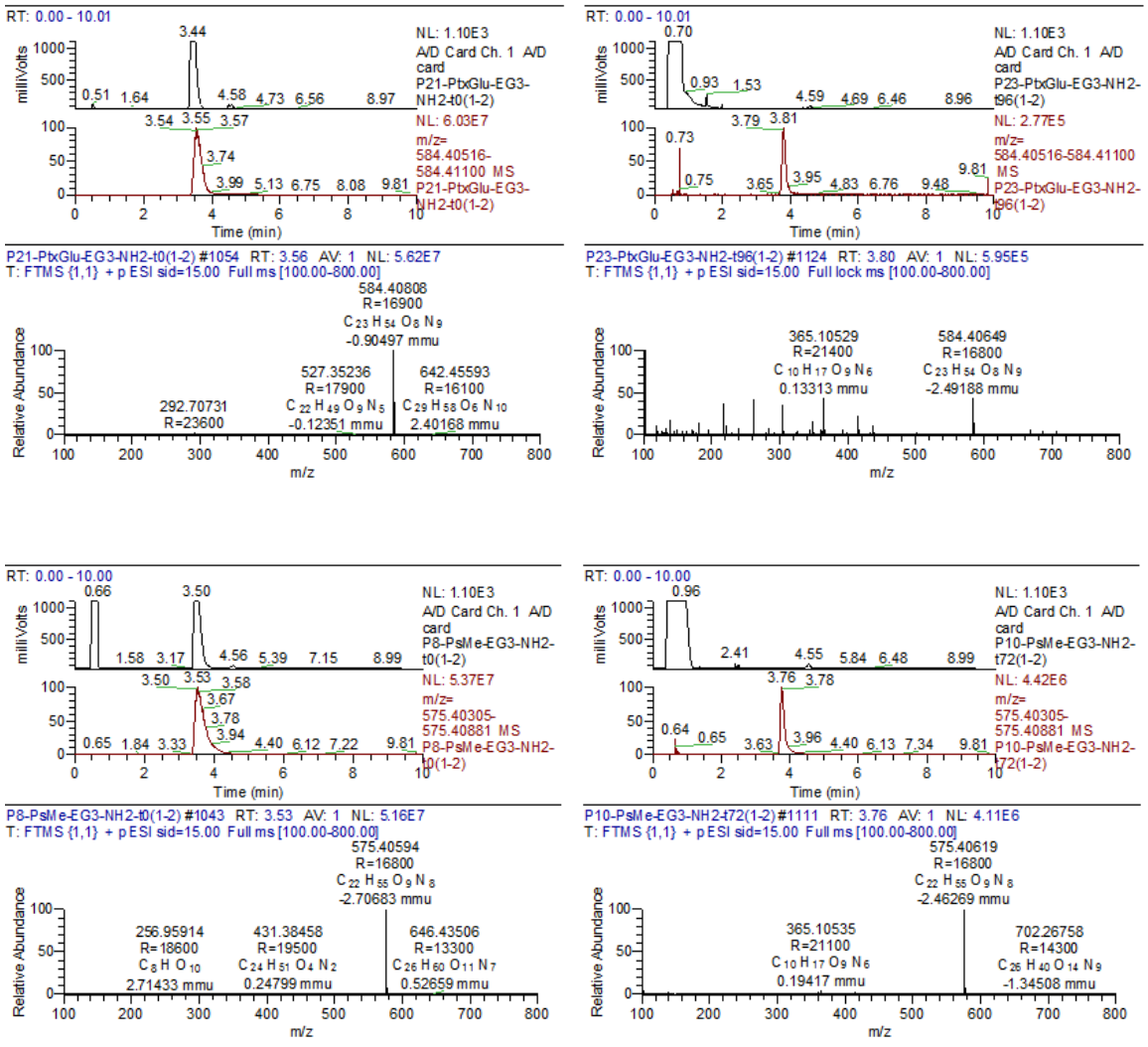

Figure C.5. Characterization of reaction yields for the preparation of PtxGlu-EG$_3$-Agarose (**137**, above) and Ps-EG$_3$-Agarose (**138**, above) by LC-HRESIMS.

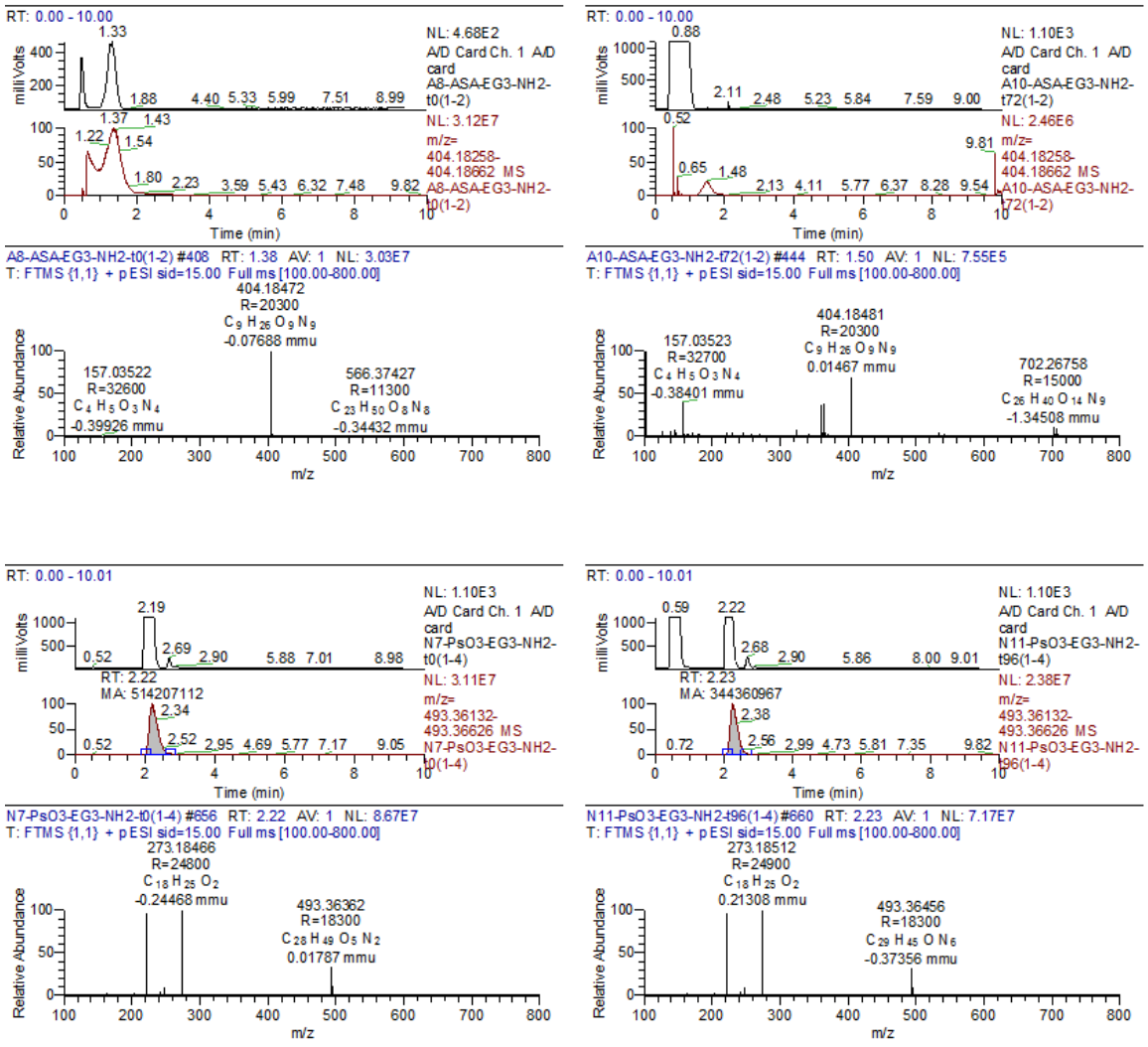

Figure C.6. Characterization of reaction yields for the preparation of ASA-EG_3-Agarose (**139**, above) and Agarose -EG_3-PsOH (**140**, above) by LC-HRESIMS.